The metallochemistry of the prion protein

Davies, Paul

Award date:
2009

Awarding institution:
University of Bath

The Metallochemistry of the Prion Protein

Paul Davies

Submitted in fulfilment for the degree of Doctor of Philosophy

University of Bath
Department of Biology and Biochemistry

April 2009

Abstract

The Prion protein (PrP) is a cell surface glycoprotein that has been directly implicated in the pathogenesis of a range of neurological disorders referred to as the transmissible spongiform encephalopathies (TSE's). The protein has been shown to bind copper within its unstructured N-terminus but the affinity and stoichiometry of the association is a matter of some debate. In addition, the functional significance of this copper binding has yet to be elucidated. This study aimed to determine accurate metal binding parameters for PrP through the use of calorimetry and to provide insight into the potential redox implications of metal once bound. A method of analysis for complex binding to proteins is thoroughly assessed and found to be suitable. The study also aimed to qualify the involvement of metals in the proteins remarkable ability to survive in the environment.

This study confirms that PrP binds copper with an affinity relative to the amount of copper available to the protein. A high nanomolar affinity is reported within two regions on the protein, the octarepeat and the 5^{th} site. Binding within the octarepeat region is found to be highest at low copper concentrations, reducing to micromolar affinity when copper levels exceed equivalents of 1. There is also strong evidence of a complex and cooperative binding mechanism. The 5^{th} site also displays high nanomolar affinity for a single atom of copper. These two regions on the protein also interact in the coordination of copper (II). The copper bound protein is highly redox active and is capable of fully reversible cycling of electrons that are dependent mainly on the octarepeat. The protein does bind other divalent cations but none appear to be physiologically relevant considering the amount of these free metal ions in the body. When adsorbed to model clays, PrP is able to survive for long periods at room temperature. This longevity is increased significantly by the presence of metals in the soil, especially manganese.

These data provide confirmation of the precise parameters of divalent cation binding to PrP. It also confirms that the copper bound protein is capable of a physiological redox role.

Acknowledgments

I wish to acknowledge the expert guidance of Professor David Brown, who has not only provided a very high quality of scientific guidance throughout my PhD but also given me enormous opportunities not normally afforded to those in my position. I am immeasurably grateful.

This thesis is dedicated to the memory of D.W.E McAlpine, who was sadly unable to see this outcome. Also, to J.E. Davy, who supported me so much along with J.F. Goad. I would also like to thank Mr J Goad for putting up with more than he should of. Finally, this is for Michelle, Andrew and Samantha – thank you all for putting up with me during this time.

Publications

Davies P, Marken F, Brown D (2009) Thermodynamic and voltammetric characterisation of the metal binding to the prion protein insights into pH dependence and redox chemistry. Biochemistry. 2009 Feb 5. [Epub ahead of]

Davies P, Fontaine SN, Moualla D, Wang X, Wright JA, Brown DR (2008) Amyloidogenic metal-binding proteins: new investigative pathways. Biochem Soc Trans. 36(Pt 6):1299-303.

Davies P, Brown DR. (2008) The chemistry of copper binding to PrP: is there sufficient evidence to elucidate a role for copper in protein function? Biochem J. 1;410(2):237-44.

Stevens DJ, Walter ED, Rodríguez A, Draper D, Davies P, Brown DR, Millhauser GL. (2009) Early onset prion disease from octarepeat expansion correlates with copper binding properties. PLoS Pathog. Apr;5(4):e1000390.

Chang, B., Gray, P., Piltch, M., Bulgin, M.S., Sorensen-Melson, S., Miller, M.W., Davies, P., Brown, D.R., Coughlin, D.R., Rubenstein, R., (2008) Surround optical fiber immunoassay (SOFIA): An ultra-sensitive assay for prion protein detection, Journal of Virological Methods doi:10.1016/j.jviromet.2009.02.019

Brazier MW, Davies P, Player E, Marken F, Viles JH, Brown DR. (2008) Manganese binding to the prion protein. J Biol Chem. 9;283(19):12831-9.

Zhu F, Davies P, Thompsett AR, Kelly SM, Tranter GE, Hecht L, Isaacs NW, Brown DR, Barron LD. (2008) Raman optical activity and circular dichroism reveal dramatic differences in the influence of divalent copper and manganese ions on prion protein folding. Biochemistry. 26;47(8):2510-7.

Klewpatinond M, Davies P, Bowen S, Brown DR, Viles JH. (2008) Deconvoluting the Cu2+ binding modes of full-length prion protein. J Biol Chem. 25;283(4):1870-81.

Alderton A, Davies P, Illman K, Brown DR. (2007) Ancient conserved domain protein-1 binds copper and modifies its retention in cells. J Neurochem. 103(1):312-21.

Butowt R, Davies P, Brown DR. (2007) Anterograde axonal transport of chicken cellular prion protein (PrPc) in vivo requires its N-terminal part.J Neurosci Res.;85(12):2567-79.

Abbreviations

BSA	Bovine serum albumin
BSE	Bovine spongiform encephalitis
CD	Circular dichroism
CJD	Creutzfeldt-Jacob disease
CMCA	Competitive metal capture analysis
CV	Cyclic voltammetry
CWD	Chronic wasting disease
EDTA	Ethylenediaminetetraacetic acid
ENDOR	Electron nuclear double resonance
EPR	Electron paramagnetic resonance imaging
ESEEM	Electron spin echo envelope modulation
EXAFS	X-ray absorbance fine structure spectroscopy
FBS	Foetal bovine serum
FCS	Fluorescence cross-correlation spectroscopy
FFI	Famial fatal insomnia
GPI	Glycosylphosphatidylinisotol
GSS	Gerstmann Straussler syndrome
ITC	Isothermal titration calorimetry
K_a	Association constant
K_d	Disassociation constant
Kte	Kaolinite
Mte	Montmorillonite
NMR	nuclear magnetic resonance imaging
OS	oxidative stress
PI	Point of ionisation
PMCA	Protein misfolding cyclic amplification
PCR	Polymerase chain reaction
PrP	Prion protein
PrP^c	Cellular prion protein
PrP^{sc}	Scrapie prion protein
rPrP	Recombinant prion protein
RT-SPR	Real time surface plasmon resonance
ROS	Reactive oxygen species
SIFT	Scanning for intensely fluorescent targets
SOD	Superoxide dismutase
TSE	Transmissible spongiform encephalopathy
Vis-CD	Visible circular dichroism

Contents

Contents - Figures

Contents – Tables

CHAPTER ONE

Introduction

1.1 The Transmissible Spongiform Encephalopathies

The transmissible spongiform encephalopathies (TSE's) or prion diseases are a range of neurodegenerative disorders in which a cell surface glycoprotein known as the prion protein (PrP) has been directly implicated in pathogenesis. These conditions include Creutzfeldt-Jacob disease (CJD), Gerstmann Straussler syndrome (GSS), Familial Insomnia (FFI) and kuru in humans beings as well as bovine spongiform encephalopathy (BSE) in cattle, chronic wasting disease (CWD) in deer and elk and scrapie in sheep (Gajdusek 1991; Prusiner 1996; Prusiner 1998; Prusiner 1998). The diseases have a distinctive neuro-pathology where spongiform degeneration occurs within the brain accompanied by deposition of amyloid plaques. Symptomatically, there is a rapid onset of dementia, loss of coordination, paralysis and invariably death.

The earliest reported cases of TSE date back to the mid eighteenth century (Brown and Bradley 1998), where the first incidents of scrapie in sheep were noted. It was then not until the 1980's that the now familiar BSE emerged (Prusiner 1998) where cattle developed scrapie like symptoms, probably as a result of eating feed containing infected sheep material. The British epidemic of BSE, labelled by the media as 'mad cow disease', caused the deaths of nearly 200,000 cattle in the late 1980's and 1990's (Anderson et al. 1996). It is generally now accepted that the epidemic was as a result of the introduction of new rendering procedures in the preparation of cattle feed (Harris 1999). Since the epidemic arose, government restrictions on how cattle feed is produced has led to a significant reduction in the number of cases on a year on year bases. The disease, however, has yet to be fully eradicated. In addition, since 1996, a human form of disease known as new variant CJD, has been linked with consumption of infected material from BSE cattle (Will et al. 1996). Inter human transmission of CJD has also been linked to tissue grafts and other forms of surgery as well as blood transfusion (Brown et al. 1992; Brown 1998).

Human forms of the TSE's can be put into three epidemiological categories, infectious

(5%), sporadic (80%), and inherited (15%) (McKintosh et al. 2003). The sporadic form of the human disease, sCJD, occurs with an incidence of around 1 case per 2 million people and is likely to occur as a result of a single prion misfolding and becoming infectious to neighbouring PrP. Alternatively, the condition may occur as a result of somatic mutations in the prion gene, prnp (Will et al. 1996). GSS and FFI are both inherited forms of disease with a pattern of autosomal dominance (Collins et al. 2001). The most common inherited form, GSS, usually occurs in middle age as a chronic cerebral ataxia (McKintosh et al. 2003). Dementia then follows with death occurring around 5 years following onset of symptoms. The mutation causing GSS was first identified in 1989 as being P102L, although several other mutations in the prion protein gene have since been shown to cause the disease (Hsiao et al. 1992). The other inherited form of disease, FFI, is typified by an increasing inability to sleep along with a steady decline in autonomic function (Lugaresi et al. 1986; Lugaresi et al. 1986). FFI patients exhibit atrophy of the anterior-ventral and medial-dorsal thalamic nuclei and carry mutations within codon 178 in the prion gene (Medori et al. 1992). Of note with these inherited forms is that it has been shown that the disease prions formed in the brains of these patients are still infectious and can be used to infect other individuals (Medori et al. 1992; Kretzschmar et al. 1995).

The infectious forms of TSE are by far the rarest and depend upon acquisition of an infectious form of the protein and consequent transfer across the blood brain barrier. This acquisition can be through ingestion or direct blood or tissue transfer from an infected individual. For direct modes of transmission, there are recorded cases of infection from contaminated dura mater grafts, corneal transplants, neurosurgical instruments, and cadaveric growth hormone (Brown et al. 1992). Transmission via ingestion was first recorded for animal populations and later for human populations through the discovery of Kuru (McKintosh et al. 2003). These cases involved intra-species transmission and exhibited extremely high communicability with a relatively consistent incubation before symptom onset. Where different species are concerned, infection is limited considerably by a species barrier. This is exemplified when material is taken from an infected individual and used to challenge an individual from another species. The rate of infection is significantly less and also carries a much longer incubation period (McKintosh et al. 2003). This species barrier has been identified as being caused by differing PrP primary structures between species (Collinge and Palmer

1994). However, this is not always the case as BSE can be transmitted readily to species where the protein has a significantly different sequence (Bruce et al. 1994). The most relevant example of this phenomenon is the transmission of prion disease to humans from cattle, leading to vCJD.

Transmission itself is thought to involve only PrP and no genetic material, hence the formation of the 'protein only' hypothesis proposed by Griffiths in 1967 (Griffith 1967) and later adapted by Stanley Prusiner (Prusiner 1982). This hypothesis sees an abnormally folded form of the prion protein (PrP^{sc}) cause the normal cellular form (PrP^{c}) to become misfolded itself. This then leads to a chain reaction in which PrP^{sc} leads to the conversion and formation of more PrP^{sc} using endogenous PrP^{c} as substrate. This conversion is catalysed by the nucleation of endogenous PrP using the disease form as a seed or template. With this knowledge, transmission via surgical procedure has been minimised by new procedures and techniques such as recombinant forms of donor hormone and familial screening of potential tissue donors (McKintosh et al. 2003). Transmission to humans via the ingestion of infected material caused vCJD cases to peak in 2002 with a total of 115 total deaths but has been declining exponentially since (Andrews 2009). For humans at least, the possibilities of an epidemic now seem unlikely. For the animal population, however, cases still persist.

The possible modes of prion disease pathogenesis can be divided into three categories; loss of PrP function, gain of PrP function or subversion of PrP function (Westergard et al. 2007). The exact cause of pathogenesis is hotly debated, but may involve one or more of these categories. Loss of function centres on PrP^{c} being converted to PrP^{sc} and losing an essential physiological role. The most commonly suggested role for PrP^{c} in this regard is one of anti-apoptosis leading to a loss of neuronal cells. Subversion of function involves the conversion of PrP from a transducer of neuro-protective signals to a transducer of neuro-toxic signals. Gain of function would see PrP^{sc} act directly as a toxic entity, possibly through the aggregation of the protein leading to disruption of axonal transport and synapse transmission or the triggering of apoptotic pathways (Westergard et al. 2007).

The different classifications or strains of the TSE's are identified by several means. Firstly, each type of TSE produces symptoms specific to the strain type. Post mortem

analysis can also reveal different patterns of damage to the brain. Perhaps the most distinguishing feature however, is the ability to identify strain types on a polyacrylamide gel. Following digestion using the protease proteinase K, PrP^{sc} has different migration characteristics specific to the strain type (Wadsworth et al. 1999). This allows for an accurate determination of the source of infection.

1.2 The Prion Protein

As discussed, PrP exists in at least two distinct forms, the cellular prion protein (PrP^{c}) and the pathogenic or scrapie form (PrP^{sc}) associated with disease. PrP^{c} has a large α-helical content and binds copper strongly within the N terminus (DeArmond and Bouzamondo 2002). The 3D solution NMR structure of the cellular form is shown in figure 1.01. PrP^{sc} or the scrapie isoform, does not bind copper (Wong et al. 2001), has a high β-sheet content and is resistant to protease degradation (Prusiner SB, 1998). It is the copper binding characteristics of PrP^{c} that have led to the current postulated functions of the protein, including as an antioxidant (Brown *et al,* 1999), a copper transporter (Brown *et al,* 2001) and a copper sequester (Brown, 1999). The conversion of PrP^{c} to PrP^{sc} through interaction with the abnormal form, leads to a metal imbalance associated with a loss of copper binding and the formation of plaques in the brain linked with the tendency of PrP^{sc} to aggregate. This interaction does not appear to involve any covalent modifications to the protein and the amino acid sequence remains the same (Chiesa and Harris 2001).

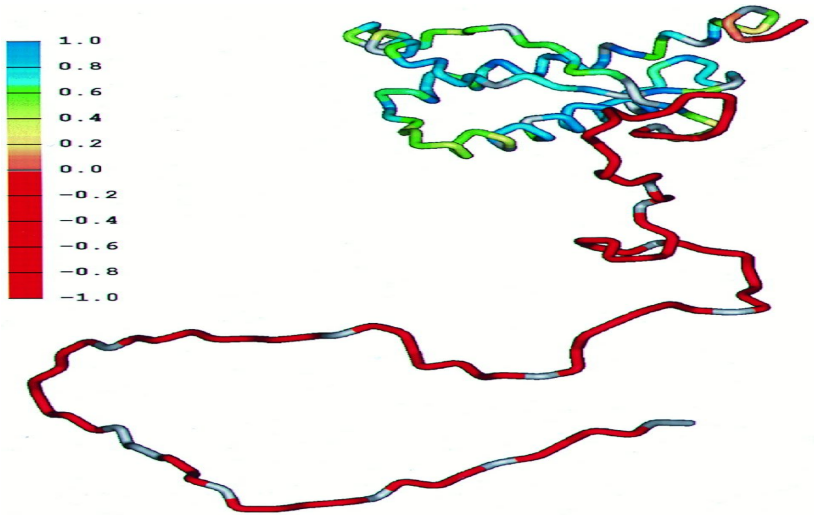

Figure 1.01 3D solution NMR structure of mouse PrP (23-231) showing the flexibility of the N-terminal domain. Donne *et al* (1997)

Although the role of PrP^{sc} in disease is relatively well characterised, the physiological role of PrP^{c} remains unclear. It is now fairly well accepted, however, that PrP^{c} binds copper *in vivo* (Brown et al. 2001). Several possible functions have been suggested that tie in with this association with copper including copper sequestration and internalisation (Pauly and Harris 1998; Brown 1999), protection against oxidants (Kuwahara et al. 1999) , and direct superoxide dismutase activity (Brown et al. 1999; Brown et al. 2001; Wong et al. 2001; Thackray et al. 2002; Cui et al. 2003). In addition, there have been some studies that suggest copper independent roles such as an involvement in cell signalling (Mouillet-Richard et al. 2000; Mange et al. 2002) and neurone growth (Santuccione et al. 2005). However, these non copper related functions have usually been suggested after studies that monitor changes in cellular activity following manipulation of the protein rather than observation of the proteins activity. What is very likely is that the copper binding to the protein is key to its function.

1.3 PrP and Copper Binding

1.3.1 The octarepeat region – coordination

Figure 1.1 shows a schematic of the primary structure of mouse PrP. The mature prion protein, when cleaved from its signal sequence and GPI motif, is some 209 amino acids long with a structured C terminus and, in the absence of copper at least, an unstructured N terminus.

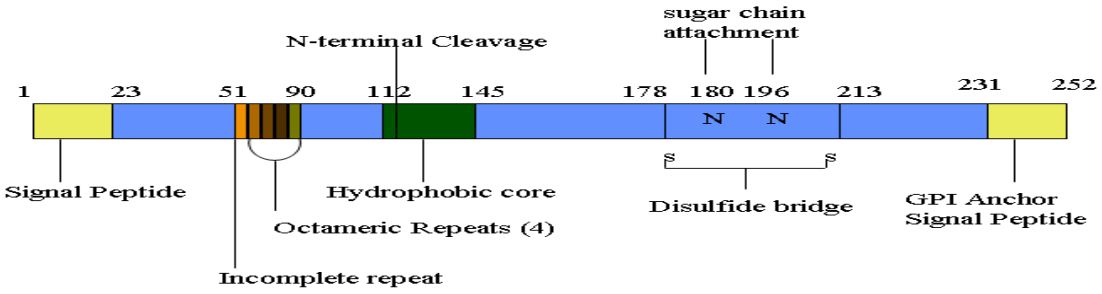

Figure 1.1 The primary structure of the mouse prion protein. This protein is anchored to the cell membrane by a GPI anchor. The signal peptide for entry into the endoplasmic reticulum and the GPI signal peptide are cleaved off before the protein reaches the cell surface. Glycosylation can occur on one two or none of the asparagine residues indicated. A hydrophobic region envelopes a cleavage point where the protein is cleaved during normal metabolic breakdown. A disulphide bond links two regions of the protein which form separate alpha-helices in the three dimensional structure.

It is within this unstructured N terminal region that the primary copper binding domain is found within residues 60 – 91, known as the octarepeat region(Hornshaw et al. 1995; Qin et al. 2002; Millhauser 2004) and more controversially within residues 91-111, or the so called 5th site (Aronoff-Spencer et al. 2000; Qin et al. 2002; Jones et al. 2005). The octarepeat region in the human protein is composed of a sequence of eight amino acids (PHGGGWGQ) repeated four times, each containing a histidine which is generally accepted to be the primary residue responsible for the copper coordination (Aronoff-Spencer et al. 2000; Burns et al. 2002). The first real hard evidence for this association of copper with PrP came from the work of Brown *et al* in 1997. By carrying out equilibrium dialysis on the recombinant N terminal region (residues 23-98), they were able to show that between five and six atoms of copper bound per recombinant fragment. Further detailed studies involving electron paramagnetic resonance imaging (EPR) and X-Ray crystallography on recombinant peptide fragments have demonstrated that a single copper is coordinated by each octarepeat segment in a pentacoordinate complex involving residues HGGGW only (Aronoff-Spencer et al. 2000; Burns et al. 2002) . This study by Arnoff-Spencer *et al,* 2000 revealed an equatorial coordination involving the Histidine imidazole, deprotonated amides from the adjacent two glycines and a deprotonated carbonyl from the last glycine. A water molecule was also identified as being involved by allowing an oxygen to coordinate axially forming a bridge to the NH of the indole on the last tryptophan. Further work by this group, however, has revealed a more complex binding system. In 2005, the same group demonstrated that the coordination of copper was dependent on the degree of copper occupancy on the protein (Chattopadhyay et al. 2005). They revealed three distinct coordination modes, clearly divisible at different relative concentrations of copper. Using X-band and S-band EPR and electron spin echo envelope modulation (ESEEM) to analyse a library of modified peptides, they showed a multiple His coordination mode at low copper occupancy, moving through a transitional coordination to the maximal occupancy at a physiological pH 7.4. Figure 1.2 shows the proposed coordination modes from their data.

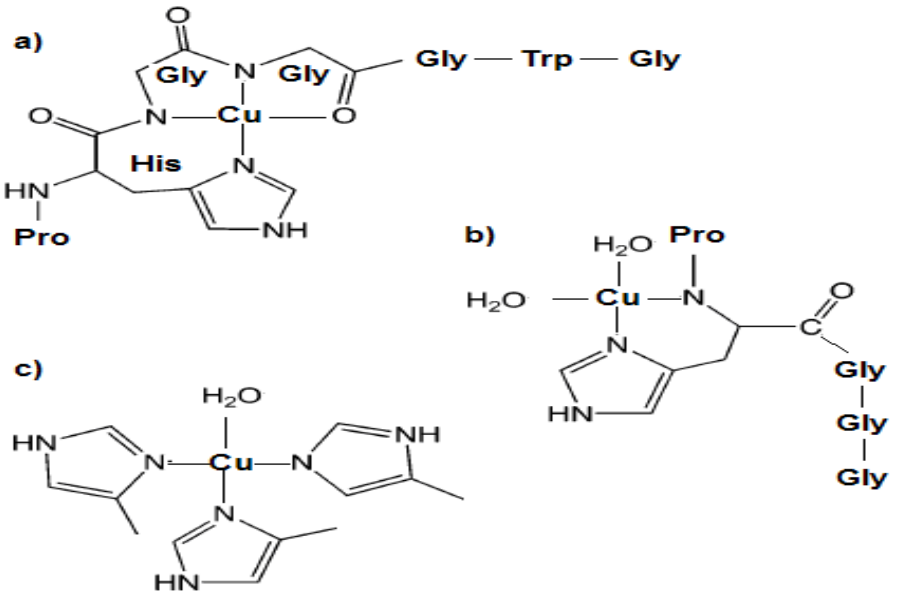

Figure 1.2 Models of the 3 equatorial coordination modes of copper binding to the octarepeat region. a) Component 1, b) Component 2 and c) component 3. For component 3, the 4th ligand involving water may also be another imidazole. After Chattopadhyay *et al,* 2005.

Component 1 coordination dominates at high copper occupancy of 2 copper equivalents and above. As the group previously revealed, a 3N1O arrangement coordinated a single copper per HGGGW motif. Figure 1.3 shows a three dimensional model of this mode for clarity.

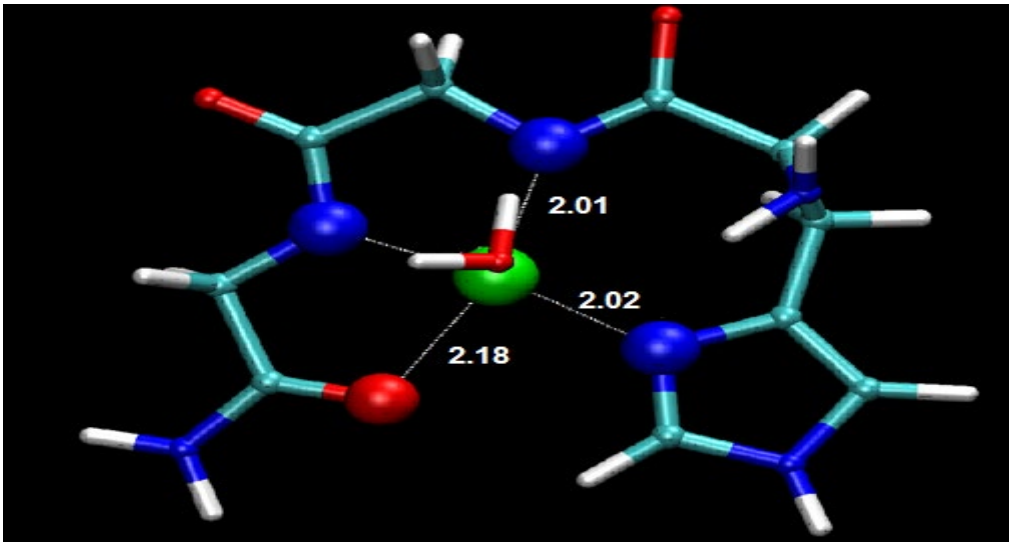

Figure 1.3 Three-dimensional model representing component 1 of the equatorial coordination mode of copper binding to the octarepeat region
Bond lengths shown are in angstroms (1 A° =0.1 nm).

EPR also revealed evidence of dipolar copper-copper centres in approximately 20% of the spectra suggesting a close copper-copper proximity of between 3.5 Å and 6 Å, close

enough for van der Waals interactions. These interactions may be responsible for driving a hydrophobic collapse and consequent N terminal structural organisation at full copper occupancy. The possible implications of this structural change are discussed in a later section of this introduction. Component two coordination is present only as a transition between low copper occupancy of one atom or less and full copper occupancy. The precise coordination mode of this component was extremely difficult to accurately characterise as the authors found it to be mixed with other modes in all the conditions tested. However, by methylating the second glycine residue in each octarepeat, they were able to successfully block component 1 formation and resolve the coordination mode for component 2. The results suggest a 2N2O arrangement at the expected neutral charge state and this is illustrated in figure 2. These findings suggest an intermediate coordination involving the His imidazole and its exocyclic nitrogen. Further contributions appear to stem from the oxygens of two water molecules within the equatorial arrangement. Component 3, present at low copper occupancy only, is likely to provide the highest affinity copper binding within the octarepeat due to its multi-His coordination. This coordination mode involves either a 3N1O or 4N arrangement and is only available at above pH 6.5 and when multiple histidine residues are present. This groups combined data points towards a mechanism for dramatic structural change within the N terminus of PrP that is entirely dependent on the amount of copper bound to the protein.

Recent work by Weiss *et al,* 2007 employed extended X-ray absorbance fine structure spectroscopy (EXAFS), EPR, electron nuclear double resonance (ENDOR) and molecular modelling to resolve the copper coordination to PrP. In contrast to many of the previous studies (Viles et al. 1999; Aronoff-Spencer et al. 2000; Burns et al. 2002; Morante et al. 2004; Chattopadhyay et al. 2005), they concentrated on spectra from full length recombinant human PrP. Although the authors report multiple configurations dependent on copper occupancy, they only identified two distinct modes of binding, models of which are shown in figure 1.4. As found previously (Mentler et al. 2005), a coordination identified as species 1 was evident that utilised a 3N1O configuration. Contributions are from the imidazole nitrogen, two glycine amides and a carbonyl oxygen from the last glycine.

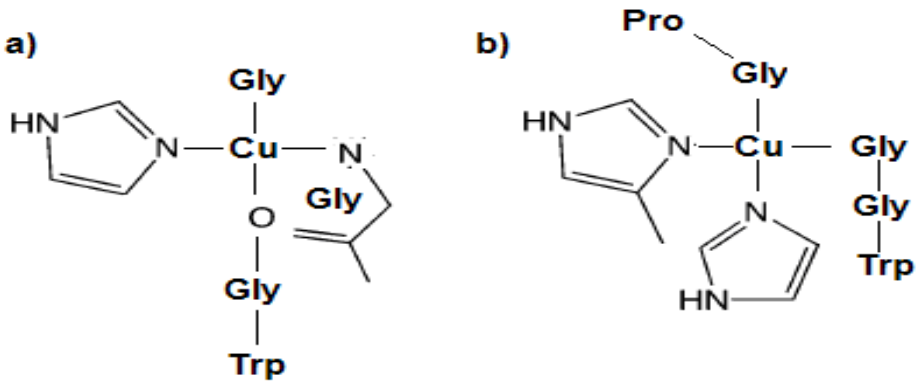

Figure 1.4. Models of the 2 Cu^{2+} coordination modes. a) species 1 and (b) species 2. After Weiss *et al,* 2007.

It is clear that this is exactly the same model as that was proposed previously (Aronoff-Spencer et al. 2000; Burns et al. 2002). The second model, or species 2, was obtained through analysis of the super hyperfine element of the EPR spectra, based on the principle that multiplicity relates to the number of nitrogen ligands. They revealed a 4N arrangement when looking at low to intermediate copper occupancy on full length protein and the entire octarepeat segment. This in itself is not strikingly different from previous findings, however the author's conclusions, in light of their ENDOR data are dramatically at odds with anything previously proposed. An intermediate structure involving two imidazole nitrogens and two glycine nitrogens was proposed.

A very interesting article utilising *ab initio* simulations (Furlan et al. 2007) produced some coordination models that were very similar to those proposed experimentally. They supported the idea of multi-his coordination under certain conditions. Interestingly, however, they suggested that the axial water thought to be involved in a pentacoordination was actually only bound to the indole of tryptophan and not directly involved. They went on to verify this and confirmed that the Cu-water interaction was extremely weak.

The relative difficulty of resolving structures accurately by nuclear magnetic resonance imaging (NMR) when paramagnetic elements, such as copper, are present has led to an interest in finding copper analogues to help elucidate the

Copper-octarepeat environment. One group investigated Ni^{2+}, $Pd^{2+,}$ Pt^{2+} and Au^{3+} ions for their suitability as a diamagnetic probe of Cu^{2+} binding (Garnett et al. 2006). The authors found that Pd^{2+} would form a square planar complex (the other ions would not) but in a different coordination than that seen for copper. Hence, they conclude that for the octarepeat at least, there are no suitable analogues. Another study (Shearer and Soh 2007) also showed Ni^{2+} was an unsuitable analogue.

1.3.2 The 5th site – coordination

A large body of literature now exists that demonstrates that copper is able to bind outside of the octarepeat region of PrP (Hasnain et al. 2001; Jackson et al. 2001; Kramer et al. 2001; Burns et al. 2003; Jones et al. 2004). Work by Jones *et al,* in 2004 and 2005 highlighted these copper binding regions as His96 and His111 in the human protein. They also identified the minimum sequence necessary for Copper binding to this region of PrP are amino acids 92-96 and 107-111. Recently, the same group utilised NMR and visible circular dichroism (Vis-CD) to fully elucidate the coordination of copper to this so called 5th site (Klewpatinond and Viles 2007). Interestingly, they found that the coordination of copper changed dramatically dependent on chain length and pH. The Vis-CD spectra for 90-126 were strikingly different from 91-115, despite only two sites being present on both fragments. By studying each individual site on each fragment by replacing the histidine at either 96 or 111 with alanine and comparing the spectra of these mutant fragments with that from the original fragments, they determined that this change in spectra was not caused by differences in coordination. They concluded that the spectra differences were caused by a change in relative affinity of His 96 and His 111 for copper. Although His111 seems to display the highest affinity for copper, His96 affinity increases dramatically on the addition of the eleven amino acid hydrophobic segment. Interestingly, the relative affinity of these two sites is reversed for nickel, with His96 demonstrating the tightest binding. They also discovered a multi coordination mode that was strongly influenced by pH. Figure 1.5 illustrates these 3 possible coordination modes. Although all display a square planar geometry, the differences are clear. At pH 7.5 and above, a 4N complex dominates, while at pH6, a ligand rearrangement shifts the coordination to a 3N1O configuration. At low pH, a multi His 2N2O coordination dominates. By combining this EPR data with Vis-CD, the authors conclude that the histidines at 96 and 111 bind copper independently except at low pH,

where it appears that both histidines are involved in the coordination of a single copper atom. Analysis by ^{1}H-NMR using nickel as a probe further confirms these findings. Another study also reported the key binding site as being present between residues 106 and 114 (Shearer and Soh 2007).

In stark contrast with the finding that His111 is most important for copper binding, another group reported that His96 was the key site involved (Treiber et al. 2007). Using real time surface plasmon resonance (SPR) analysis on synthetic peptides and recombinant protein, they also discovered a binding site for manganese within the region 91-231.

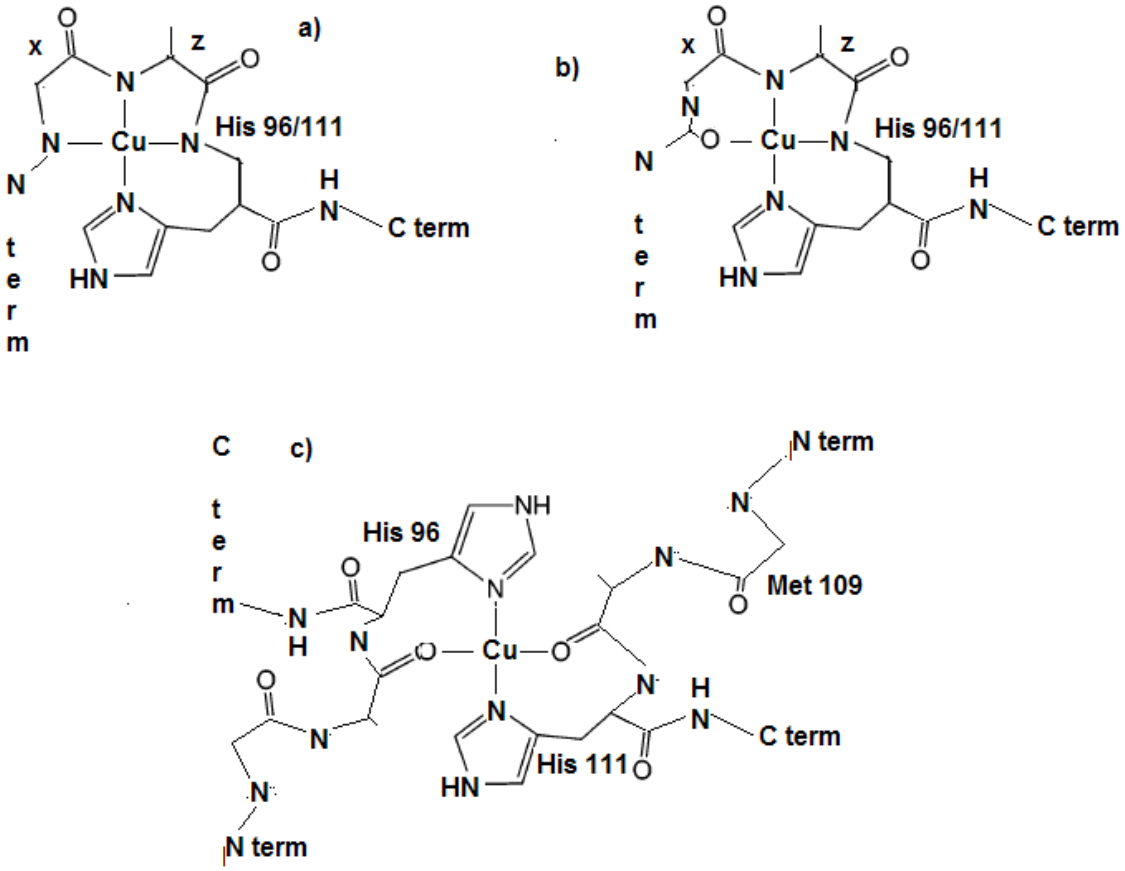

Figure 1.5 Models of the Cu^{2+} coordination modes for the 5th site. Square-planar metal-binding sites at His^{96} and His^{111} in PrP-(90-126). Z represents Thr^{95} or Lys^{110}. X represents Gly^{94} or Met^{109}. a) component 1 is a 4N complex that dominate at pH 7.5 and above. b) component 2 is a 3N1O complex that exists at pH 6 and c) component 3 is a 2N2O complex that may exist at pH 5.5. After Klewpationd and Viles, 2007.

1.3.3 The affinity of copper for PrP

Clearly, in order to understand the physiological importance of copper binding to PrP, it is necessary to know the affinity of the metal for the protein. With copper so tightly regulated in the body (Linder and Hazegh-Azam 1996), any functional copper protein must be able to chelate the copper and keep hold of it through its functional life. There have been a great number of attempts made to calculate the disassociation constants of copper and other metals from PrP but there is, unfortunately, much difference of opinion.

The first real attempt to assess the affinity of copper for PrP was in the mid 1990s, first on synthetic peptides (Hornshaw et al. 1995) by X-ray fluorescence, revealing a K_d of 6.7 μM and then on full length protein (Stockel et al. 1998) yielding a K_d of 14 μM. Following on from this, another group used various spectroscopic techniques and found the affinity for copper within the octarepeat to be k_d~6 μM when two octarepeat segments present (Viles et al. 1999). When three or four coppers were present, cooperative binding was observed. These early results were all in close agreement. In 2001, however, Jackson *et al,* utilised fluorescence quenching and discovered a very different story. They discovered that a very tight binding event was followed by a significantly weaker event. Using glycine competition, they calculated the initial binding event occurred with a k_d~8 fM and subsequent binding with a K_d~15 μM. Another group then published further data in support of positive cooperation (Garnett and Viles 2003). Using CD spectroscopy and competitive collators, they ruled out the previously reported femtomolar affinity by showing that glycine was successfully able to compete with PrP for copper. As glycine has a nanomolar affinity for copper, this meant that the affinity range had to be between the micromolar to nanomolar range. Further work (Walter et al. 2006) sought to assess the affinities for copper within each of the coordination modes they discovered. They found evidence for negative cooperativity, reporting a high affinity initial binding event in the nanomolar range followed by 3 subsequent events in the micromolar range. Data obtained by a two different methods (Thompsett et al. 2005) also demonstrated a negative cooperation between binding events in the octarepeat region. By utilising isothermal titration

calorimetry (ITC) and competitive metal capture analysis (CMCA) they reported an initial binding event in the low femtomolar range followed by three subsequent events in the picomolar range. Recently, Treiber *et al,* 2007 used RT-SPR (real time surface plasmon resonance) to assess the affinity of the octarepeat for copper and found the K_d to be in the nanomolar range.

The affinity of the 5th site for copper is also a subject of much debate. Jones *et al*, 2004, spectroscopically assessed the 5th site to bind copper with nanomolar affinity. The same group then showed that the affinity of the 5th site for copper was higher than that of the octarepeat for copper (Jones et al. 2005). This was considerably more conservative than the femtomolar affinity proposed by Jackson *et al,* 2001. Then, in 2007, two independent groups both produced data from very different methods suggesting the affinity of the 5th site was in the mid-micromolar range (Shearer and Soh 2007; Treiber et al. 2007). The later group also compared the 5th site with the octarepeat and found that the relative affinity was higher in the octarepeat region.

1.4 The Implications of Copper Binding

A key factor in the physiological relevance of copper binding to PrP is the effect that copper has when bound. There is an enormous body of evidence reporting on the ability of PrP to aggregate, form amyloid, alter its resistance to proteases, carry out electrochemical activities and transport metals through membranes. The next section of this introduction, therefore, looks at the evidence for the effects of copper on PrP.

1.4.1 Protein Stability

Metals have been implicated in the tendency of PrP to aggregate and form amyloid fibrils in disease. The first real evidence for an effect of copper on PrP stability came in 1996 (Miura et al. 1996). This group detected an increase in α-helix content in the presence of copper and therefore away from the β-sheet evident in disease. In 2004, another group showed that Cu was able to block *de novo* aggregation that had been induced by exposure to manganese (Giese et al. 2004). To quantify and characterize PrP aggregates, they used fluorescently labelled PrP and applied fluorescence cross-correlation spectroscopy analysis (cross-correlation FCS) as well as scanning for

intensely fluorescent targets (SIFT) in a confocal single molecule detection system. Another group in 2005, showed that copper inhibited the *in vitro* conversion of PrP to its abnormal form (Bocharova et al. 2005). Using a variety of techniques including ThT assay and FTIR spectroscopy, they carried out cell free assay on recombinant human protein showed that, at physiological pH, copper was the more effective than other metals tested at preventing amyloid formation. Interestingly, they showed that although less efficient, this inhibition still occurred even in the absence of the octarepeat. They also demonstrated that, despite this apparent protective effect, copper was also able to stabilise preformed non-amyloidogenic PrP that was resistant to protease (PrPres) and copper could also stabilise existing fibrils. Another group also utilised ThT assays to show that copper prevented fibril formation by human PrP whereas other metals such as aluminium and zinc induced aggregation (Ricchelli et al. 2006). Several studies have used protein misfolding cyclic amplification (PMCA) to look into the effect of copper on the ability of PrP^{sc} to generate more misfolded protein (Kim et al. 2005; Sarafoff et al. 2005). Both these studies showed that Copper was able to weakly facilitate the process, but less so than other divalent cations.

In contrast, another study in 2006, demonstrated that copper could actually induce amyloid formation in sheep carrying certain allelic variants (Tsiroulnikov et al. 2006). This idea is certainly not in isolation, however. For example, one study showed that Copper could increase β-sheet, increase protease resistance and cause aggregation, but only in the aged protein, where Asn-107 is converted to Asp by covalent modification (Qin et al. 2000). This finding was also supported by work carried out by another group (Jones et al. 2004; Klewpatinond and Viles 2007). Other work demonstrated that copper bound protein was more likely to aggregate than metal free protein and also demonstrated increases in β-sheet as a result of the presence of the metal (Jobling et al. 2001).

1.4.2 Protein electrochemistry

There has been some recent work on the electrochemistry of the protein when bound to copper. It has been shown that copper is reduced from Cu^{2+} to Cu^{+} on binding to PrP (Miura et al. 2005). Brown *et al,* 1999 first suggested that PrP displayed superoxide dismutase like activity by carrying out assays with both native and recombinant mouse

protein. They demonstrated, by modifying sections of the protein, that it was the copper bound octarepeat that was responsible for the enzymatic activity of PrP. They further demonstrated this in 2001 with native protein and showed that it was able to protect against oxidative stress (Brown et al. 2001). A study in the same year showed that PrP from scrapie infected mice demonstrated a dramatic reduction in this antioxidant activity (Wong et al. 2001). Also in this year, a study demonstrated that PrP knock out mice demonstrated an increase in markers of oxidative stress such as lipid and protein oxidation (Klamt et al. 2001). Another study produced evidence that the 5th site was redox active by employing cyclic voltammetry on copper bound PrP fragments encompassing the 5th site region (Shearer and Soh 2007). Their data clearly demonstrate a quasi-reversible reaction where the 5th site is able to cycle electrons without becoming permanently oxidised or reduced. A separate study also demonstrated a quasi-reversible reaction for copper bound peptides corresponding to the octarepeat region (Hureau et al. 2006). These studies combined suggest that all copper centres on the protein are able to undergo cyclic redox chemistry. In line with this evidence, an independent study showed that PrP does not redox silence copper (Nadal et al. 2007). They found that the protein was able to dramatically reduce the amount of hydroxyl radicals present in a Cu^{2+}/ascorbate/oxygen system without affecting hydrogen peroxide levels. The conclusion is clearly that the protein is quenching these radicals by a method other than Fenton chemistry and is doing so sacrificially. Interestingly, they also showed that the octarepeat region was protective against residue oxidation within the 5th site, suggesting that the 90-231 form of the protein may be more susceptible to oxidative damage.

One recent study has focused on the ability of PrP to generate the free radical superoxide (Kawano 2007). The study provides compelling evidence that copper PrP is able to catalyse the formation of superoxide and become damaged irreversibly by the radical. It suggests that these oxidative effects are able to produce an intermediate form of the protein designated PrPrdx which is then able to undergo conversion to the disease form. This evidence for electrochemical activity with PrP is supported by numerous others articles including (Walz et al. 1999; White et al. 1999; Frederikse et al. 2000; Wong et al. 2000; Dupuis et al. 2002; Huber et al. 2002; Miele et al. 2002; Curtis et al. 2003; Rachidi et al. 2003; Zeng et al. 2003)

More recently, studies involving our research group have focused more on the quantifying and qualifying the precise mode and action of the transfer of electrons involving the copper centres of PrP. The first highlighted the effects of disrupting the proteins electrochemistry by exposing PrP to manganese (Brazier et al. 2008). The study clearly demonstrated that it was the copper within the octarepeat region that was necessary for redox cycling. A more detailed study (Davies et al. 2009) then defined the electron transfer kinetics and pH dependence of PrP redox activity when copper is bound. The results demonstrated that PrP was able to undergo stable redox cycling and provided evidence for a redox related function for PrP. In contrast to this rather compelling evidence for the electrochemical properties of PrP, two other studies have cast serious doubt on the ability of PrP to act as a superoxide dismutase, demonstrating that neither the *in vivo* protein (Hutter et al. 2003) or recombinant protein (Jones et al. 2005) posses any superoxide dismutase like activity.

1.4.3 Protein behaviour and turnover

There have been several publications that have looked into the physical behaviour of PrP when exposed to copper. Pauly and Harris, 1998, showed that exposure to copper at the cell surface increased the rate of PrP internalisation. They also proved that the N-terminal region of the protein was important for the rate increase of internalisation. This data was later supported by other work (Lee et al. 2001; Marella et al. 2002). Additionally, another area of the protein located at the far N-terminal region of basic residues was also identified as key to the internalisation process (Lee et al. 2001; Walmsley et al. 2003). These findings were supported by a study that showed that copper induced PrP internalisation was abolished in the disease state (Perera and Hooper 2001). Another group showed that copper accelerated internalisation to transferrin containing early endosomes and golgi departments (Brown and Harris 2003). Work by Brown in 1999 showed that PrP expression aided cellular copper uptake and in 2004 further supported this by showing that PrP expression influenced cellular uptake in astrocytes (Brown 2004). Further work by our group discovered that physiological levels of copper were sufficient to drive the internalisation process and that no other metal could stimulate it (Haigh et al. 2005).

In contrast to this seemingly overwhelming evidence, work in 2000, suggested that brain copper levels and cuproenzyme activity was unaffected by PrP expression levels (Waggoner et al. 2000), calling into question the importance of any sequestration role by PrP. Additionally, Rachidi *et al,* 2003 also showed that PrP expression did not affect copper delivery.

1.5 Copper and the Function of PrP

1.5.1 Antioxidant Role

There can be little doubt that PrP does not stifle the ability of copper to undergo redox cycling. Recent studies have clearly demonstrated that copper bound PrP is fully able to accept electrons and donate electrons cyclically (Hureau et al. 2006; Shearer and Soh 2007; Brazier et al. 2008; Hureau et al. 2008; Davies et al. 2009). The evidence showing that PrP does not redox silence copper (Nadal et al. 2007) is supportive of an electrochemical role for the protein. There is an enormous body of literature supporting a role for PrP directly as a superoxide dismutase (Brown et al. 1999; Brown et al. 2001; Klamt et al. 2001; Wong et al. 2001; Dupuis et al. 2002; Huber et al. 2002; Miele et al. 2002; Curtis et al. 2003; Rachidi et al. 2003; Zeng et al. 2003; Brown 2005). This evidence, however, really only links PrP to having an effect on oxidative stress rather than a direct observation of antioxidant activity. It is likely that any protein that bound significant amounts of copper would have some effect on oxidant levels or provide some protection from oxidative stress, if only by chelating a metal capable of producing oxidants itself. A clear piece of evidence that would discount or allow for PrP as a enzymatic antioxidant is the affinity for copper. Unfortunately, the reported affinity values range from micromolar (Viles et al. 1999) to femtomolar (Jackson et al. 2001). The majority view, however, is that there is at least one nanomolar binding event (Garnett and Viles 2003; Walter et al. 2006; Treiber et al. 2007). Even a nanomolar disassociation constant, however, would not fit with what is know a protein with superoxide dismutase activity would need (Kramer et al. 2001). The variation in affinity values means a superoxide dismutase like role cannot be ruled out. What seems more likely from the available evidence though is that PrP is protecting against oxidative damage by simply chelating redox active copper or possible acting as a sacrificial quencher of ROS (Nadal et al. 2007).

1.5.2 Copper Sequestration / Buffering / Sensing

The extensive work on the metal binding characteristics of both recombinant and native PrP (Aronoff-Spencer et al. 2000; Burns et al. 2002; Burns et al. 2003; Morante et al. 2004; Chattopadhyay et al. 2005; Redecke et al. 2005) all suggest PrP has multiple metal binding sites with a high specifity for copper. The question remains, however, is the affinity of PrP for copper high enough to directly chelate copper from copper serum transporters with disassociation constants in the region of 10^{-10} to 10^{-11} (Linder and Hazegh-Azam 1996; Linder 2001). The evidence for the affinity of PrP for copper is simply too variable to make a reasoned assessment. The highest values given of femtomolar (Jackson et al. 2001; Thompsett et al. 2005) would allow for a sequestration role whereas values in the micromolar range (Viles et al. 1999) or nanomolar range (Garnett and Viles 2003; Walter et al. 2006) would not. Additionally, does the protein become loaded with copper inside the cells, transporting to the outside for a protective or catalytic purpose (Brown et al. 1998) or is the protein presented to the extracellular environment without copper loaded or partially loaded so as to chelate copper from the outside? Certainly PrP is involved in copper (II) uptake in cells (Brown 1999; Brown 2004). These concepts are illustrated in figure 1.6 and are key to understanding the role of PrP. It would seem plausible given the multiple reports of a negative cooperation and multiple disassociation constants within the octarepeat binding region (Jackson et al. 2001; Garnett and Viles 2003; Thompsett et al. 2005; Walter et al. 2006) that there would be at least some available copper binding sites free on presentation to the extracellular environment. This would leave open the interesting possibility that the dramatic restructuring seen in the N-terminus of the protein during maximum copper occupancy (Chattopadhyay et al. 2005; Weiss et al. 2007) could be a trigger for internalisation of the protein. Clearly there is much direct evidence showing that copper increases the rate of internalisation (Pauly and Harris 1998) and that the N terminus was key to this process (Lee et al. 2001; Marella et al. 2002). Additionally, it is now known that physiologically relevant amounts of copper are sufficient to drive the internalisation process (Haigh et al. 2005). This may suggest that PrP is able to function as a concentration sensitive sequester of copper, activated when extracellular copper reaches peak levels during synaptic transmission and depolarisation of between 15 μM and 300 μM (Kardos et al. 1989). This copper may then be transferred back into the cells for recycling.

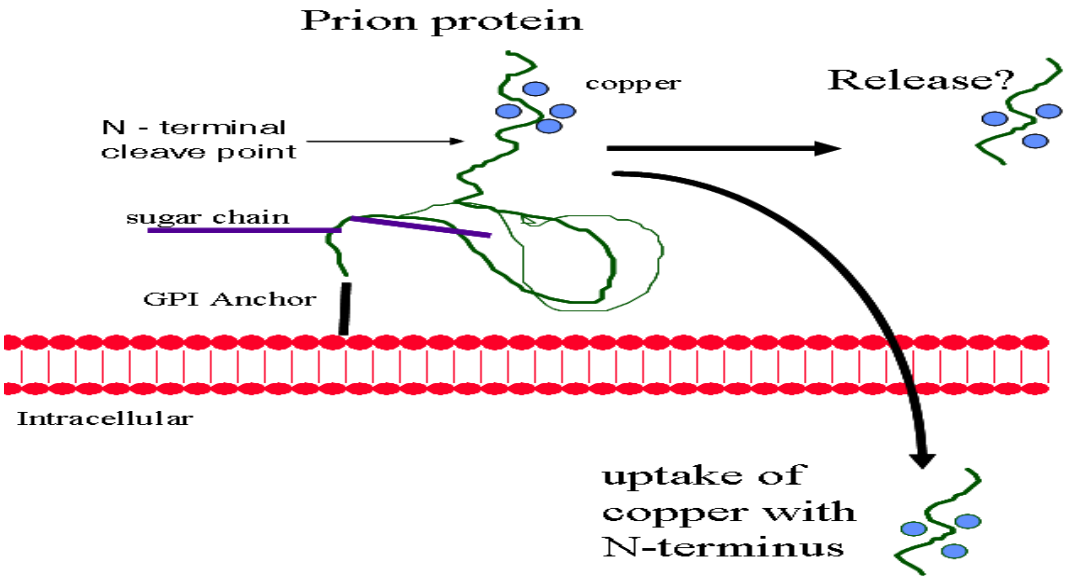

Figure 1.6 The majority of PrP synthesized by cells is anchored to the outside of the cell membrane by a GPI (glycosylphosphatidylinositol) anchor
The PrP may be bind copper before appearing at the cell surface or it might bind additional copper on reaching the cell surface. The turnover of PrP is very fast. The protein has a half-life of an hour or less. The primary question here is whether the protein is internalized on binding with copper or whether copper is transported from inside the cell to the extracellular environment for some catalytic role.

1.6 PrP Survival in the environment

Despite concerted efforts by many affected countries to eradicate the TSEs, it still remains a major problem. Clusters of outbreaks rule out spontaneous disease so this raises the question of where is the source of infection? A great deal of focus has been generated at the environment as a possible reservoir of infection, more specifically the soil that animals are exposed to when grazing (Leita *et al,* 2006). Certainly there is some evidence of sheep occupying grazing land that has previously supported infected animals becoming infected themselves (Greig, 1940). In addition, more modern, controlled studies have clearly shown infection from the environment (Hadlow *et al,* 1982; Miller *et al*, 2004). It is proposed that infectious prions may enter the soil via the disposal of infected carcasses, meat products or farm effluent (Gale and Stanfield, 2001). This is supported somewhat by evidence showing that the amount of material required for oral infection is very low, in the region of 10-100 mg of infected brain (Leita *et al,* 2006). Clearly a concern when considering that a single bovine brain would then contain enough material to infect around 2500 animals, although this would be dependent on factors such as genetic susceptibility and cross-species infectivity barriers.

A big question that is raised by this evidence is how could a protein exist in a stable form for extended periods in a hostile environment such as soil? One fascinating study even showed that some residual infectivity remained after three years in soil that had been exposed to infected material (Brown and Gajdusek, 1991). The study left many unanswered questions, however, as no information was given on how the prions were interacting with the soil or the precise conditions of the soil. Nevertheless, the study does show that prions can exist for long periods in environments that are normally hostile to proteins. Clearly, natural processes in the soil such a bacterial activity, exposure to UV radiation and soil acidity should be deleterious for even the most resilient organic material.

Interactions with metals may be able to contribute to the proteins stability and resistance against degradation. For example, it has been shown that manganese can cause PrP to fold into a proteinase resistant form (Brown et al. 2000). Certainly many metals exist within soils and it may therefore be possible that these interactions contribute to PrPs longevity in the environment. There is also some evidence of high manganese and low copper levels in areas of high scrapie incidence (Zucconi et al. 2007). The mechanism of protein adsorption on to soil particles is far from straight forward. Complicating factors include soil pH and constituents and protein PI, conformation, size, charge, solubility and flexibility (Stumm et al. 1992; Norde and Giacomelli 2000). There have been many studies of soil/protein interaction, especially with constituent clays such as kaolonite and montmorillonite (mte). One study (Servagent-Noinville et al. 2000) showed the importance of electronegative interactions in the adsorbance of bovine serum albumin (BSA) onto mte and how the strength of these interactions could alter the conformation and properties of the protein. Other studies have shown specifically the very strong adsorpative nature of soil clays to proteins, especially prions. One study, (Genovesi et al. 2007) for example, demonstrated the difficulty in deadsorbing prions from clay, especially mte and suggested that the conditions in most soils would favour an accumulation of stable prions in soils exposed to contaminated material. Another such study confirmed this and went further to suggest that mte would promote an orientation of PrP towards the soil involving elements across the entire protein in both the N and C terminus, making the adsorption almost irreversible in it's strength (Revault et al. 2005). One recent study looked specifically at the disease isoform PrP^{sc} and concluded that it was able to adsorb to many different types of soil/clay and remain

infectious following deadsorption, even if it's removal caused cleavage of the protein (Johnson et al. 2006).

1.7 Aims

The overriding aim of this study is to investigate the association of metals, especially copper, with PrP. This is achieved through the application of new and innovative techniques to address the inconsistencies within the literature. Using thermodynamic and electrochemical procedures, along with more traditional biochemical techniques, the stoichiometry, affinity and redox properties of PrP are fully qualified and quantified. Existing techniques are optimised and new methods of data analyses are evaluated. Additionally, new methods of electrochemical analysis are employed.

The purpose of such a study is to address two specific questions. Firstly, is it possible to elucidate a role for copper in normal PrP function? As indicated in this introduction, it is not possible to assign a likely function to PrP with such enormous variation within the literature surrounding copper binding. Secondly, is the proteins association with metal significant to its ability to survive in the environment? Such information could be key to understanding the transmission of infection amongst affected species.

CHAPTER TWO

General Methods

Unless otherwise stated, all reagents were purchased from Sigma-Aldrich (Poole, Dorset) and were of analytical grade

2.1 Recombinant Protein Production

2.1.1 Materials

Plasmid Constructs

pET vectors were supplied by Novagen (Nottingham). A vector map for pET 23a+ is shown in appendix A

PCR Mutagenesis

Restrictions enzymes, dNTP's and assay buffers were supplied by New England Biolabs (Hitchin, Hertfordshire).

Primers were produced by MWG (Germany).

PWO polymerase was purchased from Roche (Welwyn Garden City, Hertfordshire).

Transformations

E.coli XL2 strain were supplied by Stragene (Cedar Creek, Texas).

LB broth, agar and Carbenicillin were supplied by Melford (Ipswich, Suffolk).

All sequencing reactions were undertaken by Gene service (Cambridge, UK).

DNA purification

All DNA purifications kits were purchased from QIAGEN (Crawley, West Sussex).

Agarose Gel Electrophoresis

10 x Bluejuice loading dye and 1 kb gene ladder was from Invitrogen

Agarose and ethidium bromide was supplied by Melford

Protein Expression and Purification

Urea/carbamide, agar, Tris, phenylmethanesulphonylfluoride (PMSF) and carbenicillin were all obtained from Melford (Ipswich, Suffolk).

Isopropyl β-D-1-thiogalactopyranoside (IPTG) was obtained from Apollo Scientific (Stockport, England).

Chelating sepharose and C10 gravity columns were purchased from GE healthcare (Chalfont St Giles, Buckinghamshire).

Ultra filtration equipment, including filters, was from Millipore (Watford, Hertfordshire).

Dialysis membrane was obtained from Medicell (London, England)

EDTA from Fisher (Loughborough, Leicestershire)

Triton X from Fisher

Igepal 50

Sodium Chloride

Copper (II) sulphate penta hydrate

Protein Determination

BCA Reagent

Copper (II) sulphate

Bradford reagent

Bovine serum albumin (BSA)

2.1.2 Cloning and mutagenesis

The construct for wildtype mouse PrP was provided by Andrew Thompsett, University of Bath. The construct (mPrP 23-231) encodes for the full expressed mouse prion protein with the signal peptide (sequence 1-22) and the glycosylphosphatidylinositol (GPI) anchor (sequence 232-254) removed. The original construct was produced as previously described (Cui et al. 2003) and cloned into a pET 23(+) a expression vector. The sequencing data for the wildtype construct is listed in appendix A.

A PCR based mutagenesis reaction was carried out on wild type mPrP constructs using the standard protocol as supplied by Novagen. Paired oligonucleotide primers were designed and constructed to replace histidine residues within the octarepeat and 5th site

regions with alanine, an amino acid considered to have no copper binding characteristics when present within a peptide and with all amino groups occupied. Table 2.1 lists the primer designs used.

Table 2.1 The primers designed for mutating primer copper binding sites on mouse PrP.

H60 to A60 For	5'–GGGGCAGCCCGCCGGTGGTGGCTG–3'
H60 to A60 Rev	5'–CAGCCACCACCGGCGGGCTGCCCC–3'
H68 to A68 For	5'–GGGACAACCCGCTGGGGGCAGCTGG–3'
H68 to A68 For	5' –CCAGCTGCCCCCAGCGGGTTGTCCC–3'
H76 to A76 For	5'–GGGGACAACCTGCTGGTGGTAGTTGGGG– 3'
H76 to A76 For	5' –CCCCAACTACCACCAGCAGGTTGTCCCC– 3'
H84 to A84 For	5' –GGGTCAGCCCGCTGGCGGTGGATG– 3'
H84 to A84 For	5' –CATCCACCGCCAGCGGGCTGACCC– 3'
H95 to A95 For	5'–GGAGGGGGTACCGCAAATCAGTGGACCAAG-3'
H95 to A95 For	5'–GCTTGTTCCACTGATTTTGCGTACCCCCTCC–3'
H110 to A110 For	5'–CCAAAAACCAACCTCAAGGCAGTGGCAGGGGC–3'
H110 to A110 For	5'–GCCCCTGCCACTGCCTTGAGGTTGGTTTTT–3'

In each case, the histidine at the locations shown is mutated to alanine, an amino acid known to have no copper binding characteristics when within a peptide.

Solutions containing 120 ng of DNA per ml of nuclease free ddH_2O were prepared for each forward and reverse primer. 1.25 µl of forward and reverse primer solution were then added to a reaction mixture containing 5 µl 10x reaction buffer (100 mM Tris-HCl pH8.8, 250 mM KCl, 20 mM $MgCl_2$, 50 mM $(NH_4)_2SO_4$), 5 µl plasmid DNA, 1 µl dNTP mix, 1 µl PWO polymerase and nuclease-free ddH_2O to a final volume of 50 µl. The reaction was then carried out in a Hybaid thermal cycler.

The PCR program consisted of a melting stage of 30 seconds at 95 °C followed by 12 cycles of 30 seconds at 95 °C, 1 minute at 55 °C and 30 minutes at 72 °C. On completion, 1 µl of Dpn 1 (10 U/µl) restriction enzyme was added to digest template DNA and the reaction mixture incubated at 37 °C for 1 hour.

2.1.3 Transformations

Transformations were then carried out using E.coli XL2 amplification strain. 5 µl of product from the mutagenesis reaction was incubated with 20 µl of E.coli XL2 bacteria for 30 minutes on ice. After a 45 second heat shock at 42 °C the transformation mix was incubated on ice for a further 2 minutes and 450 µl of LB broth added. The mixture

was then incubated at 37 °C shaking at 200 rpm for 30 to 45 minutes. The transformation mixture was then spread onto 6 % agar/LB plates containing 50 µg/ml carbenicillin, to allow for selection of transformed colonies. Individual colony forming units (CFU's) were then cultured in LB broth overnight.

2.1.4 DNA Purification

Plasmid DNA was harvested by DNA miniprep as per the standard protocol. Overnight cultures from individual CFU's were spun down at 4000 rpm for 5 minutes to pellet the cells. The cell pellet was then resuspended in 250 µl of buffer P1 containing RNase A and transferred to 1.5 ml eppendorf tubes. 250 µl of lysis buffer P2 was then added and the tube inverted several times to mix. The lysis was then arrested by the addition of 350 µl of neutralisation buffer N3 and mixed by inversion several times. Tubes were then centrifuged at 13000 rpm for 10 minutes in a micro centrifuge. The supernatant was collected and run over a miniprep spin column at 13000 rpm for 1 minute. After discarding the flow through, the column was washed in 750 µl ethanol wash buffer before the DNA was eluted in 50 µl elution buffer.

2.1.5 Agarose Gel Electrophoresis

In order to determine whether mutagenic amplification of the target plasmid was successful, samples from the mini prep were submitted to agarose gel electrophoresis. 2 µl of sample was loaded onto a 0.8 % agarose gel, made with TAE buffer (40 mM Tris, pH 8, 20 mM glacial acetic acid, 1 mM EDTA) containing 0.5 µg/ml ethidium bromide. The gel was elctrophoresed using a BioRad gel tank and power pack at 110 volts, 400 mA for 45 minutes. Gels were then imagined under UV light.

Purified plasmids were then sent for sequence analysis. Successfully mutated constructs were then used to transform E.coli BL21 expression strain. Table 2.2 lists all the mutants targeted for construction with the number and location of copper binding sites available.

2.1.6 Protein Expression

Figure 2.1 shows a schematic representation of the entire protein production method.

Table 2.2 The mPrP copper binding mutants targeted by site directed mutagenesis compared with wildtype mPrP.

	Number of copper sites*			Number of copper sites*	
Protein¥	Octarepeat	5th Site	Protein¥	Octarepeat	5th Site
Wildtype	4	2	H60,68,76,84A	0	2
H95A	4	1	H60,68,76,84,95A	0	1
H110A	4	1	H60,68,76,84,95,110A	0	1
H95,110A	4	0	H60,95,110A	3	0
H60A	3	2	H68,95,110A	3	0
H68A	3	2	H76,95,110A	3	0
H76A	3	2	H84,95,110A	3	0
H84A	3	2	H60,68,95,110A	2	0
H60,68A	2	2	H60,76,95,110A	2	0
H60,76A	2	2	H76,84,95,110A	2	0
H76,84A	2	2	H60,84,95,110A	2	0
H60,84A	2	2	H68,76,95,110A	2	0
H68,76A	2	2	H60,68,76,95,110A	1	0
H60,68,76A	1	2	H60,68,84,95,110A	1	0
H60,68,84A	1	2	H68,76,84,95,110A	1	0
H68,76,84A	1	2	H60,76,84,95,110A	1	0
H60,76,84A	1	2			

* Denotes the number of potential copper locations based on the accepted theory of one copper per histidine residue

¥ Proteins are listed by the location of the histidines targeted for mutation to alanines

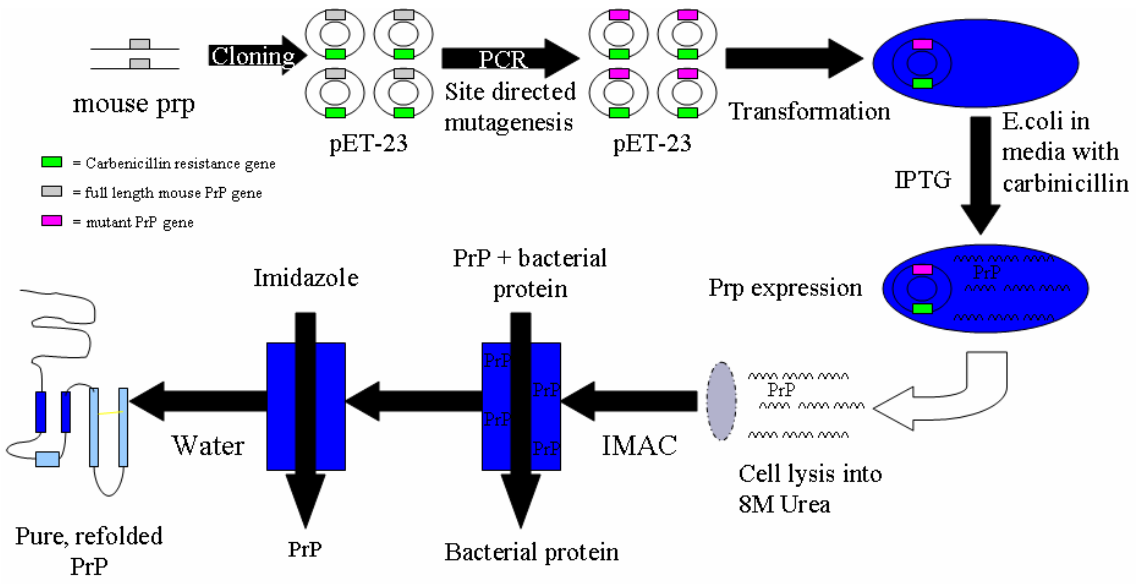

Figure 2.1 Schematic of the production and purification of recombinant mouse PrP. The gene for wildtype mPrP is cloned into pET-23 expression vector and site directed mutagenesis carried out in-situ. Protein is then expressed in BL21 E.coli and recovered from inclusion bodies by sonication in urea. Immobilised metal affinity chromatography is then used to separate the strongly copper binding PrP from bacterial proteins. Water is then added to dilute out the urea and allow the protein to refold to the most thermodynamically favourable state. Repeated dialysis is then used to remove all contaminating material

Protein production was based on a previously published method (Brown *et al*, 2000). The transformation products were used to inoculate overnight cultures containing 50 μg/ml carbenicillin. Flasks containing 1L LB broth and carbenicillin (50 μg/ml) were then inoculated with the BL21 cultures and incubated for 2-4 hours shaking at 37°C until optical density readings at 600 nm indicated exponential growth. Protein expression was then induced by the addition of IPTG to a final concentration of 1 μM. After a further 4 hours, the BL21s were harvested by centrifugation at 6000 rpm for 10 minutes.

Cell pellets were resuspended in lysis buffer (200 mM Tris-HCL pH 7.6, 1 mM EDTA, 150 mM NaCl) and PMSF added to prevent degradation by serine proteases. Lysis was achieved enzymatically using chicken egg white lysozyme (4 mg/ml lysis buffer), sodium deoxycholate (4 mg/ml lysis buffer) and DNase (20 μg/ml lysis buffer). The recombinant protein product was released as insoluble inclusion bodies.
Two different methods were then were employed to purify the protein from the inclusion bodies. For all proteins where at least 2 copper binding sites remained, purification method A was employed. For all other proteins, method B was adopted.

2.1.7 Purification Method A

Inclusion bodies containing protein that was expected to have a high affinity for copper were first washed 6 times in lysis buffer and pelleted by centrifugation at 10000 rpm for 20 minutes. The pellet was then solublised in binding buffer (8 M urea, 200 mM Tris-HCl pH 7.6, 150 mM NaCl) by sonication for 3 minutes at 80% power and filtered through 0.45 μm membrane. A 5 ml immobilised metal affinity column (IMAC) was then prepared by charging it with 0.3 M copper sulphate solution before washing with 5 bed volumes of distilled water, pH 7 to remove any unbound copper. The column was then equilibrated with binding buffer before applying the protein. Impurities were washed from the column with binding buffer until the absorbance at 280 nm was 0. The protein was then eluted with a binding buffer solution containing 300 mM imidazole.

2.1.8 Purification Method B

Inclusion bodies containing protein that was not expected to bind copper with high affinity were purified by a wash method developed from a protocol used in our lab.

Lysed cellular material was centrifuged at 10000 rpm. for 20 minutes. The pellet was then washed 6 times in wash buffer A (1 mM EDTA, 200 mM sodium chloride, 200 mM Tris pH 7, 0.5 % Triton X and 1% Igepal), with sonication at 30 % power in between. The pellet was then washed 6 times in wash buffer B (1 mM EDTA, 200 mM sodium chloride, 200 mM Tris pH 7, 0.1 % Triton X), with further sonication at 3 % power. The pellet was then washed 6 more times in a lysis buffer and then solubilised in binding buffer by sonication at 80 % power for 3 minutes.

2.1.9 Protein Refolding and Concentration

Purified protein was first checked for purity by submitting it to SDS-page analysis. The protein was then refolded in water by adding small amounts of milliQ water pH 7 until precipitation occurred. After removal of the precipitation by centrifugation, more water was added until a dilution factor of 10 had been achieved. All protein was then dialysed repeatedly against 10 l of Chelex treated MilliQ water for a minimum period of 6 hours and until > 1000000 fold dilution had been achieved. Chelex resin is a chelator with a very high affinity for copper, thereby ensuring that no free copper could contaminate the protein. Proteins were then concentrated to either 10 μM, 12 μM, 15 μM, 20 μM or 30 μM, by passing them through an Ultrafiltration cell with a 10 kDa filter fitted at 4.5 times atmospheric pressure. Protein concentration was confirmed by BCA assay, Bradford assay and absorbance at 280 nm using a molar extinction coefficient of 62250 (Expassy). Samples were then frozen at -80 °C in 3ml aliquots ready for analysis.

2.1.10 Determination of Protein Concentration

2.1.10.1 BCA assay

Triplicate protein standards of 0 to 1 mg/ml bovine serum albumin (BSA) in 0.1 mg/ml intervals were prepared using MilliQ water to 50 μl. For each protein of interest, 50 μl samples were also prepared. BCA(bicinchoninonic acid) reagent and 4 % (w/v) copper (II) sulphate were mixed to a ratio of 50:1 respectively. 1 ml of this solution was then added to each of the standards and samples, vortexed and incubated at 37 °C for 30 minutes. The solutions were then transferred to plastic cuvettes and spectrographically analysed at 562 nm in a Cary UV Vis spectrophotometer. From the standards, a

calibration curve was calculated and used to determine the protein concentration of the samples.

2.1.10.2 Bradford Assay

Triplicate protein standards of 0 to 1 mg/ml bovine serum albumin (BSA) in 0.1 mg/ml intervals were prepared using MilliQ water to 10 µl. For each protein of interest, 10 µl samples were also prepared. Bradford reagent was then diluted 5 fold n MilliQ water. 1ml of this solution was then added to each of the standards and samples, vortexed and incubated at 25 °C for 5 minutes. The solutions were then transferred to plastic cuvettes and spectrographically analysed at 595 nm in a Cary UV Vis spectrophotometer. From the standards, a calibration curve was calculated and used to determine the protein concentration of the samples.

2.2 Protein Purity and Identification

2.2.1 Materials

2D Gels

30 % acrylamide protogel from Fisher
1.5 M Tris pH 8.8
Ammonium Persulphate (APS) from Melford
N,N,N,N – Tertamethylethylene-diamine (TEMED)
Glycerol from Fisher
Tris from Melford
Bromohphenol blue
B-mercaptoethanol
Sodium Dodecyl Sulfate (SDS) from Melford
Glycine
Coomassie brilliant blue
Methanol from Fisher
Glacial acetic acid

Western Blotting

Methanol supplied by Fisher
Marvel dry semi-skimmed milk

PVDF membrane – Millipore (Watford, UK)
Blotting paper (Fisher)
Tween 20
ICMS-18 C-terminal mPrP antibody
8B4 N-terminus mPrP antibody
Goat anti mouse HRP secondary antibody from DAKO (ELY, UK)
ECL reagent supplied by Millipore
Hyperfilm XL – Amersham (Bucks, UK)

2.2.2 SDS 2D Gel Electrophoresis

Samples for analysis were mixed with 4 x Loading Dye (For 10 mls : 4 ml glycerol, 2 ml 1.5 Tris pH 6.8, 0.4 ml 0.5 % bromohphenol blue, 0.4 g (4 % w/v) SDS, 200 mM B-mercaptoethanol, ddH_2O to 10 ml) to a ratio of 1:3 respectively.
Gels, (12%) were prepared by mixing 2.3 ml ddH_2O, 2.8 ml 30 % acrylamide, 1.75 ml 1.5 M Tris (pH 8.8), 70 µl 10 % SDS, 70 µl APS, 7 µl TEMED and pouring this mixture into ATTO (USA) plates and allowed to set. A protein stacking layer was then added to the top of this gel by pouring on a mixture containing 1.18 ml ddH_2O, 260 µl 30 % acrylamide, 0.5 ml 1.5 M Tris (pH 8.8), 40 µl 10 % SDS, 20 µl APS, 2 µl TEMED. A 12 well comb was then set in this stacking layer to create wells for the sample. Protein samples were then loaded into the wells and the gel immersed in a ATTO gel tank containing running buffer (For 1 L of 10x : 188 g Glycine, 30.2 g Tris, 100 ml 10 % SDS to 1 L with ddH_2O) and electrophoresed for 55 minutes at 35 mA and 250 V.

Following electrophoresis, gels were removed from the apparatus and immersed in Coomassie stain (For 100 ml : 0.25 g Coomassie brilliant blue, 45 ml Methanol, 45 ml ddH_2O, 10 ml acetic acid) for 1 hour. They were then destained in a destain buffer containing 170 ml acetic acid and ddH_2O for 24 hours.

2.2.3 Western Blotting

Protein immobilised within the 2D gel was transferred to a PVDF membrane by a semi-dry transfer method. Blotting paper was soaked in transfer buffer (500 ml 1 x running buffer, 200 ml methanol and 300 ml ddH_2O). PVDA membrane (pre-soaked in

methanol) was placed on top of the blotting paper with the 2D gel placed on top of this. A final piece of blotting paper was placed on top. The transfer was run for 90 minutes at 50 mA, 25 V using a Bio-Rad semi-dry blotter. The membrane was then blocked in tris buffered saline containing 0.1% (v/v) Tween and 5% (w/v) (TBS-T) milk powder for 1 hour, shaking. Membranes were probed with either ICMS-18 or 8B4 monoclonal mPrP primary antibody. After rinsing the membrane in TBS-T 3 times, the antibody was diluted 15000 times in TBS-T containing 5 % milk powder overnight at 4 ºC overnight. The membrane was then washed again in TBS-T 5 times before being incubated to secondary HRP antibody, again diluted 15000 times in TBS-T containing 5 % milk powder for 45 minutes at room temperature. Following extensive washing in TBS-T, the membrane was developed for 2 minutes with ECL reagent and exposed to film for between 15 seconds and 30 minutes. A Compact X-ray processor was used to develop the film. The relative amount of protein present on the blot was quantified using the densitometer function in Adobe Photoshop.

2.3 Isothermal Titration Calorimetry

2.3.1 Materials

Copper (II) sulphate anhydrous

Copper (II) sulphate pentahydrate

Manganese sulphate

Zinc sulphate

Nickel sulphate

Iron (II) sulphate

MES hydrate

Sodium acetate

MOPS

HEPES

Tris and Glycine from Melford

2.3.2 Procedure

Proteins for calorimetric analysis were dialysed against buffer to achieve the target pH for the study. For pH 4-5.5, 10mM sodium acetate was used. For pH 5.5 to 7, 10 mM MES was used and for pH > 7, 10 mM Tris or HEPES was chosen. All protein solutions

were filtered through a 0.22 µm membrane and degassed thoroughly in a vacuum chamber before use. Metal solutions were prepared by dissolving the metal sulphate salt in milliQ water and then buffered with the appropriate buffer (as above). In the case of Cu^{2+}, the metal was chelated to either a 2 or 4 fold molar excess with glycine. At pH ≥ 5, copper remains insoluble, forming hydroxide species and forming precipitant. When chelated to an amino acid, this problem is overcome and the metal can be delivered in a predictable and quantifiable way to the protein.

ITC experiments were carried out on a Microcal VP-ITC (Milton Keynes, England). Figure 2.2 shows a diagram of the equipment used. A series of 30 x 4 µl injections of buffered metal or buffered metal chelate were made into an isolated chamber containing 1.2 ml of buffered protein at various concentrations at a constant temperature of 25 °C. A space of 2 minutes was allowed between injections to ensure equilibration between reactants. The reaction cell was stirred at a constant speed of 300 rpm.

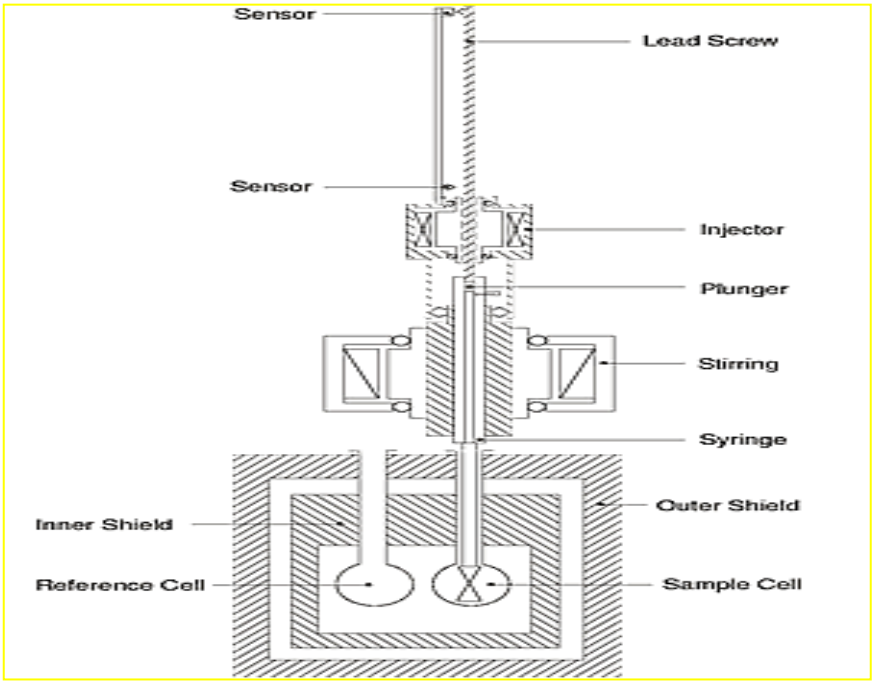

Figure 2.2. Diagram of the MicroCal VP-ITC. The protein for analysis is injected into the sample cell and the metal ligand drawn into the syringe. A small amount of sample buffer is then injected into the reference cell, in order to provide a reference temperature for the machine to equilibrate with after each injection. The chamber is shielded from the outside environment by a double casing. The syringe is then locked into place over the sample cell and set to stir the sample at 300rpm. After a period of time to allow the entire system to equilibrate, the plunger descends and releases a fixed amount of metal into the sample chamber. Any change in heat is then recorded and the system re-equilibrates in preparation for the next injection.

Heat changes within the cell were monitored during each injection of metal and recorded as the total heat change per second over time. A binding isotherm was then fitted to data and expressed as heat change per mole of metal against the metal to protein ratio. For each protein and for each condition, at least 3 runs were carried out to ensure reproducibility. Between each run, the chamber was thoroughly washed with at least 10 chamber volumes of MilliQ (Millipore, England) water and the syringe rinsed thoroughly again with at least 10 volumes of MilliQ water.

From the isothermic data, a regression model was used to predict the number of binding sites on the protein involved in the reaction, the association constants of the binding (Ka) and the change in enthalpies (ΔH). These models are discussed further in chapter 3. The choice of buffers was based on initial trials which revealed that these buffers offered the minimum of background noise. Each experimental condition had a blank run with protein in the chamber replaced with buffer. This data was then subtracted from the run with protein present to take into account any energy of dilution or metal/buffer reaction.

2.4 Cyclic voltammetry

2.4.1 Materials

Reference electrode supplied by Radiometer, (Denmark).
5 mm diameter edge plane pyrolytic graphite Pyrocarbon by Le Carbon, (UK)
3 mm diameter boron-doped diamond by Windsor Scientific, (UK).
Micro cloths and 1 micron alumina supplied by Buehler (UK).
Nitrogen (BOC, UK)

2.4.2 Method

Voltammetric measurements were conducted with a μ-Autolab III potentiated system (Eco Chemie, The Netherlands) in a conventional three-electrode electrochemical cell. Figure 2.3 shows the cyclic voltammetry equipment set-up. Experiments were performed in staircase voltammetry mode with platinum gauze counter and saturated calomel reference electrode (SCE, REF401).

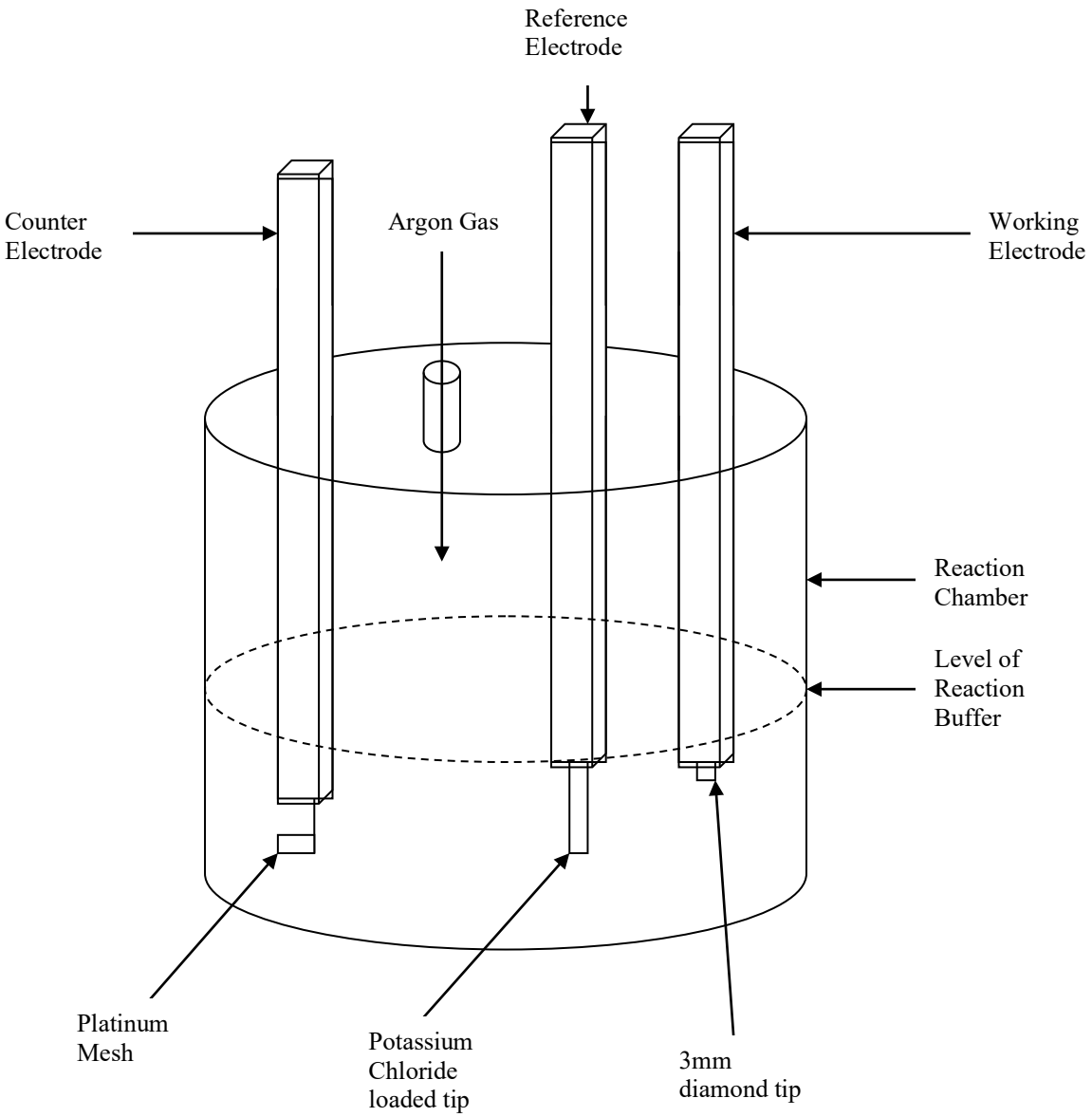

Figure 2.3 The cyclic voltammetry set-up. A current is passed into the system via the counter electrode. The voltage is increased and then decreased over a range pre-determined at the start of the experiment. Protein is adsorbed onto the diamond surface of the working electrode, where electrons leaving or entering the anaylate can be detected. The reference electrode has a tip saturated with potassium chloride and thus a constant potential is known throughout the experiment. The chamber is kept saturated with argon to ensure that no oxygen is present. (Bard and Faulkner 1980)

The working electrodes used were 5 mm diameter edge plane pyrolytic graphite or 3 mm diameter boron-doped diamond. Electrodes were polished on fresh micro cloths with alumina as polishing aid. After the final polish on a clean micro cloth, electrodes were rinsed with demineralised water. Aqueous solutions were thoroughly de-aerated with nitrogen prior to recording data. All measurements were undertaken at 22 ± 2 ºC.

Voltammetric measurements were conducted in aqueous buffer solution (5 mM MES at pH 5.5 or 5 mM HEPES pH 7) thoroughly de-aerated with nitrogen. Voltammetric sweeps were generally from a 0 start potential to +450 mV and then reversed to -450 mV. The working electrode was polished and the background current recorded in the absence of protein. Next, the working electrode was immersed into a protein solution (containing 20 µM recombinant mPrP in buffer) and after 60 seconds removed and rinsed with water. The resulting protein-modified electrode was re-immersed into the pure buffer solution in the measurement cell and cyclic voltammograms were recorded.

2.5 Mass Spectrometry

Mass spectrometry was carried out on a Bruker ESI-Mcro-TOF I. Samples of protein at a concentration of 1mg/ml were injected into the electrospray ionisation chamber (esi) using a mix of 70 % acetonitile 30 % milliQ water and at a flow rate of 50 µl min. All measurements were carried out in positive ion reflectron mode with a mass/charge (m/z) range of 800-3000. Deconvolution software supplied by Bruker was used to fit likely exact masses to the mass/charge peaks evident.

2.6 Circular Dichroism

Circular Dichroism (CD) measurements were recorded on an Applied Photophysics Chirascan instrument (London, England) at 25 °C. The cell containing the sample, typically 0.1mg/ml, had a path length of 1mm and was thoroughly cleaned and rinsed in water before being dried in the presence of acetate. Spectra were recorded in the near UV with a range of 180 nm to 260 nm. Sampling points were taken every 0.5 nm and at least 3 scans were recorded and averaged for each condition. A baseline spectra for buffer alone was recorded and subtracted from sample runs. Data was processed using the Applied Photophysics Chrirascan Viewer and transferred to Microsoft Excel for plotting and interpretation. The direct CD measurements in millidegrees (θ) were converted to molar ellipticity ($\Delta\varepsilon$ in M^{-1} cm^{-1}) using the relationship $\Delta\varepsilon = \theta/33000.c.l$, where c is concentration and l is pathlength. For an approximation of alpha to beta sheet structure, CD-Pro software (Colorado State University, Fort Collins, Colorado). The modules used were CDSTTR, CONTINLL and SELCON 3 all using protein reference set SP29 (Johnson 1999).

2.7 Cell Culture

2.71 Materials

SMB and SMB-PS cell lines were from a laboratory supplied line

Dulbecco's modified eagles media (DMEM) from Lonza (Berkshire, UK)

Foetal bovine serum (FBS) from Lonza

Trypsin-EDTA from Lonza

2.72 Method

Cells were maintained at 37 ºC and 5 % CO_2 in a humidified incubator. Cells were cultured in DMEM supplemented with 10 % FBS in 75 ml culture flasks. Following achievement of 95% confluency, cells were split 1 in 4 to ensure continued health. This was carried out by aspirating off the used media and releasing the cells by digestion with 2 ml trypsin for 5 minutes at room temperature. Trypsin was then inactivated by the addition of 10 ml fresh media and the cells divided into 4 fresh flasks.

CHAPTER THREE

Isothermal titration calorimetry regression model development

Isothermal titration calorimetry (ITC) is a key biochemical tool in the analyses of metal – ligand interactions. Over the last decade, it has been used with increasing frequency to obtain key data on the enthalpy and stoichiometry of small molecule interactions with proteins and macromolecules of interest (Liang 2008) . Since an understanding of metal associations with proteins are often important to understand their physiological roles, a key use of ITC has been to fully characterise these interactions (Okhrimenko and Jelesarov 2008). ITC directly quantifies the change in the enthalpy of binding (ΔH) as the concentration of ligand [L] to metal [M] or metal to ligand changes in real time. This is achieved by either a series of titrations of L/M into M/L or one continuous titration. The overall change in enthalpy is recorded and from the slope of the isotherm, there is usually enough resolution to be able to determine the change in complex concentration. The enthalpy data itself is usually analysed via mathematical modelling systems based on previously published equations. For simple mode binding where one or more identical but independent sites are involved, the reaction can be described by a relatively straightforward cubic equation, and can be fitted by a least squares non linear regression routine (Lin et al. 1991). More complex cooperative systems, however, are analysed via a sequential model where the number of variables and inevitably uncertainties increase as the number of likely binding events increase.

A key problem in the study of the interactions of proteins with metal ions is that some, such as copper ions, are largely insoluble at physiologically relevant pH. Cu^{2+}, for example, tends to form insoluble hydroxide species at pH > 5. Other complications with the use of redox active metal ions can be the introduction of redox chemistry to the overall reaction. Cu^{2+} can catalyse Fenton chemistry (Halliwell and Gutteridge 1992) which contributes to the overall enthalpy in the reaction and can modify the target protein of interest. Additionally, the sensitivity of ITC is generally limited to the determination of binding constants from 10^3 to 10^8 (Wiseman et al. 1989). Another concern with using a free ionic metal such as copper is the tendency for non-specific

binding. The interaction of copper ions with proteins at multiple weak sites leads to complications in the interpretation of thermodynamic data. An approach that deals with all of these issues is to chelate the metal to a second entity capable of holding the ion until transfer to the target macromolecule, hence reducing the overall degree of enthalpy change, protecting against any oxidative effects and maintaining the total amount of metal in solution. This then, however, creates additional complexity in the interpretation of the isotherm. Several attempts have been made at creating methods and principles for the analyses of such data but all have centred on simple single site binding or multiple independent sites (Sigurskjold 2000; Zhang et al. 2000; Nielsen et al. 2003). These new approaches have centred on two different principles. The first approach has been to directly modify the equations used in the regression analysis before the fitting of the data. Wang first described a mathematical expression for competitive binding in 1995 (Wang 1995). Sigurskjold then produced a full method for the analyses of the thermodynamics of competing ligand binding which allowed for the quantification of binding outside the normal sensitivity of ITC (Sigurskjold 2000). Despite the key importance of this work, the method is limited to binding events whereby the number of sites on the target macromolecule is the same for both the target and competing ligand. Nielsen *et al* then adapted this method for the analyses of data from experiments involving a competing chelator (Nielsen et al. 2003). They designed a regression routine which overcame the previous stoichiometric limitations so the competing chelator could have a different number of sites than the target macromolecule. Again, however, the model is limited to simple independent site binding. This pre-regression modification approach was successful in describing the data. However, it is dependant on a clear distinction between when binding involving the competing metal/chelator saturates and the macromolecule of interest starts. The other approach used was pioneered by Zhang *et al* and attempted to account for buffer and chelator interactions post regression analysis (Zhang et al. 2000). They showed that they could successfully account for the effects of chelator on simple independent site binding.

These methods are useful only for simple, independent binding whereby one or two groups of sites facilitate binding events of identical stability and enthalpy of association. Many proteins of interest, however, do not conform to this assumption. Many metal/protein associations involve multiple binding events of varying stability and enthalpy and some display cooperativity between sites. Where such binding chemistry

exists, the use of the cubic root method is entirely inappropriate and leads to enormous error within the calculations of the enthalpy of binding and resultant stability constants. A regression model exists, however, whereby multiple sites of varying stability and cooperativity may be analysed. Microcal provide a sequential model regression package within the Origin architecture of their analyses system. The model assumes that each site on the ligand is filled sequentially either because of inter-site cooperativity or large differences in affinity between binding events. The correct use of this model for systems involving chelated metals, however, has yet to be defined. A set of principles for the treatment of more complex binding is therefore needed.

PrP has been previously reported to bind copper within its octarepeat region in a complex and cooperative manner (Walter et al. 2006). It is therefore critical that an approach be adopted for the analyses of this cooperativity when the ionic cooper is delivered in its chelated form. First, multiple potential chelators are evaluated for their suitability. Secondly, and based on previous attempts to address the chelation problem with simple mode binding, two methods have been developed to deal with the data. The first method (method A) involves adapting the 'sequential model' commonly used for the analyses of cooperative binding and incorporating the equations for the chelator species into the overall equilibrium. These equations are then solved iteratively using the circular reference facility in Microsoft's Excel. The second method (method B) uses the 'sequential sites' model directly, solving the equations via the Levenberg-Marquardt minimization routine in Origin 5. The resulting enthalpies and constants of binding are then used to solve equations for the overall reaction equilibrium to produce the final binding constants for the macromolecule of interest. A synthetic peptide of the 4 octarepeats of the prion protein is used to assess the suitability of the two methods.

3.1 The Mathematical Theory

3.1.1 Method A

Consider a macromolecule L with n sites for metal M chelated to C where each site on L is occupied sequentially by M. In this case, C is based on the amino acid glycine where two molecules of C are required for stable binding of a single molecule of M. In such an example, the binding constants $K_1, K_2 \ldots K_n$ are defined in order of the process

of saturation. The concentration of each species in the reaction can then be defined by equations 1, 2 and 3.

$$[\mathrm{L}] = \frac{[\mathrm{L}_t]}{(1 + K_1[\mathrm{M}] + K_1K_2[\mathrm{M}]^2 + K_1K_2K_3[\mathrm{M}]^3 + K_1K_2K_3K_4[\mathrm{M}]^4 + K_{1\ldots\ldots}K_n[\mathrm{M}]^n)} \quad (1)$$

$$[\mathrm{C}] = \frac{[\mathrm{C}_t]}{(1 + 2K_i[\mathrm{C}][\mathrm{M}])} \quad (2)$$

$$[\mathrm{L}] = \frac{[\mathrm{L}_t]}{(1 + K_i[\mathrm{C}]^2 + K_1[\mathrm{L}][\mathrm{M}] + 2K_1K_2[\mathrm{M}][\mathrm{L}]^2 + 3K_1K_2K_3[\mathrm{M}][\mathrm{L}]^3 + 4K_{1\ldots\ldots}K_n[\mathrm{M}][\mathrm{L}]^n)} \quad (3)$$

Where $[M_t]$, $[C_t]$ and $[L_t]$ are the bulk concentrations.

Then the fractional species can be defined by the equations 4

$$\begin{aligned}
[\mathrm{LM}] &= K_1[\mathrm{L}][\mathrm{M}] \\
[\mathrm{LM}_2] &= K_1K_2[\mathrm{L}][\mathrm{M}]^2 \\
[\mathrm{LM}_3] &= K_1K_2K_3[\mathrm{L}][\mathrm{M}]^3 \\
[\mathrm{LM}_n] &= K_{1\ldots\ldots}K_n[\mathrm{L}][\mathrm{M}]^n \\
[\mathrm{C}_2\mathrm{M}] &= K_i[\mathrm{C}]^2[\mathrm{M}]
\end{aligned} \quad (4)$$

Where the fractions $F_1, F_2 \ldots\ldots F_n$ can be defined by

$$\begin{aligned}
F_0 &= \frac{1}{X} \\
F_1 &= \frac{Ki[\mathrm{L}]}{X} \\
F_2 &= \frac{KiK_1[\mathrm{L}]}{X}
\end{aligned} \quad (5)$$

$$F_3 = \frac{KiK_1K_2[\mathrm{L}]^2}{X}$$

$$F_n = \frac{KiK_1K_2.....K_n[\mathrm{L}]^n}{X}$$

Where

$$X = 1 + Ki[\mathrm{L}]K_1[\mathrm{L}] + KiK_1K_2[\mathrm{L}]^2 + ... + KiK_1K_2...K_n[\mathrm{L}]^n$$

This can now be related to the total heat content within the reaction cell by equation 6

$$Q = L_tV_o(F_1\Delta H_1 + F_2[\Delta H_1 + \Delta H_2] + ... + F_n[\Delta H_1 + \Delta H_2 + ... + \Delta H_n) \quad (6)$$

Where V_o is the working volume of reactants in the cell.

After an allowance is made for the displaced volume as each injection is made into the cell, an iterative solution may be found from the initial guesses of *K* and *n* by using the circular reference facility in Excel.

3.1.2 Method B

As before, the binding constants K_n are defined relative to the process of saturation, as shown be equation 7

$$K_1 = \frac{[\mathrm{LM}]}{[\mathrm{L}][\mathrm{M}]} \quad K_2 = \frac{[\mathrm{LM_2}]}{[\mathrm{LM}][\mathrm{M}]} \quad K_3 = \frac{[\mathrm{LM_3}]}{[\mathrm{LM_2}][\mathrm{M}]} \quad K_n = \frac{[\mathrm{LM_n}]}{[\mathrm{LM}_{n-1}][\mathrm{M}]} \quad (7)$$

As all concentrations of bound species $[\mathrm{LM_n}]$ can be defined relative to unbound species [L] then the various fractions of L with n bound M can be defined by F_n in equations (8)

$$F_0 = \frac{1}{X} \quad F_1 = \frac{K_1[\mathrm{M}]}{X} \quad F_2\frac{K_1K_2[\mathrm{M}]^2}{X} \quad F_n = \frac{K_1K_2.....K_n[\mathrm{M}]^n}{X} \quad (8)$$

Where

$$X = 1 + K_1[\mathrm{M}] + K_1K_2[\mathrm{M}]^2 + ... + K_1K_2...K_n[\mathrm{M}]^n \quad (9)$$

The parameter n and K can now be assigned through trial and error, allowing equations 8 and 9 to be solved by the Bisection method. The total fractions can then be determined and related to the heat content Q after each titration of ligand by 10

$$Q = L_tV_o(F_1\Delta H_1 + F_2[\Delta H_1 + \Delta H_2] + ... + F_n[\Delta H_1 + \Delta H_2 + ... + \Delta H_n) \quad (10)$$

Using the same definitions as before. The effect of each injection i, allowing for a correction for the displaced volume after i is then defined by 11

$$\Delta Q(i) = Q(i) + \frac{dV_i}{V_o}\left[\frac{Q(i) + Q(i-1)}{2}\right] - Q(i-1) \quad (11)$$

Which is then submitted to the Levenburg-Marquardt minimization routine.
The values produced from this are then used in the total equilibrium for the reaction, including the chelator, and the final enthalpies and constants of binding are calculated using equation 12.

$$K_n = \frac{K_d(\mathrm{app})K_d(\mathrm{che})}{[\mathrm{che_{total}}]^2} \quad (12)$$

Where K_n is the actual stability constant for a given copper binding event, K_d(app) is the apparent value from the ITC data, K_d(che) is the stability constant relating to the chelator species and [che] is the concentration of the chelator species. Where the chelator species is a bis chelator, the value for K_d(che) is the β_2 value obtained by multiplying the 2 stability constants together.

3.2 The Thermodynamics of Free Ionic Copper Binding to PrP

In order to illustrate the difficulties in the use of free ionic copper in the thermodynamic determination of stability constants, unchelated copper was used as a direct titrant into

the ITC reaction cell. PrP octarepeat peptide (PHGGGWGQPHGGSWGQPHGGSWGQPHGGGWGQ) based on mouse PrP residues 51-89 was synthesized as previously described (Brown et al. 2000). The protein was dry weighed and dissolved in a 10mM HEPES buffer, pH 7 or 10 mM MES buffer pH 6 to a final concentration of either 25 or 50µM. All buffers used where prepared with Chelex resin treated milliQ water, filtered through a 0.22µm membrane. Figure 3.1 shows a thermodynamic trace for the titration of free ionic copper into mPrP at pH 7.

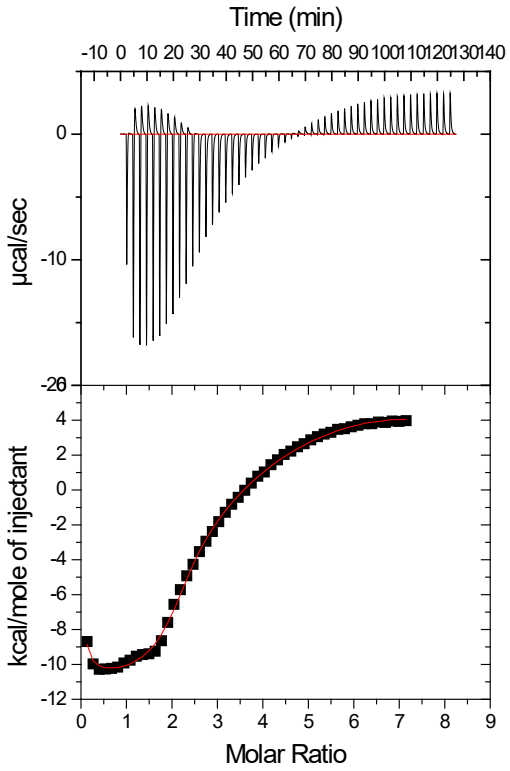

Figure 3.1 The isothermic trace from the titration of 4mM $CuSO_4$ into 50µM mPrP octa region pH 7. Both the titrant and protein is buffered at pH 7 with 20mM MOPS buffer and carried out at 25°C.

The isotherm begins with an endothermic reaction and rapidly switches to exothermic before reverting once again to endothermic at a molar ratio of 5:1 copper to protein. Such a variant trace makes analysis difficult and in fact no regression model could be confidently fitted to the data. The closest fit to the isotherm was a 7 site sequential model but errors exceeded 10% and were therefore deemed statistically uncertain.

By reducing or increasing the relative concentration of copper in each titration, in may be possible to reduce the endothermic effects of non specific binding. Figure 3.2

compares isotherms for both a high concentration delivery of copper and a low concentration delivery.

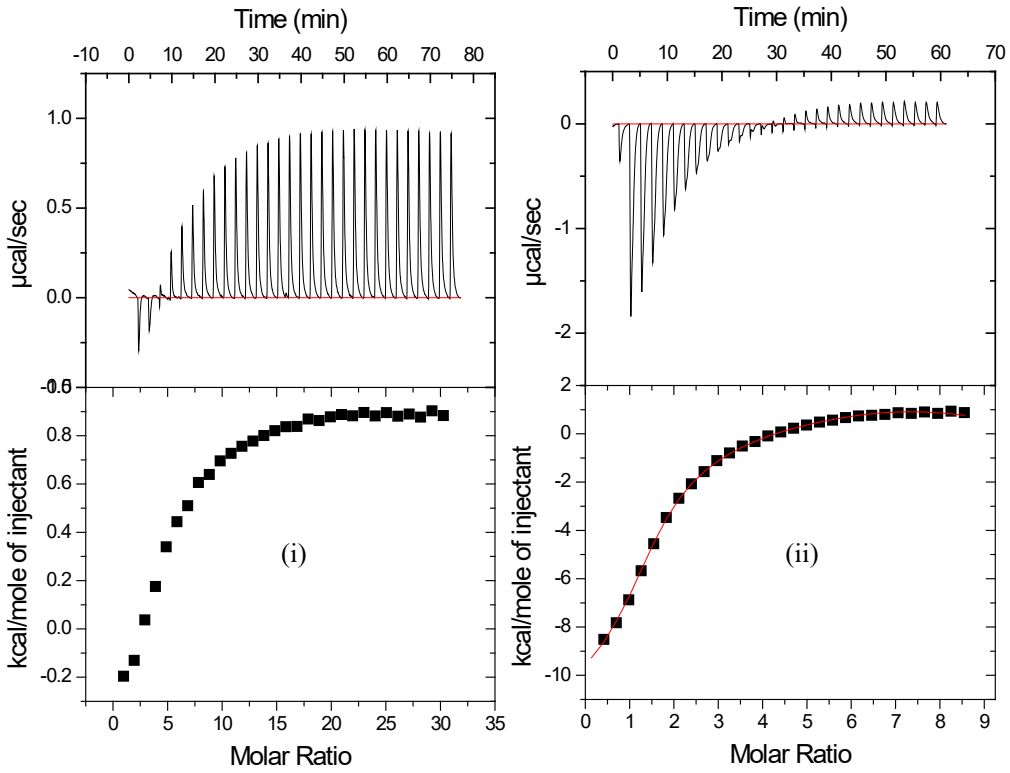

Figure 3.2 Isotherms for 50µM mPrP octarepeat region titrated with (i) 10mM $CuSO_4$ in 8µl injections and (ii) 2mM $CuSO_4$ in 2µl injections. Both reaction were buffered with 20mM HEPES pH 7 and carried out at 25°C.

The isotherm from (i) shows a far greater degree of endothermic character whereas (ii) is more exothermic overall. Both still show a mix of endo and exo thermicity. Neither isotherm is able to be analysed with a regression model within acceptable errors.

3.3 Evaluating Potential Chelators

The use of buffers and chemical reagents to chelate copper is well characterised within the literature (Martell and Smith 1974). Two well described chelators, Tris and EDTA were therefore used to deliver copper to the protein in the ITC reaction cell. These chelators were chosen due to their well reported affinity values and stoichiometry for copper. Tris binds Cu^{2+} in a $Cu[Tris]_4$ complex at pH 7 with a stepwise stability constant of log*K* 14.1. EDTA binds 1 molecule of copper with a log*K* of 18.8. Figure 3.2 compares isotherms for EDTA chelated copper and Tris chelated copper respectively.

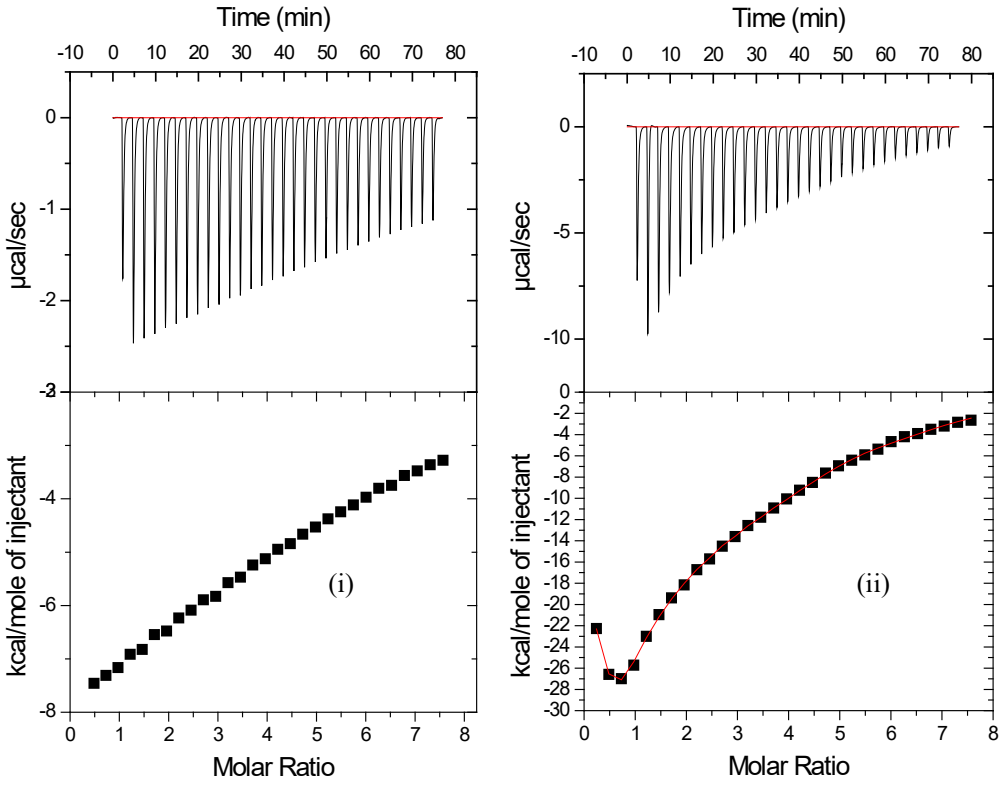

Figure 3.3 Isotherms for mPrP octarepeat region titrated with (i) 4mM Cu:EDTA in a 1:1 ratio and (ii) 4mM Cu:Tris in a 1:4 ratio. Both reaction are buffered with 20mM HEPES, pH 7 at 25°C.

The isotherm for the titrated copper chelated to EDTA (figure 3.3 (i)) shows no evidence of achieving saturation and as such is not able to be analysed. Figure 3.3 (ii) representing the titrated copper chelated to Tris does show evidence of reaching saturation. On analysis of the multiple repeats, however, large variation between calculated stability constants and even stoichiometry indicate a secondary interaction not accounted for in the predicted equilibria.

Another class of compounds known for their well characterised copper binding are amino acids. Figure 3.4 shows typical isotherms for chelated copper titrated into PrP octa region using various amino acids as chelators at pH 7, 25°C.

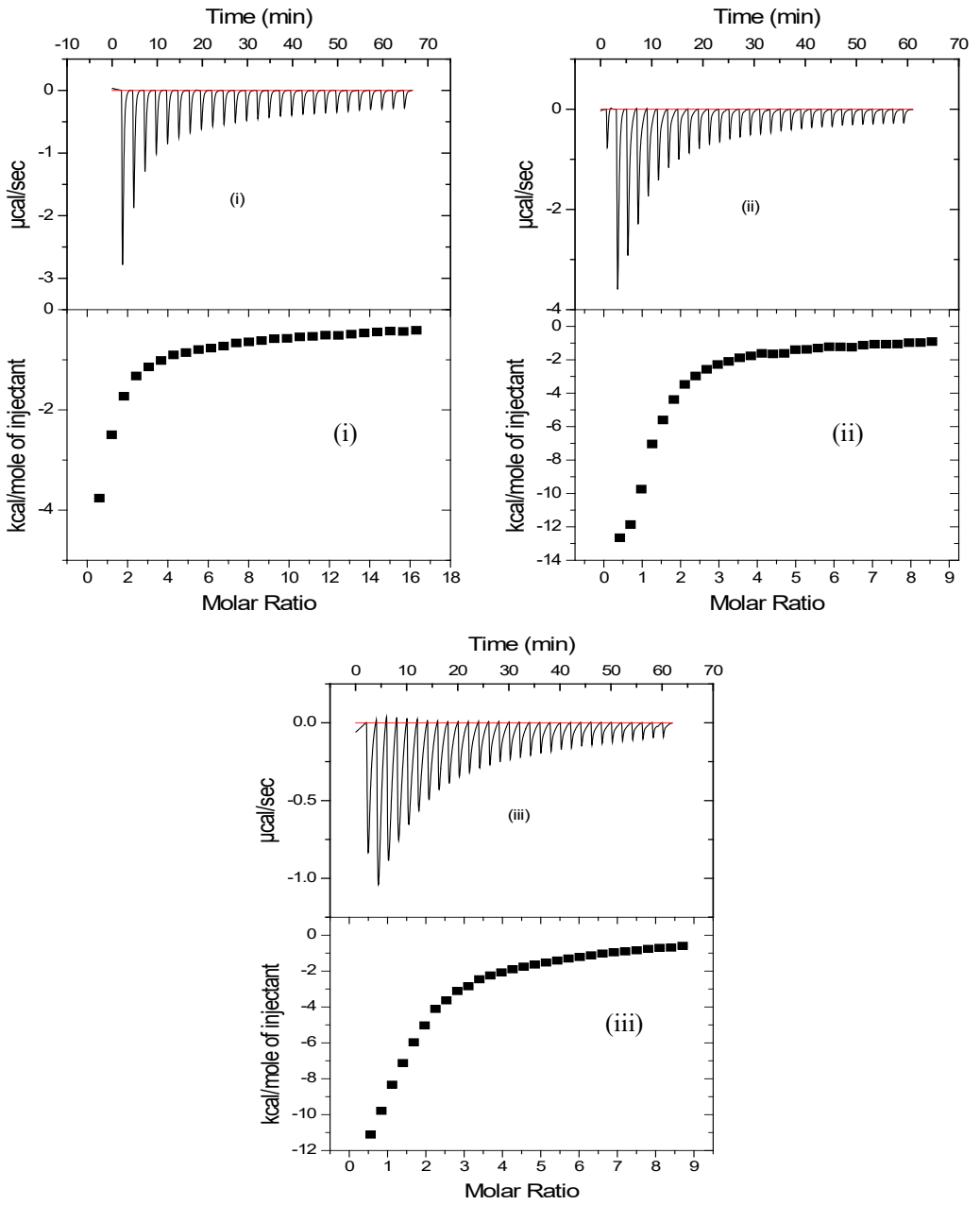

Figure 3.4 Representative isotherms for 20uM mPrP octarepeat region in HEPES pH 7 titrated with 2mM $CuSO_4$ in HEPES pH 7 chelated with (i) 4mM glycine, (ii) 4mM valine and (iii) 4mM tryptophan

Valine, tryptophan and glycine were chosen to obtain the data due to their different affinities for the ion. In each case, copper sulphate and the chelator were mixed and made up with the above buffers to a final metal to chelator molar ratio of 1:2. Typically, final concentrations of chelated metal were 2.5 or 5 mM. As with all chelator conditions tested, the titration of chelated copper into PrPocta resulted in a net exothermic reaction with a predictable transition to saturation. All isotherms are analysable by regression

analyses. All 3 amino acids are therefore considered suitable for the delivery of copper to the macromolecule of interest

3.4 Evaluation of the Two Methods of Regression

3.4.1 Method A Shows Variation Between Chelator Species

The stable and reproducible thermodynamic data produced when using amino acids as chelators enable the two theoretical regression methods to be evaluated. Table 3.1 presents the analysed data via method A for copper titrated into PrP octa region. For the chelator binding constants and enthalpies, the pH adjusted literature values were used (Martell and Smith), derived from the observation that where the pK_a of the acid used is more than one unit above the pH of the reaction, the log of the absolute stability constant K is reduced by logα where

$$\log\alpha = pK_a - pH \qquad (13)$$

and the log of the cumulative stability constant β_2 is reduced by 2logα and so on.

Table 3.1 The log *K* of affinities and the enthalpies of copper binding to PrPocta at pH 7 when using various amino acids as chelators and analysing the data by method A.

	Copper/Glycine into PrP octa		Copper/Valine into PrP octa		Copper/Tryptophan into PrP octa	
Binding Event	Log *K*	ΔH (Kcal/mole)	Log *K*	ΔH (Kcal/mole)	Log *K*	ΔH (Kcal/mole)
1	6.80	-21.80	6.90	-22.40	5.2	-21.90
2	6.30	-23.70	6.50	-25.80	3.8	-24.00
3	4.70	-15.60	4.70	-17.00	3.3	-15.80
4	4.50	-19.10	4.70	-21.30	3.2	-21.40
Total	22.30	-80.20	22.8	-86.50	15.5	-83.10

K values reported are pH dependent.The mean of three independent experiments were calculated, with errors between *K* values not exceeding 5%.

The residuals from fitting to the isotherm by least squares were used to calculate a χ^2 value for the best fit. In all cases, a 4 site sequential model best described the data, although it should be noted that the χ^2 difference between 4 and 3 or 5 sites was only 1.5% and 2.9% respectively. This represents a statistical uncertainty within values derived from so many variables. Additionally, *K* values varied significantly depending on what chelator was used, with calculated values for the overall equilibrium ranging from log*K* 22.8 for copper chelated to valine to log*K* 15.5 for the tryptophan chelate.

Different approaches with this method were then made by adjusting the way the equilibrium equations were processed in Excel. For example, the fractional species (F_1 *to* F_n) were defined more directly with reference to the bulk species, as detailed in method B. Despite this, the values remained similar, as did the variation between chelator species. Additionally, the statistical differences between model fits remained too low. This approach is therefore unsuitable for complex binding determination.

3.4.2 Method B Produces Consistent and Predictable Results

Using the same data derived from the ITC experiments using valine, glycine and tryptophan as copper chelators, method B was used to calculate the buffer/chelator independent *K* and enthalpy values. Table 3.2 shows the results of this analysis.

Table 3.2 The log *K* of affinities and the enthalpies of copper binding to PrPocta at pH 7 when using various amino acids as chelators and analysing the data by method B.

	Copper/Glycine into PrP octa		Copper/Valine into PrP octa		Copper/Tryptophan into PrP octa	
Binding Event	Log *K*	ΔH (Kcal/mole)	Log *K*	ΔH (Kcal/mole)	Log *K*	ΔH (Kcal/mole)
1	10.70	-20.67	10.70	-22.54	10.50	-21.12
2	6.20	-3.46	6.50	-5.71	6.50	-3.99
3	7.70	-17.12	7.70	-19.67	7.60	-17.56
4	7.30	-17.44	7.10	-18.95	7.60	-17.49
Total	31.90	-58.69	32.0	-66.87	32.20	-60.16

K values reported are pH dependent. log*K* values have been adjusted to account for the relative contribution of the chelator species to the overall equilibrium at the relevant pH, 25°C. The mean of three independent experiments were calculated, with errors between *K* values not exceeding 5%.

The predicted equilibrium for the entire reaction with glycine is shown in equation 14.

$$4Cu[gly]_2 + OctaPrP + 8H^+ \leftrightarrow 4Cu[OctaPrP] + 8glyH \quad (14)$$

Where $Cu[Gly]_2$ represents the copper chelated to glycine and [OctaPrP] represents the Octarepeat region of PrP. The chelator independent values can then be calculated from equation 12.

In all cases, a 4 sequential site model best described the data with χ^2 values at least 50% greater for all other models tested and frequently an order of magnitude greater. Log*K*

for all binding events were in close agreement for all three chelators used, with errors <1% for all values of *K* and ΔH. The sum of the log*K* was used for comparison between chelators and found to vary by only 0.8%. Enthalpy values varied between chelators by a predictable amount.

3.4.3 Comparison of the results using method B with the literature derived *K* and enthalpy values

Previous work has suggested that the octarepeat peptide binds 4 coppers cooperatively (Chattopadhyay et al. 2005) with detailed information about the exact copper coordination available. It is known that, at the first equivalent of copper, the 4 histidine imidazoles coordinate the metal together (mode 1). At increasing copper concentrations, coordination then reverts to mode 2 whereby each copper is coordinated by a single histidine imidazole and 2 deprotonated amides from adjacent glycines, with further contribution from a glycine carboxyl group. This information was used to predict the energies and *K* values of binding from the literature, using the equilibrium derived from (Walter et al. 2006) based on two sequential modes of binding dependent on cooper concentration. Mode 1 at copper occupancy ≤ 1 is shown by equation 15 and mode 2 at higher copper occupancy by equation 16.

$$Cu^{2+} + 4His^{I} \rightleftharpoons Cu[His^{I}]_4 \quad (15)$$

Where His^{I} represents binding centred around the imidazole of histidine.

$$4Cu^{2+} + 4HGGG \rightleftharpoons 4CuHGGG + 8H^{+} \quad (16)$$

Where HGGG represents the four amino acids within the octarepeat involved in copper coordination at high copper occupancy. The equilibrium for the disassociation of copper from the chelator glycine can be described by 17.

$$4Cu[gly]_2 + 8H^{+} \rightleftharpoons 4Cu^{2+} + 8GlyH \quad (17)$$

At both pH used for this study, the protonation of imidazole would not be expected to contribute significantly to the overall equilibrium (p*Ka*=6.02)(Martell and Smith). This knowledge enables an accurate assessment of the ITC data by comparing it with the predicted enthalpies and *K* values from the literature. Table 3.3 shows the individual *K* and ΔH values from ITC runs using copper/glycine into PrPocta at pH 6 and pH 7.

Table 3.3 The log *K* of affinities and the enthalpies of copper binding to PrPocta at pH 6 and pH 7 when using glycine as a chelator and analysing the data by method B.

	Copper/Glycine into PrP octa pH6		Copper/Glycine into PrP octa pH 7	
Binding Event	Log *K*	ΔH (Kcal/mole)	Log *K*	ΔH (Kcal/mole)
1	9.70	-20.53	10.70	-20.67
2	5.10	-3.81	6.20	-3.46
3	6.80	-17.24	7.70	-17.12
4	6.50	-17.39	7.30	-17.44
Total	28.10	-58.97	31.90	-58.69

K values reported are pH dependent. log*K* values have been adjusted to account for the relative contribution of the chelator species to the overall equilibrium at the relevant pH, 25°C. The mean of three independent experiments were calculated, with errors between *K* values not exceeding 5%.

This data is then compared to the predicted values obtained from the literature for the total equilibrium. Table 3.4 shows this comparison. The total literature Log *K* and ΔG° are compared to the totals for all 4 binding events from the ITC. ΔG° was derived from 18.

$$G = \Delta H - T\Delta S \qquad (18)$$

The Log*K* and ΔG° have been adjusted to account for the chelator in equation 17. The first set of literature values are obtained using data from four copper binding peptides HGGG as individual units. The experimental log*K* values obtained at pH 7 are 7.1% lower than the literature values and for pH 6, 5.9% lower. The overall ΔG° for reactions at pH 7 and pH 6 varied by 4.2% and 6.8% respectively. This lower than predicted energy and log*K* of binding probably results from the effect of the peptide backbone. Having the 4 octarepeats together as a single peptide means that the peptide must fold around the copper during the first binding mode and then move to a square planar geometry at higher copper occupancy. The second set of literature values are based on values obtained from whole octarepeat peptides(Chattopadhyay et al. 2005), but are

only available for pH 7 and include no thermodynamic information. The experimental value was just 5.6% higher than that reported in the literature. This suggests that the model was able to give a reasonable account of the enthalpies and association constants of binding.

Table 3.4 Comparison of the product of the experimental ITC values for Log*K* affinity and ΔG° for chelated copper into PrPocta at pH 7 and pH 6 with the values obtained from the predicted total literature equilibrium

	Copper/Glycine into PrP octa pH7 – Method B		Copper/Glycine into PrP octa pH6 – Method B	
Reaction	Log *K*	ΔG°	Log *K*	ΔG°
ITC equilibrum[a]				
$K_1K_2K_3K_4ITC$	31.90	-19.39[d]	28.10	-18.90[d]
Literature equilibrium[b]				
$Cu + 4His^I \rightleftharpoons Cu[His^I]_4$	12.60	-17.04	12.60	-17.04
$Cu[His^I]_4 \rightleftharpoons Cu[His^I] + 3His$	-10.50	14.23	-10.50	14.23
$4Cu + 4HGGG \rightleftharpoons 4CuHGGG + 8H^+$	32.08	-17.39	27.66	-17.39
Total	34.18	-20.20	29.76	-20.20
Difference a-b	-2.28	0.81	-1.66	1.30
Literature equilibrium[c]				
1st event	10.00	n/a	n/a	n/a
2,3 and 4th event	20.20	n/a	n/a	n/a
Total	30.20	n/a	n/a	n/a
Difference a-c	1.7	n/a	n/a	n/a

[a] Derived from ITC runs described and accounting for the overall effect of the chelator at the pH tested.
[b] Derived from the equilibrium for the reaction from ref (x using values from ref (x)
[c] From ref (x)
[d] With allowance made for the ΔG° of the chelator reaction

3.5 Discussion

ITC is a highly sensitive and versatile system capable of providing important insight into the associations between molecules of interest. Its use in the analysis of metal/protein associations can reveal much information of use in determining the nature and importance of metals to the function or possibly misfunction of protein *in vivo*. Studies involving metals, however, can be complicated by some ions remaining insoluble at physiological pH. Additionally, ions such as Cu^{2+} can oxidatively modify proteins through the generation of redox active species. These issues mean that the metal has to be delivered as a chelated species to the protein. This limitation adds obvious complications in the analysis of thermodynamic data from the reaction. Previous studies have sought to describe chelated ligand systems but have only looked

at simple independent site binding(Sigurskjold 2000; Zhang et al. 2000; Nielsen et al. 2003). To my knowledge, no assessment has previously been made as to the suitability of ITC in the analyses of complex, sequential chelated metal binding to macromolecules. This represents a major issue when faced with proteins that clearly display cooperativity between binding sites. This study indicates that ITC is able to distinguish sequential binding from independent site binding and that the enthalpies and association constants of the reaction can be fully accounted for post analyses.

The principle of the two methods of analysis used is simple. Method A attempts to account for the chelator during the fitting of the curve to the enthalpy data whereas method B accounts for the chelator effect post fitting. It is clear from this study that the most consistent and accurate method is method B. The reasons for this are likely to be in the necessary complexity of inserting extra variables within an equation with 16 existing unknowns. This would seem largely unnecessary as the effect of the chelator on the transfer of metal to the target macromolecule would clearly be included within the overall enthalpy change at any given point. This is because the very principle of ITC depends on the model being able to distinguish gross change with the enthalpy of the reaction. These changes, or inflections, within the isotherm are indicative of a change of binding and hence a different site being occupied. This information, along with the starting concentrations of all reactants, is all that is required to calculate the concentrations of reactants at any given point and hence the enthalpy relating to each event and association values. The effect of the chelator is therefore on the absolute enthalpy change from each binding event but not to the number of binding events on the target macromolecule. This has the effect of reducing the calculated association constant for each event. These data clearly show that, when allowing for the overall effect of the chelator, an accurate assessment of the target – ligand association constant can be produced. The values obtained are somewhat lower than that predicted from the literature values based on isolated 4 residue peptides. This is unsurprising as the effect of the peptide backbone on the overall association constant is absent in these values. Additionally, some complication is likely to come from the enthalpy of folding as the octarepeat peptide folds and unfolds at different copper concentrations. These experimental values matched previous data on the octarepeat region reasonably closely, and perhaps critically I was able to accurately distinguish the stoichiometry of binding from the data. The principle of this method should also be able to be applied to more

straight forward binding events. By using the origin software package to ascertain the stoichiometry and chelator dependent association constants and then taking account of the chelator in the overall equilibrium, an accurate assessment of binding can be produced.

There is, however, a clear requirement for a set of principles in the use of such thermodynamic analyses. Firstly, the chelator used must be a well characterised binding partner for the ligand, with predictable equilibrium across the pH range. Secondly, the chelator must not interact with the target molecule in any significant way. Thirdly, any other effects, such as those from buffer-buffer or buffer-ligand must also be taken into account within the equilibrium. Although I had the benefit of predetermined coordination data about the peptide of interest, this was only necessary for assessing the suitability of the method. It is clear that, if sequential binding is suspected, the sequential model can account for the number of sites and their affinity for the ligand.

CHAPTER FOUR

pH Dependence of and Location of Metal Binding Sites

Despite the almost universal acceptance that PrP^c is a cell surface protein that binds copper (Brown et al. 2001), the function of the protein continues to be debated. Although a number of hypotheses concerning the function of PrP do not require the protein to bind copper these studies are usually related to changes in cellular activity following manipulation of the protein rather than observation of the proteins activity. These activities include cell adhesion of cell signalling (Mouillet-Richard et al. 2000; Schmitt-Ulms et al. 2001; Mange et al. 2002) and neurite outgrowth (Santuccione et al. 2005). The two main copper dependent activities suggested for the protein are copper sequestration/internalisation (Pauly and Harris 1998; Brown 1999; Haigh et al. 2005) and antioxidant/survival promoting factor (Kuwahara et al. 1999; Roucou et al. 2004). Most proteins that bind copper offer some protection against copper's toxic effects. A significant body of data suggest that PrP^c is an antioxidant, possibly a superoxide dismutase (Brown et al. 1999; Brown et al. 2001; Wong et al. 2001; Thackray et al. 2002; Cui et al. 2003). However, further studies cast doubt on this theory (Hutter et al. 2003; Jones et al. 2005). With recent new data confirming the superoxide dismutase activity (Stanczak and Kozlowski 2007; Treiber et al. 2007) further investigation has become necessary.

PrP binds 4-5 atoms of copper at sites within an N-terminal octameric repeat region (Brown et al. 1997). The sites are centred around histidine residues within each repeat. Reported affinity of copper for full length PrP is in the range that would bind nanomolar to picomolar concentrations of copper (Thompsett et al. 2005). However, studies with smaller fragments produce more variable measures (Hornshaw et al. 1995; Jackson et al. 2001). The co-ordination of metal appears to vary with the number of available octameric repeats and the number of copper atoms involved (Chattopadhyay et al. 2005; Stanczak et al. 2005; Wells et al. 2006). It is also believed that positive cooperativity (Brown et al. 1997; Garnett and Viles 2003; Morante et al. 2004) plays a role in the binding but there could also be negative co-cooperativity at high copper concentrations (Walter et al. 2006). Structural changes in the protein occur on binding of copper (Miura

et al. 1996; Wong et al. 2001; Tsenkova et al. 2004) but a clear picture of the structural changes and their importance to PrP function remains unknown.

Despite considerable study of the copper binding capacity of PrP^c, there remain many unresolved issues. Many studies on copper binding to PrP have been based on peptides (Hornshaw et al. 1995; Miura et al. 1996; Viles et al. 1999; Jackson et al. 2001) but comparison to studies of full length recombinant PrP suggested that these studies do not fully reflect the story in the full length protein due to inter site cooperativity (Thompsett et al. 2005). In particular, it remains unclear whether the so called 5th copper binding site plays a major role in copper binding or not. Other issues that have not been assessed fully include pH dependence of the individual sites, which metals besides copper bind to PrP and the electrochemical properties of the copper once bound to the protein. This chapter reports on the investigations into the affinity and pH dependence of copper binding to PrP and what other metals associate with the protein. This is achieved through the application of ITC as discussed in the previous chapter. Previous reports of cooperativity within the octameric region are also investigated and confirmed in real time.

4.1 Recombinant Protein Production

4.1.1 Mutagenesis

Figure 4.1 shows agarose gel images for all the mutant constructs used for this chapter. Full sequences for all the mutants are listed in appendix A.

1 2 3 4 5

Figure 4.1 Agarose gel of mutated pET 23 plasmids encoding for mPrP copper binding mutants. Lane 1 – 5^{th} site region, Lane 2 – Octarepeat region, Lane 3 – null, Lane 4 and 5 – wildtype for reference.

Little optimisation was required from the standard protocol listed in chapter 2 and an overall mutagenesis efficiency of approximately 50% was achieved. In order to achieve multiple site mutants, a sequential series of mutagenesis was carried out. For example, for the mutant '5th site only', where the 4 histidines in the octarepeat region are replaced with alanine, an initial mutagenesis for the histidine at location 60 was first carried out. Once confirmed by agarose gel and sequencing, a second round of mutagenesis was carried out to mutate the next histidine at position 68 to alanine. This process was then repeated until all the targeted sites were successfully mutated to alanine to annul copper binding at this site. The 3 mutants used for this chapter are listed in figure 4.2, along with the wildtype protein for comparison.

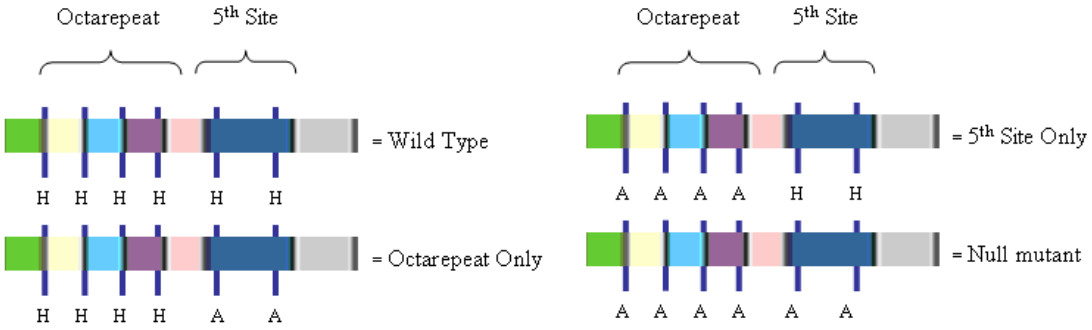

Figure 4.2 Schematic of the copper binding region of PrP highlighting the histidine residues mutated to alanines and compared to wildtype protein. The histidines within the octarepeat region are located at positions 60,68,76,84 and with in the 5th site at positions 95 and 110.

4.1.2 Protein Expression and Purification

All mutated plasmids were successfully transformed into E.coli BL21 expression strain and grown for 3-4 hours in LB media at 37°C shaking at 200rpm. Protein expression was successfully induced after addition of IPTG to a final concentration of 1mM. Protein expression was then allowed to proceed for 4 hours or overnight. Overnight expression did not produce significantly greater yields. All mutants and wildtype protein formed inclusion bodies that were successfully released by chemical lysis and solubilised in 8M urea. Protein loaded on an IMAC column charged with copper was effectively purified and eluted with 300 mM imidazole. Figure 4.3 shows the purified elusion fraction from the column for wildtype protein. For the null protein, the detergent wash purification was effective at removing contaminants and figure 4.4 shows the washes and purified product.

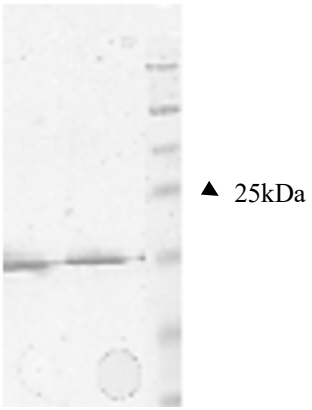

Figure 4.3 SDS gel showing the purified wildtype PrP elution fractions. Lanes 1 and 2 are the eluted protein and lane 3 the marker

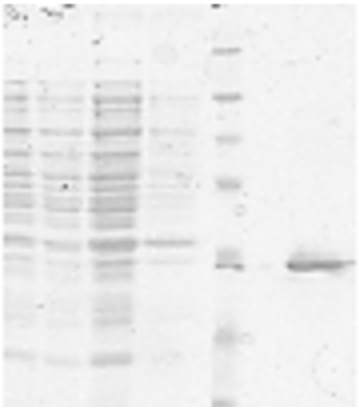

Figure 4.4 SDS gel showing the purified null protein (lane 6). Lanes 1 to 4 are the washes and lane 5 the marker

Following purification, the proteins were refolded to their most thermodynamically state by diluting out the urea with 10 mM sodium acetate buffer, pH 5.5. Natively folded PrP has a disulfide bridge within its C-terminus. To ensure the refolding process allowed correct folding and formation of this bridge, protein was refolded in the presence of 6mM oxidised and reduced glutathione and the UV-CD spectra compared with protein refolded in the normal way. Figure 4.5 shows the spectra from this experiment. The two spectra are identical in the spectral regions associated with secondary structure. This allows for the refolding of PrP in the absence of glutathione which reduces costs and complexity within the purification process.

Once refolded, all proteins were concentrated to the required concentration and dialysed at least 1000000 times against either buffer or MilliQ water to remove all remaining contaminants. Typically, final concentrations of 12, 15, 20 or 24 μM were achieved and then different concentrations of protein used for each condition to ensure reproducibility during data analysis

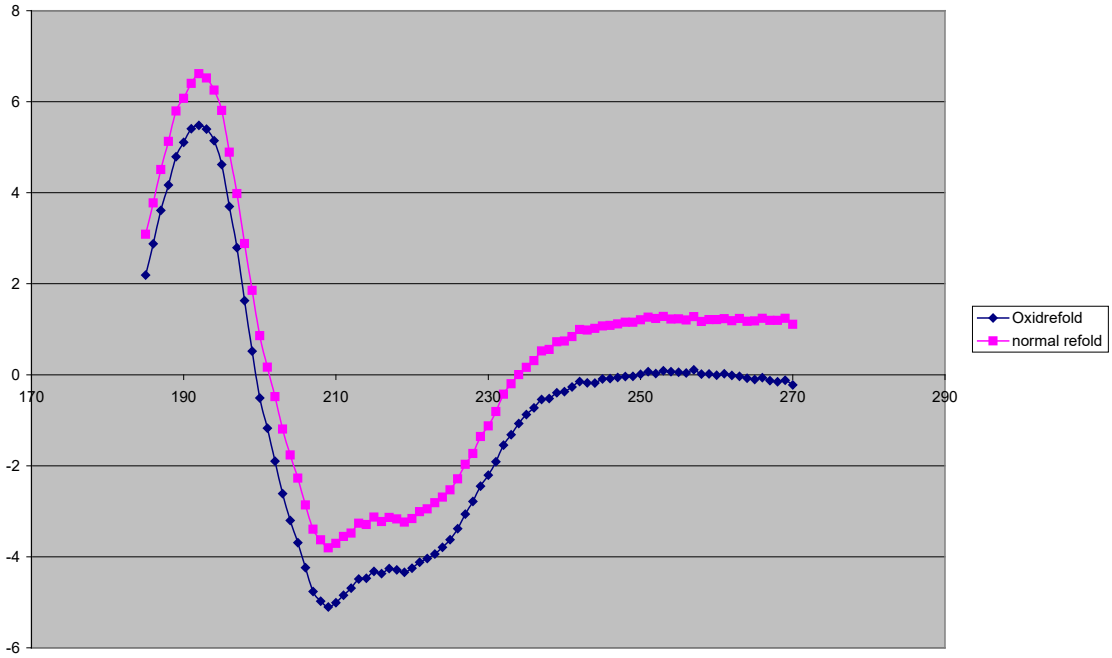

Figure 4.5 CD spectra for purified wildtype PrP comparing oxidatively and non-oxidatively refolded protein.

4.2 pH Sensitivity of Copper Binding

The copper binding sites of PrP consist of the octameric repeat region and the so called 5th site. The octameric region has been reported to contain four binding sites each consisting of an octameric repeat for which copper binding is largely dependent on the histidine of each(Hornshaw et al. 1995; Millhauser 2004). The fifth site consists of a region containing two histidines distal to the octameric repeat. Two mutants, 5th site only and octarepeat only were used to assess the pH dependence of copper binding at these two sites. Although the histidines suspected to be responsible for copper coordination have been replaced with alanine to annul binding, the proteins are still full length in order to study the effects within the intact protein as opposed to peptide fragments that may not fully represent the full copper chemistry. By comparing these two mutants with wildtype PrP, it should be possible to distinguish the relative contribution of each region on PrP to the overall copper binding seen on the wildtype protein. For each condition, copper (II) is added a glycine chelate in a 4:1 glycine to copper ration and buffered in 10 mM of an appropriate buffer. Protein was buffered with the same agent and at the same pH to minimise energies of dilution. All solutions were thoroughly degassed prior to use. ITC experiments were carried out as described in the chapter 2 and 3.

4.2.1 pH Sensitivity, Graphical Comparisons

For each condition, plots of the ITC traces from each protein are shown for comparison. The degree of slope in an isotherm is a direct indication of the tightness of binding at any given site. Where differences in affinity exist between independent binding events, a clear inflection point, or change in the acuteness of the slope, would be expected. Affinity values for wildtype, octarepeat only and 5th site only across the pH range were determined for three separate experiments using a one or two sets of sites model supplied with Microcal origin software. These models are discussed in chapter 3. The stability constants were then corrected to fully account for the relative contribution of chelating species within the overall equilibrium, as described in chapter 3. A data summary listing the least squares χ^2 values, enthalpy values for the overall reaction (quoted as Δ°G) and the stability constants corrected for chelator effects is included at the end of this section. All raw ITC traces are included as appendix B

4.2.1.1 No copper binding is detected at pH 4 or below

In order to detect the lowest pH at which sites become available on PrP for copper, experiments were carried out at pH 4. Figure 4.6 shows the plot comparing the isothermal data from the three proteins.

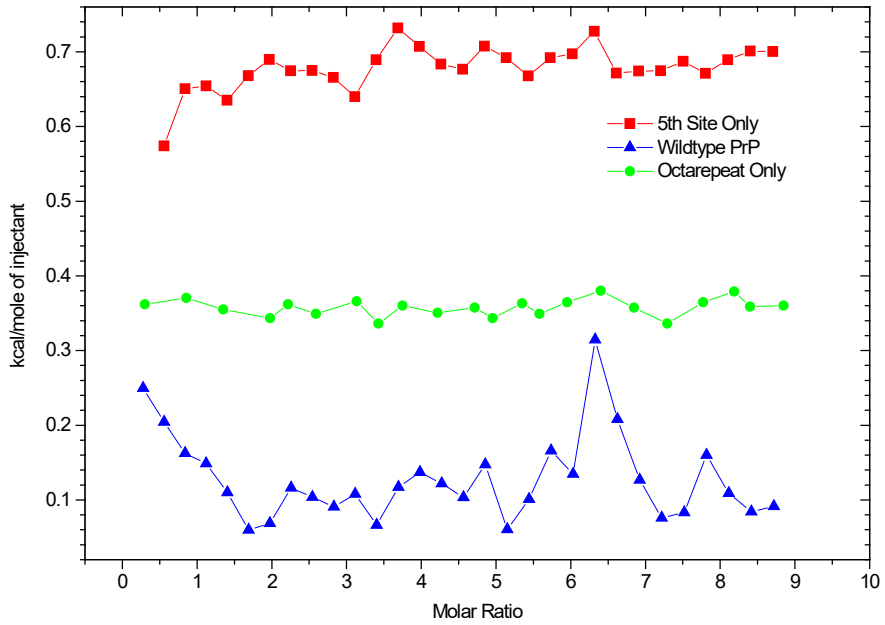

Figure 4.6 Comparison of thermodynamic plots from wildtype, 5th site only and octarepeat only titrated with copper/glycine at pH 4, 25°C, after subtraction of the buffers. 10mM sodium acetate is used in both reaction cell and syringe to ensure stable pH throughout the experiment.

Proteins were analysed at the concentrations stated and the pH was maintained by buffering with 10mM sodium acetate. Isotherms for all three constructs are consistently flat with no true inflection points after subtraction of buffers. This is consistent with no interaction between reactants over that of the energy of dilution. This suggests that, at this pH, protons are able to out compete copper at potential binding sites such as amides or histidine imidazole.

4.2.1.2 pH 5 sees the first thermodynamic evidence for copper binding

At pH 5, the first evidence for copper binding is apparent. Figure 4.7 compares the thermodynamic data for the three proteins following subtraction of buffer energies of dilution. The isotherm from the 5th site only protein shows an initial sharp slope followed by a large inflection point at a 1:1 copper to protein ratio. A gradual transition to saturation then follows. Although thermodynamic modelling showed a 1 site fit was most appropriate for the isotherm, the gradual transition from a molar ratio of 1:1 to saturation may be indicative of a very weak interaction at a second site. The octarepeat region produces an isotherm indicative of a slow and steady transition to near saturation at this pH, with little energy change over background from a protein:copper ratio of 1:6. When the wildtype isotherm is looked at, the initial slope is intermediate between the two regions. Again, near saturation occurs at around 6 copper equivalents.

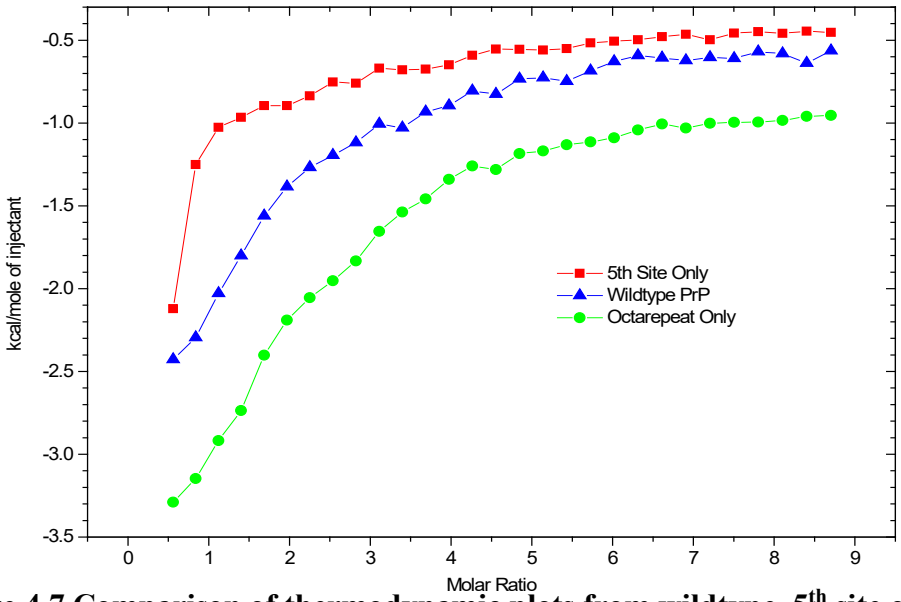

Figure 4.7 Comparison of thermodynamic plots from wildtype, 5th site only and octarepeat region titrated with copper/glycine at pH 5, 25°C, after subtraction of the buffers. 10mM sodium acetate is used in both reaction cell and syringe to ensure stable pH throughout the experiment.

4.2.1.3 At pH 6, initial isotherm slopes increase

Figure 4.8 compares the thermodynamic data for the three proteins following subtraction of buffer energies of dilution. At pH 6, the isotherm for the wildtype protein shows clear evidence of two stage binding, with a gentle inflection point apparent from 2 copper equivalents. This is indicative of multi-stage binding with an initial high affinity event followed by multiple events with a lower tightness of binding. The 5th site produces an isotherm with a steep slope to a molar ration of 1.1 with the second stage slope evident in the isotherm at pH 5 almost non existent. This strongly suggests that the possible weaker second interaction seen at pH 5 becomes less significant as the pH increases. The octarepeat region shows an initial steep slope followed by a gradual transition to near saturation. The wildtype protein shows evidence of a similar binding pattern, but the initial slope is 12% more acute.

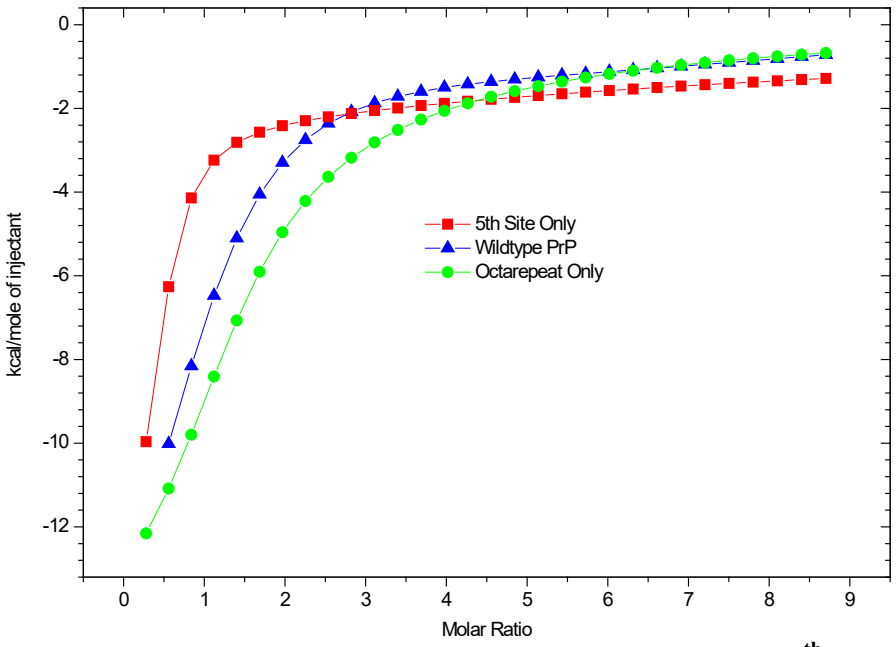

Figure 4.8 Comparison of thermodynamic plots from wildtype, 5th site only and octarepeat region titrated with copper/glycine at pH 6, 25°C, after subtraction of the buffers.

4.2.1.4 At pH 7 Wildtype PrP shows optimal binding

At pH 7, all three proteins show their optimal binding isotherm. Figure 4.9 compares the thermodynamic data for the three proteins following subtraction of buffer energies of dilution. All three isotherms now display steep initial slopes followed by rapid transition to a point of saturation, indicating that the very low affinity interactions seen at low pH are more significant at pH 7. The 5th site is saturating at a clear molar ratio of 1, with no

real evidence of a second interaction. For the point of saturation to be so distinct with rapid transition from steep slope to no change, the affinity of copper for this sight is relatively high. The octarepeat is now reaching a more defined point of saturation, with the initial slope showing similar characteristics to the 5th site and wildtype, indicating a relatively high affinity binding event. The wildtype protein now achieves a clear point of saturation at between 6 and 7 copper equivalents, confirming the proteins ability pull copper (II) at relatively low concentrations of strongly chelated copper.

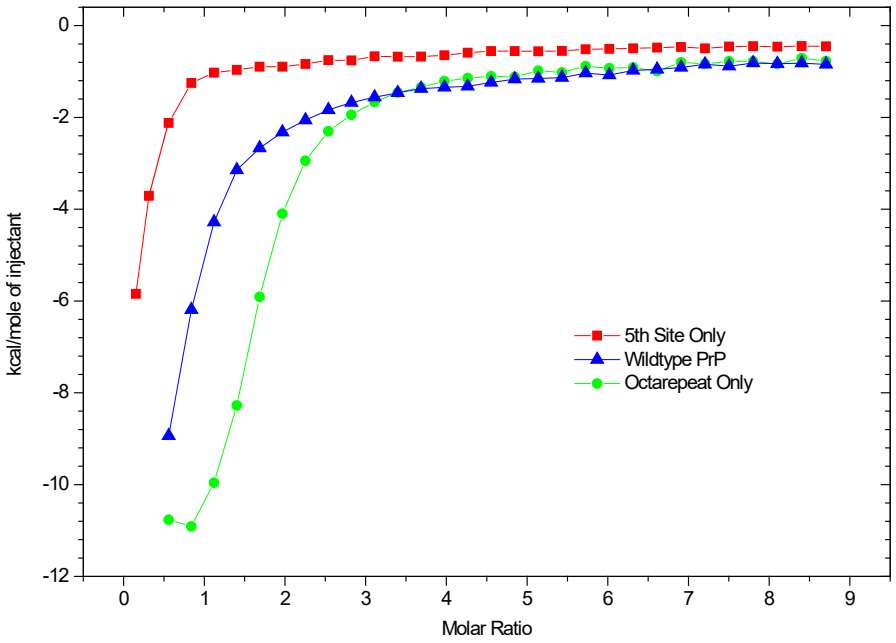

Figure 4.9 Comparison of thermodynamic plots from wildtype, 5th site only and octarepeat region titrated with copper/glycine at pH 7, 25°C, after subtraction of the buffers

4.2.1.5 At pH 8, the octarepeat region's copper binding is disrupted.

Figure 4.10 shows the isothermic data for the three proteins titrated with chelated copper at pH 8. An expectation of increasing tightness of binding at increasing pH is not satisfied. This effect is most apparent in the octarepeat region, where the isotherm has adopted a less acute transition to saturation. It would be expected that the competition with protons for copper binding sites becomes less significant at higher pH. This should lead to copper (II) binding more tightly. However, it is clear, especially within the octarepeat region, that this is not the case. In contrast, the 5th site still displays a pattern of high affinity binding and the wildtype still maintains its pattern of high affinity two stage binding.

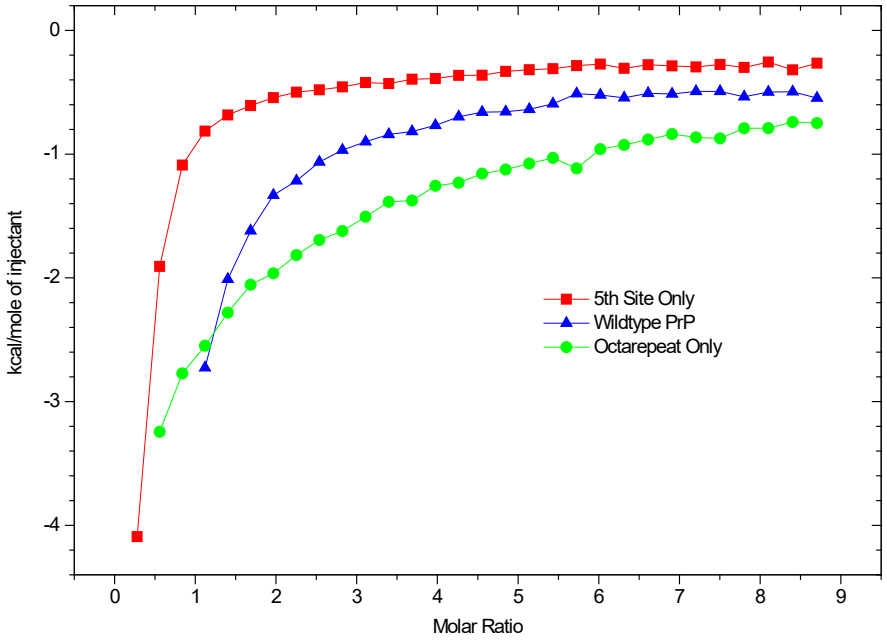

Figure 4.10 Comparison of thermodynamic plots from wildtype, 5th site only and octarepeat region titrated with copper/glycine at pH 8, 25°C, after subtraction of the buffers.

4.2.1.6 At pH 9, Only the 5th Site Maintains Familiar Binding Isotherms

Figure 4.11 compares isotherms for copper (II) binding to widtype, octarepeat region and 5th site region at pH 9.

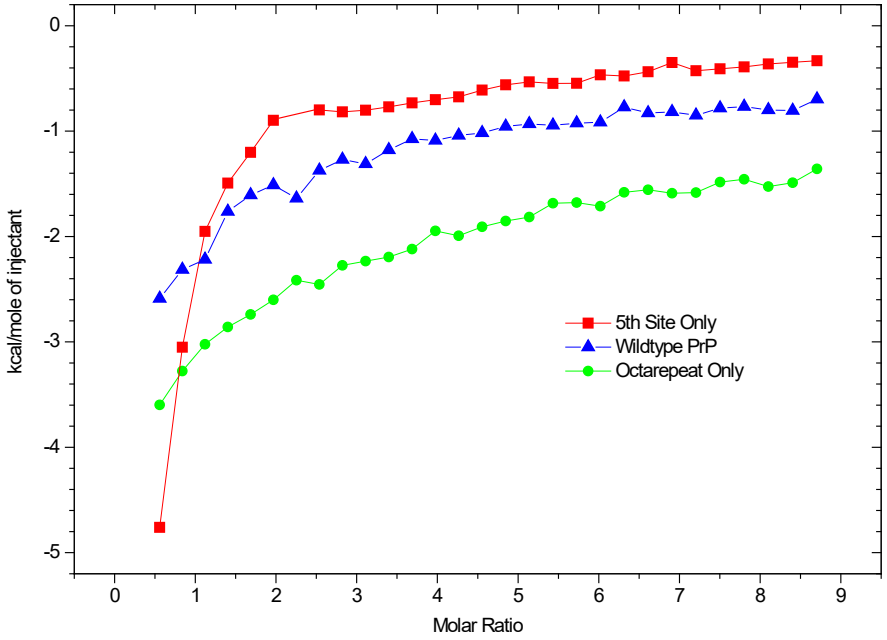

Figure 4.11 Comparison of thermodynamic plots from wildtype, 5th site only and octarepeat region titrated with copper/glycine at pH 9, 25°C, after subtraction of the buffers

At this pH, copper (II) binding within the wildtype and octarepeat proteins has altered significantly, with narrow poorly defined isotherms indicating a decrease in affinity and in number of sites. The 5th site maintains its steep binding isotherm but now fails to achieve definitive transition to saturation, indicating a decrease in affinity for copper (II). This reduction in affinity is most likely due to protein aggregation as the pH approaches the PI for PrP of 9.63.

4.2.2 Comparing the calculated affinities and stoichiometry of copper binding across the pH range

Tables 4.1 to 4.3 compare the stoichiometry and stability constants for the three proteins across the pH range. In all cases, a 'two independent sets' of sites model was used, with the exception of the octarepeat only at pH 5 and the 5th site only at pH 5, 6 and 9, where a 'one set of sites' model produced a better fit. The 'one set of sites' model use regression to fit a binding isotherm model that assumes single or multiple independent sites of similar affinity and enthalpy. The 'two sets of sites' model takes this one further with the assumption that there are 2 groups of single or independent sites with intra group similarity in affinity and stoichiometry.

4.2.2.1 The most stable copper (II) binding to PrP occurs within the physiological pH range.

Table 4.1 lists the stoichiometry and stability of the copper binding sites on PrP across the pH range. Wildtype PrP is able to bind only 2 equivalents of copper at pH 5, within 2 independent groups of sites. As pH increases, so the number of sites available to copper increase until at pH 7, the optimal 5 coppers are able to bind. The best fit model indicates that these 5 sites are divided into 2 independent sets of sites of 1 and 4 sites respectively. The stability of these copper associations also increases with pH. Optimal stability occurs at pH 7.5, with 1 copper binding with an affinity constant of log 10.8 and 4 other coppers binding with an affinity of log 7.3 within another set of sites. As conditions move into more basic conditions, so the number of sites and their affinity for copper decrease.

Table 4.1 The log stability constants and number of sites for copper on wildtype PrP across the pH range as determined by ITC using a 2 independent site model.

pH	n_1	logK_1	n_2	logK_2
4	n/d	-	n/d	-
5	1.019 ± 0.084	4.3	1.000 ± 0.000	5.1
5.5	1.008 ± 0.012	6.3	1.031 ± 0.051	6.9
6	1.021 ± 0.026	8.4	1.985 ± 0.249	6.1
6.5	1.017 ± 0.051	9.2	3.741 ± 0.219	6.5
7	1.092 ± 0.116	10.2	4.031 ± 0.102	6.9
7.5	0.946 ± 0.037	10.8	4.048 ± 0.897	7.3
8	1.058 ± 0.123	10.4	4.007 ± 0.195	7.0
9	1.142 ± 0.083	9.6	2.091 ± 0.281	6.4

K values reported are pH dependent.n_1 and n_2 represent the number of sites detected within each group of sites. The total number of binding events is therefore $n_1 + n_2$. log*K* values have been adjusted to account for the relative contribution of the chelator species to the overall equilibrium at the relevant pH, 25°C. The mean of three independent experiments were calculated, with errors between *K* values not exceeding 5%.

4.2.2.2 In acidic conditions, wildtype copper sites can be mapped to each region

Tables 4.2 and 4.3 show the stoichiometry and stability for copper binding to the octarepeat region and 5th site only. From table 4.2, it is clear that from pH 6, the copper binding sites within the octarepeat can be grouped into two sets of sites. One set of sites consists of one high affinity event that at pH 7 displays a stability constant of log 10.5. The second set of sites consists of 3 binding events of similar affinity with a stability of log 6.4 at pH 7.

Table 4.2 The log stability constants and number of sites for copper binding to octarepeat across the pH range as determined by ITC using a 1 or 2 independent site model.

pH	n_1	logK_1	n_2	logK_2
4	n/d	-	n/d	-
5	1.026 ± 0.162	4.2	n/d	-
6	1.061 ± 0.009	8.7	2.001 ± 0.052	5.8
7	1.198 ± 0.043	10.5	2.896 ± 0.376	6.4
8	1.062 ± 0.101	10.1	2.961 ± 0.061	6.1
9	1.035 ± 0.109	9.0	1.117 ± 0.151	7.4

K values reported are pH dependent.n_1 and n_2 represent the number of sites detected within each group of sites. The total number of binding events is therefore $n_1 + n_2$. log*K* values have been adjusted to account for the relative contribution of the chelator species to the overall equilibrium at the relevant pH, 25°C. The mean of three independent experiments were calculated, with errors between *K* values not exceeding 5%.

Table 4.3 lists the affinity and stoichiometry of copper (II) within the 5th site region. High affinity binding is apparent from pH 6, with the optimal being between pH 7 and

pH 8. At this pH, the region appears to bind 2 molecules of copper (II) in two sets of sites, one with high affinity of stability log 10.5 and one of lower affinity log 6.1.

Table 4.3. The log stability constants and number of sites for copper binding to the 5th site region across the pH range as determined by ITC using a 1 or 2 independent site model.

pH	n_1	logK_1	n_2	logK_2
4	n/d	-	n/d	-
5	1.096 ± 0.140	5.3	n/d	-
6	1.047 ± 0.066	8.5	n/d	-
7	0.962 ± 0.030	10.5	1.057 ± 0.018	6.1
8	1.019 ± 0.092	10.3	1.104 ± 0.131	6.1
9	1.301 ± 0.251	9.3	n/d	-

K values reported are pH dependent.n_1 and n_2 represent the number of sites detected within each group of sites. The total number of binding events is therefore $n_1 + n_2$. log*K* values have been adjusted to account for the relative contribution of the chelator species to the overall equilibrium at the relevant pH, 25°C. The mean of three independent experiments were calculated, with errors between *K* values not exceeding 5%.

At pH 5, the octarepeat region binds only 1 copper, with almost identical affinity to the second site seen on the wildtype protein. The first site on the wildtype construct can be matched to the site apparent on the 5th site region at this pH. As pH increases, the first binding event apparent on the wildtype construct closely matches the high affinity site seen in the 5th site region. However, at pH 7 and 8, a second low affinity site, log stability constant 6.1, appears which is not reflected in the matched 5th site on the wildtype protein. Additionally, when looked at in isolation, the octarepeat region appears to bind copper with greater complexity than first indicated by the wildtype data. Two sets of sites are detectable on the octarepeat region at pH > 5, with a high affinity binding event followed by multiple lower affinity events. At pH 7, the lower affinity events increase to 3, with the single site increasing to log stability constant 10.5. As with the wildtype construct, the number of sites and their affinity decrease from pH 8.

4.2.2.3 Sequential modelling is able to reveal site location at pH 7

Where sites within a group of sites are non-identical, it leads to a degeneracy within the two sites model (Zhang et al. 2000). Under such circumstances, it may be appropriate to analyse such data using a thermodynamic model that assumes that sites are filled sequentially and each site is affected by the previous binding event. Such a model exists within the Origin software supplied by Microcal but makes the factoring of the chelator effect to the overall equilibrium complicated and potentially error prone. We have

previously demonstrated the feasibility of this model, however (Davies and Brown 2008) and can now apply it to the data from the three constructs. Chapter 3 shows justification for this process. Table 4.4 compares the data from wildtype, octarepeat and 5th site constructs analysed by a sequential binding model.

Table 4.4 The log stability constants and number of sites for copper binding to 3 PrP constructs across the pH range as determined by ITC using a sequential site model

Construct	logK_1	logK_2	logK_3	logK_4	logK_5
Wildtype	10.4	10.1	5.9	6.9	7.1
Δ 5th site	10.6	6.1	n/d	n/d	n/d
Δ octarepeat	10.5	6.0	7.0	7.0	n/d

K values reported are pH dependent.log*K* values have been adjusted to account for the relative contribution of the chelator species to the overall equilibrium at the relevant pH, 25°C. The mean of three independent experiments were calculated, with errors between *K* values not exceeding 5%.

Comparing the affinity constants of the three proteins, similarities can be seen between the first two binding events on the wildtype protein and the first event on the two mutants. The next three wildtype binding events closely match the pattern and affinity of the last three events on the octarepeat construct. This suggests that there are two high affinity sites on the wildtype protein, one within the octarepeat region and one within the 5th site. It cannot be totally ruled out that the octarepeat region binds only three copper ions and the 5th site two copper ions at pH 7. However, the affinity values for copper and the octarepeat region do more closely match the last four events on the wildtype protein.

4.2.2.4 Sequential modelling reveals cooperative copper binding to PrP

As well as successfully mapping the relative contribution of the two regions on PrP to copper binding, sequential modelling reveals a cooperative binding mechanism within the octarepeat region. Although previous studies have suggested a cooperative binding mechanism within the octarepeat region (Walter et al. 2006) , we are able to observe this mechanism thermodynamically and in real time. It is clear from table 4 that a high affinity event, log stability constant 10.6 within the octarepeat region is followed by binding with an affinity of over four orders of magnitude less in the subsequent site. The affinity for copper with the last two binding events is then similar, both demonstrating a log stability constant 7.0. This is suggestive of negative cooperativity, within 4 identical copper binding sites. This pattern can be closely matched to the last

four binding events within the wildtype protein, where following the first two high affinity events matched to the 5th site and first copper within the octarepeat region, 3 events of much lower affinity are apparent.

4.3 pH Dependence and Location of Other Metal Binding Sites

There have been numerous suggestions that PrP can bind other metals such as nickel, zinc and iron. As these can be found in a free ionic form and do not necessarily form complexes with glycine, ITC experiments were carried out to assess the affinity of ionic zinc, iron and magnesium for recombinant mouse WT-PrP in the absence of glycine. Table 4.4 lists the values obtained at (i) pH 5.5 and (ii) pH 7.

Table 4.5 The log stability constants and number of sites for other divalent cat ion binding to 3 PrP constructs as determined by ITC.

(i)	Wild Type		Octarepeat		5th Site Only	
pH 5.5	Site 1	Site 2	Site 1	Site 2	Site 1	Site 2
Ni^{2+}	n/d	n/d	n/d	n/d	n/d	n/d
Zn^{2+}	n/d	n/d	n/d	n/d	n/d	n/d
Fe^{2+}	3.1	n/d	n/d	n/d	3.3	n/d
Mg^{2+}	n/d	n/d	n/d	n/d	n/d	n/d
(ii)	Wild Type		Octarepeat		5th Site Only	
pH 7	Site 1	Site 2	Site 1	Site 2	Site 1	Site 2
Ni^{2+}	4.3	3.2	4.4	3.2	n/d	n/d
Zn^{2+}	4.6	3.7	4.6	3.4	2.4	n/d
Fe^{2+}	4.0	2.7	2.8	n/d	3.9	n/d
Mg^{2+}	n/d	n/d	n/d	n/d	n/d	n/d

K values reported are pH dependent. Values quoted are logK stability constants derived from either 1 or 2 independent site models. All experiments were conducted in triplicate using buffers and concentrations previously described at 25°C. Iron II was prepared in anaerobic conditions to prevent oxidation to Fe III

At pH 7, mPrP bound all the divalent cat ions tested at two sites with the exception of magnesium, which did not bind. Zinc, nickel and iron all displayed similar affinities in the first site with zinc and nickel similar at the second site, suggesting the protein is able to bind these metals in the micromolar range. The second iron site displayed affinities in

the millimolar range. When metal binding was analysed in the mPrP mutant lacking the 5th site or the octarepeat, it was found that both nickel and zinc bound at two sites within the octarepeat with affinities matching those in the Wildtype protein. Interestingly, it was also found that protein with only the 5th site also had a low affinity site for zinc that was not apparent in the Wildtype. In contrast, iron seems to bind with highest affinity within the 5th site with the second low affinity site seen in the Wildtype appearing in the octarepeat region. At pH 5.5, only iron showed binding and that appeared to be at the micromolar affinity site within the 5th site region.

4.4 Discussion

There has been a long and somewhat inconsistent line of publications on the relationship between PrP and copper (Hornshaw et al. 1995; Miura et al. 1996; Brown et al. 1997; Jackson et al. 2001; Wong et al. 2001; Garnett and Viles 2003; Morante et al. 2004; Tsenkova et al. 2004; Chattopadhyay et al. 2005; Stanczak et al. 2005; Thompsett et al. 2005; Walter et al. 2006; Wells et al. 2006). Such an enormous variation in opinion on what is fundamental knowledge for a metalloprotein deserves and demands an explanation and re-examination. I present here a thorough thermodynamic study of copper binding to recombinant PrP and through use of single amino acid changes, demonstrate the contribution of each binding site in the wildtype protein to the overall copper binding equilibrium.

The key aspects of the protein still under debate are its function and the role of metal binding in its physiological role and in disease. These questions are difficult to answer when reports of the protein's affinity for copper range from micromolar (Hornshaw et al. 1995) to femtomolar (Jackson et al. 2001). Although it is almost universally accepted that the protein binds copper (Brown et al. 2001) and more recently binds copper in a complex and cooperative way (Chattopadhyay et al. 2005) some aspects of the metal – protein complex require further clarification. Among these unknowns are the pH dependence of metal binding, what other metals bind and where and what implications to the function of the protein these associations have. Although there has been much work focused on the individual binding regions of the protein by use of peptide fragments, there is little data on how the individual regions behave when in the intact protein. This study uses the complete protein to study these individual metal binding

regions and provides a thorough insight into its metallochemistry and its relevance in the native protein.

In order to explore the effect of pH on copper binding to the prion protein, isothermal titration calorimetry is employed to predict the number of sites and their affinity for the copper ion across a range of pH4 to pH 9. The affinities, stoichiometries and degree of cooperativity I report here are in very close agreement with a previous study (Millhauser 2007). The protein's optimal binding is between pH 7 and pH 7.5 which would mean that *in vivo* conditions of pH 7.4 would favour a tight copper association. I have demonstrated that both the octameric repeat and the 5th site region of wildtype PrP can bind copper with high affinity. The two copper sites within the 5th site highlighted by other studies using peptides (Jones et al. 2004), do not appear to be present in the complete protein. It seems that, in the presence of the octarepeat region, the 5th site binds a single copper, pointing towards a repressive effect by the octarepeat region. The combined affinity of the two sites with the 5th binding region identified by this and other studies of log 16.7 would appear to be reduced to a single binding event of around log 10.4 in the wildtype protein. The octarepeat region binds 4 coppers in both the wildtype protein and in the protein with 5th site silenced at physiological pH. This study has demonstrated the different binding modes of the octarepeat reported in previous studies (Chattopadhyay et al. 2005) by studying copper binding at different pH. Under acidic conditions of between pH 5 and pH 6, strong competition from protons for the glycine amides, PI 9.63 (Martell and Smith) mean that only the imidazoles from the 4 histidines PI 6.03 (Martell and Smith) are available for copper coordination. This results in a single complex involving one copper ion to four histidine imidazoles, irrespective of the copper concentration. As pH increases to 6, the four imidazole complexes split to bind one copper to two imidazoles, representing an intermediate copper coordination, as previously reported (Wells et al. 2006). As pH increases further, so the copper is able to compete with protons for glycine amides and hence four copper (II) atoms are able to bind in the classic single copper to single histidine coordination, with contributions from the deprotonated amides from the adjacent glycine residues. This multi-stage coordination is clearly also occurring in the octarepeat region at physiological pH, but driven by copper concentration as opposed to competition from protons. Using a sequential binding model, a clear negative cooperativity in copper binding can be seen as copper concentration increases. At copper equivalents of below one, a high affinity

binding site is immediately obvious, involving the four histidine complex. As copper concentration increases further, a binding event four orders of magnitude less is apparent, with two further sights of slightly higher affinity. It is likely that the sequential affinity for copper at this second binding site is adversely affected by the disruption of three imidazole bonds as the coordination mode changes. Again, in the presence of the other region, the octarepeat appears to suffer a slight reduction in the affinity for copper within its high affinity site. There can be no doubt that this remarkable ability to alter coordination and hence structure at different copper concentrations will be highly significant to the function of the protein and, combined with previous studies indicating a copper concentration dependent uptake and internalisation (Pauly and Harris 1998; Haigh et al. 2005), supports a potential role in copper sensing, sequestering and internalisation within the synaptic cleft. This ability would be highly dependent on copper binding to the octarepeat region. Any such function would have an important role in reducing the toxic effects from copper within the brain.

The affinities reported here are comparable to much of the recent studies on full length protein. The initial early work on the affinity of PrP for copper was carried out on synthetic or recombinant protein. For example, Hornshaw *et al,* 1995, showed each octarepeat region to bind copper with an affinity of 6.7μM. This was corroborated by Viles *et al,* 1997, who found the affinity to be 6μM. It is likely these studies failed to produce the high affinity associations shown by this and other studies due to the small fragments used and therefore the lack of the inter histidine cooperativity seen in the full length protein. Previous studies on full length have demonstrated the much higher affinity binding seen by this study. Jackson *et al,* 2001 showed the first copper equivalent binds with a femtomolar affinity and Thompsett *et al*, 2006 confirmed this. Both these studies were somewhat generous in their values, however, due to treatment of the data with reference to the chelator. Much other work (Garnet and Viles, 2003; Walter *et al*, 2006; Klewpatinond and Viles 2008) on full length protein has produced values in the same region as this study.

The values reported here are also in very close agreement to work I was involved in, (Klewpatinond et al, 2008). This study reported that at physiological pH, Cu2+ initially binds to full-length PrP in the amyloidogenic region between the octarepeats and the

structured domain at His(95) and His(110). Only subsequent Cu2+ ions bind to single histidine residues within the octarepeat region. Ni2+ ions were used to further probe metal binding and, like Cu2+, Ni2+ will bind individually to His(95) and His(110), involving preceding main chain amides. Competitive chelators were used to determine the affinity of the first mole equivalent of Cu2+ bound to full-length PrP; this approach placed the affinity in the nanomolar range.

Studies on the binding of other metals with PrP are largely in agreement with the published pattern of cat ion binding to amino acids (Gilli et al. 1998). These data suggest that the affinity of amino acid residues with metals follow the pattern of alkali metals < earth metals < transition metals. There is no apparent binding of Mg to PrP but all of the transition metals tested do produce isothermal data. As with copper, this binding is dependant on pH. Ni and Zn both bind with highest affinity to the octarepeat region and at pH 7 whereas Fe binds with highest affinity at the 5^{th} site. In acidic conditions, only Fe is able to bind and at he 5^{th} site. This is again further evidence of two very different binding mechanisms within the octarepeat and the 5^{th} site. Divalent cat ions which are able to bind the 5^{th} site appear to do so in acidic or neutral conditions whereas binding within the octarepeat is always optimal at neutral to mildly basic conditions. This would suggest the involvement of histidines for the binding of other metals as well as copper. Even under optimal conditions, it would seem unlikely that the associations of these metals with PrP play a role in its physiological function due to their relatively low stability constants from PrP. When compared to physiological systems associated with these metals, it is clear that such low affinity values would be unlikely to enable PrP to have a role in transport, storage or catalysis in connection with Fe, Ni or Zn. For example, transferrin has been shown to bind Fe with an affinity of 10^{23} (Aisen et al. 1974) and Cu/Zn SOD binds Zn with an affinity of 4.2×10^{14} (Crow et al. 1997). It is also clear that, under physiological conditions, these metals would be unable to displace copper from the protein even in a free ionic form.

Chapter Five

Focus on the Thermodynamics Within The Two Copper Binding Regions of PrP

The octarepeat region in the human protein is composed of a sequence of 8 amino acids (PHGGGWGQ) repeated four times, each containing a histidine which is generally accepted to be the primary residue responsible for the copper coordination (Aronoff-Spencer et al. 2000; Burns et al. 2002). Detailed studies involving electron paramagnetic resonance imaging (EPR) and X-Ray crystallography on recombinant peptide fragments have demonstrated that a single copper is coordinated by each octarepeat segment in a pentacoordinate complex involving residues HGGGW (Aronoff-Spencer et al. 2000; Burns et al. 2002) . This equatorial coordination involves the Histidine imidazole, deprotonated amides from the adjacent two glycines and a deprotonated carbonyl from the last glycine. A water molecule may also be involved by allowing an oxygen to coordinate axially forming a bridge to the NH of the indole on the last tryptophan. Recent work has demonstrated that the coordination of copper was dependent on the degree of copper occupancy on the protein (Chattopadhyay et al. 2005). Three distinct coordination modes were proposed, clearly divisible at different relative concentrations of copper. These consisted of a multiple His coordination mode at low copper occupancy, moving through a transitional coordination to the maximal occupancy at a physiological pH 7.4. Work on the octarepeat region has also revealed evidence of dipolar copper-copper centres suggesting a close copper-copper proximity of between 3.5Å and 6Å, close enough for van der Waals interactions (Chattopadhyay et al. 2005). These interactions may be responsible for driving a hydrophobic collapse and consequent N terminal structural organisation at full copper occupancy.

A large body of literature also exists that demonstrates that copper is able to bind outside of the octarepeat region of PrP (Hasnain et al. 2001; Jackson et al. 2001; Kramer et al. 2001; Burns et al. 2003; Jones et al. 2004). Work by Jones *et al,* in 2004 and 2005 highlighted these copper binding regions as His96 and His111 in the human protein. They also identified the minimum sequence necessary for Copper binding to this region of PrP are amino acids 92-96 and 107-111. Recently, the same group utilised NMR and visible circular dichroism (Vis-CD) to fully elucidate the coordination of copper to this

so called 5th site (Klewpatinond and Viles 2007). Interestingly, they found that the coordination of copper changed dramatically dependent on chain length and pH. They concluded that this striking effect was caused by a change in relative affinity of His 95 and His 110 for copper. Although His110 seems to display the highest affinity for copper, His96 affinity increases dramatically on the addition of the 11 amino acid hydrophobic segment. They also discovered a multi coordination mode that was strongly influenced by pH.

The complexity of copper coordination to the regions of PrP deserve a more detailed study to elucidate the degree of contribution of the individual motifs to the overall stability of binding. Evidence suggesting very close copper / copper proximity and dramatic structural change on copper binding within both regions raise questions concerning the impact of each copper (II) molecule as it associates. The degree of positive or negative cooperativity both within and between each region may also be further resolved by such a study.

5.1 Recombinant Protein Production

5.1.1 Mutagenesis

Figure 5.1 shows agarose gel images for a selection of the mutant constructs used for this chapter. Full sequences for all the mutants are listed in appendix A.

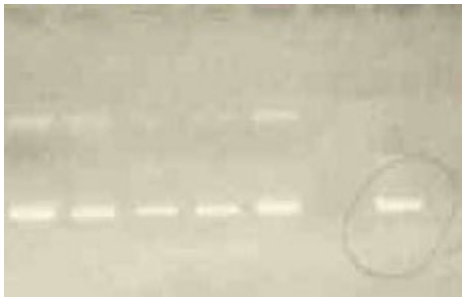

1 2 3 4 5 6

Figure 5.1 Agarose gel of mutated pET 23 plasmids encoding for mPrP copper binding mutants. Lane 1 – Site 1,5,6 present; Lane 2 – Site 4,5,6 present; Lane 3 – Site 1,2,5,6 present; Lane 4 - Site 1,2,3,5,6 present; Lane 5 – Site 6 present, Lane 6 - wildtype for reference.

In order to achieve multiple site mutants, a sequential series of mutagenesis was carried out. For example, for the mutant ‘site 3,4’, where the first 2 histidines in the octarepeat

region and the 2 histidines within the 5th site are replaced with alanine, the octarepeat only mutant was used as a template. An initial mutagenesis for the histidine at location 60 was first carried out. Once confirmed by agarose gel and sequencing, a second round of mutagenesis was carried out to mutate the next histidine at position 68 to alanine. The 19 mutants used for this chapter are listed in figure 5.2, along with the wildtype protein for comparison.

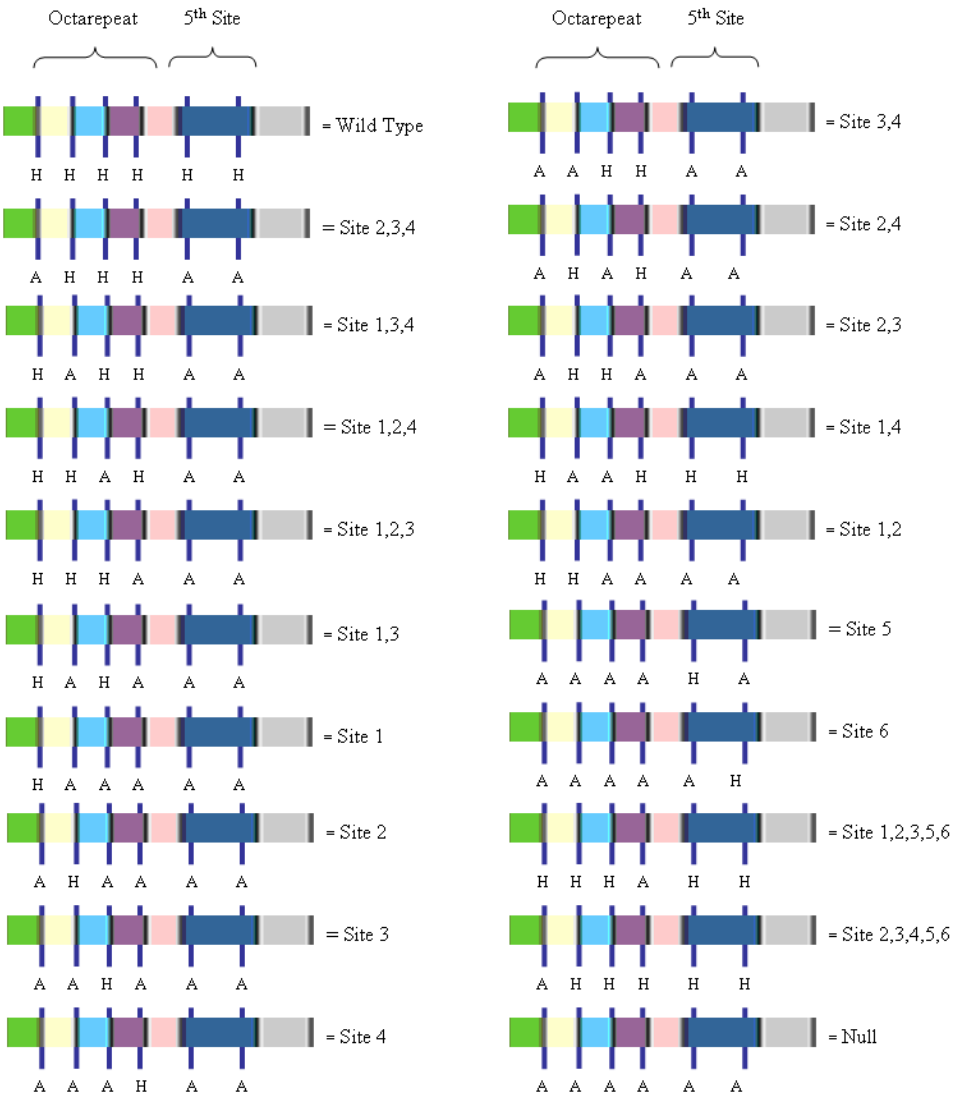

Figure 5.2 Schematic of the copper binding region of PrP highlighting the histidine residues mutated to alanines and compared to wildtype protein. The mutant names refer directly to which histidine residues are present. The histidines within the octarepeat region are located at positions 60,68,76,84 and with in the 5th site at positions 95 and 110.

5.1.2 Protein Expression and Purification

All mutated plasmids were successfully transformed into E.coli BL21 expression strain and grown for 3-4 hours in LB media at 37°C shaking at 200 rpm. Protein expression was successfully induced after addition of IPTG to a final concentration of 1 mM. Protein expression was then allowed to proceed for 4 hours or overnight. Overnight expression did not produce significantly greater yields. All mutants and wildtype protein formed inclusion bodies that were successfully released by chemical lysis and solubilised in 8 M urea. Protein loaded on an IMAC column charged with copper was effectively purified and eluted with 300 mM imidazole. Figure 5.3 shows the purified elusion fraction from the column for the mutant with sites 1,5,6 present and 2,3,4 present.

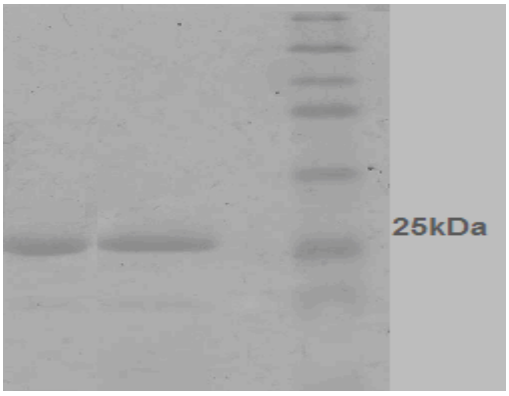

Figure 5.3 SDS gel showing the purified mutant protein.. Lane 1 shows 'Site 1.5.6' and lane 2 shows 'Site 2,3,4'. Lane 3 is the marker

Following purification, the proteins were refolded to their most thermodynamically favourable state by diluting out the urea with 10 mM sodium acetate buffer, pH 5.5. Once refolded, all proteins were concentrated to the required concentration and dialysed at least 1000000 times against either buffer or MilliQ water to remove all remaining contaminants.

5.2 Thermodynamic Assessment of Intra Region Interactions for Copper (II) Binding to the octarepeat of PrP

For each mutant protein, copper (II) was added as a glycine chelate in a 4:1 glycine to copper ratio and buffered in 10mM MOPS. Protein was buffered with the same agent and at the same pH to minimise energies of dilution. All solutions were thoroughly degassed prior to use. In order to factor in the thermodynamics of the energies of dilution, runs were carried out of chelated copper into buffer only and subtracted from the data. ITC experiments were carried out as described in the chapter 2 and 3.

Plots of the ITC traces from each protein are shown for comparison. The degree of slope in an isotherm is a direct indication of the tightness of binding at any given site. Where differences in affinity exist between binding events, a clear inflection point, or change in the acuteness of the slope, would be expected. Affinity values for all the mutants listed above were determined for three separate experiments using a sequential sites model supplied with Microcal origin software. These models are discussed in chapter 3. A sequential model was tested and found to provide the most consistent regression fit for the data. Additionally, the use of such a model allows insight into copper (II) binding site interaction. The stability constants were then corrected to fully account for the relative contribution of chelating species within the overall equilibrium, as described in chapter 3. A data summary graph is then included as a comparison between mutants.

5.2.1 The removal of one histidine residue has dramatic consequences for copper binding affinity within the octarepeat

Figure 5.4 compares the isotherms for each of the mutants with the 5th site missing along with one site missing in the octarepeat region. When looking at the isotherms from each mutant, clear differences can be observed.

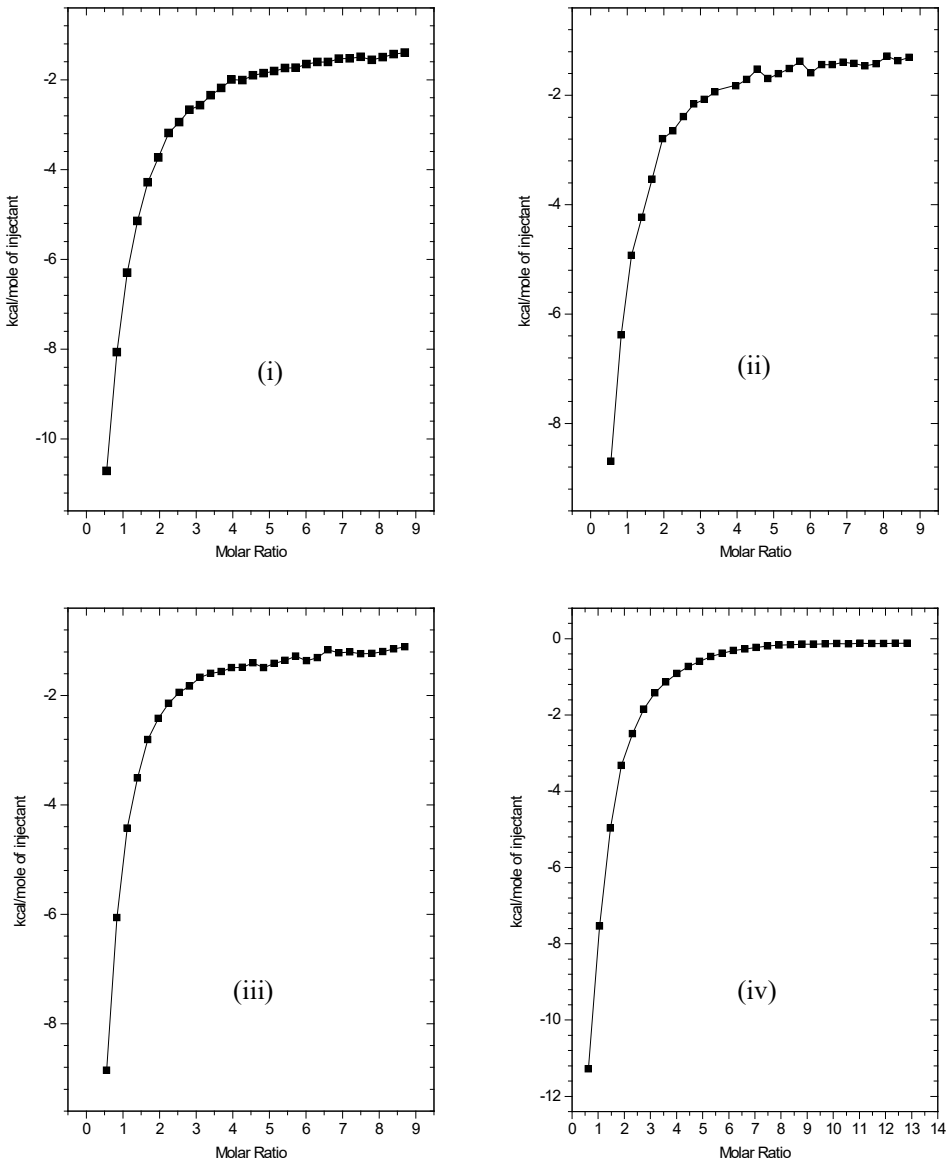

Figure 5.4 Isotherms for the titration of copper (II) : glycine into the mutants of PrP lacking the 5th site and one of the sites within the octarepeat. (i) Sites 1,2,4 present. (ii) sites 1,3,4 present. (iii) sites 1,2,3 present. (iv) sites 2,3,4 present.

The isotherms for the mutants with sites 1,2,4 present and 1,3,4 present (i and ii respectively) do not display such a defined transition from steep slope to eventual saturation as the mutants where the sites remaining within the octarepeat are all together. Additionally, only the mutant with sites 2,3,4 present achieves complete saturation, evidenced by reduction of ΔH to 0 by a molar ration of 5 copper to 1 protein. The location of the remaining histidine residues within the octarepeat when one is removed is therefore clearly important. Where the missing histidine is within the sequence of octarepeat histidines (i.e. at location 2 or 3) then the remaining sites are less able to cooperate in the coordination of the copper (II). Where the missing histidine is on the periphery of the octarepeat region (i.e. at location 1 or 4) then the remaining sites

are still able to interact. Figure 5.5 compares the log stability constants for the 4 mutants with the protein with the complete octarepeat region.

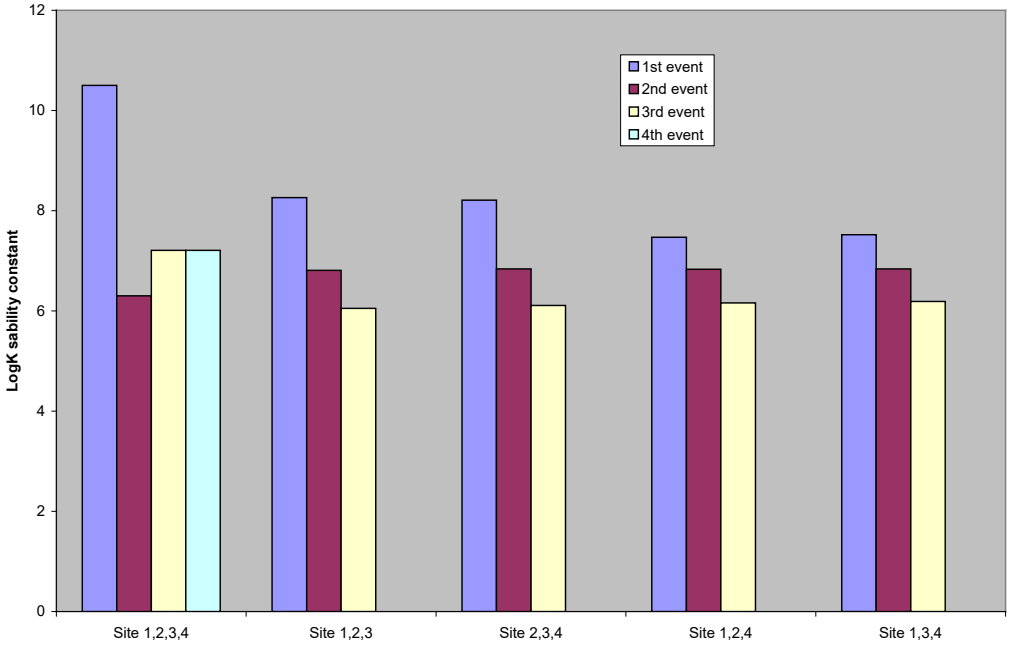

Figure 5.5 Comparison of the log stability constants for the four mutants with the 5th site absent as well as one histidine within the octarepeat with the complete octarepeat region. All errors are within 2 % for calculated stability constants and within 5 % for the mean of each value

The deductions made from the graphical comparison are confirmed by the regression analysis of the isotherms. In all cases, a sequential model was used to fit the data to the number of sites and their affinity for copper. All 4 mutants were fitted to a 3 site sequential model, with χ^2 values all at least 50% lower than other model possible fits. All errors for stability constants were below 5% and below 10% for calculated enthalpy of binding. Comparing the affinities of the 4 mutants with the complete octarepeat, striking differences are immediately apparent. For the complete octarepeat region, 4 binding events are apparent. The first event is one of high affinity, with a log stability constant of 10.5. There then follows an event 4.5 orders of magnitude lower before two events of equal affinity log stability constant 7.0. When looking at the mutants with the 3 sites remaining in sequence, they both display an initial binding event around 2.5 orders of magnitude lower than the first event on the protein with the complete octarepeat. The mutant with sites 1,2,3 remaining shows 3 sequential sites with log stability constants 8.2, 7.1, 6.2 and the mutant with sites 2,3,4 remaining 3 sites log stability constant 8.3, 7,1, 6.4. The mutants with the 3 remaining sites separated by a

histidine to alanine mutation, however, both display a more disrupted binding pattern, with an initial event some 3 orders of magnitude less than that on the complete octarepeat region. The mutant with sites 1,2,4 remaining shows 3 sequential sites with log stability constants 7.3, 6.9, 6.1 and the mutant with sites 1,3,4 remaining 3 sites log stability constant 7.4, 7,0, 6.1. These data therefore clearly highlight the importance of histidine residue location within the octarepeat for the degree of cooperativity between binding sites.

5.2.2 The removal of two histidine residues has even more striking effects on copper binding affinity within the octarepeat

Figure 5.6 compares the isotherms for each of the mutants with the 5th site missing along with two sites missing in the octarepeat region. There are 6 possible combinations for these mutants. Remaining histidine residues are either situated in adjacent octarepeats (sites remaining 1,2 or 2,3 or 3,4) or separated by 1 octarepeat (sites remaining 1,3 or 2,4) or separated by 2 octarepeats (sites remaining 1,4). When looking at the isotherms from each mutant, clear differences can again be observed. The 3 mutants with remaining histidine residues situated in adjacent octarepeat (figure 5.6 (i),(ii) and (iii)) all produce isotherms with a defined inflection point at around 3 copper equivalents. There is also a clear transition to saturation. When these are compared to mutants with histidine residues situated in octarepeats separated by 1 or more mutated octarepeats, it is clear that the distance between functional copper binding sites is critical to the coordination and stability of binding. The isotherms for these mutants (figure 5.6 (iv), (v) and (vi)) all display a much less defined inflection point and barely achieve saturation by 10 copper equivalents. This pattern of binding is indicative of a significant affect on copper (II) binding stability between mutants. Figure 5.7 compares the log stability constants for the 6 mutants with the protein with the complete octarepeat region.

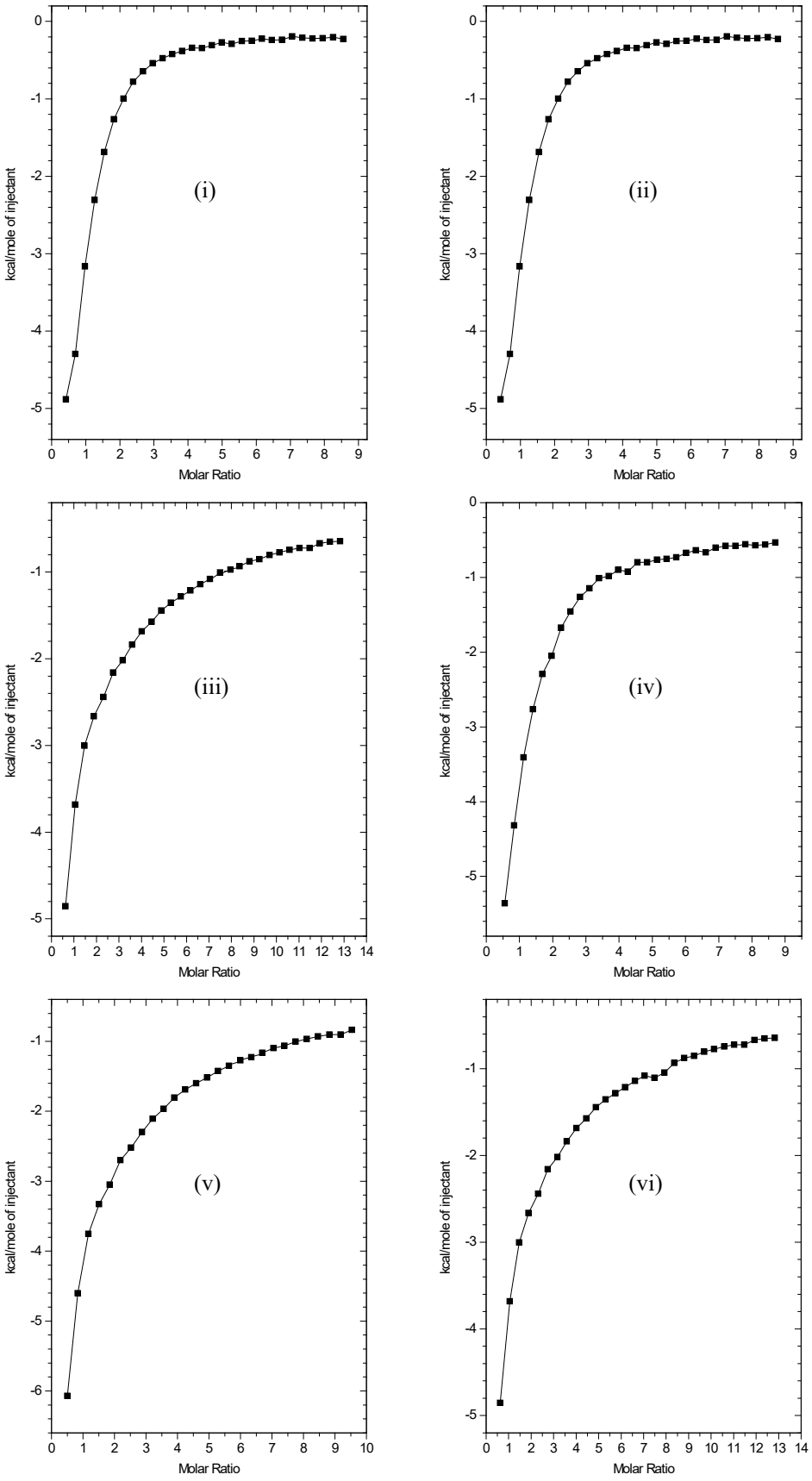

Figure 5.6 Isotherms for the titration of copper (II) : glycine into the mutants of PrP lacking the 5th site and two of the sites within the octarepeat. (i) Sites 3,4 present. (ii) sites 1,2 present. (iii) sites 2,3 present. (iv) sites 1,4 present. (v) sites 1,3 present. (vi) sites 2,4 present.

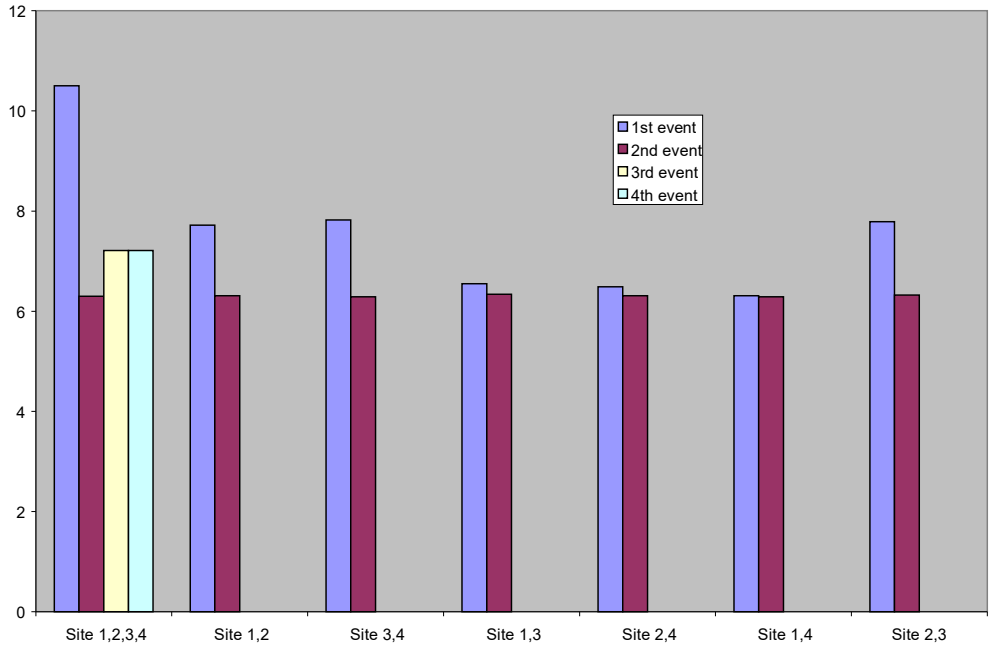

Figure 5.7 Comparison of the log stability constants for the four mutants with the 5th site absent as well as two histidines within the octarepeat. All errors are within 2 % for calculated stability constants and within 5 % for the mean of each value

In all cases, a sequential model was used to fit the data to the number of sites and their affinity for copper. All 6 mutants were fitted to a 2 site sequential model, with χ^2 values all at least 62% lower than other model possible fits. All errors for stability constants were below 5% and below 8% for calculated enthalpy of binding. Comparing the affinities of the 6 mutants with the complete octarepeat, striking differences are again apparent. For the complete octarepeat region, 4 binding events are apparent with log stability constants 10.5, 6.0, 7.0 and 7.0. When looking at the mutants with the 2 sites remaining in sequence, they all display an initial binding event around 3 orders of magnitude lower than the first event on the protein with the complete octarepeat. The mutant with sites 1,2 remaining shows 2 sequential sites with log stability constants 7.7 and 6.2. The mutants with sites 3,4 and 2,3 remaining both produce 2 events log stability constant 7.8 and 6.2. The 2 mutants with remaining histidine residues separated by 1 non-functional octarepeat, however, both display log stability constants of only 6.4 and 6.2. The mutant with the two functioning octarepeats most distal to one another suffers the greatest effect, with identical affinities of log stability 6.2. These striking differences between mutants further highlight the interaction between copper binding sites.

5.2.3 The removal of three histidine residues highlights the affinity of each octarepeat for copper (II) in the absence of binding site interactions

Figure 5.8 compares the isotherms for each of the mutants with the 5th site missing along with only 1 site remaining within the octarepeat region.

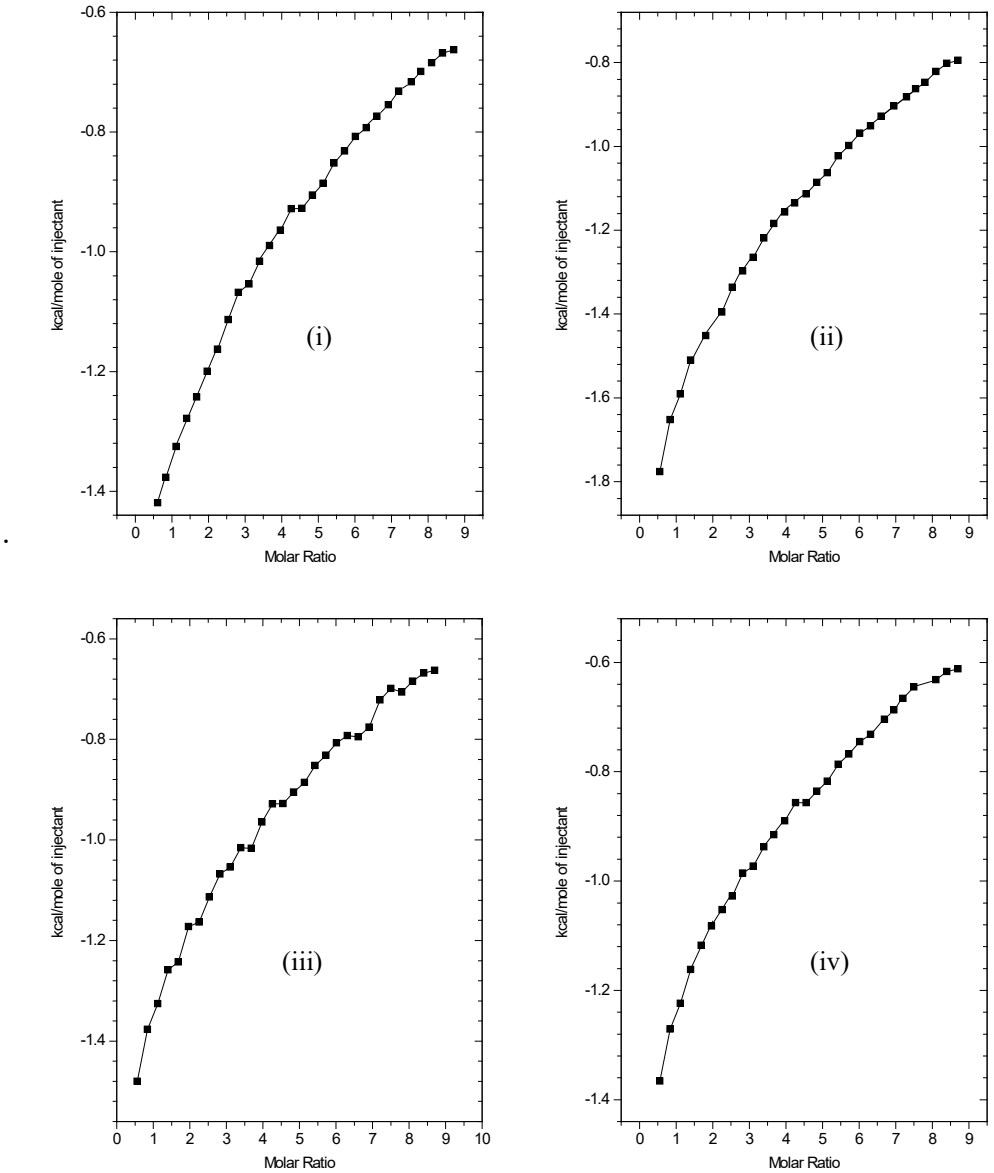

Figure 5.8 Isotherms for the titration of copper (II) : glycine into the mutants of PrP lacking the 5th site and three of the sites within the octarepeat. (i) Site 1 present. (ii) site 2 present. (iii) site 3 present. (iv) site 4 present

When looking at the isotherms from each mutant, it is immediately obvious that all are strikingly similar. All 4 isotherms show no clear inflection point and do not reach

independent saturation. Regression modelling predicts saturation at around 20 copper equivalents. This is highly indicative of a single binding event of relatively low affinity. Figure 5.9 compares stability constants of the single site mutants with those of the complete octarepeat region.

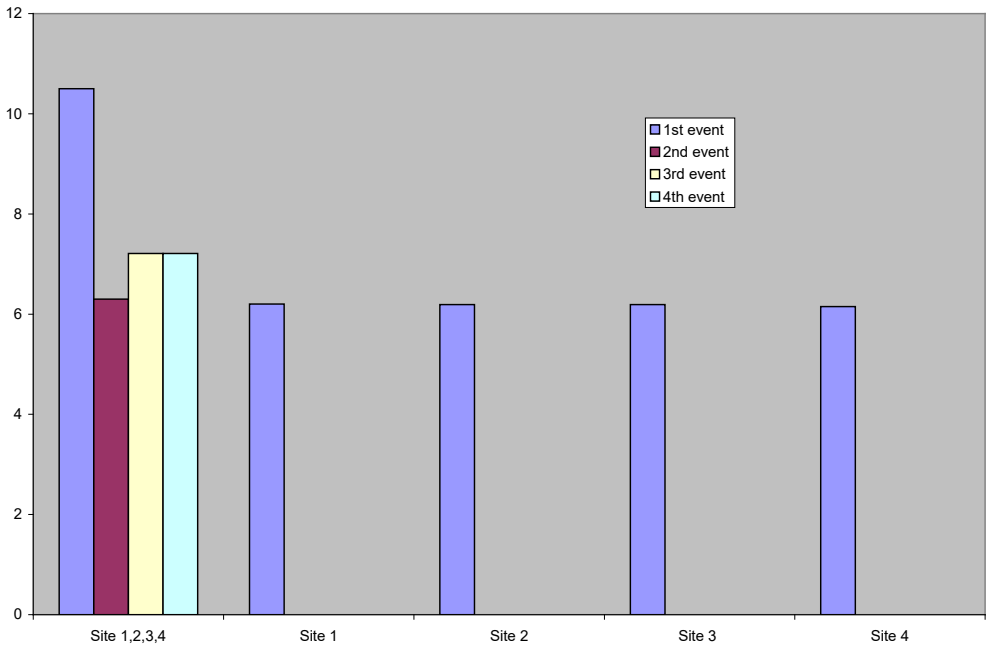

Figure 5.9 Comparison of the log stability constants for the four mutants with the 5th site absent as well as three histidines within the octarepeat with the complete octarepeat region. All errors are within 4 % for calculated stability constants and within 5 % for the mean of each value

All four mutants now produce identical affinities for copper (II) with log stability constants of 6.2 at their one site. This effectively means that each octarepeat region can independently coordinate copper with K_d in the high micromolar range (0.1 to 1 μM).

5.3 Thermodynamic Assessment of Intra Region Interactions for Copper (II) Binding to the 5th site of PrP

For the three mutant proteins focusing on the 5th site, copper (II) was added as a glycine chelate in a 4:1 glycine to copper ratio and buffered in 10mM MOPS. Protein was again buffered with the same agent and at the same pH to minimise energies of dilution. All solutions were thoroughly degassed prior to use. In order to factor in the thermodynamics of the energies of dilution, runs were carried out of chelated copper

into buffer only and subtracted from the data. ITC experiments were carried out as described in the chapter 2 and 3.

Plots of the ITC traces from each of the three proteins are shown for comparison. Affinity values for all the 3 mutants were determined for three separate experiments using a sequential sites model supplied with Microcal origin software. These models are discussed in chapter 3. A sequential model was tested and found to provide the most consistent regression fit for the data. Additionally, the use of such a model allows insight into copper (II) binding site interaction. The stability constants were then corrected to fully account for the relative contribution of chelating species within the overall equilibrium, as described in chapter 3. A data summary graph is then included as a comparison between mutants.

5.3.1 The removal of the octarepeat region allows a detailed assessment of binding interactions within the 5th site

Figure 5.10 shows isotherms for the 3 mutants with the octarepeat missing.
It is immediately noticeable that the 5th site is more than the simple sum of its parts. The mutant with the only histidine remaining at site 5 shows no evidence of copper binding, with the isotherm flat following deduction of energies of dilution. The mutant with the histidine at site 6 does show evidence of copper binding, but the isotherm is similar to that seen with single octarepeat residues and as such is of low affinity. Interestingly, the isotherms for all repeats on this mutant produced variable results, leading to the rather inconsistent isothermic data. When both sites are present, however, there is a remarkable transformation to an isotherm indicative of very high affinity binding. Table 5.1 compares the log stability constants for the three mutants as defined by a sequential model.

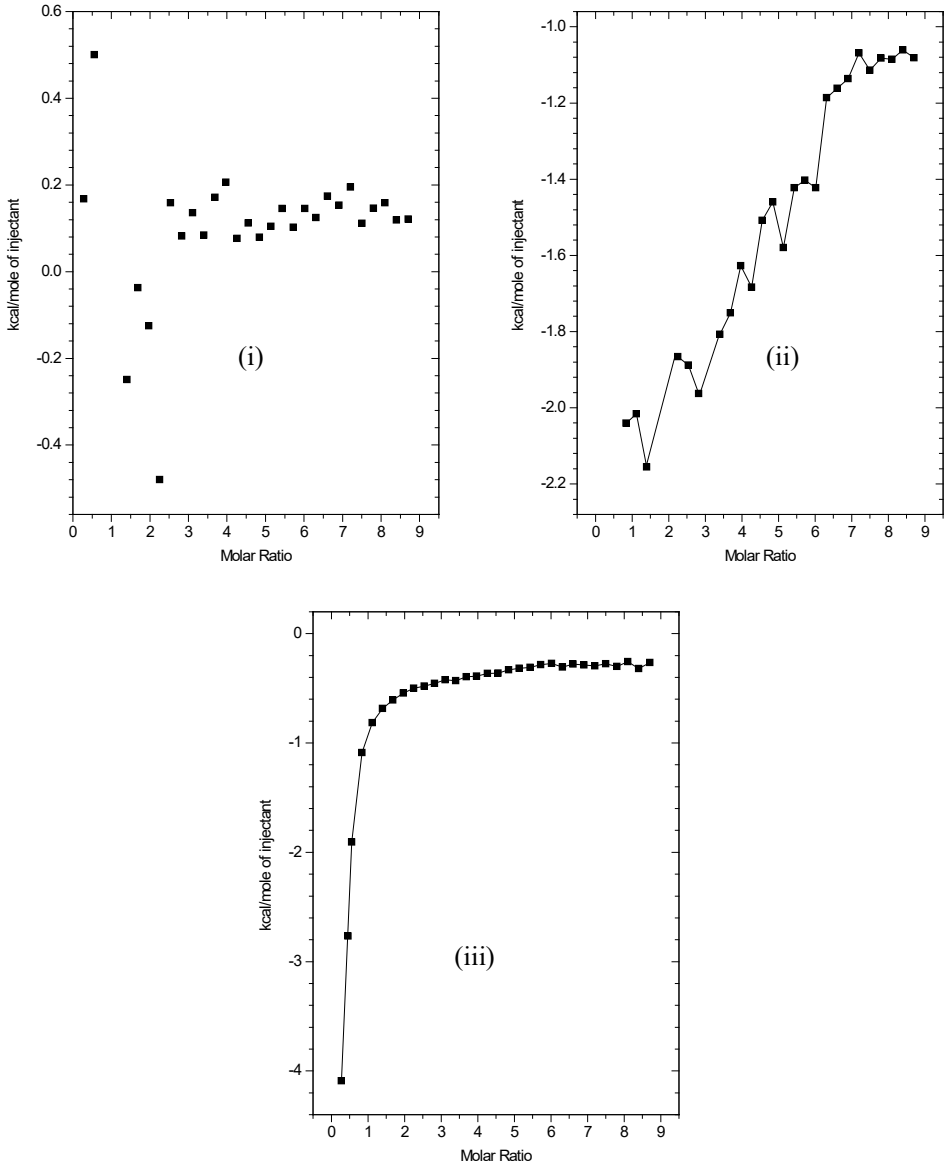

Figure 5.10 Isotherms for the titration of copper (II) : glycine into the mutants of PrP lacking the octarepeat. (i) Site 5 present. (ii) Site 6 present. (iii) Site 5,6 present. All errors are within 2 % for calculated stability constants and within 5 % for the mean of each value

Table 5.1 compares stability constants and number of sites for copper on the mutant with the 5th site present (sites 5 and 6) and mutants with one histidine within the 5th site removed (sites 5 or 6)

Mutant (site present)	LogK Stability Site 5	Site 6
Site 5,6	10.6	6.1
Site 5	n/d	n/d
Site 6	6.3	n/d

All errors within stability constants are within 5% and 2% between means

The intact 5th site shows two sites with a combined affinity of nearly log stability 17. When each site is looked at in isolation, only site 6 is able to coordinate copper (II) and with an affinity in the high micromolar range. This is striking evidence of the importance of binding site interaction for the coordination of copper to the 5th site region.

5.4 Thermodynamic Assessment of Inter Region Interactions for Copper (II) Binding to the 5th site and octarepeat regions of PrP

Considering the remarkable degree of interaction between sites within each copper binding region of PrP, it would be of interest to see if this pattern is seen between regions of the protein. In order to obtain this information, thermodynamic assessment was carried out using two mutants, both with the 5th site present but one with an octarepeat histidine adjacent to the 5th site and one with an octarepeat histidine distal to the 5th site. Figure 5.11 compares the two isotherms.

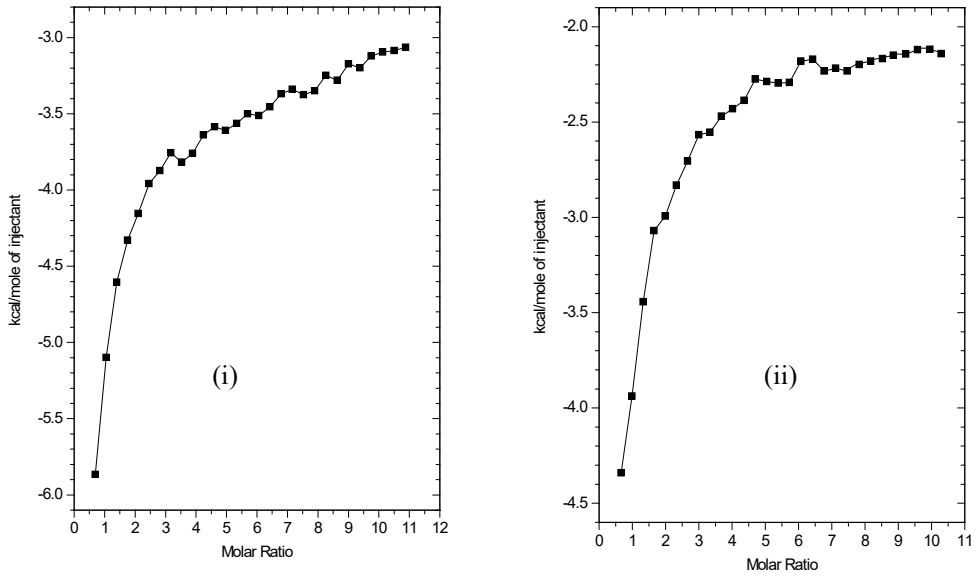

Figure 5.11 Isotherms for the titration of copper (II) : glycine into the mutants of PrP. (i) Site 4,5,6 present. (ii) Site 1,5,6

Isotherms are similar with the mutant with sites 1,5,6 present showing slightly higher copper binding stability. Table 5.2 compares the stability constants from the two mutants. Regression analysis was carried out using a 2 site sequential model.

Table 5.2 compares stability constants and number of sites for copper on the two mutants with the 5th site present (sites 5 and 6) either the first or the last histidine within the octarepeat

Mutant (site present)	LogK stability Site 1	Site 2
Site 1,5,6	10.2	7.14
Site 4,5,6	9.6	7.18

All errors within stability constants are within 5% and 2% between means

The affinity for copper within the 5th site is affected by copper coordination within the octarepeat region. Where copper (II) coordinates at the histidine most distal to the 5th site, there is a reduction in affinity within the region form log stability 10.6 to log stability 10.2. This effect is more striking, however, when the copper coordinated by the octarepeat is closer to the 5th site. When copper (II) is coordinated by the histidine at site 4, the 5th site shows log stability constant for copper of only 9.6. Also of note is the observation that the stability of copper within the remaining single octarepeat is an order of magnitude higher than that seen when the single remaining histidine coordinate copper in the absence of the 5th site. These data therefore indicate that the 5th site has a positive affect on the octarepeat but the octarepeat has a repressive affect on the 5th site.

5.5 Discussion

In order to explore the inter and intra region cooperativity suggested by earlier chapters in more detail, isothermal titration calorimetry was employed to elucidate how copper interacts within and between each PrP region. The use of single or multiple histidines to alanine mutations within each region represents a new approach to the detailed study of copper binding at each individual site. Previous studies using truncation peptides (Hornshaw et al. 1995; Miura et al. 1996; Viles et al. 1999; Jackson et al. 2001) are at risk of missing important aspects of the copper binding chemistry by not allowing for protein folding and inter region interactions.

The data from the mutants with the 5th site histidines replaced allow for a detailed assessment to be made of the copper (II) binding within the octarepeat region. The affects of these mutations are illustrated graphically in figure 5.2.

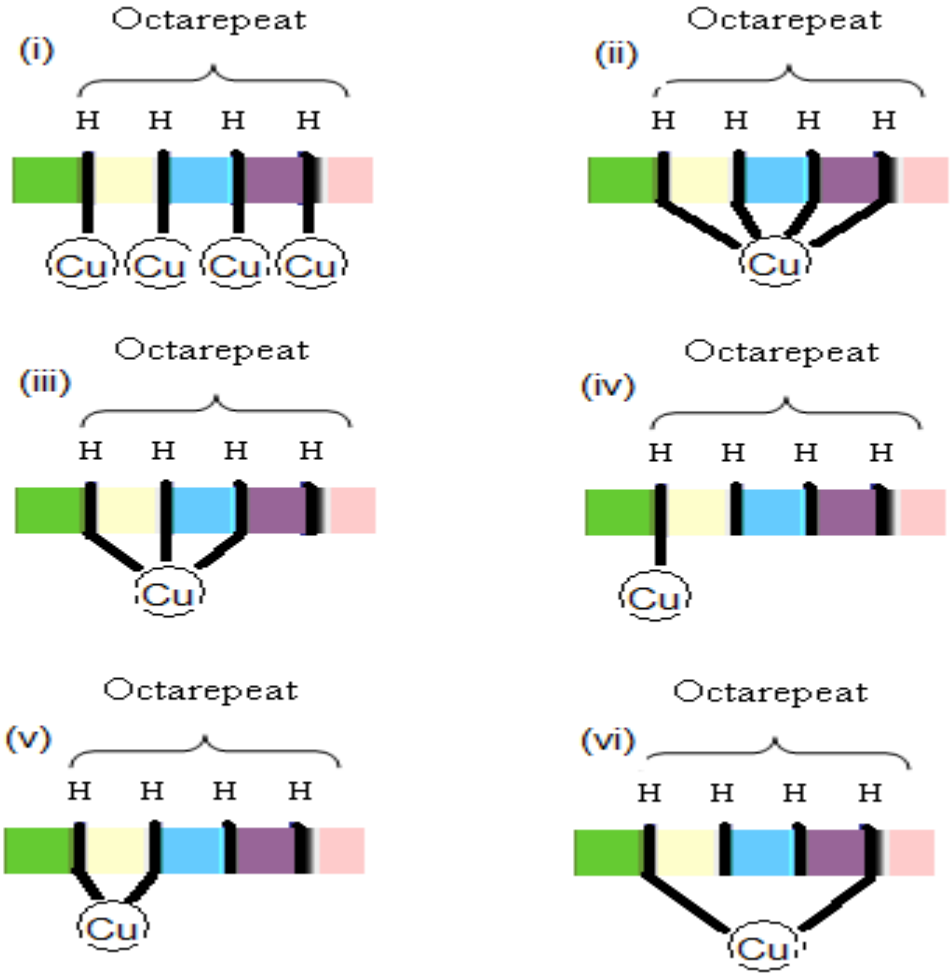

Figure 5.2 Copper coordination within the octarepeat region of full length PrP. (i) When saturated with copper (component 1). (ii) When one equivalent of copper available. (iii) When one equivalent of copper available in the mutant with one histidines remaining. (iv) When one equivalent of copper available in the mutant with one histidine remaining. (v) When one equivalent of copper available in the mutant with two histidines remaining adjacent to one another. (vi) When one equivalent of copper available in the mutant with two histidines remaining distal to one another.

When one histidine is replaced within the region, a dramatic affect on the stability of copper binding at low copper occupancy is apparent. When compared to the intact octarepeat region, the high affinity event in the 0.1 nM range is no longer detectable and is replaced with an event with an event 10-100 nM range. This represents a significant

reduction in the stability of copper (II) binding during the first equivalent of the ion. Previous structural work by Chattopadhyay *et al*, 2005 revealed a complex, multi-stage coordination of copper (II) within the octarepeat region that was dependent on copper occupancy. They showed that, at a copper occupancy of one or below, all four octarepeat histidines were responsible for the coordination of one metal ion by forming a 4N binding arrangement. The group predicted that this 'component 3' binding mode would be of significantly higher stability relative to binding modes at higher copper occupancy. The affect of this remarkable feature of the octarepeat region is highlighted by the thermodynamic data. With one histidine and therefore one octarepeat region unavailable for copper (II) coordination, the highly stable 4N arrangement is replaced by a 3N or 3N1O configuration, resulting in a reduction of binding stability by at least 2.5 orders of magnitude. As the ability of the octarepeat region to bind copper (II) in this multi-histidine mode is utterly dependent on dramatic protein folding around the ion (Aronoff-Spencer et al. 2000), it would be expected that the location of histidines within the octarepeat region is critical to the stability of the copper (II) site. This is exemplified by the thermodynamic data. In mutants with the remaining histidine residues located sequentially, the first binding event is of significantly higher stability than is the mutants where the sequence of remaining histidines is broken. Where the missing histidine is within the sequence of histidines, the reduction in the stability of the first copper (II) site is reduced by 3.5 orders of magnitude.

Further evidence for the component three binding mode involving multiple histidine coordination is apparent in the mutants with two octarepeat histidines replaced. When the two remaining histidines are in sequence, the stability of the first binding event (~50 nM) is almost identical to that seen in the mutants with just one histidine removed and with two of the histidines in sequence. This provides strong evidence that the initial event involves both remaining histidine residues in a likely 2N2O configuration with the oxygen ligands coming from water molecules present in solution. This configuration and stability is strongly suggestive of a primary contribution from the two remaining histidine imidazoles. In contrast, when the remaining histidines are separated by a mutated octarepeat, the stability for the first copper drops into the 500 nM nanomolar range. As the stability is higher than that expected for a single octarepeat (see below), there must be some surviving inter octarepeat cooperativity. This can be explained by findings that show an intermediate binding mode within the intact octarepeat

(Chattopadhyay et al. 2005). This 'component 2' mode involves not only an imidazole nitrogen but also an exocyclic nitrogen from one other histidine residue and two oxygens from water molecules. Only existing for an instant in the complete region when copper occupancy is increasing, this mode of copper (II) coordination is usually extremely difficult to resolve (Burns et al. 2002). This mutant with the two remaining histidines separated may then provide a model for the study of this intermediate binding mode. Further evidence for this type of coordination comes from the fact that increasing the distance between histidine residues further produces two identical copper (II) binding events, with a stability almost identical to two individual octarepeats.

The single octarepeats display a stability of binding for copper (II) that is identical irrespective of where they are located. This provides good evidence that it is the inter octarepeat interactions that are responsible for the high degree of stability for copper (II) at low occupancy. The affinity of each octarepeat for copper (II) very closely matches that previously reported (Walter et al. 2006). This single copper to single octarepeat binding mode is described in the literature at 'component 1' (Chattopadhyay et al. 2005) and consists of a primary coordinating imidazole ligand with contributions from deprotonated amides from adjacent glycines and a carboxyl from the last glycine in the HGGGW sequence. This would naturally form an equatorial arrangement.

Copper binding within the 5th site region has been the cause of much debate within the prion field. By removing the affect of the octarepeat region through the mutation of all four histidines to alanine, a detailed assessment of the contribution of the two 5th site histidines can be made. The most striking observation from the thermodynamic data presented here is that binding within the 5th site appears to be more than the sum of its contributing parts. By removing the histidine at location 110, it is clear that the histidine at location 95 is unable to coordinate copper (II) independently. By reversing this process and looking at the site at 110, only very low nanomolar binding is apparent. When compared to the intact 5th site region, however, two atoms of copper (II) are coordinated with one in the 0.1 nM range and one in the 1 μM range. This must surely represent the most striking example yet of intra region cooperation on PrP. The best source of comparison for any data relating to the 5th site region has to be from John Viles of Queen Mary's University in London. His group has devoted much of its resources into unravelling the mysteries of 5th site copper coordination. Work by the

group confirms my findings of the relative importance of the two histidines, with the 110 site providing the primary coordinating ligand (Klewpatinond and Viles 2007). The observation that the copper binding at either site is so dramatically different from that when both sites are present is very difficult to explain but is likely to involve structural affects from either the mutation of histidine to alanine or copper – copper interactions. This effect will be exaggerated greatly by the presence of multiple proline residues with the 5th site region. Of interest, and in support of using full length protein for binding studies, they showed that the relative stability of each histidine for copper was dependent of peptide chain length.

Data from previous chapters suggested an interaction between the two regions of PrP when coordinating copper. To investigate this phenomena, mutants with the 5th site present and one site within the octarepeat present either close or distal to the 5th site are utilised. It is clear from the data that the presence of copper within the 5th site has a significant effect on copper binding within the octarepeat. The stability of copper binding within a single octarepeat region increases by an order of magnitude when copper is present within the 5th site. Also of note is that copper binding within the octarepeat region appears to reduce the stability of the copper (II) within the 5th site. This affect is dependent on the distance of the octarepeat site from the 5th site. Where the remaining copper site is close to the 5th site region, a relatively large reduction in 5th site stability is observed, approaching an order of magnitude. Where the remaining site is distal, from the region, a very small reduction in 5th site stability is apparent. This effect can be seen in studies involving the entire protein (Davies et al. 2009) and involves the affects of dramatic structural changes in the presence of copper within the octarepeat region. This is evidenced by the fact that the affect is more pronounced in the mutant with the remaining histidine in close proximity to the 5th site. This is also strong evidence for why the 5th site, when in isolation, can bind 2 copper atoms but only 1 when the octarepeat region is present.

CHAPTER SIX

The Electrochemistry of Metal Bound PrP

A clear factor in determining the physiological role of PrP has to be the functional implications of copper when bound to the protein. Most proteins that bind copper offer some protection against copper's toxic effects and many cupro-proteins use copper to catalyse redox reactions. There is a large body of data indicating a catalytic role for copper bound PrP (Brown et al. 1999; Brown et al. 2001; Wong et al. 2001; Thackray et al. 2002; Cui et al. 2003; Hutter et al. 2003; Jones et al. 2005; Stanczak and Kozlowski 2007; Treiber et al. 2007) but this work concentrates on indirect evidence such as enzyme activity assays. Data concerning the electrochemistry of such activity is harder to find, although some does exist. It has been shown that copper is reduced from Cu2+ to Cu+ on binding to PrP (Miura et al. 2005). Another study produced evidence that the fifth site was redox active by employing cyclic voltammetry on copper-bound PrP fragments encompassing the fifth site region (Shearer and Soh 2007). Their results clearly demonstrate a quasi-reversible reaction where the fifth site is able to cycle electrons without becoming permanently oxidized or reduced. A separate study also demonstrated a quasireversible reaction for copper-bound peptides corresponding to the octarepeat region (Hureau et al. 2006). Together, these studies suggest that all copper centres on the protein are able to undergo cyclic redox chemistry. In line with this evidence, an independent study showed that PrP does not redox-silence copper (Nadal et al. 2007). They found that the protein was able to dramatically reduce the amount of hydroxyl radicals present in a Cu2+/ascorbate/oxygen system without affecting hydrogen peroxide levels. Another study looked at the ability of PrP to generate the free radical superoxide (Kawano 2007). The study provides compelling evidence that copper-bound PrP is able to catalyse the formation of superoxide and become damaged irreversibly by the radical.

Previous attempts to directly study the redox activity of PrP, including those above has centred on traditional electrochemical systems whereby soluble protein is analysed in free solution contained within a conventional 3 electrode cell system. These systems have severe limitations including having to correct for the effect of protein migration through the solution on varying the electrode potential. These systems usually produce a

very high level of background, making precise determination of voltammetric peaks difficult. Additionally, large amounts of protein at relatively high concentrations are required. Combining copper to protein in solution can also add complications and requires large volumes of protein to carry out the necessary number of experiments with varying copper concentrations. It was therefore important to first design and optimise a system which could overcome these issues by adsorbing the protein to the working electrode. This would have the affect of eliminating migratory complications and dramatically reducing the volume of protein required. Additionally, copper equivalents can be easily added to the protein before being immersed into the electrochemical cell.

6.1 Electrochemical System Design and Optimisation

Cyclic voltammetry (CV) was employed to gain insight into the redox properties of PrP. The CV system and cell was set up as described in chapter 2. Initial experiments were carried out using a 5 mm diameter edge plane pyrolytic graphite working electrode. PrP has been shown to adhere strongly to mineral surfaces (Johnson et al. 2006) due to its strong positive charge originating from arginine and lysine residues at neutral pH. A 5 mM MES/Tris buffer combination was used to buffer the system at pH 7 as this proved to contribute minimal background to the voltammagram. The working electrode was prepared as previously described and immersed in the voltammetric cell to record background readings. The electrode was then immersed in apo-protein or copper bound protein for 1 minute before being rinsed thoroughly in buffer to eliminate any loosely adsorbed protein. The electrode was then replaced in the CV cell and sweeps recorded between 450 mV and -450 mV. Figure 6.1 shows the voltammagram obtained at 0.1 mV/s at pH 7. A stable redox cycle is observable over background noise, but it is unclear from the voltammagram just how much signal is buried within the background. Further optimisation revealed no improvement in signal and different materials were therefore tested to reduce background.

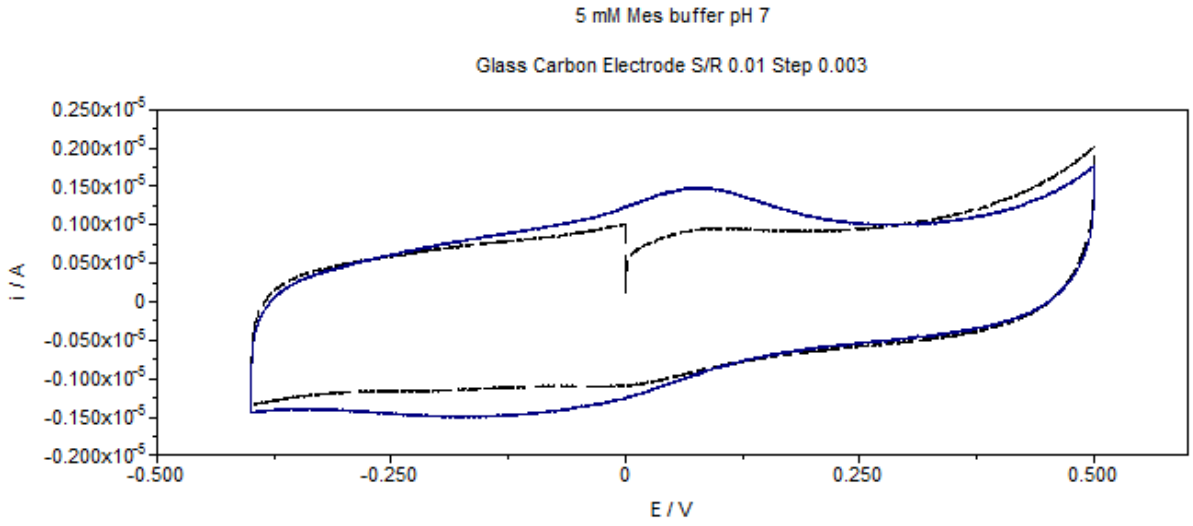

Figure 6.1 Cyclic voltammagram of mPrP wildtype refolded with copper (II) (blue line) at a scan rate of 0.01 V/s using a 5 mm glass carbon working electrode against standard reference SCE. The black line represents no protein adsorbed and indicates background noise.

Where a high degree of sensitivity is required, highly inert minerals have been shown to dramatically reduce background noise (Bard and Faulkner 1980). A 3 mm boron doped diamond electrode was therefore chosen for further optimisation. Protein was adsorbed to the electrode using its electronegative properties as before. All other experimental conditions were the same as for the glass carbon system. Figure 6.2 shows the voltammagram for mPrP adsorbed onto the boron doped diamond electrode.

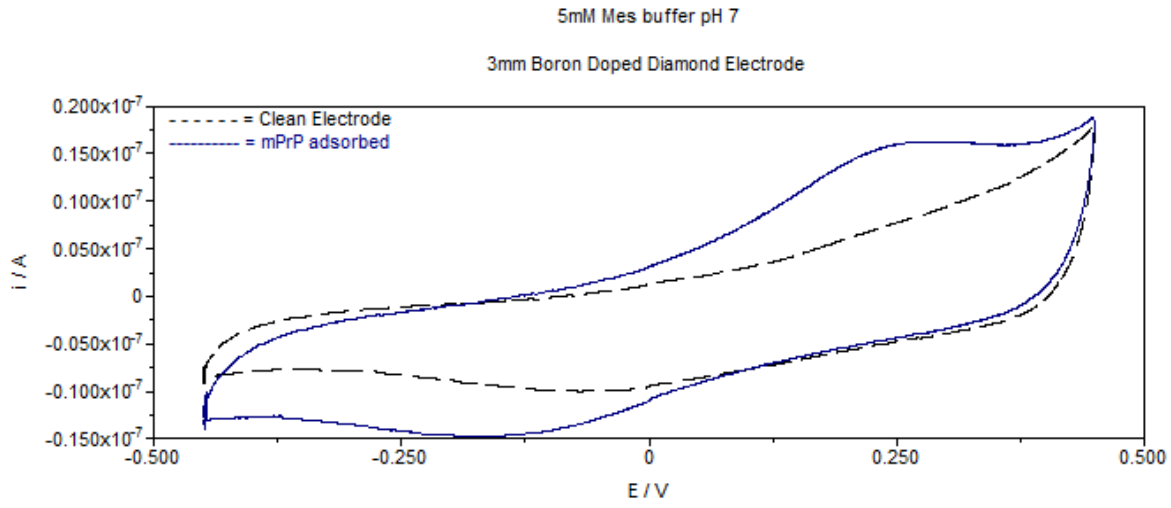

Figure 6.2 Cyclic voltammagram of mPrP wildtype refolded with copper (II) (blue line) at a scan rate of 0.01 V/s using a 3 mm glass carbon working electrode against standard reference SCE. The black line represents no protein adsorbed and indicates background noise.

It is clear from the voltammagram that there is a significant reduction in background noise when using the boron doped diamond system. All signals were fully reversible and reproducible so this system was chosen over others tested.

6.2 The Electrochemistry of Copper Bound Wildtype PrP

To ensure that the protein is stably adsorbed to the electrode, so complications such as migration are eliminated, a range of experiments were carried out at different scan rates, using wildtype mPrP adsorbed to the 3 mm boron doped diamond electrode against SCE. Figure 6.3 shows the results from this analysis.

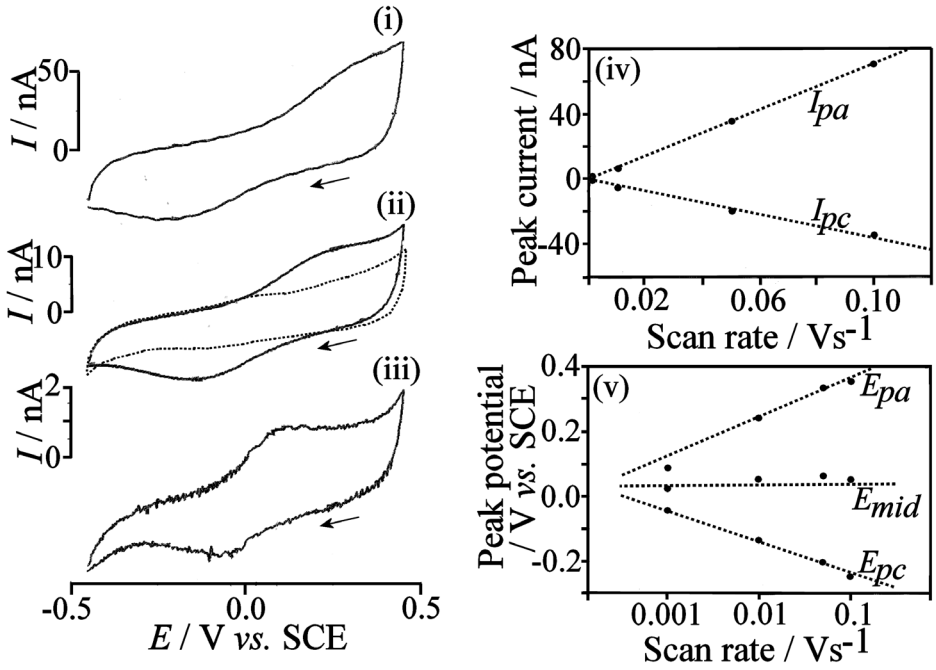

Figure 6.3 Cyclic voltammograms recorded at scan rates of (i) 50 mVs^{-1}, (ii) 10 mVs^{-1}, and (iii) 1 mVs^{-1} for the reduction and re-oxidation of copper refolded mPrP adsorbed onto a 3 mm diameter boron-doped diamond disc electrode and immersed in 5 mM Mes/tris buffer solution at pH7. The dashed line indicates the background signal without protein. (iv) Plot of the peak current versus the scan rate. (v) Plot of the peak potentials versus the scan rate (in logarithmic scale).

Figure 6.3 (i) to 6 (iii) shows a typical sequence of voltammetric data and the plot in figure 6 (iv) clearly demonstrates a linear relationship between peak current and scan rate. This confirms a permanently surface bound protein and electron transfer directly into the protein bound copper. The effect of the scan rate on the peak potentials is shown in Figure 6 (v). The characteristic logarithmic dependence is consistent with a

electron transfer rate limited process and a fit of the corresponding equation for the peak potential (Bard and Faulkner 2001) give good agreement with $\alpha = 0.5$ and $k^0 = 0.05\ s^{-1}$.

$$E_p = E_{mid} + \frac{RT}{\alpha F}\ln\left(\frac{RT}{\alpha F}\frac{k^0}{v}\right) \quad (1)$$

In this equation the peak potential E_p is correlated to the midpoint potential, E_{mid}, the gas constant, R, the absolute temperature, T, the transfer coefficient, α, the Faraday constant, F, the standard rate constant for electron transfer, k^0, and the scan rate, v. The copper bound protein contains 5 copper centres, 4 localised relatively closely together in the octarepeat unit and 1 within the 5th site of PrP. The charge under the voltammetric response, ca. 255 nC, can be investigated and converted into the approximate area per protein adsorbed onto the boron doped diamond surface. This calculation gives a very realistic area of 4.7 nm × 4.7 nm for each Cu-PrP molecule (molecular weight 23kDa) assuming that 5 copper centres are reduced in one electron processes (5 electrons consumed per protein). These 5 copper centres may be electronically distinct but coupled and therefore may not be individually resolved. The reversible or midpoint potential for this process is 0.03 +/- 0.01 V vs. SCE, which is not too different when compared to the reversible potential observed for Cu(II/I) coordinated to fragments of the prion protein (Hureau et al. 2006; Hureau et al. 2008).

6.3 The Distribution of PrP on the Electrode Surface

In order to confirm the calculated surface distribution and stability of PrP on the boron doped diamond surface, atomic force microscopy (AFM) was utilised to image the actual protein on the mineral surface. The AFM measurements were carried out as described in chapter 2. Figure 6.4 shows the forced volume map for a section of the boron doped diamond surface. Force-distance curves were recorded between a conventional AFM cantilever and gold tip and the PrP coated surface at a loading rate of up to 6 nN/s. The adhesion force histogram revealed a bimodal distribution with average rupture forces of 4.2 ± 0.23 nN. This provides good evidence of a highly stable association between the protein and the boron doped diamond surface.

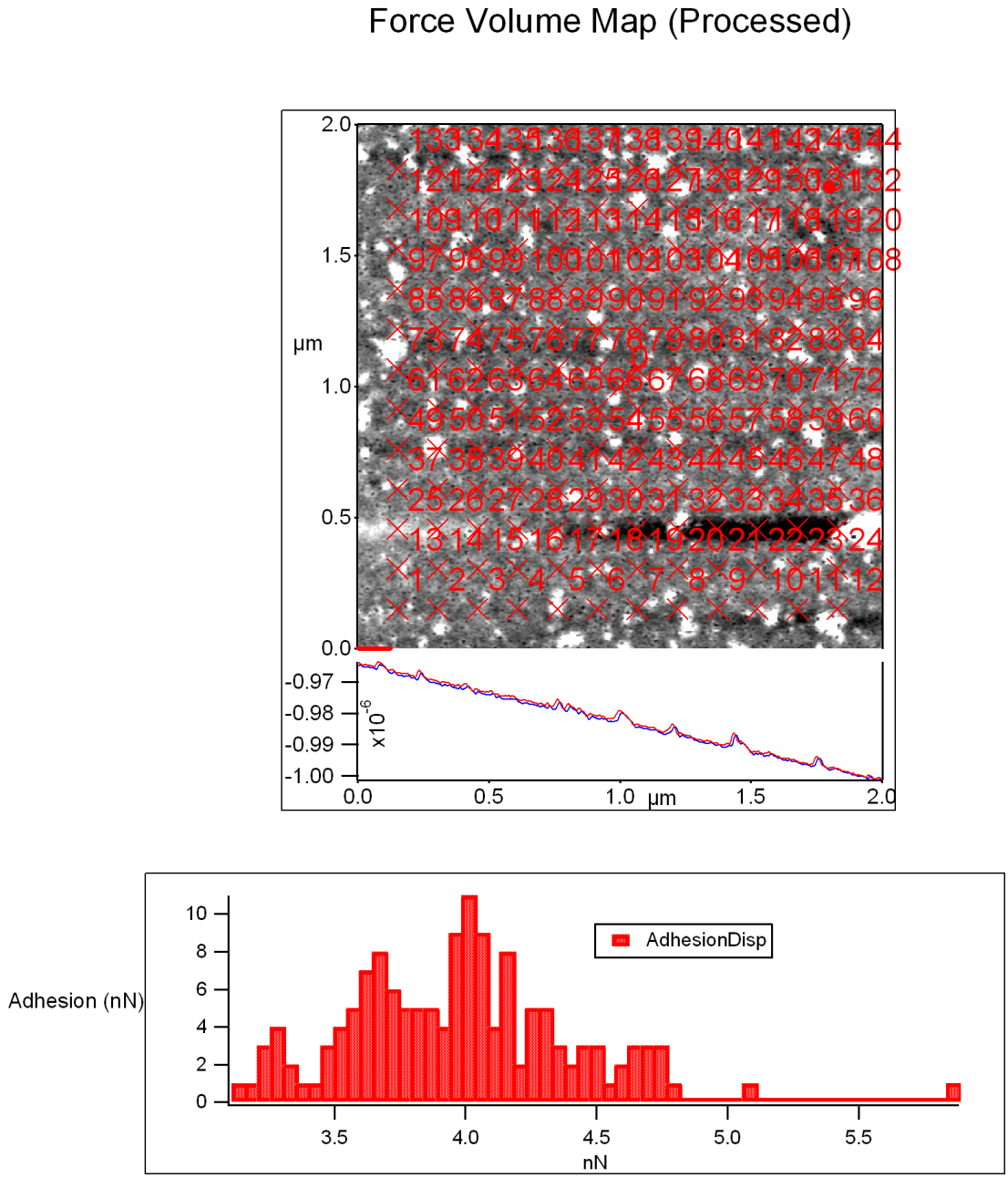

Figure 6.4 Forced volume map for a section of the boron doped diamond surface recorded between a conventional AFM cantilever and gold tip and the PrP coated surface at a loading rate of up to 6 nN/s.

In order to assess the distribution of the protein across the boron doped diamond surface, imaging of 2 µm sections of the surface were carried out in a forced volume interference mode. Figure 6.5 shows the image map for the scanned section. The white colouration over the image represents the protein with darker areas containing less material. The image clearly shows a random and uneven distribution of PrP with large clusters of protein appearing as the white areas at a height of > 2 nm. This was unexpected as there should be a linear charge across the diamond surface with no bias

towards protein adhesion. The only explanation for such a random distribution of protein is that the boron doped surface must contain imperfections leading to charge bias and differential surface adhesion properties. Analysis of further sections revealed a similar pattern of protein distribution, with a calculated average area coverage per protein of 4.8 nm^2. This represents a near perfect match for the area occupation derived from the CV data. Figure 6.6 shows a three dimensional representation of the adsorbed protein, further evidencing the clusters of protein rather than a uniform distribution. Despite this distribution, the very close match for the protein area occupied between active and imaged PrP shows that even the areas of high protein density contain mainly redox active PrP.

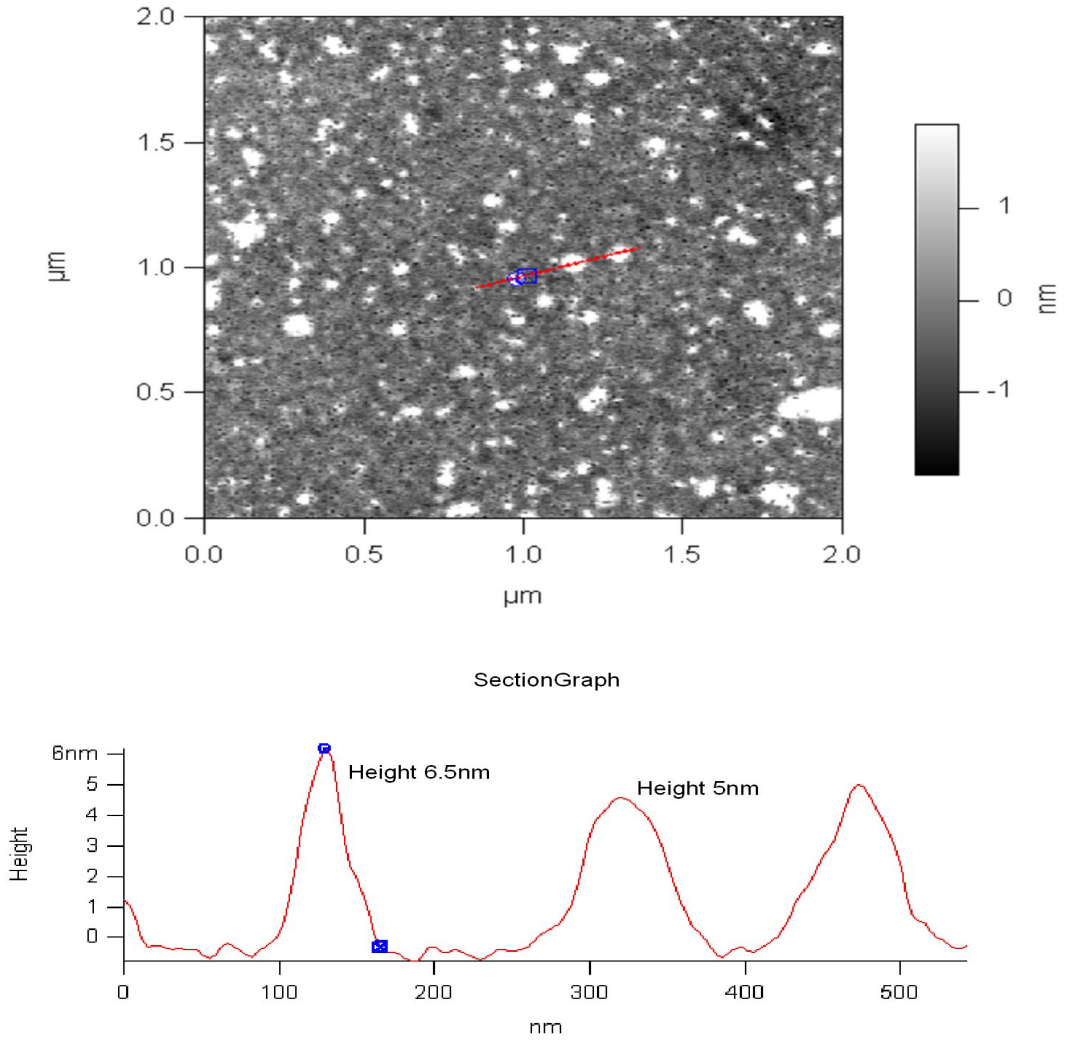

Figure 6.5 Forced volume interference map for a section of the boron doped diamond surface recorded between a conventional AFM cantilever and gold tip and the PrP coated surface at a loading rate of up to 6 nN/s

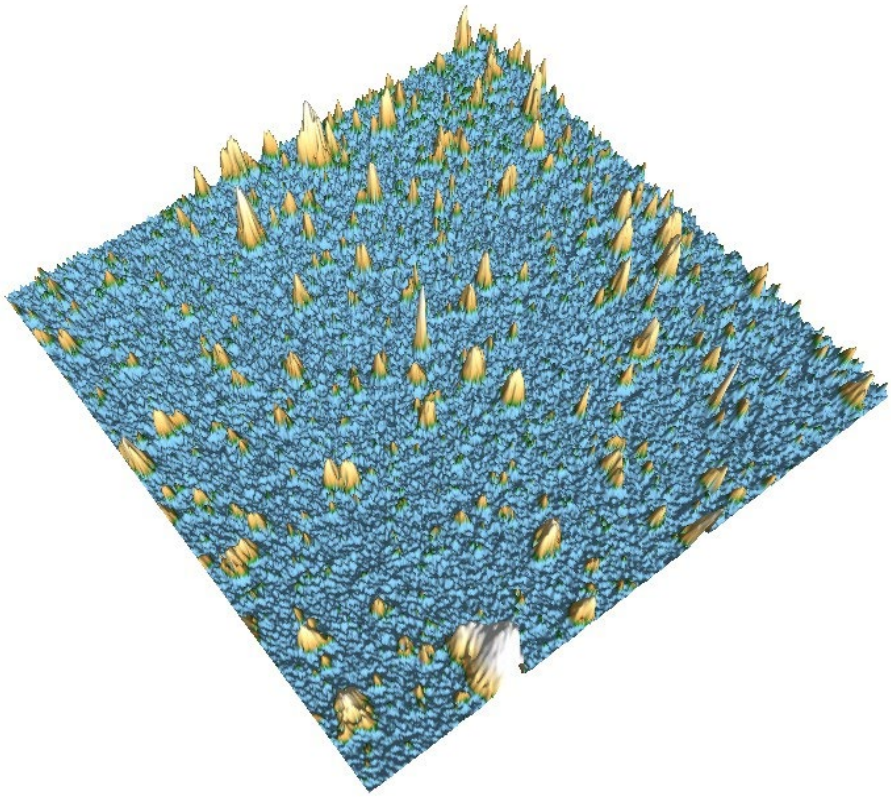

Figure 6.6 Three dimensional forced volume interference map for a section of the boron doped diamond surface recorded between a conventional AFM cantilever and gold tip and the PrP coated surface at a loading rate of up to 6 nN/s

6.4 Region Specific Redox Activity

Confirmation of stably associated PrP to the boron doped diamond surface allows for a more detailed analysis of the redox centres of the protein. In order to achieve this, the histidine mutants discussed in previous chapters are utilised to assess the relative contribution of each copper binding centre of PrP to the redox chemistry of the protein. The mutants of mPrP lacking either all the histidines in the octarepeat region (5^{th} site only), the 5_{th} site (octarepeat only) and both the 5_{th} and octarepeat (PrP-null) are used to assess region specific dependency on redox processes. Figure 6.7 shows the voltammograms for the 3 proteins. The wildtype protein (blue line) shows the characteristic reversible cycle with a redox potential of 0.03 ± 0.01 V vs. SCE. The octarepeat region shows a very similar voltammagram, but the 5^{th} site and null are dramatically different. There is no signal evident on the null protein and the 5^{th} site shows a more positive oxidation peak with a mid point potential of 0.100 ± 0.02 V vs SCE. The copper centre of the 5^{th} site therefore shows evidence of a significantly altered electron transfer kinetics.

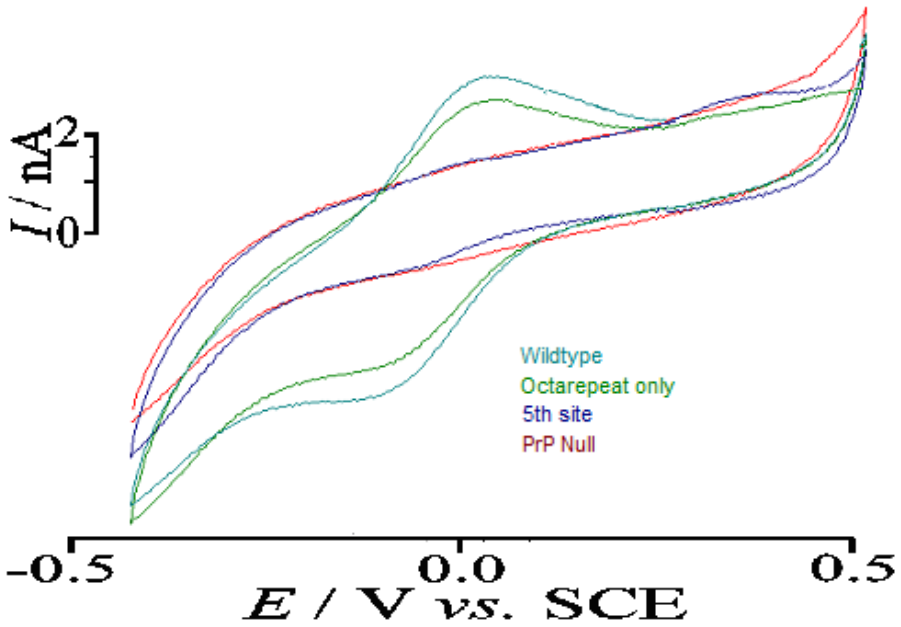

Figure 6.7. Cyclic voltammagram comparing various mPrP mutants with wild type protein at a scan rate 1 mV/s. The mutant labels refer to the positions where histidine residues have been replaced with alanine therefore abolishing copper binding in these regions. Null refers to the protein where all histidines in the copper binding N-terminus have been replaced with alanine.

Interestingly, despite an altered oxidation peak for the 5th site, the oxidation peak for the octarepeat is reduced relative to wildtype when the 5th site is absent. This would indicate a possible inter region electron transfer as the single copper within the 5th site is unlikely to contribute to both peaks. To investigate this further, the integrated peak charge for each mutant is calculated and listed in table 6.1.

Table 6.1 Comparison of the integrated peak charges (forward reaction) from wildtype PrP, octarepeat only, 5th site only and PrP Null as obtained from cyclic voltammetry.

Protein	Mid Point Potential (V vs SCE)	Integrated Oxidation Peak Charge (nC)
Wildtype mPrP-Cu	0.03 ± 0.02	255 ± 11
mPrP-Cu No 5th Site	0.03 ± 0.02	201 ± 5
mPrP-Cu No Octarepeat	0.10 ± 0.03	13 ± 1
mPrP-Cu Null Histidine	N/A	Not detected

When 5 atoms of copper are bound to the protein (4 in the octarepeat and 1 in at 5th site), an integrated charge of 255nC can be calculated from the forward reaction. When copper binding at the 5th site abolished, a drop equivalent to 20% is observed. When copper binding in the octarepeat is nullified, however, a 95%
decrease in charge is observed. This suggests that electron transfer at the 5th site is facilitated by the coppers present within the octarepeat and it is these coppers that are responsible for the protein's apparent ability to cycle electrons when adsorbed to an electrode system.

To investigate the individual copper centres within the octarepeat region in detail, the mutants with the 5th site removed along with individual histidines within the octarepeat. These mutants are discussed in more detail in previous chapters. Figure 6.8 shows the voltammograms for these mutants.

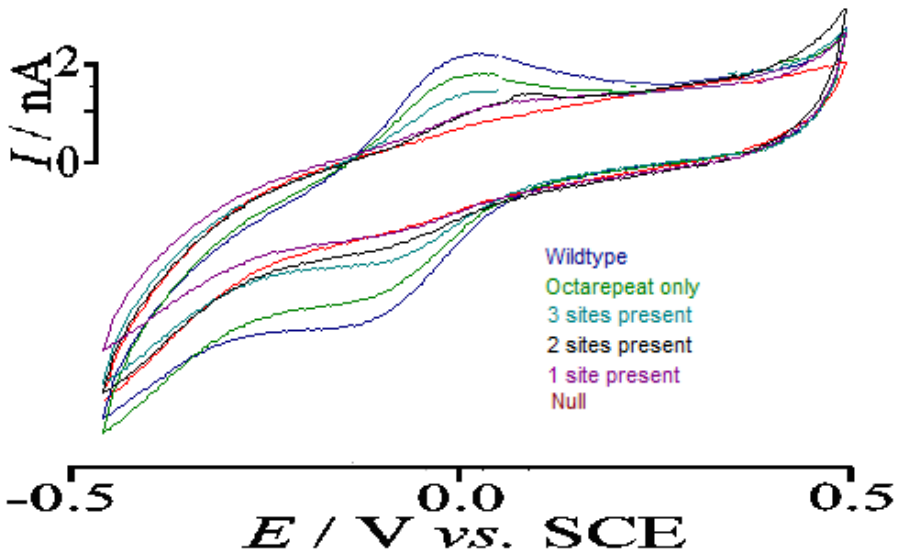

Figure 6.8. Cyclic voltammagram comparing various mPrP mutants with wild type protein at a scan rate 1 mV/s. The mutant labels refer to the number of histidine residues remaining within the octarepeat. Null refers to the protein where all histidines in the copper binding N-terminus have been replaced with alanine.

It is clear from figure 6.8 that all 4 histidines must be present within the octarepeat region for stable redox cycling. Redox peaks for the mutant with 3 sites present are ~50% that of wildtype protein. When only 2 sites remain, severe disruption of redox cycling is observable, with redox signals barely evident over background noise. As before, the null protein shows no apparent redox signal. This significant disruption of redox cycling within the octarepeat region indicates that removing a single copper centre has an affect greater would be expected for a 25% reduction in available redox centres. This is strong evidence for the channelling of electrons through the octarepeat between copper centres.

6.5 PrP Redox Activity is Copper Specific

Where a electrochemical system displays such clear evidence for redox function, it is important to establish whether the process is dependent on a specific metal centre or if any redox active metal will confer redox capability. This then takes what is an interesting observation to the potential for a functional role. In order to achieve this, the effect of manganese was assessed on the protein. Wildtype mPrP that had been refolded in either copper or manganese were examined as well as copper refolded protein that had been exposed to manganese or manganese refolded protein that had been exposed to copper. There was no obvious difference between the later two conditions so only one trace is shown. Figure 6.9 shows the voltammograms obtained with a scan rate of 1 mVs^{-1}. The voltammagram shows the back ground as a dotted line and a clear difference can be observed that can be attributed to reduction and oxidation by the manganese or copper centres. The peak current ratio on protein containing copper only was 1, suggesting a fully reversible reaction for this condition. Where protein with only manganese was tested, the oxidation peak was significantly larger than the corresponding reduction, suggesting an irreversible or partially irreversible oxidation of manganese. Protein that had been exposed to both manganese and copper showed a significantly smaller oxidation/reduction corresponding to the copper centres, suggesting that manganese had displaced some of the bound copper and thus reduced the copper redox signal. The oxidation signal produced for the wildtype copper refolded protein corresponded to an integrated peak charge of 255 ± 11 nC. For the

copper/manganese refolded protein, this was reduced to 110 nC ± 7 nC for the copper signal and 90 ± 4 nC for the manganese signal. The manganese only protein showed an integrated peak charge of 125 ± 10 nC. As this charge is directly related to the amount of metal available for electron transfer on the protein, it would appear that three atoms of copper are displaced by manganese in the copper/manganese refolded protein.

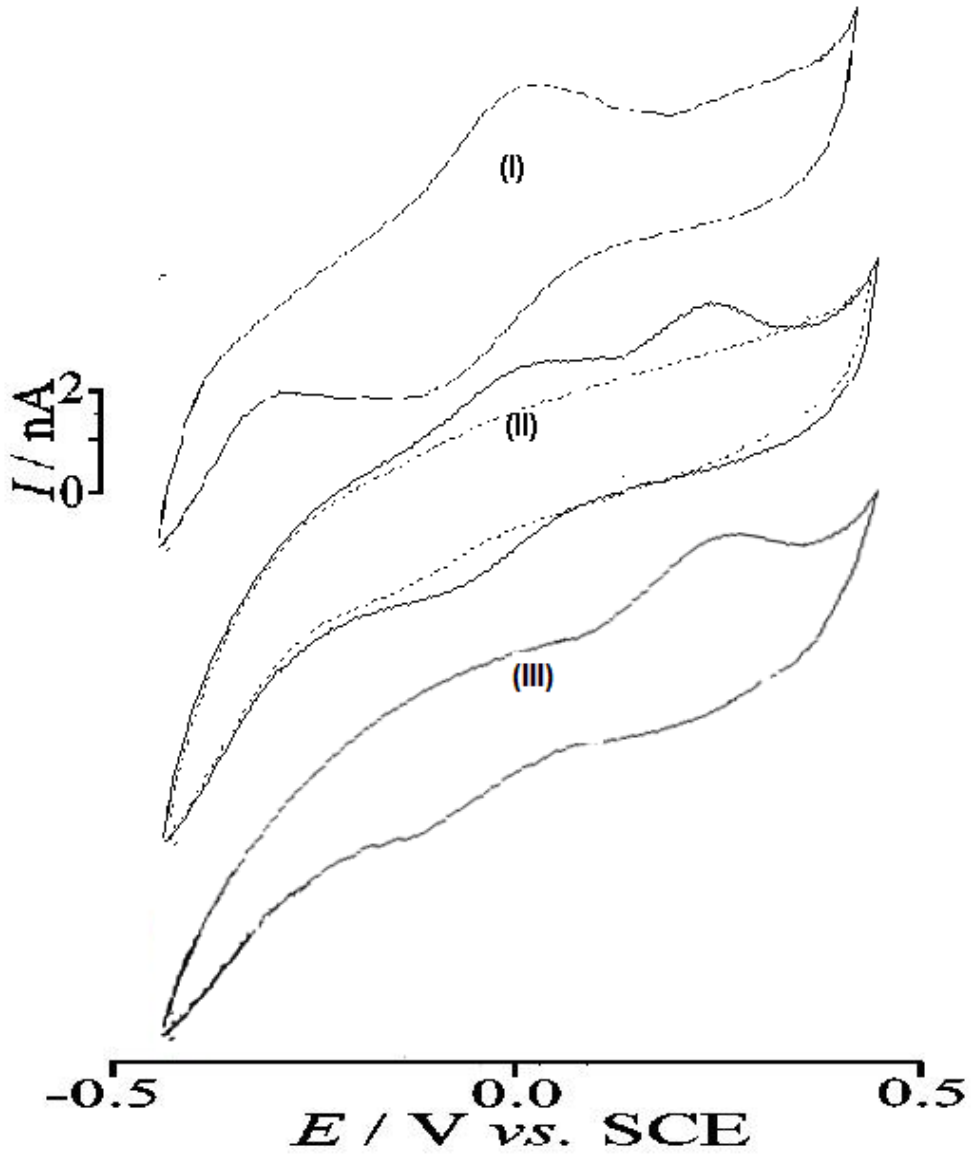

Figure 6.9 Cyclic voltammagram comparing wildtype mPrP refolded in (I) Copper, (II) Copper and manganese (III) manganese. The protein was adsorbed onto a 3mm boron doped diamond electrode by incubation in 20µM protein solution pH 7 for 60 seconds. The scan rate used was 1mV/s in an oxygen excluded buffer of 5mM Mes/Tris, pH 7 25˚C. The dashed line on scan (II) represents the background signal where protein without metal is adsorbed to the electrode.

The fact that only copper bound PrP shows stable redox cycling is good evidence that the redox capability of PrP is dependent on copper (II), the metal generally considered

to be the proteins natural binding partner. This is evidence of a potential physiological redox role for PrP.

6.6 Discussion

One of the most heated topics of debate concerning the prion protein's function is whether or not it is able to act in an antioxidant role. Much recent evidence has been contradictory, with studies confirming antioxidant activity (Brown et al. 1999; Brown et al. 2001; Wong et al. 2001; Thackray et al. 2002; Cui et al. 2003) and other studies showing this not to be so (Hutter et al. 2003; Jones et al. 2005). The need to develop a technique that can be built on to contribute to this argument is therefore desirable. I have applied a new technique to the study of metal binding to PrP which may aid further a solution to this question. Although previous electrochemical work exists on small peptide fragments analogous to single octarepeat copper binding regions (Hureau et al. 2006; Hureau et al. 2008), no study has used the entire protein stably adsorbed to the electrode surface. By adsorbing PrP to a diamond electrode and subjecting it to cyclic voltammetry, I have shown without doubt that the protein is capable of exchanging electrons when bound to copper. This electrochemistry is largely dependent on the copper bound to the octarepeat region but also involves the 5^{th} site, but not independently. The data clearly shows that the 5^{th} site is involved with channelling electrons into the octarepeat region, which needs to be complete and correctly folded to take part in this 5^{th} site oxidation and subsequent reduction. This is fascinating and may lend extra support to the finding that the octarepeat region protects the 5^{th} site from oxidative damage (Nadal et al. 2007). This appears to be further evidence for the interaction between the two copper binding regions. The redox cycling is limited by the rate of electron transfer and is fully reversible, indicating that the wildtype protein is unaffected by continuous oxidation and reduction. Despite the proposed square planer copper coordination geometry, copper (I) and copper (II) are able to remain stably bound to the protein during cycling. Previous work has demonstrated this property (Hureau et al. 2006). The calculated area taken up on the electrode by the protein, assuming 5 redox active coppers bound to each, gives a very realistic $4.7nm^2$ and experiments with various mutants lacking one or more copper further prove the results. AFM imaging also demonstrates this. The mid point potential of 0.03 mV would mean in vivo conditions would favour a redox able state. Configurational and structural

effects due to the adsorption onto the electrode are clearly identified by the AFM imaging and calculated charge per redox centre confirms that adsorbed PrP is active on the surface of the electrode.

Many blue copper proteins display some sort of redox activity (Dhillon et al. 2009). A fully reversible redox property, however, is usually reserved for type I blue copper sites as these tend to form a distorted tetrahedral environment with a strong Cu – S bond to the thiolate of cysteine residue, two Cu – N imidazole bonds and a long Cu – S bond to a methionine. The highly covalent Cu (II) – S (Cys) bond provides a strong electronic coupling into protein pathways to facilitate rapid long-range electron transfer. This ensures that the rapid transition between the two redox states of the copper does not cause the metal centre to be lost. PrP binds copper (II) in the classic type II format with a square planar geometry (Viles et al. 1999). Proteins in this class are not normally able to accommodate copper (I) so once reduced, the copper tends to fall off the protein. Type I proteins that need to cycle electrons in a stable way normally have structural elements which prevent this from happening, Superoxide dismutase (SOD), for example, has its copper centre buried deep with the protein structure (Ge et al. 2003). This pattern of protein evolution is consistent across the type II proteins and those that are able to undergo stable redox cycling all have some significant catalytic role involving redox chemistry at their copper centres (Abolmaali et al. 1998). Additionally, the pattern and mid point potentials of these catalytic proteins are all very similar. Using Cu/Zn SOD as an example, the range and potential closely match that of PrP from my data (Ge et al. 2003). With the enormous body of evidence supporting the importance of oxidative stress in prion disease (Brown 2005) and the evidence supporting PrP as an antioxidant, this new evidence strongly supports the idea that PrP contributes to both the normal defence against oxidative stress and its cause in prion disease (Stanczak and Kozlowski 2007; Treiber et al. 2007).

CHAPTER 7

Metals and PrP Survival in the Environment

TSE remains a major problem in several countries despite concerted efforts to eradicate the disease. As the pattern of rules out spontaneous outbreak of disease, evidence suggests the environment is the source of the infective agent (Leita *et al,* 2006; Greig, 1940; Hadlow *et al,* 1982; Miller *et al*, 2004). This agent may enter the soil via infected carcasses, meat products or farm effluent (Gale and Stanfield, 2001). It has been shown that some residual infectivity remains after three years in soil that had been exposed to infected material (Brown and Gajdusek, 1991). Natural processes in the soil such a bacterial activity, exposure to UV radiation and soil acidity should be deleterious for even the most resilient organic material. It is not known how PrP is able to survive. Interactions with metals may be able to contribute to the proteins stability and resistance against degradation. For example, it has been shown that manganese can cause PrP to fold into a proteinase resistant form (Brown *et al,* 2000**)**. Certainly, many metals exist within soils and it may therefore be possible that these interactions contribute to PrP's longevity in the environment. There is also some evidence of high manganese and low copper levels in areas of high scrapie incidence (Ragnarsdottir and Hawkins, 2005).

A clear understanding of how PrP interacts with soils is important in order to assess whether metals contribute to the stability of PrP in the environment. The mechanism of protein adsorption on to soil particles is far from straight forward. Complicating factors include soil pH and constituents and protein PI, conformation, size, charge, solubility and flexibility (Norde, W and Giacomelli C, 2000; Stumm 1992). The majority of soil/protein interactions have, therefore, been with model systems, especially with constituent clays such as kaolonite (kte) and montmorillonite (mte). One study (Sevegent-Noinville *et al*, 1999) showed the importance of electronegative interactions in the adsorbance of bovine serum albumin (BSA) onto mte and how the strength of these interactions could alter the conformation and properties of the protein. Other studies have shown specifically the very strong adsorptive nature of soil clays to proteins, especially prions. Leita *et al* in 2005 demonstrated the difficulty in deadsorbing prions from clay, especially mte and suggested that the conditions in most soils would favour an accumulation of stable prions in soils exposed to contaminated material. Another such study suggested that mte would promote an orientation of PrP

towards the soil involving elements across the entire protein in both the N and C terminus, making the adsorption almost irreversible in it's strength (Revault *et al,* 2005). Another study confirmed that PrP could adsorb strongly to clay and remain infectious (Johnson *et al,* 2006). With the protein/soil interactions well characterised, it is possible to construct model systems whereby the stability of both Metal bound and apo forms of PrP^{c} and PrP^{sc} can be studied.

The aims of the study were to assess the stability of recombinant PrP on a model soil over a period of 30 months in the presence or absence of various key metals. The stability of PrP^{c} and PrP^{sc} in the presence of soils and metals was also studied.

7.1 Characterisation of the association of PrP and the model soil systems of Mte and Kte

The two most commonly used model soil systems used for protein-soil interaction studies are mte and kte. Mte is a mineral clay of the smectite family and very well defined. Its composition is $(Na,Ca)_{0.33}(Al,Mg)_2Si_4O_{10}(OH)_2$ (Stumm et al. 1992). The Aluminium atoms are situated between two silicon layers sharing the valancies of the oxygens. This forms a tetrahedral structure with an expandable gap between interlayers. This space cannot expand beyond 2 nm (Juma, 1998) and will therefore not allow globular PrP to pass into the clay structure. Kaolinite is another silicate mineral of the phyllosilicate family and is also very well defined, with a composition of $Al_2Si_2O_5(OH)_4$ (Stumm et al. 1992). It is a layered silicate mineral, with one tetrahedral sheet linked through oxygen atoms to one octahedral sheet of alumina octahedral (Deer et al. 1992). Again, the gap between sheets does not allow for passage of large globular proteins into the clay. Table 7.1 compares the properties of the two minerals and figure 7.1 and figure 7.2 show schematic representations.

Table 7.1 Comparison of the properties of mte and kte (Brady and Weil 1996).

• **Property**	• **Montmorillonite**	• **Kaolinite**
• **Size (mm)**	• 0.01-1.0	• 0.5-5.0
• **Shape**	• Flakes	• Hexagonal crystals
• **External surface area (m^2/g)**	• 70-120	• 10-30
• **Internal surface area (m^2/g)**	• 550-650	• -
• **Plasticity**	• High	• Low
• **Cohesiveness**	• High	• Low
• **Swelling capacity**	• High	• Low
• **Unit-layer charge**	• 0.5-0.9	• 0
• **Interlayer spacing (nm)**	• 1.0-2.0	• 0.7
• **Bonding**	• Van der Waal's bonds (weak attractive force)	• Hydrogen
• **Net negative charge ($cmol_c/kg$)**	• 80-120	• 2-5

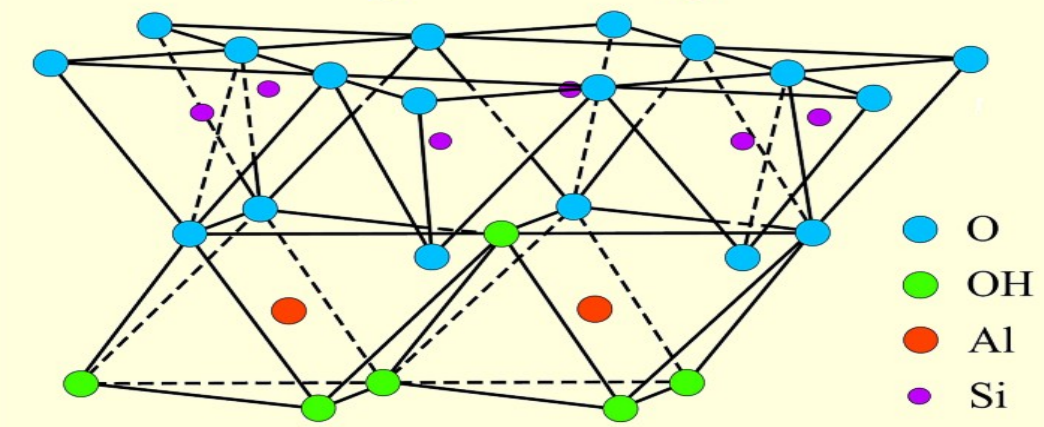

Figure 7.1 Schematic of the structure of kaolinite. Adapted from (Grim 1962)

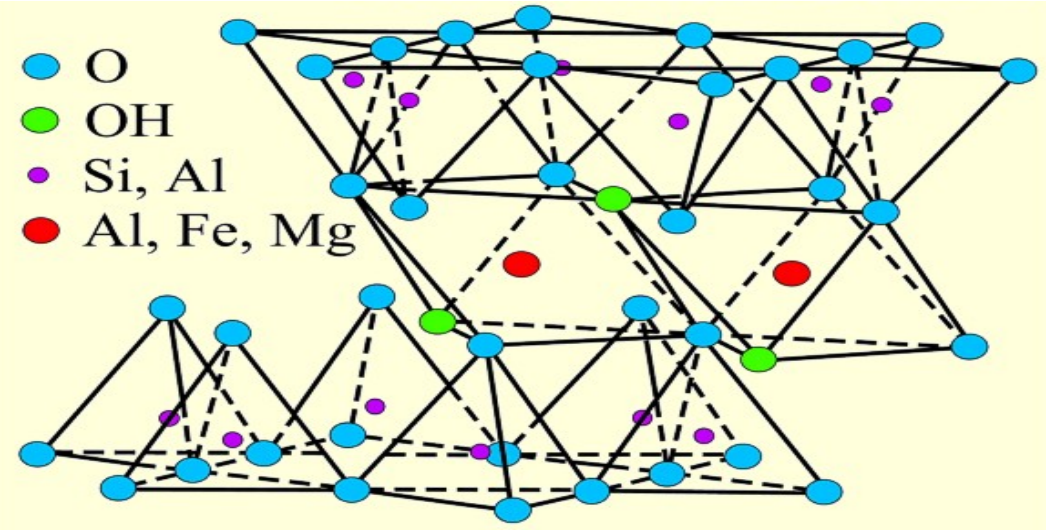

Figure 7.2 Schematic of the structure of Montmorillonite. Adapted from (Grim 1962)

Initially, an evaluation of the total capacity of mte and kte for PrP was carried out. Various amounts of mte from 0 mg to 12 mg were added to 15ml falcon tubes along with 5ml of recombinant mPrP to a final concentration of 0.2 mg/ml. The solutions were stirred for two hours before being centrifuged at 800 x g for 10minutes. The supernatant was collected and submitted to BCA analysis. The amount of mPrP remaining in solution was recorded and used to assess the amount that had adsorbed to the mte. Controls that omitted the protein or mte were used. Tables 7.2 and 7.3 compare the capacity of the clays for the protein.

Table 7.2 The adsorptive capacity of mte for recombinant wild type mPrP.

Mte (mg)	mPrP (mg) in supernatant pre adsorption	mPrP (mg) in supernatant post adsorption	mPrP (mg) adsorbed	MPrP adsorbed per mg mte (mg)
2	1	0.900	0.100	0.050
4	1	0.800	0.200	0.050
6	1	0.650	0.350	0.059
8	1	0.600	0.400	0.050
10	1	0.525	0.475	0.048
12	1	0.450	0.550	0.046
0	1	1.000	0.000	0.000
10	0	0.000	0.000	0.000

The amount of mPrP adsorbed onto mte at pH7. Column 2 shows the amount of PrP in solution before adsorption to mte. Column 3 shows the amount in solution after 2 hours incubation at room temperature with mte. Column 5 shows the calculated amount of PrP adsorbed per mg of mte. The last two rows represent experimental controls.

Table 7.3 The adsorptive capacity of mte for recombinant wild type mPrP.

Mte (mg)	mPrP (mg) in supernatant pre adsorption	mPrP (mg) in supernatant post adsorption	mPrP (mg) adsorbed	MPrP adsorbed per mg mte (mg)
2	1	0.945	0.055	0.028
4	1	0.905	0.095	0.024
6	1	0.856	0.144	0.024
8	1	0.784	0.216	0.027
10	1	0.760	0.240	0.024
12	1	0.700	0.300	0.025
0	1	1.000	0.000	0.000
10	0	0.000	0.000	0.000

The amount of rPrP adsorbed onto kte at pH7. Column 2 shows the amount of PrP in solution before adsorption to kte. Column 3 shows the amount in solution after 2 hours incubation at room temperature with mte. Column 5 shows the calculated amount of PrP adsorbed per mg of kte. The last two rows represent experimental controls.

Under the conditions used, mte has an adsorptive capacity of 50 μg of mPrP per mg of mte. The controls excluding the mte or protein prove that no other factors are responsible for the data obtained. Based on the known physical characteristics of the clay used, this gives a specific adsorbance of 150 μg PrP/M^{-2} mte. Kte has an adsorptive capacity of 25 μg of mPrP per mg of kte. This translates to a specific adsorbance of 750 μg PrP/M^{-2} kte. Therefore, 40 mg of both kte and mte was used to adsorb 1mg of protein for future experiments.

7.2 The Initial Desorption of rPrP from Kte and Mte

Previous reports have suggested that the adsorption of PrP to clay is irreversible (Revault et al. 2005). Various desorption conditions were therefore tested to confirm whether desorption was possible. Mte or Kte (40 mg) was added to 1.5 ml eppendorfs along with 1ml of recombinant mPrP to a final concentration of 1mg/ml protein. The tubes were then rotated for two hours at room temperature before being centrifuged at 800 x g for 10 minutes and the supernatant collected. A variety of solutions were then added to the tubes and thoroughly mixed by vortexing. The tubes were then incubated for 10 minutes at either 25 °C or 100 °C. The solutions used were sodium acetate at pH 3 or pH 5, MES/Tris at pH 8 or pH 10, 10 % SDS, Desorption buffer (100 mM Tris-pH 8, 10 % SDS, 7.5 mM EDTA, 100 mM DTT, 30% glycerol), 2 M sodium chloride and MilliQ water. After treatment in the solutions, the tubes were allowed to equilibrate to room temperature before again being centrifuged at 800 x g and the supernatant collected. The supernatant was then submitted to BCA assay and Western blot analysis. Two antibodies were used, ICMS-18 (anti PrP C-terminal residues 143-153) and 8B4 (anti-PrP N-terminal residues 35-45). Table 7.4 summarises the attempts at the deadsorption of mPrP from mte and kte. All methods were more efficient at recovering the protein at 100 °C. By far the most successful method was by boiling the mte in deadsorption buffer, which yielded over 95 % recovered protein. Figure 7.3 shows Western blots for the desorbed protein from the three most successful conditions at 25 ºC and 100 ºC from mte.

Table 7.4 Summary of the results from the methods used to deadsorb PrP from mte and kte

Desorption Solution	Temperature (°C)	Amount of mPrP adsorbed onto 40mg mte or kte (mg)	Amount of mPrP released from mte		Amount of mPrP released from kte	
			mg	%	mg	%
Sodium acetate pH 3	25	1	0.05	5	0.01	1
Sodium acetate pH 5	25	1	0.04	4	0.01	1
MES/Tris pH 8	25	1	0.09	9	0.03	3
MES/Tris pH 10	25	1	0.09	9	0.05	5
10 % SDS	25	1	0.18	18	0.09	9
Desorption buffer	25	1	0.39	39	0.20	20
2 M Sodium Chloride	25	1	0.13	13	0.07	7
MilliQ water	25	1	0.01	1	n/d	n/d
Sodium acetate pH 3	100	1	0.14	14	0.11	11
Sodium acetate pH 5	100	1	0.10	10	0.10	10
MES/Tris pH 8	100	1	0.11	11	0.09	9
MES/Tris pH 10	100	1	0.14	14	0.10	10
10 % SDS	100	1	0.28	28	0.24	24
Desorption buffer	100	1	0.95	95	0.70	70
2 M sodium chloride	100	1	0.24	24	0.21	21
MilliQ water	100	1	0.05	5	0.08	8

n/d – not detected

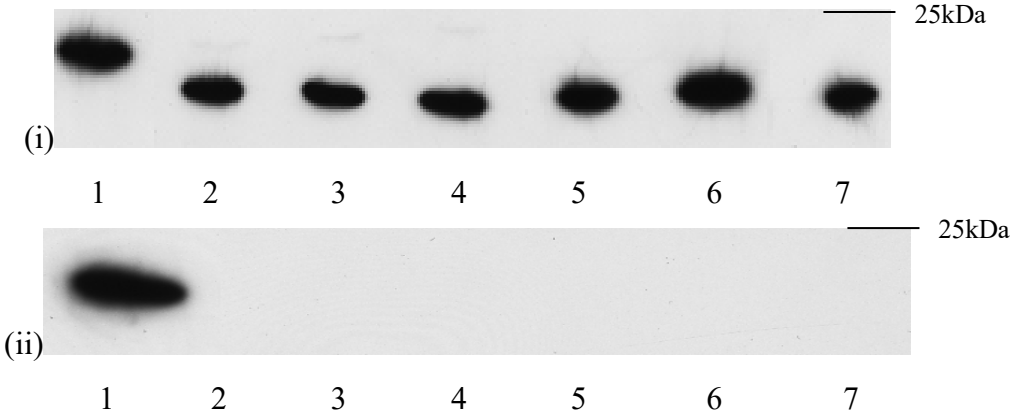

Figure 7.3 Blot comparing protein desorbed from the clay probed with (i) ICMS-18 and (ii) 8B4 ant-PrP antibody. The conditions are compared with 1) Fresh recombinant PrP and rPrP desorbed from mte with 2) 10 % SDS 25 ºC, 3) desorption buffer 25 ºC, 4) 2M NaCl 25 ºC, 5) 10 % SDS 100 ºC, 6) desorption buffer 100 ºC, 7) 2 M NaCl 100 ºC

When compared to fresh recombinant PrP, the desorbed protein is smaller than expected (figure 7.3i) by around 2-3 kDa. The antibody used, ICMS-18, is specific to the C-terminus of the protein. Antibody raised to the N-terminus region 35-45 (figure 7.2ii) produced no reactivity to protein desorbed by any of the conditions. This suggests that a section of protein at least 20 residues long is missing from PrP post deadsorption. It is

not clear at this stage whether this fragment is cleaved by the desorption conditions or if it is left adsorbed to the clay.

7.3 The Adsorption and Deadsorption of PrP from Cell Lysates

In order to relate the cellular form of PrP to the recombinant work, experiments were carried out with mouse PrP from cultured cells. An infected cell line was derived from scrapie infected mouse brains (SMB). The control cell line was derived from scrapie infected mouse brains cured with pentosan sulphate (SMB-PS). The cells were cultured as described in chapter two. The cells were then lysed in phosphate buffered saline containing 1 % Igepal and 1 % Triton X and the lysates collected. Lysates were then mixed with 40mg of mte in 1.5ml eppendorfs and rotated for two hours. The tubes were then centrifuged for 10 minutes at 800 x g and the supernatant collected and labelled primary supernatant. Buffer G (see above) was then added to the tubes and boiled for 20 minutes at 100 °C. The tubes were again centrifuged for 10 minutes at 800 x g before the supernatant was collected and labelled secondary supernatant. These supernatants were then submitted for western blot analysis and compared with lysates before adsorption. Figure 7.4 shows these results.

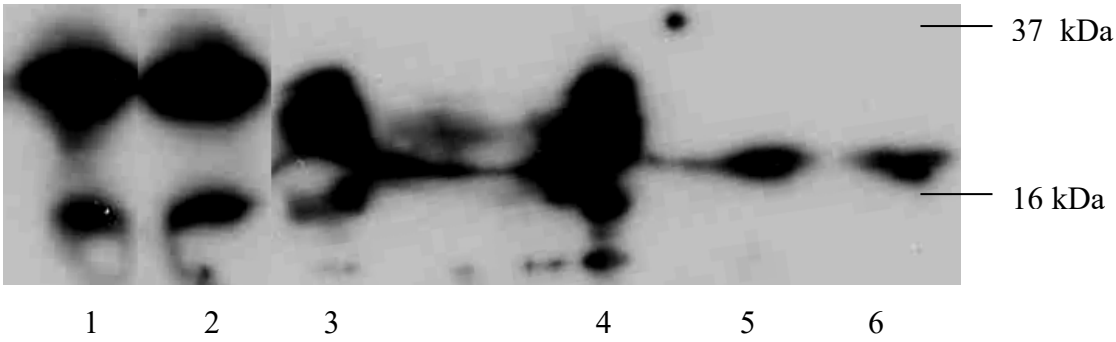

Figure 7.4 Western blot comparing PrP desorbed from mte using deadsorption buffer. The primary antibody used was ICMS-18 raised to the C-terminal region. 1) SMB-PS lysates, 2) SMB lysates, 3) PrP from SMB-PS desorbed from mte with desorption buffer, 4) PrP from SMB desorbed from mte with desorption buffer, 5) PrP from SMB-PS boiled in desorption buffer 6) PrP from SMB boiled in desorption buffer

Controls that were not adsorbed but still boiled in buffer G were used to assess if any observed changes to the protein were as a result of the adsorption process or deadsorption. It is clear that the protein desorbed from the clay is smaller than that

before adsorption. Controls that were boiled in desorption buffer without clay also showed evidence of cleavage or degradation. This suggests that a portion of the protein is cleaved during the deadsorption process but this is due simply to the desorption process.

In order to ascertain where the protein is cleaved, experiments were carried out with antibody 8B4, a monoclonal mouse PrP antibody raised against N-terminal sequence 35-45. Figure 7.5 shows a western blot of cell lysates before and after adsorption to mte and lysates just treated with deadsorption buffer.

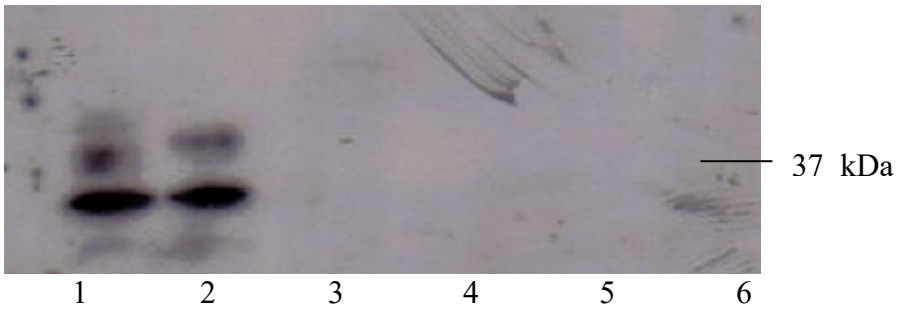

Figure 7.5. Western blot of PrP^{c} and PrP^{sc} from mte using deadsorption buffer. The primary antibody used was the N-terminus antibody 8B4 which is specific to the region 35-45 on mPrP. 1) PrP^{c} lysates, 2) PrP^{sc} lysates, 3) PrP from SMB-PS desorbed from mte with desorption buffer, 2) PrP from SMB desorbed from mte with desorption buffer, 5) PrP from SMB-PS boiled in desorption buffer 6) PrP from SMB boiled in desorption buffer

The N-terminus part of the protein is clearly lost from the protein following deadsorption, but not due to the adsorption process. The samples of lysates that were not adsorbed but treated in the deadsorption buffer also show a loss of the N-terminus, suggesting that it is the deadsorption process that is responsible. This method then is suitable for basic determination of PrP longevity when adsorbed to clay but not for more detailed studies on the effects of clay association.

7.4 The Development of a Method to Deadsorb PrP From Clay in its Native State

There is clearly a need to develop a method to remove the adsorbed protein from the clay in a way that will allow for more detailed analysis. A method that does not expose

the protein to high temperatures or harsh denaturing conditions was therefore developed. The base idea behind the method is to use the proteins existing electrostatic charge by developing a polar potential difference across the clay, while trapping the substrate and allowing the protein to deadsorb and become trapped on a membrane. PrP is a basic protein with a PI of 9.6. Figure 7.6 illustrates the theory.

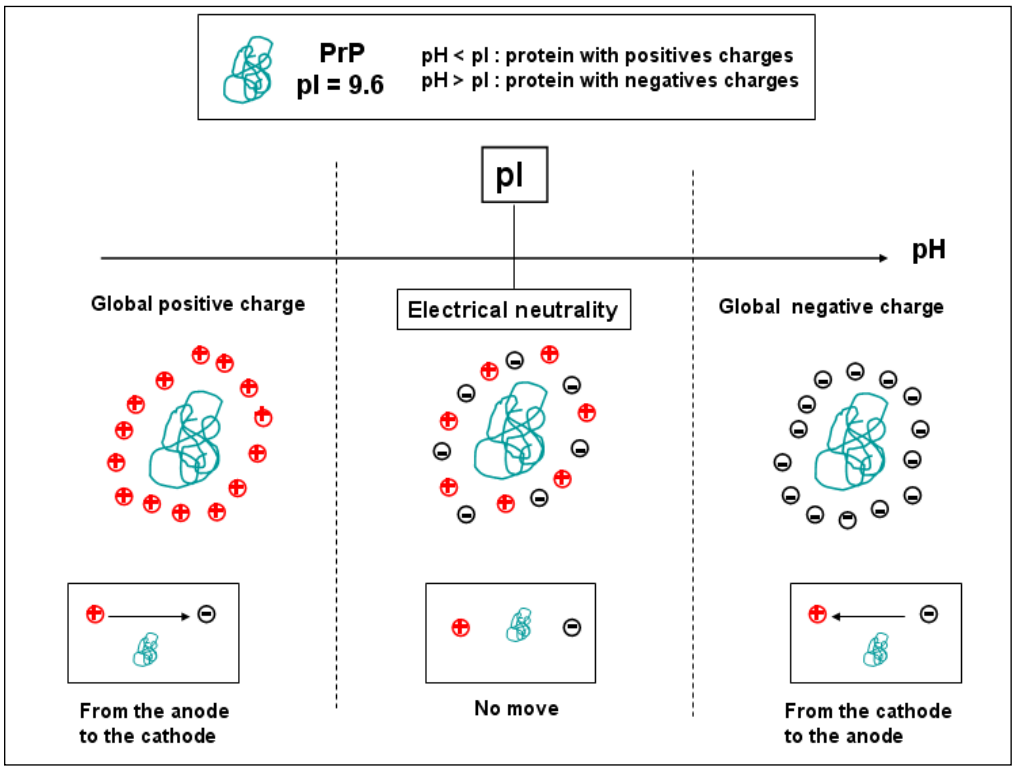

Figure 7.6 Illustration of the theory behind the electrostatic deadsorption method. Where the pH is above the protein PI, a charge is expected to pull the protein towards the cathode. Where the pH is below the protein PI, a charge is expected to pull the protein towards the anode.

Using this theory, a desorption apparatus was constructed. Protein/clay mixtures in 20 mM MES buffer, pH 5 were set in cooling polyacrylamide gel inside plastic tubes of 5mm diameter. A 20 % polyacrylamide plug was then set into the top of the tube to seal it. Figure 7.10 shows this.

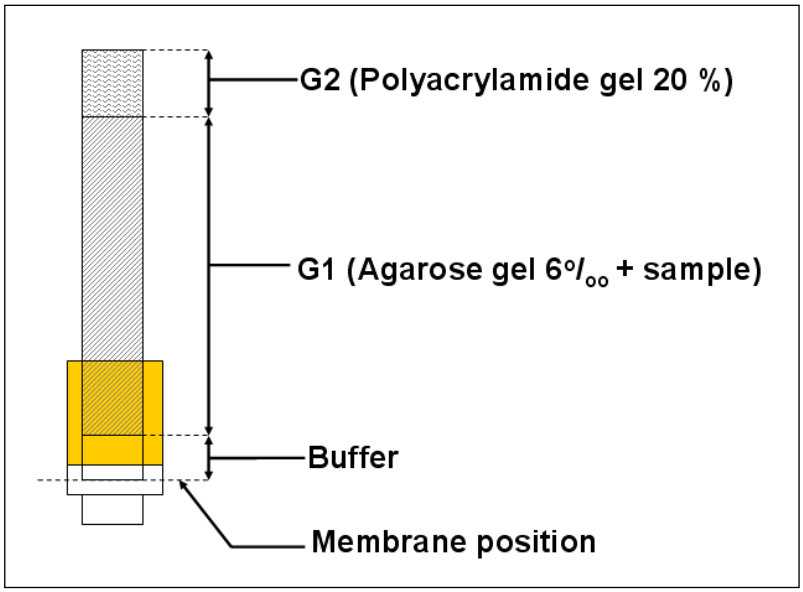

Figure 7.7 Illustration of the tube used to set the protein/clay mix.

These tubes where then attached to 3 kDa membranes at one end and set into 0.8 % agarose gel. The gel was then submerged in a gel tank containing TAE buffer, pH 5 and a current of 35 mV passed across the gel. Figure 7.7 illustrates the apparatus set up. The entire apparatus was cooled in ice to prevent overheating.

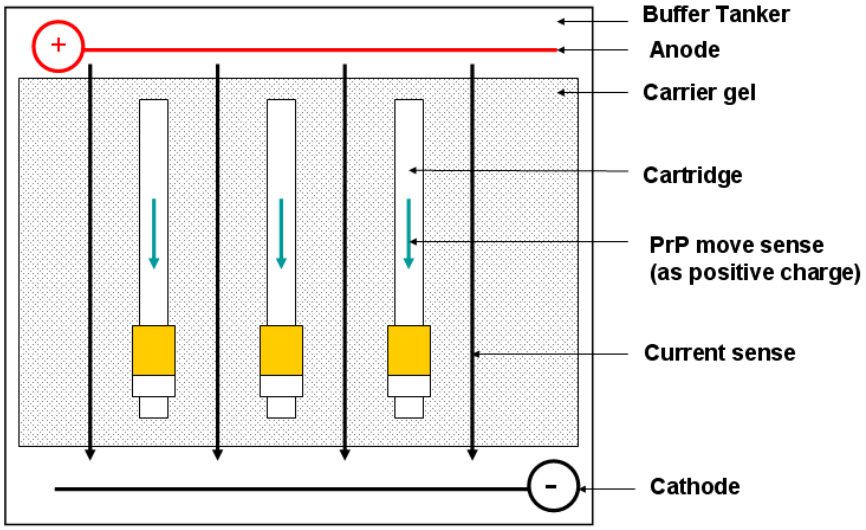

Figure 7.7 Illustration of the desorption apparatus used.

The apparatus was tested using 40 mg amounts of recombinant protein/clay mixtures that had been incubated for 2 years at room temperature and electrophoresed for 24 hours. The membranes at the cathode were then removed and submitted to Western

analysis using ICMS-18. Figure 7.8 shows the blots. Controls using adsorbed bovine serum albumin (BSA) and no protein were included.

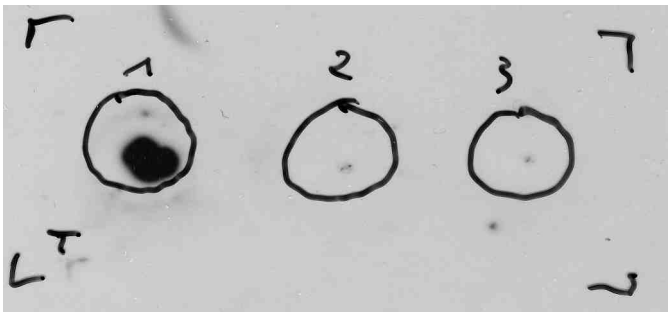

Figure 7.8 Blot of the membranes from the apparatus using ICMS-18.
1 = PrP. 2 = BSA. 3 = No protein.

The apparatus is clearly able to efficiently remove PrP from the clay matrix. As no denaturing or reducing agents are used, the protein is as close to its state while adsorbed to the clay as possible. Figure 7.9 shows a blot comparing recombinant protein before and after extraction using 8B4 N-terminal antibody.

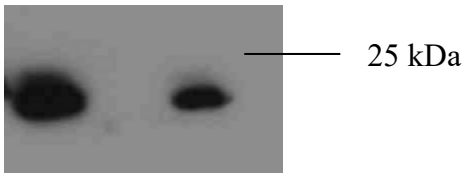

Figure 7.9 Blot comparing recombinant rPrP using ICMS-18. 1) before extraction and 2) after extraction

It is clear from figure 7.9 that the N-terminal region previously lost by the harsh desorption conditions is still present when the protein is extracted by this method. This method of protein desorption was therefore adopted for future studies.

Although the use of recombinant PrP is an indicator of how the protein may behave in soil, it is clearly the cellular or disease forms of the protein that carry some significance in the environment. Figure 7.10 shows a Western blot carried out with ICMS-18 on the extracts from the aqueous clay incubated with SMB and SMB-PS lysates for 6 months. Each cell lysate was incubated with proteinase K for 1 hour at 37 ºC to a final concentration of 8 µg/ml lysates.

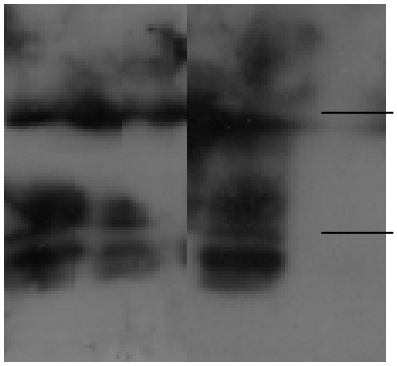

Figure 7.10 Western blot (ICMS-18) of the extracted cell lysates after 6 months incubation on mte. 1) SMB , 2) SMB after PK digest, 3) SMB-PS, 4) SMB-PS after PK digest

From figure 7.10, it is apparent that protein from both SMB and SMB-PS lysates survive equally well on the clay. After exposure to the clay, the cell lysates from the SMB's still demonstrate resistance to PK digest. This is indicative of infectious PrP^{sc} remaining intact on the clay. The lysates from the SMB-PS cell line showed no resistance to PK digest and therefore contained only PrP^{c}.

7.5 Investigation Into the Effect of Soil Metals on PrP stability

In order to investigate whether key metals played any role in the stabilisation of PrP in soil, mte was contaminated with copper and manganese. Manganese has been shown to increase PrP resistance to protease degradation (Brazier et al. 2008) and has been associated with increased incidence of scrapie (Ragnarsdottir and Hawkins, 2005; (Zucconi et al. 2007) and copper is the natural binding partner of PrP (Brown et al. 1997). To contaminate the clay, 1 mM solutions of the sulphate salt of each metal were mixed with mte for 2 hours shaking at room temperature. The mixture was then centrifuged to sediment the clay and the supernatant discarded. The clay was then dried in a dessicator for 72 hours before use. rPrP solutions of 1mg/ml were then mixed with the clay to produce an aqueous metal/clay/protein mixture and incubated at room temperature for either 0, 12 or 24 months. The protein was then extracted from the clay by the electrophoresis method described above and submitted to Western blot. Figure 7.11 shows the blot for the protein extracted immediately after 24 hours incubation on the clay.

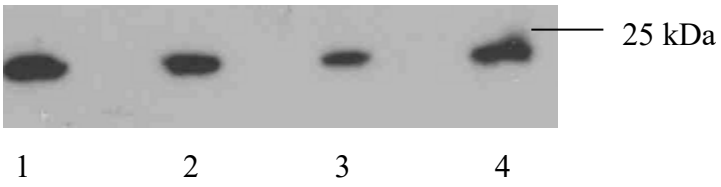

Figure 7.11 Western blot (ICMS-18) of the extracted rPrP from 1) mte with no metals, 2) mte with copper, 3) mte with manganese and 4) fresh protein not adsorbed to clay.

There is no evidence of any degradation product in any condition after 24 hours. There is, however, evidence of differences in the amount of protein extracted from the clay. Densitometer analysis shows the best recovery from the metal free clay. Relative to this condition, there was a 22% ± 4% reduction in recovery from the clay with copper and a 57% ± 17% reduction in recovery from the clay with manganese. This suggests that the presence of metals increases the degree of protein adsorption to clay. Figure 7.12 shows the blot comparing recombinant protein that had been incubated for 12 months on the aqueous clay with different metals.

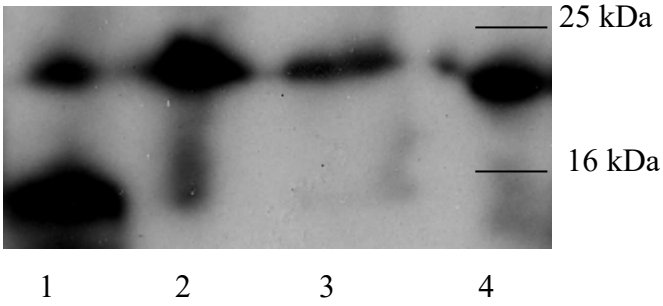

Figure 7.12 Western blot (ICMS-18) of the extracted 12 month old rPrP from 1) mte with no metals, 2) mte with copper, 3) mte with manganese and 4) fresh protein

When compared to fresh recombinant protein (lane 4), PrP that had been incubated with aqueous clay in the absence of metals (lane 1) is showing evidence of significant degradation, with only a relatively small proportion of protein left intact, as evidenced by the top band at around 23 kDa. In contrast, PrP incubated in aqueous clay with copper, shows very little degradation (lane 2). The protein incubated with manganese (lane 3) shows no evidence of any degradation. This suggests that metals play an important role in stabilising the protein in soil, with copper and manganese seeming to provide an equal measure of protection after 12 months.

Figure 7.13 shows the material from the SMB lysates after 12 month incubation with various metals

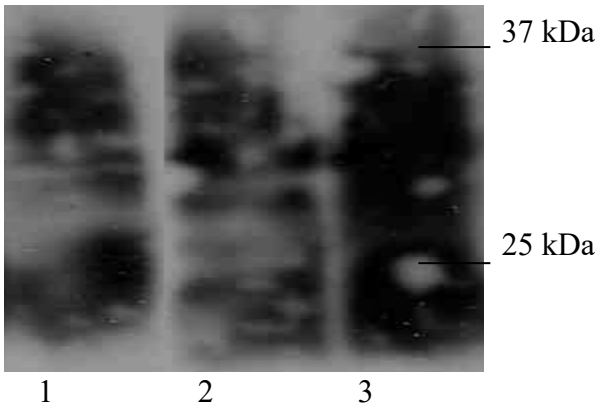

Figure 7.13 Western blot (ICMS-18) of the extracted 12 month old SMB lysates from 1) mte with no metals, 2) mte with copper, 3) mte with manganese

It is clear from the blot that all extracts from the aqueous clay in both the presence or absence of metals still contain material form infected mice. The aqueous soul containing manganese seems to stabilise the protein more effectively. Densitometric analysis reveals that there is a 52% ± 13% increase in protein recovery from the clay with manganese relative to the metal free clay. There is no significant difference between protein recovery from the metal free and copper clay.

Following two years of incubation on the clays, extraction of any residual protein was carried out as before. Figure 7.14 shows the blot for the extracts from aqueous clay in the presence and absence of metals. When compared to fresh recombinant protein (lane 4), PrP that had been extracted from aqueous soil with no metal (lane 1) shows clear evidence of substantial degradation with very little of the full length protein remaining. The protein incubated in aqueous soil with copper (lane 2) has also suffered significant degradation, but has faired much better than the protein with no metal present.

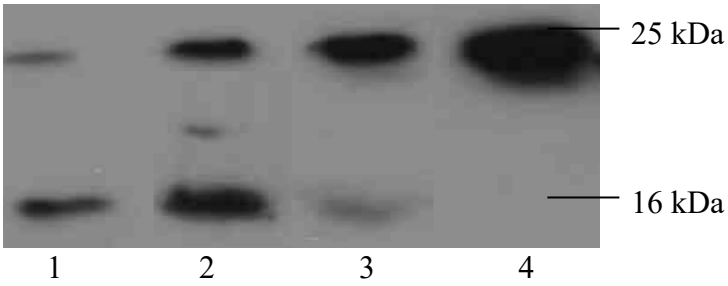

Figure 7.14 Western blot (ICMS-18) of the extracted 24 month old rPrP from 1) mte with no metals, 2) mte with copper, 3) mte with manganese and 4) fresh protein

What is most striking, however, is that the protein incubated in aqueous soil with manganese is virtually intact, with only very faint evidence of degradation. This strongly suggests that manganese in soil is able to significantly increase the survival of PrP in soil. Figure 7.15 compares the three conditions in respect of the degree of recovery of the intact protein.

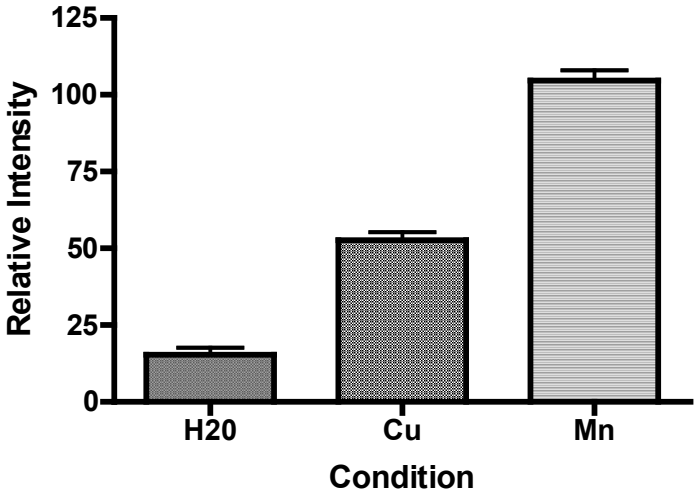

Figure 7.15 Comparison of the amount of rPrP recovered from the clay in the presence or absence of metals after 2 years incubation at room temperature. Quantification was achieved by densitometric analyses of 3 western blots for each condition. All intensity readings are relative to the protein desorbed from the clay with manganese.

It is clear from figure 7.15 that, after 2 years incubation on the clay, PrP is able to survive better when in the presence of metals, especially manganese. Relative to the manganese condition, there is around half as much protein recovered from the clay with copper ($p<0.001$) and around 6 times less protein from the clay with no metals present ($p<0.001$).

In order to draw significance from this observation however, the experiments with the material from infected mouse brains would need to show a similar pattern of stabilisation. Figure 7.16 shows the blot from the extracted material and figure 7.17 compares the amount of protein recovered relative to the manganese condition by densitometric analyses.

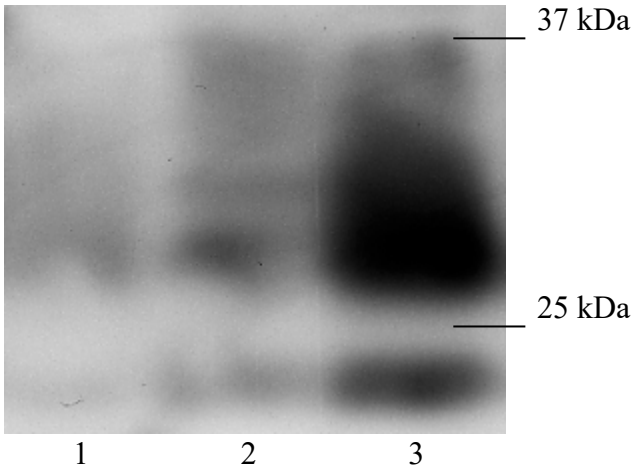

Figure 7.16 Western blot (ICMS-18) of the extracted 24 month old SMB lystaes from 1) mte with no metals, 2) mte with copper, 3) mte with manganese

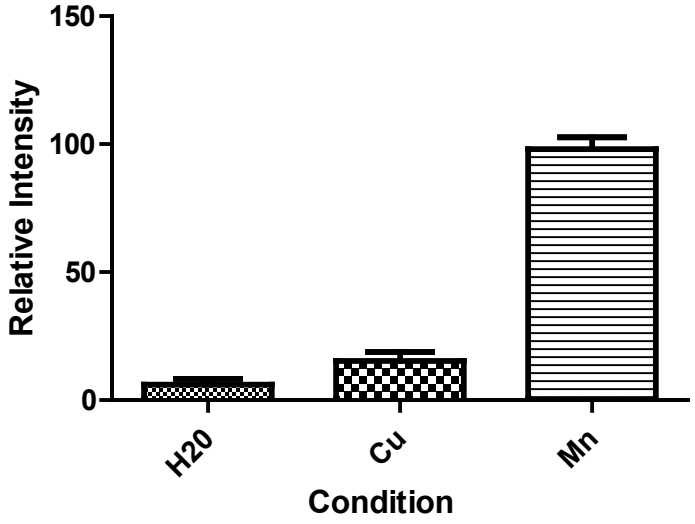

Figure 7.17 Comparison of the amount of PrP from SMB lysates recovered from the clay in the presence or absence of metals after 2 years incubation at room temperature. Quantification was achieved by densitometric analyses of 3 western blots for each condition. All intensity readings are relative to the protein desorbed from the clay with manganese.

The extracts from the aqueous clay with no metals present (lane 1) show only traces of protein remaining. Densiometric analyses reveals only 8 ± 3% protein present relative to

the manganese condition ($p<0.01$). The extracts from the aqueous clay in the presence of copper (lane 2) show evidence of an increase in protein stability, but have still suffered significant degradation, with only 16 ± 2% protein relative to the manganese ($p<0.001$). Alarmingly, the extracts from the clay containing the infectious material in the presence of manganese (lane 3) show a significant amount of PrP still remaining. This is very strong evidence for the mechanism behind which PrP may be able to remain in soil for many years and lead to pockets of TSE outbreaks in localised areas. This finding ties in well with studies showing a correlation between high manganese levels in soil and high incidence of TSE's (Purdey 2000; Purdey 2001; Nishida 2003; Purdey 2004; Purdey 2005; Ragnarsdottir and Hawkins 2005).

In all studies undertaken so far, aqueous clays are used as this is most likely to resemble conditions in the environment. It would be expected, however, that the affect of using anhydrous clays would be to stabilise the protein further by removing the hydrolysis activities of water. At the beginning of this study, clays were therefore prepared as before but were fully desiccated after the addition of the protein. Figure 7.18 shows the blot from the extracts of rPrP from the dried clay after 2 years of incubation with protein.

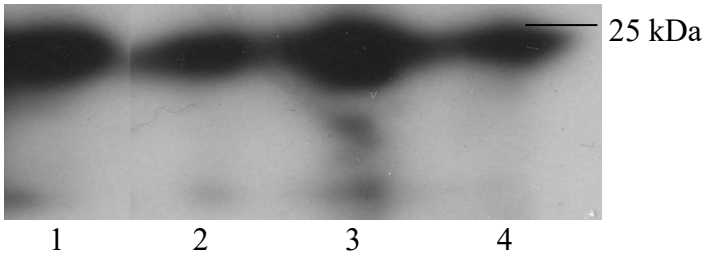

Figure 7.18 Western blot (ICMS-18) of the extracted 24 month old rPrP from dried mte with 1) no metals, 2) copper, 3) manganese compared to 4) fresh protein

As expected, protein incubated on the dried clay was very stable, irrespective of which metals are present. This is evidence for a hydrolytic mechanism of degradation of PrP when in soil.

7.6 The Importance of the Known Metal Binding Sites on PrP for the Metal Dependent Stability

It is impossible to know whether it is a direct interaction between the metal and protein that leads to increased stability or an indirect affect of the metal being present. In order to ascertain whether the differences in protein stability seen with the various metals are dependent on the known metal binding sites on PrP, the mutants lacking various histidine residues were used in the study. The mutant lacking the 5th site (octarepeat region present), the mutant lacking the octarepeat (5th site present) and the mutant lacking all 6 histidines (null) were used. Each mutant was incubated on the clay for a period of 12 months and then extracted as described above. Figure 7.19 shows the Western blot for the octarepeat region present mutant incubated in aqueous clay with various metals.

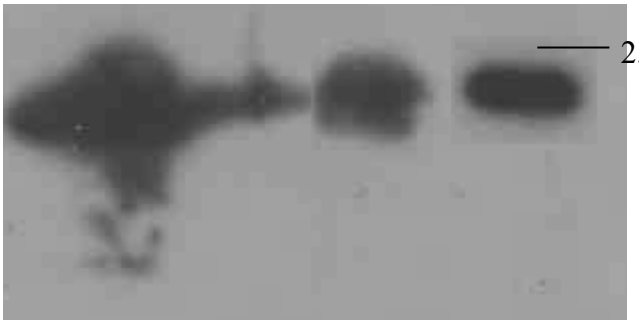

Figure 7.19 Western blot (ICMS-18) of the extracted rPrP octarepeat region present from 1) mte with no metals, 2) mte with copper, 3) mte with manganese and 4) fresh protein

In the absence of the 5th site, the results following 12 months incubation of rPrP on the aqueous clay show a similar pattern to the wildtype protein. The only condition in which degradation is evident is where no metals are present (lane 1), with metals seemingly reducing protein degradation after 12 months. Figure 7.20 compares the amount of protein extracted from the clay as revealed by densitomtric analysis. In the absence of the 5th site, the protein extracted from the clay in the presence of copper was significantly reduced relative to both the manganese present and metals absent ($p<0.01$). This suggests that copper interaction at the 5th site is important for protein stability on the clay.

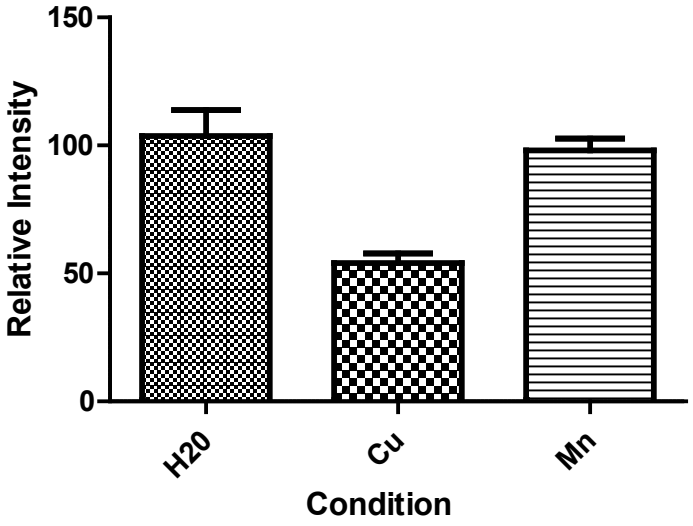

Figure 7.20 Comparison of the amount of rPrP with the 5th site absent recovered from the clay in the presence or absence of metals after 2 years incubation at room temperature. Quantification was achieved by densitometric analyses of 3 western blots for each condition. All intensity readings are relative to the protein desorbed from the clay with manganese.

Figure 7.21 shows the blot for the protein with octarepeat absent incubated on aqueous clay in the presence and absence of metals.

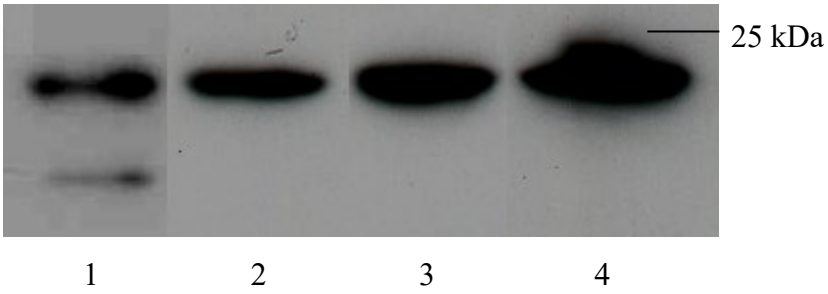

Figure 7.21 Western blot (ICMS-18) of the extracted rPrP 5th site region present from 1) mte with no metals, 2) mte with copper, 3) mte with manganese and 4) fresh protein

Figure 7.22 shows the densitometric analyses for the three conditions. Relative to the clay containing manganese, only 51 ± 4 % protein was recovered from the copper containing clay and 43 ± 2 % from the clay in the absence of metals. This is almost exactly the same result as for the wildtype protein suggesting the octarepeat has no role in metal driven stabilisation of PrP on soil.

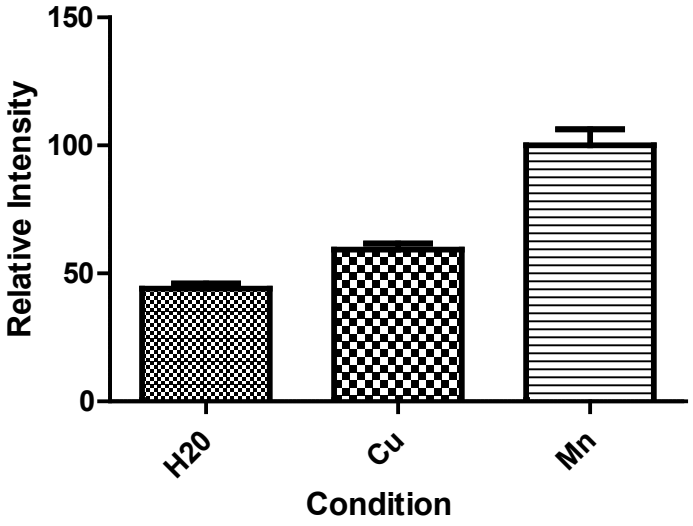

Figure 7.22 Comparison of the amount of rPrP with the octameric region absent recovered from the clay in the presence or absence of metals after 2 years incubation at room temperature. Quantification was achieved by densitometric analyses of 3 western blots for each condition. All intensity readings are relative to the protein desorbed from the clay with manganese.

Figure 7.23 shows the blot of the extracts from the null protein incubated on the aqueous clay for 12 months in the presence of absence of metals and figure 7.24 shows the densitometric analyses.

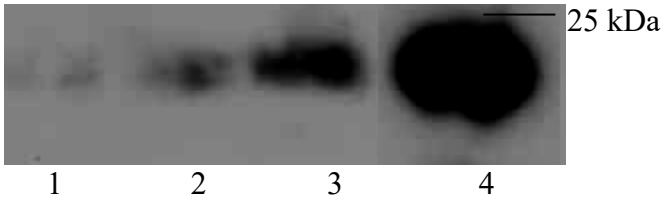

Figure 7.23 Western blot (ICMS-18) of the extracted rPrP null present from 1) mte with no metals, 2) mte with copper, 3) mte with manganese and 4) fresh protein

Striking differences can be observed between this protein and wildtype PrP. In the extract from the clay with no metals present (lane 1), the protein has all but completely degraded. A similar level of degradation is evident with the extract from the clay with copper present (lane 2). The extract from clay with manganese present, however, shows a high degree of resistance to degradation. It is likely then, from these results, that the differences between these mutants of PrP are

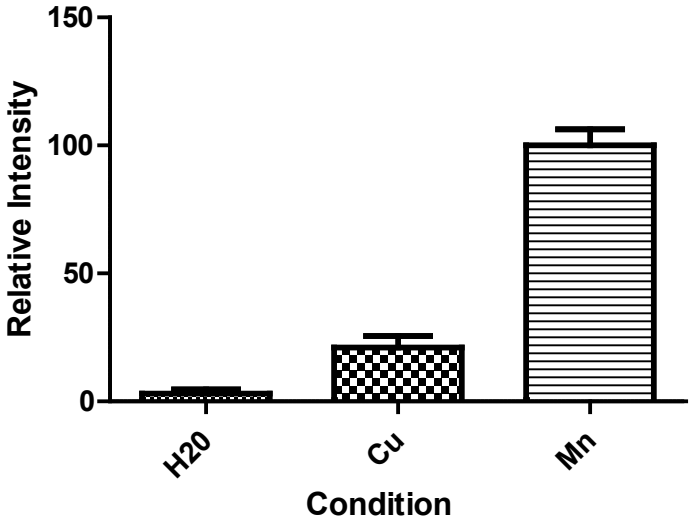

Figure 7.24 Comparison of the amount of null rPrP recovered from the clay in the presence or absence of metals after 2 years incubation at room temperature. Quantification was achieved by densitometric analyses of 3 western blots for each condition. All intensity readings are relative to the protein desorbed from the clay with manganese.

mainly due to a reduction in overall protein stability as a result of the mutation themselves. There is some evidence that copper associations with the 5th site may be important for protein stability but this is not the case for manganese. This is good evidence that the ability of manganese to stabilise PrP is not due to the known metal binding regions on PrP but due to an interaction elsewhere on the protein or a secondary effect not predicted by this study

7.7 Discussion

There is a strong need to establish how TSE's are transmitted from one infected entity to another. Without this knowledge, the full eradication of the disease from both animal and human populations will remain little more than a pipedream. Most evidence suggests that the mode of infection within animals is via the ingestion of infected material (Wiggins 2009) and that some of this material is sourced from the environment such as contaminated soil that animals are grazing on (Revault et al. 2005; Vasina et al. 2005; Pucci et al. 2008; Saunders et al. 2008). As the TSE's are caused by an infectious protein (Prusiner 1996; Prusiner 1998; Prusiner 1998) , this evidence raises more questions than it answers, the primary one concerning the proteins mechanism of stability within soil.

There have been many attempts to correlate unusual distributions of soil metals and minerals with incidence of TSE outbreak (Purdey 2000; Nishida 2003; Chihota et al. 2004; Purdey 2004; Johnson et al. 2006; Johnson et al. 2007; Polano et al. 2008; Imrie et al. 2009; Russo et al. 2009). These studies have produced a varied group of results, some strongly suggesting that soil mineral and metal contents are important for survival (Purdey 1998; Purdey 2000; Purdey 2001; Nishida 2003; Purdey 2004; Purdey 2005; Ragnarsdottir and Hawkins 2005; Purdey 2006; Imrie et al. 2009) and others proving otherwise (Chihota et al. 2004). Of these studies, many have highlighted imbalances of copper and manganese as possible factors (Purdey 2000; Purdey 2001; Nishida 2003; Purdey 2004; Purdey 2005; Ragnarsdottir and Hawkins 2005). When this factor is combined with evidence showing these metals have significant affects on protein stability (Brown et al. 2000) and that infected animals show imbalance of these metals (Wong et al. 2001; Wong et al. 2001; Thackray et al. 2003; Wong et al. 2004; Hesketh et al. 2007) there is clearly a need to assess what affect these metals have on PrP in soil.

The first aim of this study was to assess whether it was possible to remove PrP once adsorbed to the surface of common minerals found in soils. The clay montmorillonite is used to provide a controlled substrate for the analysis. Initial attempts to remove the protein from the clay provided evidence of just how strong the PrP-mte association is. Despite all the methods tested, it was impossible to remove much protein unless severe denaturing and heat treatments were used. These methods, although effective, meant that any useful information stored within the protein would be lost on deadsorption. Additionally, significant degradation to the protein was observed which proved to be N-terminal loss, an element not only required for infection but also for stable adsorption to the clay (Cooke et al. 2007). This fits in well with other tandem studies that have shown PrP is difficult to remove (Johnson et al. 2006; Leitaa et al. 2006; Pucci et al. 2008; Wiggins 2009) or even impossible (Revault et al. 2005). None of these methods are therefore suitable for removing protein from the clay matrix.

All proteins carry a specific charge at pHs above or below their point of ionisation (PI). For PrP, a basic PI of 9.6 confers a strong positive charge at neutral or acidic pH. By using this property of protein, PrP was removed successfully from the clay without any need to denature secondary structure. This allowed for an assessment of how well the

entire protein survived on the clay over time. Even in the absence of metals, rPrP resisted degradation remarkable well and after 12 months was still clearly detectable. This supports other studies which have shown increased PrP stability when associated with clays (Johnson et al. 2006; Johnson et al. 2007). In fact, these studies have demonstrated that PrP may even be more infectious via oral ingestion when associated with clay. My studies do indicate however, that disease, cellular and rPrP all degrade within around 24 months when on clay alone, unless the clay is anhydrous. As this later condition seems unlikely in climates such as ours, a period of around 2 years does appear to reduce the amount of PrP surviving significantly. There is, however, a clear difference between protein adsorbed to clay with metals present and absent. PrP adsorbed to a Cu-mte matrix resisted degradation significantly better than that adsorbed to clay alone, although after 2 years exposure, the majority of the protein had degraded to a 16 kDa fragment. The most striking affect was when protein was adsorbed to a Mn-mte matrix. Even after 24 months, there was little evidence of any significant degradation and the full length protein was still apparent on Western blots. This effect was mirrored by the studies using cellular and disease PrP, an important fact that allows the recombinant work to have some context for the 'real world'. This observation is closely supported by studies showing that manganese can cause PrP to fold into a protease resistant form (Brown et al. 2000) and further studies highlighting increased manganese levels in brains of affected individuals (Hesketh et al. 2007). It also provides a potential link to whether studies showing elevated manganese in soil are relevant to disease outbreak (Purdey 2000; Purdey 2001; Nishida 2003; Purdey 2004; Purdey 2005; Ragnarsdottir and Hawkins 2005). Our lab has previously demonstrated some interesting consequences when manganese is bound to PrP, not least the dramatic affects on the proteins redox chemistry (Brazier et al. 2008). Our work showed that the protein was capable of taking part in and being altered by manganese catalysed redox chemistry that could significantly alter the properties of PrP. This ties in well with other work that demonstrated an affect by manganese oxides on PrP (Russo et al. 2009), although this study did suggest a deleterious affect, although not in the presence of soil.

The mechanism of PrP stabilisation in the presence of manganese does not appear to involve known metal binding elements within the protein. Studies with Mn-mte using a mutant PrP with all N-terminal histidines removed did not reduce the proteins resistance to degradation when compared to wildtype protein. There are differences between the

wildtype and null protein when associated with Cu-mte or mte in the absence of metals. This is likely due to the stabilising effects of copper when bound to the protein (Davies and Brown 2008). The null protein has been shown to have no copper binding characteristics (Davies et al. 2009) and therefore copper in the soil may confer some increased stability to the protein. From this study, however, it would appear that the majority of the differences seen in stability between mutant PrP proteins are simply due to the structural affects of amino acid substitutions. Further and more detailed studies of the association of manganese with PrP are therefore needed but fall outside the scope of this work.

In conclusion, soil metals do have a significant affect on PrP stabilisation on clays. This is in addition to an already striking ability for the protein to stably adsorb to minerals in soils and survive the harsh conditions in the soil environment. It is therefore possible that where areas of high manganese are present, PrP in both its cellular and disease forms could survive for longer periods and hence potentially be transmitted to new hosts. The implications of this are discussed in more detail in chapter 8 of this thesis. These factors should be investigated further at both a biochemical and geological level. Such work may be critical to understand the transmission of the disease and to its eventual eradication.

Chapter Eight
General Discussion

Despite the enormous amount of research into the metallochemistry of PrP, there still remains a good deal of disagreement over several key aspects of the proteins interaction with physiological metals. These areas of debate include the stoichiometries and affinity for copper, the possible interaction with other metals and the degree and significance of redox contributions from the protein. Additionally, there has not been any detailed assessment of the pH dependence of copper binding to PrP. These factors, I believe, may provide further insight into the possible physiological function of this remarkable protein. Another area of recent debate has been the potential environmental contamination caused by PrP and its link to the transmission of prion disease amongst the animal population. This work has raised questions about how a protein could resist degradation from harsh environmental conditions.

This study aimed to produce a thorough thermodynamic and electrochemical characterisation of mature PrP. This allows for the determination of the metal binding characteristics of PrP obtained by a relatively novel method and using the full length protein. As no concrete method existed for the analysis of complex or potentially cooperative ligand binding via calorimetry, an opportunity to develop a set of principles for the treatment of such data has also been explored. New methods for the study of the electrochemistry of PrP have also been evaluated and used to reveal some exciting properties of PrP that may have significant implications for the proteins function. Finally, the questions concerning the proteins survival in the environment are addressed with an emphasis on PrP's interactions with soil metals. The information from this part of the study may provide an explanation as to how a protein can remain stable in soil for many years and why some areas seem more affected by TSE outbreak than others.

8.1 Isothermal Titration Calorimetry can be used for the Determination of Complex Ligand Binding

ITC is a highly versatile and sensitive technique that has been employed for the thermodynamic determination of association reactions in solution. The techniques ability to precisely determine the changes in enthalpy and entropy that accompany the binding of molecules can provide much insight into the balance of energies involved. All biological interactions have evolved through the underlying laws of physics and chemistry and nothing in biology occurs outside of these universal principles. This allows for the simple division of biological reactions into covalent and non-covalent interactions. ITC allows for these interactions to be directly monitored through the observation of changes in enthalpy as a reaction progresses. This then allows for the determination of fundamental parameters such as the number of binding elements involved and the stability of each distinct association. These determined parameters are invariably determined through the application of regression analysis and mathematical modelling based on basic and well known principles.

The principle behind the use of ITC for determining molecular interactions is very straight forward. A molecule M is added in small amount to a reaction cell containing molecule L. After each titration, the ML complex is allowed to come to equilibrium and the heat change for the process recorded. This process is then continued until a ration of M to L of 0.1 to > 3 is achieved (Okhrimenko and Jelesarov 2008). The total heat recorded after each addition of M to L is proportional to the total amount of ML formed and therefore relates directly to the degree of saturation Y by equation 1.

$$Y = \frac{[ML]}{[M]_{tot}} \qquad (1)$$

In this respect, the principle is similar to that used for the spectrographic determination of binding constants, but by gaining the data thermodynamically and isothermically, the total heat change post injection is also proportional to the molar enthalpy of association ΔH_A. This then allows for the determination of the stability constant K_A by equation 2.

$$K_A = \frac{\mathrm{Y}}{(1 - \mathrm{Y})[\mathrm{M}]} \quad (2)$$

From this, the other key thermodynamic parameters of change of Gibbs free energy ΔG and change in entropy ΔS can be determined by equation 3 and 4 respectively.

$$\Delta G_A = -RT\ln K_A \quad (3)$$

And

$$\Delta S_A = \frac{(\Delta H_A - \Delta K_A)}{T} \quad (4)$$

Where R is the gas constant and T is the absolute temperature.

Clearly, however, the total enthalpy change in the reaction also includes other factors such as the energies of dilution and protonation and as such these must be accounted for by running appropriate blank runs of M into buffer and subtracting this from the data. Regression analysis and application of exact mathematical expressions to describe the thermodynamic data is then applied to derive the stoichiometry and stability of the association between M and L. These expressions are discussed in detail in chapter 3.

A major factor when using ITC for the determination of multiple binding events between M and L is whether these interactions are identical or individually distinct. Also, whether each event is independent of one another or cooperative and interacting, a common phenomenon is biology. These factors can normally be determined by the fitting of multiple regression models and using the sum of the least squares to decide the best descriptive fit (Ababou and Ladbury 2006). These models are again discussed in detail in chapter 3 and will therefore not be discussed further here. ITC has, over recent years at least, been used frequently to accurately determine increasingly complex binding events in which cooperativity and multiple site coordination are present (Cliff and Ladbury 2003; Cliff et al. 2004; Whitesides and Krishnamurthy 2005; Ababou and Ladbury 2006; Ababou and Ladbury 2007; Okhrimenko and Jelesarov 2008).

The problem faced by this study is in the use of calorimetry to determine the binding parameters for PrP and copper (II), the natural binding partner of the protein (Brown et al. 1997). Copper (II) is largely insoluble at physiological pH (Linder and Hazegh-Azam 1996) and as such cannot be simply delivered to the thermodynamic chamber in solution. In addition, free copper has a tendency to cause protein aggregation (Daniels and Brown 2002), leading to thermodynamic chaos, and to catalyse significant redox chemistry (Halliwell and Gutteridge 1990) leading to further noise and complication. The fact that much of the copper (II) at pH 7 will be precipitated and therefore unavailable for copper chemistry with PrP would also mean inaccurate assessment of the free concentration of the metal leading to significant error in the determined binding parameters. All these factors mean the copper must be chelated to another entity for delivery to the protein. This adds significant complications to the regression analysis and model fitting. There are, however, several studies indicating mathematical solutions to the added complexity of using a chelator, but all have centred on simple single site binding or multiple independent sites (Sigurskjold 2000; Zhang et al. 2000; Nielsen et al. 2003). These new approaches have centred on two different principles. The first approach has been to directly modify the equations used in the regression analysis before the fitting of the data. Wang first described a mathematical expression for competitive binding in 1995 (Wang 1995). Sigurskjold then produced a full method for the analyses of the thermodynamics of competing ligand binding which allowed for the quantification of binding outside the normal sensitivity of ITC (Sigurskjold 2000). The method, however, is limited to binding events whereby the number of sites on the target macromolecule is the same for both the target and competing ligand. Nielsen *et al* then adapted this method for the analyses of data from experiments involving a competing chelator (Nielsen et al. 2003). They designed a regression routine which overcame the previous stoichiometric limitations so the competing chelator could have a different number of sites than the target macromolecule. Again, however, the model is limited to simple independent site binding. This pre-regression modification approach was successful in describing the data. However, it is dependant on a clear distinction between when binding involving the competing metal/chelator saturates and the macromolecule of interest starts. The other approach used was pioneered by Zhang *et al* and attempted to account for buffer and chelator interactions post regression analysis (Zhang et al. 2000). They showed that they could successfully account for the effects of chelator on simple independent site binding.

It is clear from the literature that PrP does not conform to simple binding kinetics, but is complex and potentially cooperative in its nature. This then was the first real challenge faced by this study – to devise and evaluate a suitable method for the analysis of copper (II) binding to PrP when the metal is delivered by a chelator. There are were two possible approaches. The first was to completely design a new regression routine to account for the chelator during the regression analyses. This was called method A and is described fully in chapter 3. The second was to use the existing 'sequential' model supplied by MicroCal and operated within the Origin architecture supplied with calorimeter. The affect of the chelator species could then be fully accounted for post regression by equation 4.

$$K_n = \frac{K_d(\text{app})K_d(\text{che})}{[\text{che}_{\text{total}}]^2} \qquad (4)$$

Where K_n is the actual stability constant for a given copper binding event, K_d(app) is the apparent value from the ITC data, K_d(che) is the stability constant relating to the chelator species and [che] is the concentration of the chelator species. Where the chelator species is a bis chelator, the value for K_d(che) is the β_2 value obtained by multiplying the two stability constants together. This approach, or method B, is by far and away the most straight forward and significantly reduces the number of functions necessary within the regression equations. The question really is which approach is most suitable.

Once establishing that amino acids served as excellent chelators of copper (Martell and Smith 1974) and that they are very well characterised in terms of their affinity and stoichiometry for copper (II), experiments could be conducted to assess the two methods. From my work., it is clear that method A produces a high degree of variation between chelator species tested. This is unsurprising when considering the enormous number of added variables accounted for by the regression analysis. Method B, however, produced consistent and realistic values when used to assess the binding parameters of copper (II) to the isolated octarepeat region of PrP. I had hypothesised that this would be the case for two reasons. Firstly, in using ITC for this purpose, I am only interested in binding events between PrP and copper (II) and therefore can consider

the disassociation of the metal from the chelator and resultant association with PrP as a single thermodynamic event. As we know precisely the concentrations of all reactants and the pre determined binding parameters for the chelator, we can apply the post regression calculation described by equation 4. Secondly, a by making the assumption in the first point, I can reduce the number of variables in the regression analysis. This allows the least squares calculation used to determine stoichiometric parameters between model fits to be more reliable.

The analyses of the thermodynamic data from the octarepeat peptide can be related to the published literature on PrP peptide fragments (Chattopadhyay et al. 2005; Walter et al. 2006) and also literature values for the known coordinating ligands on the peptide (Martell and Smith 1974). These then are in very good agreement with my data when using method B for the analysis. Additionally, when testing different chelators, the values for the stability and stoichiometry of copper (II) binding to the peptide are consistent and in agreement. Additionally, when many models are fitted from both the independent and sequential regression routines within Origin, there is clear statistical evidence that method B is able to distinguish between simple and complex interacting binding. Method B is therefore adopted as the method of analysis throughout this thesis.

8.2 PrP Binds Copper (II) with High Affinity in the Physiological pH Range

The degree of variation within the literature concerning the copper (II) binding parameters of PrP is a major issue when trying to relate this data to the function or miss-function of the protein. Wide ranging estimates of the affinity of copper (II) for PrP from micromolar (Hornshaw et al. 1995; Stockel et al. 1998) to femtomolar (Jackson et al. 2001; Thompsett et al. 2005) only serve to increase speculation of protein function and how that may relate to the copper binding characteristics of PrP. It is almost universally accepted that PrP binds 4 to 5 molecules of copper within two distinct regions, the octarepeat (Hornshaw et al. 1995; Qin et al. 2002; Millhauser 2004) and the 5^{th} site (Burns et al. 2002; Qin et al. 2002; Jones et al. 2005). The octarepeat region consists of four identical binding domains consisting of HGGG where the histidine is considered to be the primary coordinating ligand (Prusiner 1998; Aronoff-Spencer et al. 2000; Burns et al. 2002) with further contribution from deprotonated amides from the

two adjacent glycine residues and a deprotonated carbonyl from the third glycine (Aronoff-Spencer et al. 2000). In isolation, these ligands bind a single copper each but when together they form a complex and interacting arrangement that is dependent on the concentration of copper (II) available (Viles et al. 1999; Aronoff-Spencer et al. 2000; Burns et al. 2002). The 5th site consists of two small regions further up from the octarepeat, consisting of the amino acids 92-96 and 107-111 whereby the histidines at position 95 and 110 on the mouse protein (or 96 and 111 for the human protein) are the primary coordinating ligands (Hasnain et al. 2001; Jackson et al. 2001; Kramer et al. 2001; Burns et al. 2003; Jones et al. 2004). Despite the availability of 2 coordinating histidines, it is generally believed that only 1 copper binds at physiological pH (Klewpatinond and Viles 2007). The primary aim of this part of my work is to use a new approach to determine the binding parameters of these copper (II) binding regions across the pH range and to investigate the degree of any interaction both between and within the regions. The bulk of this work is carried out using recombinant PrP in order to provide a controlled environment for the study of the individual binding regions. Work by our lab has demonstrated that the affinity of copper for glycosylated PrP is equivalent to that of non-glycosylated (Davies et al. 2009). Full length recombinant protein is therefore considered a suitable model for the cellular form.

The data described in chapter 4 clearly demonstrates that the optimal copper binding conditions for PrP are within the physiological pH range of between pH 7 and pH 7.5. This is highly supportive of the proposed mechanism of coordination for PrP (Viles et al. 1999; Aronoff-Spencer et al. 2000; Burns et al. 2002; Jones et al. 2004; Morante et al. 2004; Jones et al. 2005; Mentler et al. 2005; Garnett et al. 2006; Furlan et al. 2007; Shearer and Soh 2007; Weiss et al. 2007). With histidine imidazoles being the primary coordinating ligands, the *pKa* of 6.02 (Martell and Smith 1974) would mean the imidazole nitrogen would be fully deprotonated at pH > 6.02 and would therefore be able to freely bind copper (II) without competition from protons. Under acidic conditions of between pH 5 and pH 6, strong competition from protons for the imidazole nitrogens mean that copper coordination is progressively less stable until at pH 4 the metal can no longer compete with protons. Additionally, as the pH falls, the glycine amides, PI 9.63 (Martell and Smith 1974) mean that only the imidazoles from the 4 histidines are available for copper coordination. The fact that affinity and

stoichiometry for copper (II) decline at pH 8 or above suggest that protein aggregation becomes an issue as the pH approaches the PI of 9.6.

8.21 Copper (II) Binding to the Octarepeat Region is Complex and Cooperative

The data from the pH study provide an interesting insight into how the octarepeat region behaves under differing concentrations of copper. When in acidic pH, the competition for protons mean that all four histidine ligands coordinate together to produce a 4N arrangement in the absence of the contribution from the now proton saturated glycine residues. This then resembles the low concentration copper coordination, often referred to as component 3 in the literature (Chattopadhyay et al. 2005). As pH increases and the proton affect diminishes, the four imidazole complexes split to bind one copper to two imidazoles, representing an intermediate copper coordination, as previously reported as component 2 (Wells et al. 2006). As pH increases further, so the copper is able to compete with protons for glycine amides and hence four copper (II) atoms are able to bind in the classic single copper to single histidine coordination, with contributions from the deprotonated amides from the adjacent glycine residues. This multi-stage coordination, or component 1 (Chattopadhyay et al. 2005) is clearly also occurring in the octarepeat region at physiological pH, but driven by copper concentration as opposed to competition from protons.

Sequential modelling of the copper (II) binding to the octarepeat region reveals some fascinating inter site interactions that support the current thinking on copper (II) binding well. At low copper concentration, a single high affinity binding event is apparent, with an affinity in the 0.1 nM range. As copper concentration increases, 3 other binding events are apparent, with affinities in the high micromolar to low nanomolar range. These values differ significantly from previous published work by out group (Thompsett et al. 2005). The reason for this discrepancy is simply the way the original data was handled. Although a method of analyses similar to the ITC method B highlighted in this thesis was used, the overall concentration of the chelating species was not taken into account. This had the affect of significantly over estimating the final affinity values. The pattern of copper (II) binding highlighted by this study is again very supportive of the multi-stage binding suggested by other work (Chattopadhyay et al.

2005). Additionally, the values I report here are strikingly close to recent values obtained by other groups (Millhauser 2007). The remarkable characteristics of copper (II) coordination to PrP highlighted by this work are evidence of negative cooperativity as copper concentration increases. More significantly, these data are further evidence of the way the protein is able to undergo enormous structural rearrangement within the N-terminus as the protein folds and unfolds under different coordination modes dependent on copper concentration. This is discussed later in this section with a view to protein function.

The work using mutants where the 5th site is removed in addition to one or more sites within the octarepeat region lends further support to the complexity of inter-site interaction with the region. Where only one copper (II) binding site remains, a clear assessment of the contribution by the individual repeat segments is achieved. Each segment binds copper in the high micromolar range. This ties in well with studies on peptides, revealing an affinity of 6.7 μM for each repeat (Hornshaw et al. 1995). When two repeats are present, the sites are able to interact to coordinate the copper with higher stability at low concentrations. The high degree of sensitivity of ITC as a technique to study binding reveals details that may be otherwise hidden from other techniques concerning the importance of the location of these remaining residues. Where the two remaining residues are close together, there is a clear increase in the stability of the first copper equivalent than when the two sites are more distal. This is again further evidence in support of the proposed coordination modes mentioned above. This pattern of coordination is continued in the mutant with 3 octarepeats available. These mutants display an affinity for copper (II) in the 10-100 nM range at the first equivalent of copper, reflecting the affect of the missing histidine imidazole on the stability of binding. This can be supported further by the observation that 4 histidine imidazoles will coordinate one molecule of copper (II) with a log stability constant of 12.6 (Martell and Smith 1974). Although this absolute value is unlikely to precisely match the absolute value seen in the protein due to the effects of folding and stearic interference, the reduction in the calculated literature affinity for three imidazoles of approximately log stability 2 (Martell and Smith 1974) should be evident in the experimental data. In fact this is precisely the case, with the mutant with three octarepeats showing a reduction in copper (II) stability of 2 orders of magnitude. In addition, the importance of the location of the remaining histidines is once again highlighted in this mutant as the

affinity for the first copper (II) equivalent is an order of magnitude more in the mutant with the three octarepeats in sequence. This lends further support to the inter octarepeat cooperativity and interaction.

8.22 Copper (II) Binding to the 5th Site is of Similar Affinity to that of the Octarepeat Region

Independent site modelling of the ITC data for the wild-type protein under acidic conditions allows for the mapping of a single binding event within the 5th site. This event increases in stability by 2 orders of magnitude per unit pH increase from log stability constant 4.3 at pH 5 to 10.8 at pH 7.5. This fact is somewhat confused, however, when the 5th site is looked at in isolation. In the mutant with octarepeat region histidines substituted with alanines, 2 copper (II) binding events are apparent within the 5th site. This second binding event is not apparent on the intact protein, if accepting that the octarepeat region is binding 4 coppers as the data clearly shows. This peculiarity within the data demands further investigation and so mutants with either of the histidines within the 5th replaced with alanine were looked at. Thermodynamic data from these experiments reveal that the primary coordinating ligand for copper (II) within the 5th site region is the histidine at position 110. This is supported by work from other groups showing the dominance of the last histidine (Klewpatinond and Viles 2007; Shearer and Soh 2007). Interestingly, the protein with only one histidine at position 95 showed no evidence of copper (II) binding under the conditions tested. This would mean that its relative affinity for copper is below that required to associate significantly with free copper (II) in the ITC cell. What is of striking significance is how these two binding elements interact to form a highly stable copper (II) ligand that far exceeds the sum of their individual contribution. This is especially highlighted in the mutant with only the 5th site present. Here, there are clearly 2 coppers binding with a log stability constant β_2 of 16.6 at pH 7. This is 6 orders of magnitude higher than the single 5th site binding event observed in the wild-type protein. This is strong evidence of intra site interactions. This extraordinary property has been seen by others working on this region. For example, one group showed that the relative of affinity of copper (II) for each histidine residue within the 5th site changed dependent on what other residues were present in peptide fragments representing the region (Klewpatinond and Viles 2007). They showed that the affinity of histidine 95 for copper (II) increased significantly on

addition of the hydrophobic segment just up stream of the histidine at 110. This is evidence of a highly complex and interacting system of copper (II) coordination within the 5th site.

The affinity of copper within the 5th site as revealed by sequential thermodynamic modelling is in good agreement with previously published values by a group that has produced the bulk of accepted copper binding data to the 5th site region. My calculated log stability constant of between 10.1 and 10.4 is similar to the nanomolar affinity reported by this group (Jones et al. 2004). This group also reported that the relative affinity of the 5th site for copper (II) is higher than that reported for the octarepeat region. From my data, I cannot confirm this as the octarepeat region's affinity for copper (II), at low copper concentrations at least, is almost identical to the 5th site. Where the 5th site would be able to out compete the octarepeat region for copper (II) would be under conditions where the ratio of copper (II) to protein is greater than 1.

8.23 The Two Copper (II) Binding Regions on PrP Also Show Evidence of Inter-Site Interaction

The two copper sites within the 5th site highlighted by other studies using peptides (Jones et al. 2004), do not appear to be present in the complete protein. It seems that, in the presence of the octarepeat region, the 5th site binds a single copper, pointing towards a repressive effect by the octarepeat region. The combined affinity of the two sites with the 5th binding region identified by this and other studies of log 16.7 would appear to be reduced to a single binding event of around log 10.4 in the wild-type protein. The octarepeat region binds 4 coppers in both the wild-type protein and in the protein with 5th site silenced at physiological pH. Again, in the presence of the other region, the octarepeat appears to suffer a slight reduction in the affinity for copper within its high affinity site. This data suggests an interaction between the two regions of PrP when coordinating copper. To investigate this phenomena, mutants with the 5th site present and one site within the octarepeat present either close or distal to the 5th site are utilised. It is clear from the data that the presence of copper within the 5th site has a significant effect on copper binding within the octarepeat. The stability of copper binding within a single octarepeat region increases by an order of magnitude when copper is present within the 5th site. Also of note is that copper binding within the octarepeat region

appears to reduce the stability of the copper (II) within the 5th site. This affect is dependent on the distance of the octarepeat site from the 5th site. Where the remaining copper site is close to the 5th site region, a relatively large reduction in 5th site stability is observed, approaching an order of magnitude. Where the remaining site is distal, from the region, a very small reduction in 5th site stability is apparent. This effect can be seen in studies involving the entire protein (Davies et al. 2009) and involves the affects of dramatic structural changes in the presence of copper within the octarepeat region. This is evidenced by the fact that the affect is more pronounced in the mutant with the remaining histidine in close proximity to the 5th site. This is also strong evidence for why the 5th site, when in isolation, can bind 2 copper atoms but only 1 when the octarepeat region is present.

8.24 The Affinity and Cooperative Nature of Copper (II) binding to PrP Support a Copper Dependent Role for the Protein

PrP is clearly a copper (II) binding protein that binds copper with high affinity optimally at physiological pH. This is suggestive of a role for copper in the proteins function. Elucidating this function, considering a lack of any severe consequences to PrP knock out animal models (Flechsig et al. 2003), is difficult in the extreme. This lack of consequence is not necessarily a direct indicator of irrelevance. The body, especially the brain, has a plethora of backup systems should one be depleted or lacking for any reason (Nilsson 2001). A classic example is that of a superoxide dismutase knocked out in a similar mouse model to that of the PrP knockout experiment (Kirk et al. 2000). The authors clearly show that many critical systems have back up and redundancy and by simply monitoring the affects over a single short life span, no information as to the function of the knocked out gene is revealed. Considering this fact and that PrP appears to follow the same pattern, only thorough biochemical investigation can lend any credence to possible protein function.

An affinity of copper (II) for PrP in the 0.1 nM range would allow for many potential copper based functions. This level of copper (II) stability, for example, is in a comparable range to transport proteins such as serum albumin, with a log stability constants of 11 (Brown and Besinger 1998). Other functional copper proteins such as cerruloplasmin, can bind copper in some sites with a log stability constant as low as 5 to

7 (Giroux and Schoun 1981). Many copper chaperones have relatively low affinity with log stability constant of 4.1 for CopC (Arnesano et al. 2002), 5.4 for ATOX-1 (Wernimont et al. 2004) and 6.8 for COX-17 (Abajian et al. 2004). In fact, the affinity of copper (II) for PrP is not hugely out of range from estimates of the affinity of copper for Cu/Zn SOD of log stability constant 12.6 (Hirose et al. 1988). Although this does not allow for the identification of PrP's functional role, it does at least allow for these functions as possible for the protein.

What is of enormous interest to anyone attempting an elucidation of PrP function is the way the protein coordinates copper. I have been utterly fascinated by the way PrP is able to alter the way its binds copper dependent on the concentration of the metal it is exposed to. My data strongly supports the complex cooperative nature of copper binding to PrP highlighted by many other studies. It would seem plausible then, given this and the other multiple reports of a negative cooperation and multiple disassociation constants within the octarepeat binding region (Jackson et al. 2001; Garnett and Viles 2003; Thompsett et al. 2005; Walter et al. 2006) that there would be at least some available copper binding sites free on presentation to the extracellular environment. This would leave open the interestingly possibility that the dramatic restructuring seen in the N-terminus of the protein during maximum copper occupancy (Chattopadhyay et al. 2005; Weiss et al. 2007) could be a trigger for internalisation of the protein. Clearly there is much direct evidence showing that copper increases the rate of internalisation (Pauly and Harris 1998; Brown 1999; Brown 2004) and that the N terminus was key to this process (Lee et al. 2001; Marella et al. 2002). Additionally, it is now known that physiologically relevant amounts of copper are sufficient to drive the internalisation process (Haigh et al. 2005). This may suggest that PrP is able to function as a concentration sensitive sequester of copper, activated when extracellular copper reaches peak levels during synaptic transmission and depolarisation of between 15 μM and 300 μM (Kardos et al. 1989). This copper may then be transferred back into the cells for recycling.

Comparison of the way PrP interacts with other metals lends further support to copper (II) being a functional partner of PrP. Studies on the binding of other metals with PrP are largely in agreement with the published pattern of cation binding to amino acids (Gilli et al. 1998). These data suggest that the affinity of amino acid residues with

metals follow the pattern of alkali metals < earth metals < transition metals. There is no apparent binding of magnesium to PrP but all of the transition metals tested do produce isothermal data. As with copper, this binding is dependant on pH. Nickel (II) and zinc (II) both bind with highest affinity to the octarepeat region and at pH 7 whereas iron (II) binds with highest affinity at the 5th site. In acidic conditions, only iron is able to bind and at he 5th site. This is again further evidence of two very different binding mechanisms within the octarepeat and the 5th site. Divalent cat ions which are able to bind the 5th site appear to do so in acidic or neutral conditions whereas binding within the octarepeat is always optimal at neutral to mildly basic conditions. This would suggest the involvement of histidines for the binding of other metals as well as copper. Even under optimal conditions, it would seem unlikely that the associations of these metals with PrP play a role in its physiological function due to their relatively low stability constants from PrP. When compared to physiological systems associated with these metals, it is clear that such low affinity values would be unlikely to enable PrP to have a role in transport, storage or catalysis in connection with iron, nickel or zinc. For example, transferrin has been shown to bind Fe with an affinity of 10^{23} (Aisen et al. 1974) and Cu/Zn SOD binds zinc with an affinity of 4.2×10^{14} (Crow et al. 1997). It is also clear that, under physiological conditions, these metals would be unable to displace copper from the protein even in a free ionic form.

There had also been a good deal of work on the binding of manganese to PrP carried out by my research group (Brazier et al. 2008). This work revealed two sites for the metal, one within the octarepeat region with log stability 3.6 and one within the 5th site log stability 4.2. Unlike iron, nickel or zinc, the affinity of the protein for manganese may be physiologically relevant as most manganese binding proteins have relatively low affinity for the metal (Jose et al. 1999; Garrick et al. 2006; Brazier et al. 2008). The metal transporter DMT-1 for example, displays an affinity for manganese of just 3 mM (Garrick et al. 2006). Despite this, the nanomolar concentrations of manganese within the brain would not allow for the formation of PrP-Mn complexes under normal physiological conditions. So herein lays another dichotomy with PrP. The protein should not be able to bind manganese physiologically and yet it has been shown that PrP derived from brains or cell culture has manganese bound (Brown et al. 2000; Wong et al. 2001; Thackray et al. 2002). Additionally, manganese binding to PrP occurs within the octarepeat and the 5th site (Brazier et al. 2008), and despite the proteins

strong preference for copper, my electrochemical data shows that manganese can displace copper from these sites. This is also supported by other work from my group (Brazier et al. 2008). This is an area that will need to be investigated further, not least because of the affect of manganese when bound, highlighted in both the survival studies presented in this thesis and the evidence showing that manganese can cause the protein to become protease resistant (Kim et al. 2005) and aggregate (Brown et al. 1997). Additionally, manganese displacement of copper (II) has serious consequences for the redox capabilities of the protein (Brazier et al. 2008).

8.3 Copper (II) Bound PrP may have a Role in Physiological Redox Chemistry

The electrochemistry of metalloproteins is an area of considerable interest to me and one in which, I feel, is under investigated in terms of neurodegeneration. The copper binding characteristics revealed by the thermodynamic data suggest a copper dependent role for PrP. Many proteins that bind copper have a role in catalysis, immune defence or detoxification that involves copper dependent redox chemistry. There have been many functional redox studies whereby PrP is subjected to assays attempting to indirectly monitor redox activity (Brown et al. 1999; Walz et al. 1999; White et al. 1999; Frederikse et al. 2000; Wong et al. 2000; Brown et al. 2001; Wong et al. 2001; Dupuis et al. 2002; Huber et al. 2002; Miele et al. 2002; Curtis et al. 2003; Hutter et al. 2003; Rachidi et al. 2003; Zeng et al. 2003; Jones et al. 2005; Nadal et al. 2007). However, this has not yet been thoroughly explored by direct electrochemical evidence. There have been some recent studies on peptide fragments on the octarepeat (Hureau et al. 2006; Hureau et al. 2008) and the 5th site (Shearer and Soh 2007) but, especially in the case of the later study, have only produced relativiely weak electrochemical data. The study on the 5th site did show a very low electrochemical signal over background but, in my opinion, the amount of extrapolation was not justified by the data presented. It is clear that the problem faced by the authors of these studies is one of method. This research was based on cyclic voltammetry, a system allowing direct potentiodynamic electrochemical measurement. This method ramps potential up and down across an electrode and the current recorded at this electrode and plotted against time. This then allows for the determination of the redox properties of an element in solution to be determined. This method is limited, however, in sensitivity and by its requirement to

have relatively large amount of concentrated analyte in solution (Bard and Faulkner 2001). It is also complicated by the need to factor in the migration of the analyte through the solution. A major goal of this study was to therefore design a system whereby direct cyclic voltammetric measurements could be made without these hindrances.

PrP has been shown to adhere strongly to mineral surfaces (Johnson et al. 2006) due to its strong positive charge originating from arginine and lysine residues at neutral pH. Based on this property, various electronegative surfaces were tested for there electrochemical suitability. The discovery that boron doped diamond can serve as both an excellent working electrode with very low background noise and also adsorb PrP strongly was a major step forward in the design of a suitable system. Once optimised, this system produced excellent data revealing important insight into the electrochemistry of PrP. When copper is bound to the protein, it is clear that PrP is able to undergo fully reversible redox cycling with a potential of 0.03 ± 0.01 V vs. SCE. This electrochemistry is largely dependent on the copper bound to the octarepeat region but also involves the 5^{th} site, but not independently. The data clearly shows that the 5^{th} site is involved with channelling electrons into the octarepeat region, which needs to be complete and correctly folded to take part in this 5^{th} site oxidation and subsequent reduction. This may lend extra support to the finding that the octarepeat region protects the 5^{th} site from oxidative damage (Nadal et al. 2007). This appears to be further evidence for the interaction between the two copper binding regions. The redox cycling is limited by the rate of electron transfer and is fully reversible, indicating that the wild-type protein is unaffected by continuous oxidation and reduction. Despite the proposed square planner copper coordination geometry, copper (I) and copper (II) are able to remain stably bound to the protein during cycling. Previous work has demonstrated this property (Hureau et al. 2006). The mid point potential of 0.03 mV would mean *in vivo* conditions would favour a redox able state. Configurational and structural effects due to the adsorption onto the electrode are clearly identified by the AFM imaging and calculated charge per redox centre confirms that adsorbed PrP is active on the surface of the electrode.

It is difficult to consider a non catalytic role for a protein that had evolved such interesting redox capabilities. Although there is very little direct electrochemical

evidence to compare my data with, there is an enormity of data suggesting a catalytic role for PrP, especially one involved in the detoxification of reactive oxygen species (Brown et al. 1999; Brown et al. 2001; Klamt et al. 2001; Wong et al. 2001; Dupuis et al. 2002; Huber et al. 2002; Miele et al. 2002; Curtis et al. 2003; Rachidi et al. 2003; Zeng et al. 2003; Brown 2005). Certainly, should PrP have such a function, then there would be backup systems in place that would make it difficult to detect as highlighted above. To suggest a copper dependent redox role for PrP without exploring the redox implications of other metals when bound to the protein would be inappropriate. Considering the data from the thermodynamic metal binding studies suggest a potentially significant interaction with manganese, and that the metal provides increased stability to the protein, this would be a good metal to evaluate. Exposure of the copper bound protein to manganese produced some very interesting redox data. It would appear that manganese is able to displace some redox critical copper (II) molecules and disrupt the redox properties of the protein. This is despite the proteins strong preference for copper. This would mean that in circumstances where the *in vivo* protein is exposed to manganese, it would lose its ability to undergo redox cyclic and potentially become permanently oxidised under conditions of oxidative stress. The CV data suggests that at least 2 coppers are displaced from the octarepeat region by manganese. As other work has demonstrated that this region when bound to copper (II) is protective against 5^{th} site oxidation (Nadal et al. 2007) then this may provide evidence of the mechanism by which oxidative damage to PrP could occur. Certainly my work on the electrochemistry of PrP has highlighted an interesting redox interaction between the octarepeat region and the 5^{th} site so this mechanism of oxidative damage to the protein is interesting. This may be especially relevant to the ability of the protein to survive in the environment when exposed to manganese in light of work showing that oxidised PrP may convert to a protease resistant form (Kawano 2007).

This electrochemical work, although very interesting, is relatively preliminary. In order to fully convince the scientific community of the relevance of these findings to the function or perhaps miss-function of PrP, the method needs further development. I am planning to combine CV with other biochemical techniques in order to produce a full and complete electrochemical picture of how the protein behaves in various biologically relevant situations. For example, I have theorised that CV may be combined with calorimetry to monitor the redox implications of copper (II) during it's association with

PrP. This will provide information on whether there is any reduction of copper during any of the three coordination modes within the octarepeat region. I also want to combine CV with oxidative stress assays in which the protein is exposed to or allowed to generate reactive oxygen species in solution. This will provide insight into what occurs to the protein during situations of oxidative stress and whether the protein is altered by reactive species or able to detoxify them. With recent theories on the involvement of PrP in other neurodegenerative disease involving oxidative stress (Hooper and Turner 2008), the interaction of PrP with reactive oxygen species may produce some far reaching implications. In this vein, this approach of redox analysis is already being tested for other proteins linked to neurodegeneration such as amyloid precursor protein (APP) and the synucleins. As these proteins carry very different charge states to PrP, new was of interfacing the protein to the electrode are being developed.

8.4 Metals in Environment have a Significant Affect on the stability of PrP

This study has demonstrated that even in the absence of metals, PrP resists degradation remarkably well and after 12 months is still present in clay. When the clay is anhydrous, the protein is able to resist degradation for even longer periods of time, presumably due to the absence of hydrolytic affects. This data supports other studies which have shown increased PrP stability when associated with clays (Johnson et al. 2006; Johnson et al. 2007). What is striking from my work, however, is the affect of manganese when present in the soil model. PrP exposed to Mn-mte matrices appears impervious to degradation and is still present after over 2 years of incubation at room temperature. The mechanism of PrP stabilisation in the presence of manganese does not appear to involve known metal binding elements within the protein. Studies with Mn-mte using a mutant PrP with all N-terminal histidines removed did not reduce the proteins resistance to degradation when compared to wild-type protein. This is not at all surprising. It has been shown, for example, that manganese can cause PrP to fold into a protease resistant form (Brown et al. 2000) and promote aggregation and increases in beta sheet content (Giese et al. 2004). It is likely therefore that these factors provide the mechanism for manganese stabilisation of PrP in soil.

There have been many attempts to correlate unusual distributions of soil metals and minerals with incidence of TSE outbreak (Purdey 2000; Nishida 2003; Chihota et al. 2004; Purdey 2004; Johnson et al. 2006; Johnson et al. 2007; Polano et al. 2008; Imrie et al. 2009; Russo et al. 2009). These studies have produced a varied group of results, some strongly suggesting that soil mineral and metal contents are important for survival (Purdey 1998; Purdey 2000; Purdey 2001; Nishida 2003; Purdey 2004; Purdey 2005; Ragnarsdottir and Hawkins 2005; Purdey 2006; Imrie et al. 2009) and others proving otherwise (Chihota et al. 2004). Of these studies, many have highlighted imbalances of copper and manganese as possible factors (Purdey 2000; Purdey 2001; Nishida 2003; Purdey 2004; Purdey 2005; Ragnarsdottir and Hawkins 2005). Combined with my data and evidence showing these metals have significant affects on protein stability (Brown et al. 2000) and that infected animals show imbalance of these metals (Wong et al. 2001; Wong et al. 2001; Thackray et al. 2003; Wong et al. 2004; Hesketh et al. 2007), a clear mechanism for PrP survival in the environment is apparent.

In order to determine the environmental significance of this work, it will need to be supported with field studies in which samples of soils from areas of farmland are collected and analysed. Any protein can be extracted by the methods that have evolved through this work and then analysed for manganese content and protease resistance. It is not yet known whether protein will be detected in random soil samples but my feeling from this study is it will be possible. This will require significant funding but should be investigated further at both a biochemical and geological level. Additionally, the recovered protein from the soil needs to be analysed for infectivity in animal models. Attempts were made at the beginning of this study to infect cell culture with the lysates but this proved impossible due to the toxicity of the clay itself. The cultured neurones are simply too vulnerable to such insult and cannot survive challenge from such alien substances. Such work may be critical to understand the transmission of the disease and to its eventual eradication.

8.5 Concluding Remarks

The way copper (II) coordinates to PrP has now been established beyond doubt. PrP binds copper with high affinity and in a way that it utterly dependent on the concentration of copper (II) the protein is exposed to. The structural affects and the

degree of stability of copper (II) binding, combined with the remarkable redox characteristics are highly suggestive of a copper dependent functional role for PrP. PrP itself is a highly stable and resilient protein, but in the presence of metals becomes almost immortal. The finding that manganese provides enormous stability to the protein provides a good basis for how PrP may remain in the environment and infect livestock grazing on the contaminated land.

This study has provided confirmation of many previously suggested facts concerning the metal associations of PrP. The work has also produced much preliminary data which may lead to further advances concerning PrP and other proteins involved in neurodegeneration.

References

Ababou, A. and J. E. Ladbury (2006). "Survey of the year 2004: literature on applications of isothermal titration calorimetry." J Mol Recognit **19**(1): 79-89.

Ababou, A. and J. E. Ladbury (2007). "Survey of the year 2005: literature on applications of isothermal titration calorimetry." J Mol Recognit **20**(1): 4-14.

Abajian, C., L. A. Yatsunyk, et al. (2004). "Yeast cox17 solution structure and Copper(I) binding." J Biol Chem **279**(51): 53584-92.

Abolmaali, B., H. Taylor, et al. (1998). Evolutionary aspects of copper binding centers in copper proteins. Bioinorganic Chemistry**:** 91-190.

Aisen, P., A. Leibman, et al. (1974). "The anion-binding functions of transferrin." Adv Exp Med Biol **48**(0): 125-40.

Anderson, R. M., C. A. Donnelly, et al. (1996). "Transmission dynamics and epidemiology of BSE in British cattle." Nature **382**(6594): 779-88.

Andrews, N. J. (2009). "Incidence of variant Creutzfeldt-Jakob disease diagnoses and deaths in the UK." Retrieved 10/04/2009, 2009, from http://www.cjd.ed.ac.uk/cjdq60.pdf.

Arnesano, F., L. Banci, et al. (2002). "Solution structure of CopC: a cupredoxin-like protein involved in copper homeostasis." Structure **10**(10): 1337-47.

Aronoff-Spencer, E., C. S. Burns, et al. (2000). "Identification of the Cu2+ binding sites in the N-terminal domain of the prion protein by EPR and CD spectroscopy." Biochemistry **39**(45): 13760-71.

Bard, A. J. and L. R. Faulkner (1980). Electrochemical methods : fundamentals and applications, Wiley.

Bard, A. J. and L. R. Faulkner (2001). Electrochemical methods : fundamentals and applications. New York ; Chichester, John Wiley.

Bocharova, O. V., L. Breydo, et al. (2005). "Copper(II) inhibits in vitro conversion of prion protein into amyloid fibrils." Biochemistry **44**(18): 6776-87.

Brady, N. C. and R. R. Weil (1996). The nature and properties of soils. London, Prentice Hall International.

Brazier, M. W., P. Davies, et al. (2008). "Manganese binding to the prion protein." J Biol Chem **283**(19): 12831-9.

Brown, D. R. (1999). "Prion protein expression aids cellular uptake and veratridine-induced release of copper." J Neurosci Res **58**(5): 717-25.

Brown, D. R. (2004). "Role of the prion protein in copper turnover in astrocytes." Neurobiol Dis **15**(3): 534-43.

Brown, D. R. (2005). "Neurodegeneration and oxidative stress: prion disease results from loss of antioxidant defence." Folia Neuropathol **43**(4): 229-43.

Brown, D. R. and A. Besinger (1998). "Prion protein expression and superoxide dismutase activity." Biochem J **334 (Pt 2)**: 423-9.

Brown, D. R., C. Clive, et al. (2001). "Antioxidant activity related to copper binding of native prion protein." J Neurochem **76**(1): 69-76.

Brown, D. R., F. Hafiz, et al. (2000). "Consequences of manganese replacement of copper for prion protein function and proteinase resistance." Embo J **19**(6): 1180-6.

Brown, D. R., K. Qin, et al. (1997). "The cellular prion protein binds copper in vivo." Nature **390**(6661): 684-7.

Brown, D. R., B. Schmidt, et al. (1998). "Effects of copper on survival of prion protein knockout neurons and glia." J Neurochem **70**(4): 1686-93.

Brown, D. R., B. S. Wong, et al. (1999). "Normal prion protein has an activity like that of superoxide dismutase." Biochem J **344 Pt 1**: 1-5.

Brown, L. R. and D. A. Harris (2003). "Copper and zinc cause delivery of the prion protein from the plasma membrane to a subset of early endosomes and the Golgi." J Neurochem **87**(2): 353-63.

Brown, P. (1998). "Donor pool size and the risk of blood-borne Creutzfeldt-Jakob disease." Transfusion **38**(3): 312-5.

Brown, P. and R. Bradley (1998). "1755 and all that: a historical primer of transmissible spongiform encephalopathy." Bmj **317**(7174): 1688-92.

Brown, P., M. A. Preece, et al. (1992). ""Friendly fire" in medicine: hormones, homografts, and Creutzfeldt-Jakob disease." Lancet **340**(8810): 24-7.

Bruce, M. E., P. A. McBride, et al. (1994). "PrP in pathology and pathogenesis in scrapie-infected mice." Mol Neurobiol **8**(2-3): 105-12.

Burns, C. S., E. Aronoff-Spencer, et al. (2002). "Molecular features of the copper binding sites in the octarepeat domain of the prion protein." Biochemistry **41**(12): 3991-4001.

Burns, C. S., E. Aronoff-Spencer, et al. (2003). "Copper coordination in the full-length, recombinant prion protein." Biochemistry **42**(22): 6794-803.

Chattopadhyay, M., E. D. Walter, et al. (2005). "The octarepeat domain of the prion protein binds Cu(II) with three distinct coordination modes at pH 7.4." J Am Chem Soc **127**(36): 12647-56.

Chiesa, R. and D. A. Harris (2001). "Prion diseases: what is the neurotoxic molecule?" Neurobiol Dis **8**(5): 743-63.

Chihota, C. M., M. B. Gravenor, et al. (2004). "Investigation of trace elements in soil as risk factors in the epidemiology of scrapie." Vet Rec **154**(26): 809-13.

Cliff, M. J., A. Gutierrez, et al. (2004). "A survey of the year 2003 literature on applications of isothermal titration calorimetry." J Mol Recognit **17**(6): 513-23.

Cliff, M. J. and J. E. Ladbury (2003). "A survey of the year 2002 literature on applications of isothermal titration calorimetry." J Mol Recognit **16**(6): 383-91.

Collinge, J. and M. S. Palmer (1994). "Molecular genetics of human prion diseases." Philos Trans R Soc Lond B Biol Sci **343**(1306): 371-8.

Collins, S., C. A. McLean, et al. (2001). "Gerstmann-Straussler-Scheinker syndrome,fatal familial insomnia, and kuru: a review of these less common human transmissible spongiform encephalopathies." J Clin Neurosci **8**(5): 387-97.

Cooke, C. M., J. Rodger, et al. (2007). "Fate of prions in soil: detergent extraction of PrP from soils." Environ Sci Technol **41**(3): 811-7.

Crow, J. P., J. B. Sampson, et al. (1997). "Decreased zinc affinity of amyotrophic lateral sclerosis-associated superoxide dismutase mutants leads to enhanced catalysis of tyrosine nitration by peroxynitrite." J Neurochem **69**(5): 1936-44.

Cui, T., M. Daniels, et al. (2003). "Mapping the functional domain of the prion protein." Eur J Biochem **270**(16): 3368-76.

Curtis, J., M. Errington, et al. (2003). "Age-dependent loss of PTP and LTP in the hippocampus of PrP-null mice." Neurobiol Dis **13**(1): 55-62.

Daniels, M. and D. R. Brown (2002). "Purification and preparation of prion protein: synaptic superoxide dismutase." Methods Enzymol **349**: 258-67.

Davies, P. and D. R. Brown (2008). "The chemistry of copper binding to PrP: is there sufficient evidence to elucidate a role for copper in protein function?" Biochem J **410**(2): 237-44.

Davies, P. and D. R. Brown (2008). "A Critical Assessment of Two Methods of Mathematical Analysis for Complex Protein and Chelated Ligand Thermodynamics." Dalton Trans **In Submission**.

Davies, P., F. Marken, et al. (2009). "Thermodynamic and voltammetric characterisation of the metal binding to the prion protein – insights into pH Dependence and redox chemistry." Biochemistry **Accepted for publication 6/2/9**

DeArmond, S. J. and E. Bouzamondo (2002). "Fundamentals of prion biology and diseases." Toxicology **181-182**: 9-16.

Deer, W. A., R. A. Howie, et al. (1992). An introduction to the rock-forming minerals. Harlow, Longman Scientific & Technical.

Dhillon, H., K. Sharma, et al. (2009). "Electrochemical and spectral characterization of blue copper protein models." Electrochemistry Communications **11**(4): 878-880.

Dupuis, L., C. Mbebi, et al. (2002). "Loss of prion protein in a transgenic model of amyotrophic lateral sclerosis." Mol Cell Neurosci **19**(2): 216-24.

Flechsig, E., I. Hegyi, et al. (2003). "Expression of truncated PrP targeted to Purkinje cells of PrP knockout mice causes Purkinje cell death and ataxia." Embo J **22**(12): 3095-101.

Frederikse, P. H., S. J. Zigler, Jr., et al. (2000). "Prion protein expression in mammalian lenses." Curr Eye Res **20**(2): 137-43.

Furlan, S., G. La Penna, et al. (2007). "Studying the Cu binding sites in the PrP N-terminal region: a test case for ab initio simulations." Eur Biophys J **36**(7): 841-5.

Gajdusek, D. C. (1991). "The transmissible amyloidoses: genetical control of spontaneous generation of infectious amyloid proteins by nucleation of configurational change in host precursors: kuru-CJD-GSS-scrapie-BSE." Eur J Epidemiol **7**(5): 567-77.

Garnett, A. P., C. E. Jones, et al. (2006). "A survey of diamagnetic probes for copper2+ binding to the prion protein. 1H NMR solution structure of the palladium2+ bound single octarepeat." Dalton Trans(3): 509-18.

Garnett, A. P. and J. H. Viles (2003). "Copper binding to the octarepeats of the prion protein. Affinity, specificity, folding, and cooperativity: insights from circular dichroism." J Biol Chem **278**(9): 6795-802.

Garrick, M. D., S. T. Singleton, et al. (2006). "DMT1: which metals does it transport?" Biol Res **39**(1): 79-85.

Ge, B., F. W. Scheller, et al. (2003). "Electrochemistry of immobilized CuZnSOD and FeSOD and their interaction with superoxide radicals." Biosensors and Bioelectronics **18**(2-3): 295-302.

Genovesi, S., L. Leita, et al. (2007). "Direct detection of soil-bound prions." PLoS ONE **2**(10): e1069.

Giese, A., J. Levin, et al. (2004). "Effect of metal ions on de novo aggregation of full-length prion protein." Biochem Biophys Res Commun **320**(4): 1240-6.

Gilli, R., D. Lafitte, et al. (1998). "Thermodynamic analysis of calcium and magnesium binding to calmodulin." Biochemistry **37**(16): 5450-6.

Giroux, E. and J. Schoun (1981). "Copper and zinc ion binding by bovine, dog, and rat serum albumins." J Inorg Biochem **14**(4): 359-62.

Griffith, J. S. (1967). "Self-replication and scrapie." Nature **215**(5105): 1043-4.

Grim, R. E. (1962). Applied Clay Mineralogy. [With illustrations.], pp. viii. 422. McGraw-Hill Book Co.: New York.

Haigh, C. L., K. Edwards, et al. (2005). "Copper binding is the governing determinant of prion protein turnover." Mol Cell Neurosci **30**(2): 186-96.
Halliwell, B. and J. M. Gutteridge (1990). "Role of free radicals and catalytic metal ions in human disease: an overview." Methods Enzymol **186**: 1-85.
Halliwell, B. and J. M. Gutteridge (1992). "Biologically relevant metal ion-dependent hydroxyl radical generation. An update." FEBS Lett **307**(1): 108-12.
Harris, D. A. (1999). "Cell biological studies of the prion protein." Curr Issues Mol Biol **1**(1-2): 65-75.
Hasnain, S. S., L. M. Murphy, et al. (2001). "XAFS study of the high-affinity copper-binding site of human PrP(91-231) and its low-resolution structure in solution." J Mol Biol **311**(3): 467-73.
Hesketh, S., J. Sassoon, et al. (2007). "Elevated manganese levels in blood and central nervous system occur before onset of clinical signs in scrapie and bovine spongiform encephalopathy." J Anim Sci **85**(6): 1596-609.
Hirose, J., S. Toida, et al. (1988). "Studies of copper-binding behavior of copper-free and apo-superoxide dismutase by high-performance liquid chromatography." Chem Pharm Bull (Tokyo) **36**(6): 2103-8.
Hooper, N. M. and A. J. Turner (2008). "A new take on prions: preventing Alzheimer's disease." Trends Biochem Sci **33**(4): 151-5.
Hornshaw, M. P., J. R. McDermott, et al. (1995). "Copper binding to the N-terminal tandem repeat regions of mammalian and avian prion protein." Biochem Biophys Res Commun **207**(2): 621-9.
Hornshaw, M. P., J. R. McDermott, et al. (1995). "Copper binding to the N-terminal tandem repeat region of mammalian and avian prion protein: structural studies using synthetic peptides." Biochem Biophys Res Commun **214**(3): 993-9.
Hsiao, K., S. R. Dlouhy, et al. (1992). "Mutant prion proteins in Gerstmann-Straussler-Scheinker disease with neurofibrillary tangles." Nat Genet **1**(1): 68-71.
Huber, R., T. Deboer, et al. (2002). "Sleep deprivation in prion protein deficient mice sleep deprivation in prion protein deficient mice and control mice: genotype dependent regional rebound." Neuroreport **13**(1): 1-4.
Hureau, C., L. Charlet, et al. (2006). "A spectroscopic and voltammetric study of the pH-dependent Cu(II) coordination to the peptide GGGTH: relevance to the fifth Cu(II) site in the prion protein." J Biol Inorg Chem **11**(6): 735-44.
Hureau, C., C. Mathe, et al. (2008). "Folding of the prion peptide GGGTHSQW around the copper(II) ion: identifying the oxygen donor ligand at neutral pH and probing the proximity of the tryptophan residue to the copper ion." J Biol Inorg Chem **13**(7): 1055-64.
Hutter, G., F. L. Heppner, et al. (2003). "No superoxide dismutase activity of cellular prion protein in vivo." Biol Chem **384**(9): 1279-85.
Imrie, C. E., A. Korre, et al. (2009). "Spatial correlation between the prevalence of transmissible spongiform diseases and British soil geochemistry." Environ Geochem Health **31**(1): 133-45.
Jackson, G. S., I. Murray, et al. (2001). "Location and properties of metal-binding sites on the human prion protein." Proc Natl Acad Sci U S A **98**(15): 8531-5.
Jobling, M. F., X. Huang, et al. (2001). "Copper and zinc binding modulates the aggregation and neurotoxic properties of the prion peptide PrP106-126." Biochemistry **40**(27): 8073-84.
Johnson, C. J., J. A. Pedersen, et al. (2007). "Oral transmissibility of prion disease is enhanced by binding to soil particles." PLoS Pathog **3**(7): e93.

Johnson, C. J., K. E. Phillips, et al. (2006). "Prions adhere to soil minerals and remain infectious." PLoS Pathog **2**(4): e32.

Johnson, W. C. (1999). "Analyzing protein circular dichroism spectra for accurate secondary structures." Proteins **35**(3): 307-12.

Jones, C. E., S. R. Abdelraheim, et al. (2004). "Preferential Cu2+ coordination by His96 and His111 induces beta-sheet formation in the unstructured amyloidogenic region of the prion protein." J Biol Chem **279**(31): 32018-27.

Jones, C. E., M. Klewpatinond, et al. (2005). "Probing copper2+ binding to the prion protein using diamagnetic nickel2+ and 1H NMR: the unstructured N terminus facilitates the coordination of six copper2+ ions at physiological concentrations." J Mol Biol **346**(5): 1393-407.

Jones, S., M. Batchelor, et al. (2005). "Recombinant prion protein does not possess SOD-1 activity." Biochem J **392**(Pt 2): 309-12.

Jose, T. J., L. H. Conlan, et al. (1999). "Quantitative evaluation of metal ion binding to PvuII restriction endonuclease." J Biol Inorg Chem **4**(6): 814-23.

Kardos, J., I. Kovacs, et al. (1989). "Nerve endings from rat brain tissue release copper upon depolarization. A possible role in regulating neuronal excitability." Neurosci Lett **103**(2): 139-44.

Kawano, T. (2007). "Prion-derived copper-binding peptide fragments catalyze the generation of superoxide anion in the presence of aromatic monoamines." Int J Biol Sci **3**(1): 57-63.

Kim, N. H., J. K. Choi, et al. (2005). "Effect of transition metals (Mn, Cu, Fe) and deoxycholic acid (DA) on the conversion of PrPC to PrPres." Faseb J **19**(7): 783-5.

Kirk, E. A., M. C. Dinauer, et al. (2000). "Impaired Superoxide Production Due to a Deficiency in Phagocyte NADPH Oxidase Fails to Inhibit Atherosclerosis in Mice." Arterioscler Thromb Vasc Biol **20**(6): 1529-1535.

Klamt, F., F. Dal-Pizzol, et al. (2001). "Imbalance of antioxidant defense in mice lacking cellular prion protein." Free Radic Biol Med **30**(10): 1137-44.

Klewpatinond, M. and J. H. Viles (2007). "Fragment length influences affinity for Cu2+ and Ni2+ binding to His96 or His111 of the prion protein and spectroscopic evidence for a multiple histidine binding only at low pH." Biochem J **404**(3): 393-402.

Kramer, M. L., H. D. Kratzin, et al. (2001). "Prion protein binds copper within the physiological concentration range." J Biol Chem **276**(20): 16711-9.

Kretzschmar, H. A., M. Neumann, et al. (1995). "Codon 178 mutation of the human prion protein gene in a German family (Backer family): sequencing data from 72-year-old celloidin-embedded brain tissue." Acta Neuropathol **89**(1): 96-8.

Kuwahara, C., A. M. Takeuchi, et al. (1999). "Prions prevent neuronal cell-line death." Nature **400**(6741): 225-6.

Lee, K. S., A. C. Magalhaes, et al. (2001). "Internalization of mammalian fluorescent cellular prion protein and N-terminal deletion mutants in living cells." J Neurochem **79**(1): 79-87.

Leitaa, L., F. Fornasiera, et al. (2006). "Interactions of prion proteins with soil." Interactions of prion proteins with soil **38**(7): 1638-1644

Liang, Y. (2008). "Applications of isothermal titration calorimetry in protein science." Acta Biochim Biophys Sin (Shanghai) **40**(7): 565-76.

Lin, L. N., A. B. Mason, et al. (1991). "Calorimetric studies of the binding of ferric ions to ovotransferrin and interactions between binding sites." Biochemistry **30**(50): 11660-9.

Linder, M. C. (2001). "Copper and genomic stability in mammals." Mutat Res **475**(1-2): 141-52.
Linder, M. C. and M. Hazegh-Azam (1996). "Copper biochemistry and molecular biology." Am J Clin Nutr **63**(5): 797S-811S.
Lugaresi, E., F. Cirignotta, et al. (1986). "Nocturnal myoclonus and restless legs syndrome." Adv Neurol **43**: 295-307.
Lugaresi, E., F. Cirignotta, et al. (1986). "Nocturnal paroxysmal dystonia." J Neurol Neurosurg Psychiatry **49**(4): 375-80.
Mange, A., O. Milhavet, et al. (2002). "PrP-dependent cell adhesion in N2a neuroblastoma cells." FEBS Lett **514**(2-3): 159-62.
Marella, M., S. Lehmann, et al. (2002). "Filipin prevents pathological prion protein accumulation by reducing endocytosis and inducing cellular PrP release." J Biol Chem **277**(28): 25457-64.
Martell, A. E. and R. M. Smith Critical Stability Constants. [S.l.], [s.n.].
Martell, A. E. and R. M. Smith (1974). Critical stability constants. New York ; London, Plenum Press.
McKintosh, E., S. J. Tabrizi, et al. (2003). "Prion diseases." J Neurovirol **9**(2): 183-93.
Medori, R., P. Montagna, et al. (1992). "Fatal familial insomnia: a second kindred with mutation of prion protein gene at codon 178." Neurology **42**(3 Pt 1): 669-70.
Mentler, M., A. Weiss, et al. (2005). "A new method to determine the structure of the metal environment in metalloproteins: investigation of the prion protein octapeptide repeat Cu(2+) complex." Eur Biophys J **34**(2): 97-112.
Miele, G., M. Jeffrey, et al. (2002). "Ablation of cellular prion protein expression affects mitochondrial numbers and morphology." Biochem Biophys Res Commun **291**(2): 372-7.
Millhauser, G. L. (2004). "Copper binding in the prion protein." Acc Chem Res **37**(2): 79-85.
Millhauser, G. L. (2007). "Copper and the prion protein: methods, structures, function, and disease." Annu Rev Phys Chem **58**: 299-320.
Miura, T., A. Hori-i, et al. (1996). "Metal-dependent alpha-helix formation promoted by the glycine-rich octapeptide region of prion protein." FEBS Lett **396**(2-3): 248-52.
Miura, T., S. Sasaki, et al. (2005). "Copper reduction by the octapeptide repeat region of prion protein: pH dependence and implications in cellular copper uptake." Biochemistry **44**(24): 8712-20.
Morante, S., R. Gonzalez-Iglesias, et al. (2004). "Inter- and intra-octarepeat Cu(II) site geometries in the prion protein: implications in Cu(II) binding cooperativity and Cu(II)-mediated assemblies." J Biol Chem **279**(12): 11753-9.
Mouillet-Richard, S., M. Ermonval, et al. (2000). "Signal transduction through prion protein." Science **289**(5486): 1925-8.
Nadal, R. C., S. R. Abdelraheim, et al. (2007). "Prion protein does not redox-silence Cu2+, but is a sacrificial quencher of hydroxyl radicals." Free Radic Biol Med **42**(1): 79-89.
Nielsen, A. D., C. C. Fuglsang, et al. (2003). "Isothermal titration calorimetric procedure to determine protein-metal ion binding parameters in the presence of excess metal ion or chelator." Anal Biochem **314**(2): 227-34.
Nilsson, J. (2001). "Absence of EC-SOD Does Not Promote Atherogenesis in Mice: Have We Lost Yet Another Player?" Arterioscler Thromb Vasc Biol **21**(9): 1387-1388.

Nishida, Y. (2003). "Elucidation of endemic neurodegenerative diseases--a commentary." Z Naturforsch [C] **58**(9-10): 752-8.
Norde, W. and C. E. Giacomelli (2000). "BSA structural changes during homomolecular exchange between the adsorbed and the dissolved states." J Biotechnol **79**(3): 259-68.
Okhrimenko, O. and I. Jelesarov (2008). "A survey of the year 2006 literature on applications of isothermal titration calorimetry." J Mol Recognit **21**(1): 1-19.
Pauly, P. C. and D. A. Harris (1998). "Copper stimulates endocytosis of the prion protein." J Biol Chem **273**(50): 33107-10.
Perera, W. S. and N. M. Hooper (2001). "Ablation of the metal ion-induced endocytosis of the prion protein by disease-associated mutation of the octarepeat region." Curr Biol **11**(7): 519-23.
Polano, M., C. Anselmi, et al. (2008). "Organic polyanions act as complexants of prion protein in soil." Biochem Biophys Res Commun **367**(2): 323-9.
Prusiner, S. B. (1982). "Novel proteinaceous infectious particles cause scrapie." Science **216**(4542): 136-44.
Prusiner, S. B. (1996). "Molecular biology and pathogenesis of prion diseases." Trends Biochem Sci **21**(12): 482-7.
Prusiner, S. B. (1998). "The prion diseases." Brain Pathol **8**(3): 499-513.
Prusiner, S. B. (1998). "Prions." Proc Natl Acad Sci U S A **95**(23): 13363-83.
Pucci, A., L. P. D'Acqui, et al. (2008). "Fate of prions in soil: interactions of RecPrP with organic matter of soil aggregates as revealed by LTA-PAS." Environ Sci Technol **42**(3): 728-33.
Purdey, M. (1998). "High-dose exposure to systemic phosmet insecticide modifies the phosphatidylinositol anchor on the prion protein: the origins of new variant transmissible spongiform encephalopathies?" Med Hypotheses **50**(2): 91-111.
Purdey, M. (2000). "Ecosystems supporting clusters of sporadic TSEs demonstrate excesses of the radical-generating divalent cation manganese and deficiencies of antioxidant co factors Cu, Se, Fe, Zn. Does a foreign cation substitution at prion protein's Cu domain initiate TSE?" Med Hypotheses **54**(2): 278-306.
Purdey, M. (2001). "Does an ultra violet photooxidation of the manganese-loaded/copper-depleted prion protein in the retina initiate the pathogenesis of TSE?" Med Hypotheses **57**(1): 29-45.
Purdey, M. (2004). "Elevated silver, barium and strontium in antlers, vegetation and soils sourced from CWD cluster areas: do Ag/Ba/Sr piezoelectric crystals represent the transmissible pathogenic agent in TSEs?" Med Hypotheses **63**(2): 211-25.
Purdey, M. (2005). "Metal microcrystal pollutants: the heat resistant, transmissible nucleating agents that initiate the pathogenesis of TSEs?" Med Hypotheses **65**(3): 448-77.
Purdey, M. (2006). "Auburn university research substantiates the hypothesis that metal microcrystal nucleators initiate the pathogenesis of TSEs." Med Hypotheses **66**(1): 197-9.
Qin, K., D. S. Yang, et al. (2000). "Copper(II)-induced conformational changes and protease resistance in recombinant and cellular PrP. Effect of protein age and deamidation." J Biol Chem **275**(25): 19121-31.
Qin, K., Y. Yang, et al. (2002). "Mapping Cu(II) binding sites in prion proteins by diethyl pyrocarbonate modification and matrix-assisted laser desorption ionization-time of flight (MALDI-TOF) mass spectrometric footprinting." J Biol Chem **277**(3): 1981-90.

Rachidi, W., D. Vilette, et al. (2003). "Expression of prion protein increases cellular copper binding and antioxidant enzyme activities but not copper delivery." J Biol Chem **278**(11): 9064-72.

Ragnarsdottir, K. V. and D. P. Hawkins (2005). "Bioavailable copper and manganese in soils from Iceland and their relationship with scrapie occurrence in sheep." J. Geochem. Explor. **88**: 228-234.

Redecke, L., W. Meyer-Klaucke, et al. (2005). "Comparative analysis of the human and chicken prion protein copper binding regions at pH 6.5." J Biol Chem **280**(14): 13987-92.

Revault, M., H. Quiquampoix, et al. (2005). "Fate of prions in soil: trapped conformation of full-length ovine prion protein induced by adsorption on clays." Biochim Biophys Acta **1724**(3): 367-74.

Ricchelli, F., R. Buggio, et al. (2006). "Aggregation/fibrillogenesis of recombinant human prion protein and Gerstmann-Straussler-Scheinker disease peptides in the presence of metal ions." Biochemistry **45**(21): 6724-32.

Roucou, X., M. Gains, et al. (2004). "Neuroprotective functions of prion protein." J Neurosci Res **75**(2): 153-61.

Russo, F., C. J. Johnson, et al. (2009). "Pathogenic prion protein is degraded by a manganese oxide mineral found in soils." J Gen Virol **90**(Pt 1): 275-80.

Santuccione, A., V. Sytnyk, et al. (2005). "Prion protein recruits its neuronal receptor NCAM to lipid rafts to activate p59fyn and to enhance neurite outgrowth." J Cell Biol **169**(2): 341-54.

Sarafoff, N. I., J. Bieschke, et al. (2005). "Automated PrPres amplification using indirect sonication." J Biochem Biophys Methods **63**(3): 213-21.

Saunders, S. E., S. L. Bartelt-Hunt, et al. (2008). "Prions in the environment: occurrence, fate and mitigation." Prion **2**(4): 162-9.

Schmitt-Ulms, G., G. Legname, et al. (2001). "Binding of neural cell adhesion molecules (N-CAMs) to the cellular prion protein." J Mol Biol **314**(5): 1209-25.

Servagent-Noinville, S., M. Revault, et al. (2000). "Conformational Changes of Bovine Serum Albumin Induced by Adsorption on Different Clay Surfaces: FTIR Analysis." J Colloid Interface Sci **221**(2): 273-283.

Shearer, J. and P. Soh (2007). "The copper(II) adduct of the unstructured region of the amyloidogenic fragment derived from the human prion protein is redox-active at physiological pH." Inorg Chem **46**(3): 710-9.

Shearer, J. and P. Soh (2007). "Ni K-edge XAS suggests that coordination of Ni(II) to the unstructured amyloidogenic region of the human prion protein produces a Ni(2) bis-mu-hydroxo dimer." J Inorg Biochem **101**(2): 370-3.

Sigurskjold, B. W. (2000). "Exact analysis of competition ligand binding by displacement isothermal titration calorimetry." Anal Biochem **277**(2): 260-6.

Stanczak, P. and H. Kozlowski (2007). "Can chicken and human PrPs possess SOD-like activity after beta-cleavage?" Biochem Biophys Res Commun **352**(1): 198-202.

Stanczak, P., D. Valensin, et al. (2005). "Structure and stability of the CuII complexes with tandem repeats of the chicken prion." Biochemistry **44**(39): 12940-54.

Stockel, J., J. Safar, et al. (1998). "Prion protein selectively binds copper(II) ions." Biochemistry **37**(20): 7185-93.

Stumm, W., L. Sigg, et al. (1992). Chemistry of the solid-water interface : processes at the mineral-water and particle-water interface in natural systems, Wiley.

Thackray, A. M., R. Knight, et al. (2002). "Metal imbalance and compromised antioxidant function are early changes in prion disease." Biochem J **362**(Pt 1): 253-8.

Thackray, A. M., J. Y. Madec, et al. (2003). "Detection of bovine spongiform encephalopathy, ovine scrapie prion-related protein (PrPSc) and normal PrPc by monoclonal antibodies raised to copper-refolded prion protein." Biochem J **370**(Pt 1): 81-90.

Thompsett, A. R., S. R. Abdelraheim, et al. (2005). "High affinity binding between copper and full-length prion protein identified by two different techniques." J Biol Chem **280**(52): 42750-8.

Treiber, C., R. Pipkorn, et al. (2007). "Copper is required for prion protein-associated superoxide dismutase-I activity in Pichia pastoris." Febs J **274**(5): 1304-11.

Treiber, C., A. R. Thompsett, et al. (2007). "Real-time kinetics of discontinuous and highly conformational metal-ion binding sites of prion protein." J Biol Inorg Chem **12**(5): 711-20.

Tsenkova, R. N., I. K. Iordanova, et al. (2004). "Prion protein fate governed by metal binding." Biochem Biophys Res Commun **325**(3): 1005-12.

Tsiroulnikov, K., H. Rezaei, et al. (2006). "Cu(II) induces small-size aggregates with amyloid characteristics in two alleles of recombinant ovine prion proteins." Biochim Biophys Acta **1764**(7): 1218-26.

Vasina, E. N., P. Dejardin, et al. (2005). "Fate of prions in soil: adsorption kinetics of recombinant unglycosylated ovine prion protein onto mica in laminar flow conditions and subsequent desorption." Biomacromolecules **6**(6): 3425-32.

Viles, J. H., F. E. Cohen, et al. (1999). "Copper binding to the prion protein: structural implications of four identical cooperative binding sites." Proc Natl Acad Sci U S A **96**(5): 2042-7.

Wadsworth, J. D., A. F. Hill, et al. (1999). "Strain-specific prion-protein conformation determined by metal ions." Nat Cell Biol **1**(1): 55-9.

Waggoner, D. J., B. Drisaldi, et al. (2000). "Brain copper content and cuproenzyme activity do not vary with prion protein expression level." J Biol Chem **275**(11): 7455-8.

Walmsley, A. R., F. Zeng, et al. (2003). "The N-terminal region of the prion protein ectodomain contains a lipid raft targeting determinant." J Biol Chem **278**(39): 37241-8.

Walter, E. D., M. Chattopadhyay, et al. (2006). "The affinity of copper binding to the prion protein octarepeat domain: evidence for negative cooperativity." Biochemistry **45**(43): 13083-92.

Walz, R., O. B. Amaral, et al. (1999). "Increased sensitivity to seizures in mice lacking cellular prion protein." Epilepsia **40**(12): 1679-82.

Wang, Z. X. (1995). "An exact mathematical expression for describing competitive binding of two different ligands to a protein molecule." FEBS Lett **360**(2): 111-4.

Weiss, A., P. Del Pino, et al. (2007). "The configuration of the Cu(2+) binding region in full-length human prion protein compared with the isolated octapeptide." Vet Microbiol **123**(4): 358-66.

Wells, M. A., C. Jelinska, et al. (2006). "Multiple forms of copper (II) co-ordination occur throughout the disordered N-terminal region of the prion protein at pH 7.4." Biochem J **400**(3): 501-10.

Wernimont, A. K., L. A. Yatsunyk, et al. (2004). "Binding of copper(I) by the Wilson disease protein and its copper chaperone." J Biol Chem **279**(13): 12269-76.

Westergard, L., H. M. Christensen, et al. (2007). "The cellular prion protein (PrP(C)): its physiological function and role in disease." Biochim Biophys Acta **1772**(6): 629-44.

White, A. R., S. J. Collins, et al. (1999). "Prion protein-deficient neurons reveal lower glutathione reductase activity and increased susceptibility to hydrogen peroxide toxicity." Am J Pathol **155**(5): 1723-30.

Whitesides, G. M. and V. M. Krishnamurthy (2005). "Designing ligands to bind proteins." Q Rev Biophys **38**(4): 385-95.

Wiggins, R. C. (2009). "Prion stability and infectivity in the environment." Neurochem Res **34**(1): 158-68.

Will, R. G., J. W. Ironside, et al. (1996). "A new variant of Creutzfeldt-Jakob disease in the UK." Lancet **347**(9006): 921-5.

Wiseman, T., S. Williston, et al. (1989). "Rapid measurement of binding constants and heats of binding using a new titration calorimeter." Anal Biochem **179**(1): 131-7.

Wong, B. S., D. R. Brown, et al. (2001). "Oxidative impairment in scrapie-infected mice is associated with brain metals perturbations and altered antioxidant activities." J Neurochem **79**(3): 689-98.

Wong, B. S., D. R. Brown, et al. (2001). "A Yin-Yang role for metals in prion disease." Panminerva Med **43**(4): 283-7.

Wong, B. S., S. G. Chen, et al. (2001). "Aberrant metal binding by prion protein in human prion disease." J Neurochem **78**(6): 1400-8.

Wong, B. S., T. Pan, et al. (2000). "Differential contribution of superoxide dismutase activity by prion protein in vivo." Biochem Biophys Res Commun **273**(1): 136-9.

Wong, E., A. M. Thackray, et al. (2004). "Copper induces increased beta-sheet content in the scrapie-susceptible ovine prion protein PrPVRQ compared with the resistant allelic variant PrPARR." Biochem J **380**(Pt 1): 273-82.

Zeng, F., N. T. Watt, et al. (2003). "Tethering the N-terminus of the prion protein compromises the cellular response to oxidative stress." J Neurochem **84**(3): 480-90.

Zhang, Y., S. Akilesh, et al. (2000). "Isothermal titration calorimetry measurements of Ni(II) and Cu(II) binding to His, GlyGlyHis, HisGlyHis, and bovine serum albumin: a critical evaluation." Inorg Chem **39**(14): 3057-64.

Zucconi, G. G., S. Cipriani, et al. (2007). "Copper deficiency elicits glial and neuronal response typical of neurodegenerative disorders." Neuropathol Appl Neurobiol **33**(2): 212-25.

Appendix A

Plasmid Vector Map – 23a(+)

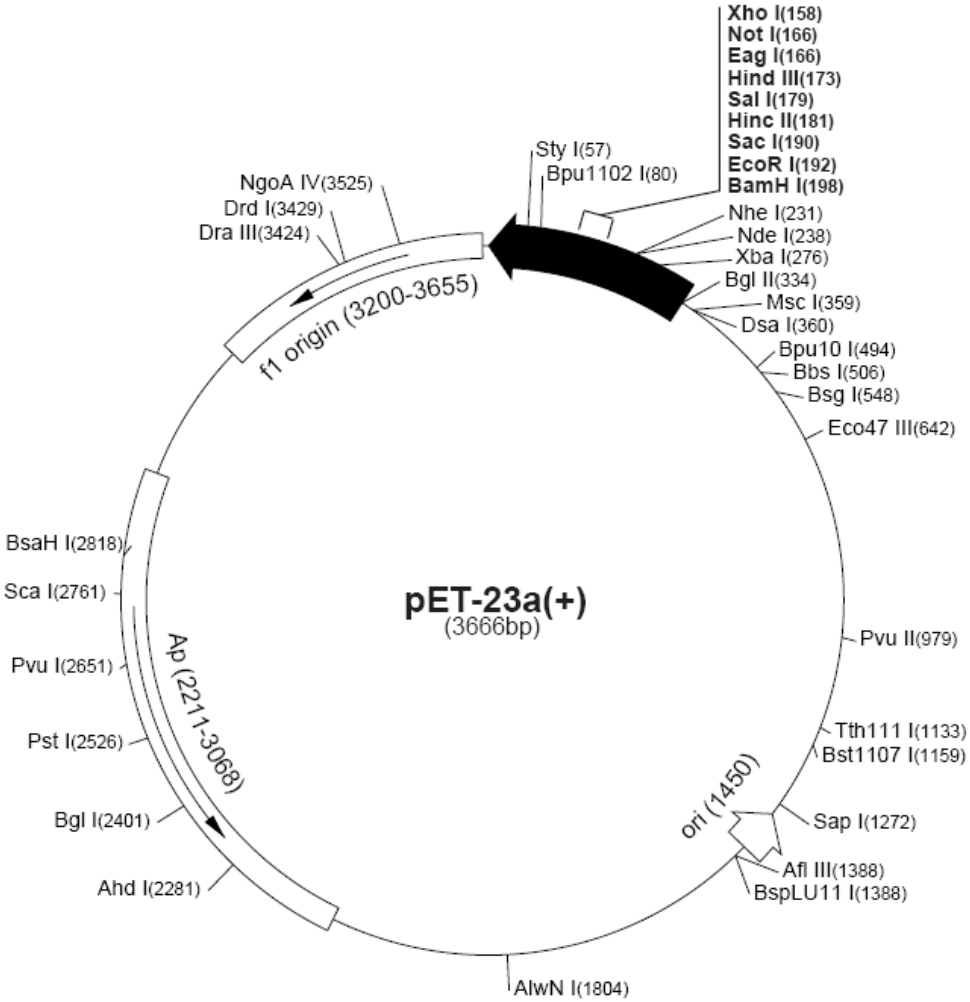

pET-23a-d(+) cloning/expression region

Wildtype rPrP Sequence

AAAAAGCGGCCAAAGCCTGGAGGGTGGAACACCGGTGGAAGCCGGTATCC
CGGGCAGGGAAGCCCTGGAGGCAACCGTTACCCACCTCAGGGTGGCACCTG
GGGGCAGCCCCACGGTGGTGGCTGGGGACAACCCCATGGGGGCAGCTGGG
GACAACCTCATGGTGGTAGTTGGGGTCAGCCCCATGGCGGTGGATGGGGCC
AAGGAGGGGGTACCCATAATCAGTGGAACAAGCCCAGCAAACCAAAAACC
AACCTCAAGCATGTGGCAGGGGCTGCGGCAGCTGGGGCAGTAGTGGGGGG
CCTTGGTGGCTACATGCTGGGGAGCGCCATGAGCAGGCCCATGATCCATTTT
GGCAACGACTGGGAGGACCGCTACTACCGTGAAAACATGTACCGCTACCCT
AACCAAGTGTACTACAGGCCAGTGGATCAGTACAGCAACCAGAACAACTTC
GTGCACGACTGCGTCAATATCACCATCAAGCAGCACACGGTCACCACCACC
ACCAAGGGGGAGAACTTCACCGAGACCGATGTGAAGATGATGGAGCGCGT
GGTGGAGCAGATGTGCGTCACCCAGTACCAGAAGGAGTCCCAGGCCTATTA
CGACGGGAGAAGATCC

Wildtype rPrP Protein Sequence

K K R P K P G G W N T G G S R Y P G Q G S P G G N R Y P P Q G G T W G Q P H
G G G W G Q P H G G S W G Q P H G G S W G Q P H G G G W G Q G G G T H N
Q W N K P S K P K T N L K H V A G A A A A G A V V G G L G G Y **M** L G S A **M**
S R P **M** I H F G N D W E D R Y Y R E N **M** Y R Y P N Q V Y Y R P V D Q Y S N
Q N N F V H D C V N I T I K Q H T V T T T T K G E N F T E T D V K **M** **M** E R V
V E Q **M** C V T Q Y Q K E S Q A Y Y D G R R S

Null PrP Sequence

AAAAAGCGGCCAAAGCCNGGAGGNTGGAACACCGGTGGAAGCCGGTATCC
CGGGCAGGGAAGCCCTGGAGGCAACCGTTACCCACCTCAGGGTGGCACCTG
GGGGCAGCCCGCCGGTGGTGGCTGGGGACAACCCGCTGGGGGCAGCTGGG
GACAACCTGCTGGTGGTAGTTGGGGTCAGCCCGCTGGCGGTGGATGGGGCC
AAGGAGGGGGTACCGCTAATCAGTGGAACAAGCCCAGCAAACCAAAAACC
AACCTCAAGGCTGTGGCAGGGGCTGCGGCAGCTGGGGCAGTAGTGGGGGG
CCTTGGTGGCTACATGCTGGGGAGCGCCATGAGCAGGCCCATGATCCATTTT
GGCAACGACTGGGAGGACCGCTACTACCGTGAAAACATGTACCGCTACCCT
AACCAAGTGTACTACAGGCCAGTGGATCAGTACAGCAACCAGAACAACTTC
GTGCACGACTGCGTCAATATCACCATCAAGCAGCACACGGTCACCACCACC
ACCAAGGGGGAGAACTTCACCGAGACCGATGTGAAGATGATGGAGCGCGT
GGTGGAGCAGATGTGCGTCACCCAGTACCAGAAGGAGTCCCAGGCCTATTA
CGACGGGAGAAGATCCTGA

Null PrP Protein Sequence

K K R P K P G G W N T G G S R Y P G Q G S P G G N R Y P P Q G G T W G Q P A
G G G W G Q P A G G S W G Q P A G G S W G Q P A G G G W G Q G G G T A N
Q W N K P S K P K T N L K A V A G A A A A G A V V G G L G G Y **M** L G S A **M**
S R P **M** I H F G N D W E D R Y Y R E N **M** Y R Y P N Q V Y Y R P V D Q Y S N
Q N N F V H D C V N I T I K Q H T V T T T T K G E N F T E T D V K **M** **M** E R V
V E Q **M** C V T Q Y Q K E S Q A Y Y D G R R S

5th Site Only PrP Sequence

AAAAAGCGGCCAAAGCCNGGAGGNTGGAACACCGGTGGAAGCCGGTATCC
CGGGCAGGGAAGCCCTGGAGGCAACCGTTACCCACCTCAGGGTGGCACCTG
GGGGCAGCCCGCCGGTGGTGGCTGGGGACAACCCGCTGGGGGCAGCTGGG
GACAACCTGCTGGTGGTAGTTGGGGTCAGCCCGCTGGCGGTGGATGGGGCC
AAGGAGGGGGTACCCATAATCAGTGGAACAAGCCCAGCAAACCAAAAACC
AACCTCAAGCATGTGGCAGGGGCTGCGGCAGCTGGGGCAGTAGTGGGGGG
CCTTGGTGGCTACATGCTGGGGAGCGCCATGAGCAGGCCCATGATCCATTTT
GGCAACGACTGGGAGGACCGCTACTACCGTGAAAACATGTACCGCTACCCT
AACCAAGTGTACTACAGGCCAGTGGATCAGTACAGCAACCAGAACAACTTC
GTGCACGACTGCGTCAATATCACCATCAAGCAGCACACGGTCACCACCACC
ACCAAGGGGGAGAACTTCACCGAGACCGATGTGAAGATGATGGAGCGCGT
GGTGGAGCAGATGTGCGTCACCCAGTACCAGAAGGAGTCCCAGGCCTATTA
CGACGGGAGAAGATCCTGA

5th Site Only PrP Protein Sequence

K K R P K P G G W N T G G S R Y P G Q G S P G G N R Y P P Q G G T W G Q P A
G G G W G Q P A G G S W G Q P A G G S W G Q P A G G G W G Q G G G T H N
Q W N K P S K P K T N L K H V A G A A A A G A V V G G L G G Y **M** L G S A **M**
S R P **M** I H F G N D W E D R Y Y R E N **M** Y R Y P N Q V Y Y R P V D Q Y S N
Q N N F V H D C V N I T I K Q H T V T T T T K G E N F T E T D V K **M** **M** E R V
V E Q **M** C V T Q Y Q K E S Q A Y Y D G R R S

Site 5 Present PrP Sequence

AAAAAGCGGCCAAAGCCNGGAGGNTGGAACACCGGTGGAAGCCGGTATCC
CGGGCAGGGAAGCCCTGGAGGCAACCGTTACCCACCTCAGGGTGGCACCTG
GGGGCAGCCCGCCGGTGGTGGCTGGGGACAACCCGCTGGGGGCAGCTGGG
GACAACCTGCTGGTGGTAGTTGGGGTCAGCCCGCTGGCGGTGGATGGGGCC
AAGGAGGGGGTACCCATAATCAGTGGAACAAGCCCAGCAAACCAAAAACC
AACCTCAAGGCTGTGGCAGGGGCTGCGGCAGCTGGGGCAGTAGTGGGGGG
CCTTGGTGGCTACATGCTGGGGAGCGCCATGAGCAGGCCCATGATCCATTTT
GGCAACGACTGGGAGGACCGCTACTACCGTGAAAACATGTACCGCTACCCT
AACCAAGTGTACTACAGGCCAGTGGATCAGTACAGCAACCAGAACAACTTC
GTGCACGACTGCGTCAATATCACCATCAAGCAGCACACGGTCACCACCACC
ACCAAGGGGGAGAACTTCACCGAGACCGATGTGAAGATGATGGAGCGCGT
GGTGGAGCAGATGTGCGTCACCCAGTACCAGAAGGAGTCCCAGGCCTATTA
CGACGGGAGAAGATCCTGA

Site 5 Present PrP Protein Sequence

K K R P K P G G W N T G G S R Y P G Q G S P G G N R Y P P Q G G T W G Q P A
G G G W G Q P A G G S W G Q P A G G S W G Q P A G G G W G Q G G G T H N
Q W N K P S K P K T N L K A V A G A A A A G A V V G G L G G Y **M** L G S A **M**
S R P **M** I H F G N D W E D R Y Y R E N **M** Y R Y P N Q V Y Y R P V D Q Y S N
Q N N F V H D C V N I T I K Q H T V T T T T K G E N F T E T D V K **M** **M** E R V
V E Q **M** C V T Q Y Q K E S Q A Y Y D G R R S

Site 6 Present PrP Sequence

AAAAAGCGGCCAAAGCCNGGAGGNTGGAACACCGGTGGAAGCCGGTATCC
CGGGCAGGGAAGCCCTGGAGGCAACCGTTACCCACCTCAGGGTGGCACCTG
GGGGCAGCCCGCCGGTGGTGGCTGGGGACAACCCGCTGGGGGCAGCTGGG
GACAACCTGCTGGTGGTAGTTGGGGTCAGCCCGCTGGCGGTGGATGGGGCC
AAGGAGGGGGTACCGCTAATCAGTGGAACAAGCCCAGCAAACCAAAAACC
AACCTCAAGCATGTGGCAGGGGCTGCGGCAGCTGGGGCAGTAGTGGGGGG
CCTTGGTGGCTACATGCTGGGGAGCGCCATGAGCAGGCCCATGATCCATTTT
GGCAACGACTGGGAGGACCGCTACTACCGTGAAAACATGTACCGCTACCCT
AACCAAGTGTACTACAGGCCAGTGGATCAGTACAGCAACCAGAACAACTTC
GTGCACGACTGCGTCAATATCACCATCAAGCAGCACACGGTCACCACCACC
ACCAAGGGGGAGAACTTCACCGAGACCGATGTGAAGATGATGGAGCGCGT
GGTGGAGCAGATGTGCGTCACCCAGTACCAGAAGGAGTCCCAGGCCTATTA
CGACGGGAGAAGATCCTGA

Site 6 Present PrP Protein Sequence

K K R P K P G G W N T G G S R Y P G Q G S P G G N R Y P P Q G G T W G Q P A
G G G W G Q P A G G S W G Q P A G G S W G Q P A G G G W G Q G G G T A N
Q W N K P S K P K T N L K H V A G A A A A G A V V G G L G G Y **M** L G S A **M**
S R P **M** I H F G N D W E D R Y Y R E N **M** Y R Y P N Q V Y Y R P V D Q Y S N
Q N N F V H D C V N I T I K Q H T V T T T T K G E N F T E T D V K **M** **M** E R V
V E Q **M** C V T Q Y Q K E S Q A Y Y D G R R S

Octarepeat Only PrP Sequence

AAAAAGCGGCCAAAGCCTGGAGGGTGGAACACCGGTGGAAGCCGGTATCC
CGGGCAGGGAAGCCCTGGAGGCAACCGTTACCCACCTCAGGGTGGCACCTG
GGGGCAGCCCCACGGTGGTGGCTGGGGACAACCCCATGGGGGCAGCTGGG
GACAACCTCATGGTGGTAGTTGGGGTCAGCCCCATGGCGGTGGATGGGGCC
AAGGAGGGGGTACCGCTAATCAGTGGAACAAGCCCAGCAAACCAAAAACC
AACCTCAAGGCTGTGGCAGGGGCTGCGGCAGCTGGGGCAGTAGTGGGGGG
CCTTGGTGGCTACATGCTGGGGAGCGCCATGAGCAGGCCCATGATCCATTTT
GGCAACGACTGGGAGGACCGCTACTACCGTGAAAACATGTACCGCTACCCT
AACCAAGTGTACTACAGGCCAGTGGATCAGTACAGCAACCAGAACAACTTC
GTGCACGACTGCGTCAATATCACCATCAAGCAGCACACGGTCACCACCACC
ACCAAGGGGGAGAACTTCACCGAGACCGATGTGAAGATGATGGAGCGCGT
GGTGGAGCAGATGTGCGTCACCCAGTACCAGAAGGAGTCCCAGGCCTATTA
CGACGGGAGAAGATCC

Octarepeat Only rPrP Protein Sequence

K K R P K P G G W N T G G S R Y P G Q G S P G G N R Y P P Q G G T W G Q P H
G G G W G Q P H G G S W G Q P H G G S W G Q P H G G G W G Q G G G T A N
Q W N K P S K P K T N L K A V A G A A A A G A V V G G L G G Y **M** L G S A **M**
S R P **M** I H F G N D W E D R Y Y R E N **M** Y R Y P N Q V Y Y R P V D Q Y S N
Q N N F V H D C V N I T I K Q H T V T T T T K G E N F T E T D V K **M** **M** E R V
V E Q **M** C V T Q Y Q K E S Q A Y Y D G R R S

Site 2,3,4 Only PrP Sequence

AAAAAGCGGCCAAAGCCTGGAGGGTGGAACACCGGTGGAAGCCGGTATCC
CGGGCAGGGAAGCCCTGGAGGCAACCGTTACCCACCTCAGGGTGGCACCTG
GGGGCAGCCCGCCGGTGGTGGCTGGGGACAACCCCATGGGGGCAGCTGGG
GACAACCTCATGGTGGTAGTTGGGGTCAGCCCCATGGCGGTGGATGGGGCC
AAGGAGGGGGTACCGCTAATCAGTGGAACAAGCCCAGCAAACCAAAAACC
AACCTCAAGGCTGTGGCAGGGGCTGCGGCAGCTGGGGCAGTAGTGGGGGG
CCTTGGTGGCTACATGCTGGGGAGCGCCATGAGCAGGCCCATGATCCATTTT
GGCAACGACTGGGAGGACCGCTACTACCGTGAAAACATGTACCGCTACCCT
AACCAAGTGTACTACAGGCCAGTGGATCAGTACAGCAACCAGAACAACTTC
GTGCACGACTGCGTCAATATCACCATCAAGCAGCACACGGTCACCACCACC
ACCAAGGGGGAGAACTTCACCGAGACCGATGTGAAGATGATGGAGCGCGT
GGTGGAGCAGATGTGCGTCACCCAGTACCAGAAGGAGTCCCAGGCCTATTA
CGACGGGAGAAGATCC

Site 2,3,4 rPrP Protein Sequence

K K R P K P G G W N T G G S R Y P G Q G S P G G N R Y P P Q G G T W G Q P A
G G G W G Q P H G G S W G Q P H G G S W G Q P H G G G W G Q G G G T H A
Q W N K P S K P K T N L K A V A G A A A A G A V V G G L G G Y **M** L G S A **M**
S R P **M** I H F G N D W E D R Y Y R E N **M** Y R Y P N Q V Y Y R P V D Q Y S N
Q N N F V H D C V N I T I K Q H T V T T T T K G E N F T E T D V K **M** **M** E R V
V E Q **M** C V T Q Y Q K E S Q A Y Y D G R R S

Site 1,3,4 Only PrP Sequence

AAAAAGCGGCCAAAGCCTGGAGGGTGGAACACCGGTGGAAGCCGGTATCC
CGGGCAGGGAAGCCCTGGAGGCAACCGTTACCCACCTCAGGGTGGCACCTG
GGGGCAGCCCCACGGTGGTGGCTGGGGACAACCCGCTGGGGGCAGCTGGG
GACAACCTCATGGTGGTAGTTGGGGTCAGCCCCATGGCGGTGGATGGGGCC
AAGGAGGGGGTACCGCTAATCAGTGGAACAAGCCCAGCAAACCAAAAACC
AACCTCAAGGCTGTGGCAGGGGCTGCGGCAGCTGGGGCAGTAGTGGGGGG
CCTTGGTGGCTACATGCTGGGGAGCGCCATGAGCAGGCCCATGATCCATTTT
GGCAACGACTGGGAGGACCGCTACTACCGTGAAAACATGTACCGCTACCCT
AACCAAGTGTACTACAGGCCAGTGGATCAGTACAGCAACCAGAACAACTTC
GTGCACGACTGCGTCAATATCACCATCAAGCAGCACACGGTCACCACCACC
ACCAAGGGGGAGAACTTCACCGAGACCGATGTGAAGATGATGGAGCGCGT
GGTGGAGCAGATGTGCGTCACCCAGTACCAGAAGGAGTCCCAGGCCTATTA
CGACGGGAGAAGATCC

Site 1,3,4 rPrP Protein Sequence

K K R P K P G G W N T G G S R Y P G Q G S P G G N R Y P P Q G G T W G Q P H
G G G W G Q P A G G S W G Q P H G G S W G Q P H G G G W G Q G G G T A N
Q W N K P S K P K T N L K A V A G A A A A G A V V G G L G G Y **M** L G S A **M**
S R P **M** I H F G N D W E D R Y Y R E N **M** Y R Y P N Q V Y Y R P V D Q Y S N
Q N N F V H D C V N I T I K Q H T V T T T T K G E N F T E T D V K **M** **M** E R V
V E Q **M** C V T Q Y Q K E S Q A Y Y D G R R S

Site 1,2,4 Only PrP Sequence

AAAAAGCGGCCAAAGCCTGGAGGGTGGAACACCGGTGGAAGCCGGTATCC
CGGGCAGGGAAGCCCTGGAGGCAACCGTTACCCACCTCAGGGTGGCACCTG
GGGGCAGCCCCACGGTGGTGGCTGGGGACAACCCCATGGGGGCAGCTGGG
GACAACCTGCTGGTGGTAGTTGGGGTCAGCCCCATGGCGGTGGATGGGGCC
AAGGAGGGGGTACCGCTAATCAGTGGAACAAGCCCAGCAAACCAAAAACC
AACCTCAAGGCTGTGGCAGGGGCTGCGGCAGCTGGGGCAGTAGTGGGGGG
CCTTGGTGGCTACATGCTGGGGAGCGCCATGAGCAGGCCCATGATCCATTTT
GGCAACGACTGGGAGGACCGCTACTACCGTGAAAACATGTACCGCTACCCT
AACCAAGTGTACTACAGGCCAGTGGATCAGTACAGCAACCAGAACAACTTC
GTGCACGACTGCGTCAATATCACCATCAAGCAGCACACGGTCACCACCACC
ACCAAGGGGGAGAACTTCACCGAGACCGATGTGAAGATGATGGAGCGCGT
GGTGGAGCAGATGTGCGTCACCCAGTACCAGAAGGAGTCCCAGGCCTATTA
CGACGGGAGAAGATCC

Site 1,2,4 only rPrP Protein Sequence

K K R P K P G G W N T G G S R Y P G Q G S P G G N R Y P P Q G G T W G Q P H
G G G W G Q P H G G S W G Q P A G G S W G Q P H G G G W G Q G G G T A N
Q W N K P S K P K T N L K A V A G A A A A G A V V G G L G G Y **M** L G S A **M**
S R P **M** I H F G N D W E D R Y Y R E N **M** Y R Y P N Q V Y Y R P V D Q Y S N
Q N N F V H D C V N I T I K Q H T V T T T T K G E N F T E T D V K **M** **M** E R V
V E Q **M** C V T Q Y Q K E S Q A Y Y D G R R S

Site 1,2,3 Only PrP Sequence

AAAAAGCGGCCAAAGCCTGGAGGGTGGAACACCGGTGGAAGCCGGTATCC
CGGGCAGGGAAGCCCTGGAGGCAACCGTTACCCACCTCAGGGTGGCACCTG
GGGGCAGCCCCACGGTGGTGGCTGGGGACAACCCCATGGGGGCAGCTGGG
GACAACCTCATGGTGGTAGTTGGGGTCAGCCCGCTGGCGGTGGATGGGGCC
AAGGAGGGGGTACCGCTAATCAGTGGAACAAGCCCAGCAAACCAAAAACC
AACCTCAAGGCTGTGGCAGGGGCTGCGGCAGCTGGGGCAGTAGTGGGGGG
CCTTGGTGGCTACATGCTGGGGAGCGCCATGAGCAGGCCCATGATCCATTTT
GGCAACGACTGGGAGGACCGCTACTACCGTGAAAACATGTACCGCTACCCT
AACCAAGTGTACTACAGGCCAGTGGATCAGTACAGCAACCAGAACAACTTC
GTGCACGACTGCGTCAATATCACCATCAAGCAGCACACGGTCACCACCACC
ACCAAGGGGGAGAACTTCACCGAGACCGATGTGAAGATGATGGAGCGCGT
GGTGGAGCAGATGTGCGTCACCCAGTACCAGAAGGAGTCCCAGGCCTATTA
CGACGGGAGAAGATCC

Site 1,2,3 Only PrP Protein Sequence

K K R P K P G G W N T G G S R Y P G Q G S P G G N R Y P P Q G G T W G Q P H
G G G W G Q P H G G S W G Q P H G G S W G Q P A G G G W G Q G G G T A N
Q W N K P S K P K T N L K A V A G A A A A G A V V G G L G G Y **M** L G S A **M**
S R P **M** I H F G N D W E D R Y Y R E N **M** Y R Y P N Q V Y Y R P V D Q Y S N
Q N N F V H D C V N I T I K Q H T V T T T T K G E N F T E T D V K **M** **M** E R V
V E Q **M** C V T Q Y Q K E S Q A Y Y D G R R S

Site 1 Only PrP Sequence

AAAAAGCGGCCAAAGCCTGGAGGGTGGAACACCGGTGGAAGCCGGTATCC
CGGGCAGGGAAGCCCTGGAGGCAACCGTTACCCACCTCAGGGTGGCACCTG
GGGGCAGCCCCACGGTGGTGGCTGGGGACAACCCGCTGGGGGCAGCTGGG
GACAACCTGCTGGTGGTAGTTGGGGTCAGCCCGCTGGCGGTGGATGGGGCC
AAGGAGGGGGTACCGCTAATCAGTGGAACAAGCCCAGCAAACCAAAAACC
AACCTCAAGGCTGTGGCAGGGGCTGCGGCAGCTGGGGCAGTAGTGGGGGG
CCTTGGTGGCTACATGCTGGGGAGCGCCATGAGCAGGCCCATGATCCATTTT
GGCAACGACTGGGAGGACCGCTACTACCGTGAAAACATGTACCGCTACCCT
AACCAAGTGTACTACAGGCCAGTGGATCAGTACAGCAACCAGAACAACTTC
GTGCACGACTGCGTCAATATCACCATCAAGCAGCACACGGTCACCACCACC
ACCAAGGGGGAGAACTTCACCGAGACCGATGTGAAGATGATGGAGCGCGT
GGTGGAGCAGATGTGCGTCACCCAGTACCAGAAGGAGTCCCAGGCCTATTA
CGACGGGAGAAGATCC

Site 1 rPrP Protein Sequence

K K R P K P G G W N T G G S R Y P G Q G S P G G N R Y P P Q G G T W G Q P H
G G G W G Q P A G G S W G Q P A G G S W G Q P A G G G W G Q G G G T A N
Q W N K P S K P K T N L K A V A G A A A A G A V V G G L G G Y **M** L G S A **M**
S R P **M** I H F G N D W E D R Y Y R E N **M** Y R Y P N Q V Y Y R P V D Q Y S N
Q N N F V H D C V N I T I K Q H T V T T T T K G E N F T E T D V K **M** **M** E R V
V E Q **M** C V T Q Y Q K E S Q A Y Y D G R R S

Site 2 Only PrP Sequence

AAAAAGCGGCCAAAGCCTGGAGGGTGGAACACCGGTGGAAGCCGGTATCC
CGGGCAGGGAAGCCCTGGAGGCAACCGTTACCCACCTCAGGGTGGCACCTG
GGGGCAGCCCGCCGGTGGTGGCTGGGGACAACCCCATGGGGGCAGCTGGG
GACAACCTGCTGGTGGTAGTTGGGGTCAGCCCGCTGGCGGTGGATGGGGCC
AAGGAGGGGGTACCGCTAATCAGTGGAACAAGCCCAGCAAACCAAAAACC
AACCTCAAGGCTGTGGCAGGGGCTGCGGCAGCTGGGGCAGTAGTGGGGGG
CCTTGGTGGCTACATGCTGGGGAGCGCCATGAGCAGGCCCATGATCCATTTT
GGCAACGACTGGGAGGACCGCTACTACCGTGAAAACATGTACCGCTACCCT
AACCAAGTGTACTACAGGCCAGTGGATCAGTACAGCAACCAGAACAACTTC
GTGCACGACTGCGTCAATATCACCATCAAGCAGCACACGGTCACCACCACC
ACCAAGGGGGAGAACTTCACCGAGACCGATGTGAAGATGATGGAGCGCGT
GGTGGAGCAGATGTGCGTCACCCAGTACCAGAAGGAGTCCCAGGCCTATTA
CGACGGGAGAAGATCC

Site 2 rPrP Protein Sequence

K K R P K P G G W N T G G S R Y P G Q G S P G G N R Y P P Q G G T W G Q P A
G G G W G Q P H G G S W G Q P A G G S W G Q P A G G G W G Q G G G T A N
Q W N K P S K P K T N L K A V A G A A A A G A V V G G L G G Y **M** L G S A **M**
S R P **M** I H F G N D W E D R Y Y R E N **M** Y R Y P N Q V Y Y R P V D Q Y S N
Q N N F V H D C V N I T I K Q H T V T T T T K G E N F T E T D V K **M** **M** E R V
V E Q **M** C V T Q Y Q K E S Q A Y Y D G R R S

Site 3 Only PrP Sequence

AAAAAGCGGCCAAAGCCTGGAGGGTGGAACACCGGTGGAAGCCGGTATCC
CGGGCAGGGAAGCCCTGGAGGCAACCGTTACCCACCTCAGGGTGGCACCTG
GGGGCAGCCCGCCGGTGGTGGCTGGGGACAACCCGCTGGGGGCAGCTGGG
GACAACCTCATGGTGGTAGTTGGGGTCAGCCCGCTGGCGGTGGATGGGGCC
AAGGAGGGGGTACCGCTAATCAGTGGAACAAGCCCAGCAAACCAAAAACC
AACCTCAAGGCTGTGGCAGGGGCTGCGGCAGCTGGGGCAGTAGTGGGGGG
CCTTGGTGGCTACATGCTGGGGAGCGCCATGAGCAGGCCCATGATCCATTTT
GGCAACGACTGGGAGGACCGCTACTACCGTGAAAACATGTACCGCTACCCT
AACCAAGTGTACTACAGGCCAGTGGATCAGTACAGCAACCAGAACAACTTC
GTGCACGACTGCGTCAATATCACCATCAAGCAGCACACGGTCACCACCACC
ACCAAGGGGGAGAACTTCACCGAGACCGATGTGAAGATGATGGAGCGCGT
GGTGGAGCAGATGTGCGTCACCCAGTACCAGAAGGAGTCCCAGGCCTATTA
CGACGGGAGAAGATCC

Site 3 only rPrP Protein Sequence

K K R P K P G G W N T G G S R Y P G Q G S P G G N R Y P P Q G G T W G Q P A
G G G W G Q P A G G S W G Q P H G G S W G Q P A G G G W G Q G G G T A N
Q W N K P S K P K T N L K A V A G A A A A G A V V G G L G G Y **M** L G S A **M**
S R P **M** I H F G N D W E D R Y Y R E N **M** Y R Y P N Q V Y Y R P V D Q Y S N
Q N N F V H D C V N I T I K Q H T V T T T T K G E N F T E T D V K **M** **M** E R V
V E Q **M** C V T Q Y Q K E S Q A Y Y D G R R S

Site 4 Only PrP Sequence

AAAAAGCGGCCAAAGCCTGGAGGGTGGAACACCGGTGGAAGCCGGTATCC
CGGGCAGGGAAGCCCTGGAGGCAACCGTTACCCACCTCAGGGTGGCACCTG
GGGGCAGCCCGCCGGTGGTGGCTGGGGACAACCCGCTGGGGGCAGCTGGG
GACAACCTGCTGGTGGTAGTTGGGGTCAGCCCCATGGCGGTGGATGGGGCC
AAGGAGGGGGTACCGCTAATCAGTGGAACAAGCCCAGCAAACCAAAAACC
AACCTCAAGGCTGTGGCAGGGGCTGCGGCAGCTGGGGCAGTAGTGGGGGG
CCTTGGTGGCTACATGCTGGGGAGCGCCATGAGCAGGCCCATGATCCATTTT
GGCAACGACTGGGAGGACCGCTACTACCGTGAAAACATGTACCGCTACCCT
AACCAAGTGTACTACAGGCCAGTGGATCAGTACAGCAACCAGAACAACTTC
GTGCACGACTGCGTCAATATCACCATCAAGCAGCACACGGTCACCACCACC
ACCAAGGGGGAGAACTTCACCGAGACCGATGTGAAGATGATGGAGCGCGT
GGTGGAGCAGATGTGCGTCACCCAGTACCAGAAGGAGTCCCAGGCCTATTA
CGACGGGAGAAGATCC

Site 4 rPrP Protein Sequence

K K R P K P G G W N T G G S R Y P G Q G S P G G N R Y P P Q G G T W G Q P A
G G G W G Q P A G G S W G Q P A G G S W G Q P H G G G W G Q G G G T A N
Q W N K P S K P K T N L K A V A G A A A A G A V V G G L G G Y **M** L G S A **M**
S R P **M** I H F G N D W E D R Y Y R E N **M** Y R Y P N Q V Y Y R P V D Q Y S N
Q N N F V H D C V N I T I K Q H T V T T T T K G E N F T E T D V K **M** **M** E R V
V E Q **M** C V T Q Y Q K E S Q A Y Y D G R R S

Site 1,3 Only PrP Sequence

AAAAAGCGGCCAAAGCCTGGAGGGTGGAACACCGGTGGAAGCCGGTATCC
CGGGCAGGGAAGCCCTGGAGGCAACCGTTACCCACCTCAGGGTGGCACCTG
GGGGCAGCCCCACGGTGGTGGCTGGGGACAACCCGCTGGGGGCAGCTGGG
GACAACCTCATGGTGGTAGTTGGGGTCAGCCCGCTGGCGGTGGATGGGGCC
AAGGAGGGGGTACCGCTAATCAGTGGAACAAGCCCAGCAAACCAAAAACC
AACCTCAAGGCTGTGGCAGGGGCTGCGGCAGCTGGGGCAGTAGTGGGGGG
CCTTGGTGGCTACATGCTGGGGAGCGCCATGAGCAGGCCCATGATCCATTTT
GGCAACGACTGGGAGGACCGCTACTACCGTGAAAACATGTACCGCTACCCT
AACCAAGTGTACTACAGGCCAGTGGATCAGTACAGCAACCAGAACAACTTC
GTGCACGACTGCGTCAATATCACCATCAAGCAGCACACGGTCACCACCACC
ACCAAGGGGGAGAACTTCACCGAGACCGATGTGAAGATGATGGAGCGCGT
GGTGGAGCAGATGTGCGTCACCCAGTACCAGAAGGAGTCCCAGGCCTATTA
CGACGGGAGAAGATCC

Site 1,3 rPrP Protein Sequence

K K R P K P G G W N T G G S R Y P G Q G S P G G N R Y P P Q G G T W G Q P H
G G G W G Q P A G G S W G Q P H G G S W G Q P A G G G W G Q G G G T A N
Q W N K P S K P K T N L K A V A G A A A A G A V V G G L G G Y **M** L G S A **M**
S R P **M** I H F G N D W E D R Y Y R E N **M** Y R Y P N Q V Y Y R P V D Q Y S N
Q N N F V H D C V N I T I K Q H T V T T T T K G E N F T E T D V K **M** **M** E R V
V E Q **M** C V T Q Y Q K E S Q A Y Y D G R R S

Site 3,4 Only PrP Sequence

AAAAAGCGGCCAAAGCCTGGAGGGTGGAACACCGGTGGAAGCCGGTATCC
CGGGCAGGGAAGCCCTGGAGGCAACCGTTACCCACCTCAGGGTGGCACCTG
GGGGCAGCCCGCCGGTGGTGGCTGGGGACAACCCGCTGGGGGCAGCTGGG
GACAACCTCATGGTGGTAGTTGGGGTCAGCCCCATGGCGGTGGATGGGGCC
AAGGAGGGGGTACCGCTAATCAGTGGAACAAGCCCAGCAAACCAAAAACC
AACCTCAAGGCTGTGGCAGGGGCTGCGGCAGCTGGGGCAGTAGTGGGGGG
CCTTGGTGGCTACATGCTGGGGAGCGCCATGAGCAGGCCCATGATCCATTTT
GGCAACGACTGGGAGGACCGCTACTACCGTGAAAACATGTACCGCTACCCT
AACCAAGTGTACTACAGGCCAGTGGATCAGTACAGCAACCAGAACAACTTC
GTGCACGACTGCGTCAATATCACCATCAAGCAGCACACGGTCACCACCACC
ACCAAGGGGGAGAACTTCACCGAGACCGATGTGAAGATGATGGAGCGCGT
GGTGGAGCAGATGTGCGTCACCCAGTACCAGAAGGAGTCCCAGGCCTATTA
CGACGGGAGAAGATCC

Site 3,4 only rPrP Protein Sequence

K K R P K P G G W N T G G S R Y P G Q G S P G G N R Y P P Q G G T W G Q P A
G G G W G Q P A G G S W G Q P H G G S W G Q P H G G G W G Q G G G T A N
Q W N K P S K P K T N L K A V A G A A A A G A V V G G L G G Y **M** L G S A **M**
S R P **M** I H F G N D W E D R Y Y R E N **M** Y R Y P N Q V Y Y R P V D Q Y S N
Q N N F V H D C V N I T I K Q H T V T T T T K G E N F T E T D V K **M** **M** E R V
V E Q **M** C V T Q Y Q K E S Q A Y Y D G R R S

Site 2,4 Only PrP Sequence

AAAAAGCGGCCAAAGCCTGGAGGGTGGAACACCGGTGGAAGCCGGTATCC
CGGGCAGGGAAGCCCTGGAGGCAACCGTTACCCACCTCAGGGTGGCACCTG
GGGGCAGCCCGCCGGTGGTGGCTGGGGACAACCCCATGGGGGCAGCTGGG
GACAACCTGCTGGTGGTAGTTGGGGTCAGCCCCATGGCGGTGGATGGGGCC
AAGGAGGGGGTACCGCTAATCAGTGGAACAAGCCCAGCAAACCAAAAACC
AACCTCAAGGCTGTGGCAGGGGCTGCGGCAGCTGGGGCAGTAGTGGGGGG
CCTTGGTGGCTACATGCTGGGGAGCGCCATGAGCAGGCCCATGATCCATTTT
GGCAACGACTGGGAGGACCGCTACTACCGTGAAAACATGTACCGCTACCCT
AACCAAGTGTACTACAGGCCAGTGGATCAGTACAGCAACCAGAACAACTTC
GTGCACGACTGCGTCAATATCACCATCAAGCAGCACACGGTCACCACCACC
ACCAAGGGGGAGAACTTCACCGAGACCGATGTGAAGATGATGGAGCGCGT
GGTGGAGCAGATGTGCGTCACCCAGTACCAGAAGGAGTCCCAGGCCTATTA
CGACGGGAGAAGATCC

Site 2,4 only rPrP Protein Sequence

K K R P K P G G W N T G G S R Y P G Q G S P G G N R Y P P Q G G T W G Q P A
G G G W G Q P H G G S W G Q P A G G S W G Q P H G G G W G Q G G G T A N
Q W N K P S K P K T N L K A V A G A A A A G A V V G G L G G Y **M** L G S A **M**
S R P **M** I H F G N D W E D R Y Y R E N **M** Y R Y P N Q V Y Y R P V D Q Y S N
Q N N F V H D C V N I T I K Q H T V T T T T K G E N F T E T D V K **M** **M** E R V
V E Q **M** C V T Q Y Q K E S Q A Y Y D G R R S

Site 2,3 Only PrP Sequence

AAAAAGCGGCCAAAGCCTGGAGGGTGGAACACCGGTGGAAGCCGGTATCC
CGGGCAGGGAAGCCCTGGAGGCAACCGTTACCCACCTCAGGGTGGCACCTG
GGGGCAGCCCGCCGGTGGTGGCTGGGGACAACCCCATGGGGGCAGCTGGG
GACAACCTCATGGTGGTAGTTGGGGTCAGCCCGCTGGCGGTGGATGGGGCC
AAGGAGGGGGTACCGCTAATCAGTGGAACAAGCCCAGCAAACCAAAAACC
AACCTCAAGGCTGTGGCAGGGGCTGCGGCAGCTGGGGCAGTAGTGGGGGG
CCTTGGTGGCTACATGCTGGGGAGCGCCATGAGCAGGCCCATGATCCATTTT
GGCAACGACTGGGAGGACCGCTACTACCGTGAAAACATGTACCGCTACCCT
AACCAAGTGTACTACAGGCCAGTGGATCAGTACAGCAACCAGAACAACTTC
GTGCACGACTGCGTCAATATCACCATCAAGCAGCACACGGTCACCACCACC
ACCAAGGGGGAGAACTTCACCGAGACCGATGTGAAGATGATGGAGCGCGT
GGTGGAGCAGATGTGCGTCACCCAGTACCAGAAGGAGTCCCAGGCCTATTA
CGACGGGAGAAGATCC

Site 2,3 rPrP Protein Sequence

K K R P K P G G W N T G G S R Y P G Q G S P G G N R Y P P Q G G T W G Q P A
G G G W G Q P H G G S W G Q P H G G S W G Q P A G G G W G Q G G G T A N
Q W N K P S K P K T N L K A V A G A A A A G A V V G G L G G Y **M** L G S A **M**
S R P **M** I H F G N D W E D R Y Y R E N **M** Y R Y P N Q V Y Y R P V D Q Y S N
Q N N F V H D C V N I T I K Q H T V T T T T K G E N F T E T D V K **M** **M** E R V
V E Q **M** C V T Q Y Q K E S Q A Y Y D G R R S

Site 1,4 Only PrP Sequence

AAAAAGCGGCCAAAGCCTGGAGGGTGGAACACCGGTGGAAGCCGGTATCC
CGGGCAGGGAAGCCCTGGAGGCAACCGTTACCCACCTCAGGGTGGCACCTG
GGGGCAGCCCCACGGTGGTGGCTGGGGACAACCCGCTGGGGGCAGCTGGG
GACAACCTGCTGGTGGTAGTTGGGGTCAGCCCCATGGCGGTGGATGGGGCC
AAGGAGGGGGTACCGCTAATCAGTGGAACAAGCCCAGCAAACCAAAAACC
AACCTCAAGGCTGTGGCAGGGGCTGCGGCAGCTGGGGCAGTAGTGGGGGG
CCTTGGTGGCTACATGCTGGGGAGCGCCATGAGCAGGCCCATGATCCATTTT
GGCAACGACTGGGAGGACCGCTACTACCGTGAAAACATGTACCGCTACCCT
AACCAAGTGTACTACAGGCCAGTGGATCAGTACAGCAACCAGAACAACTTC
GTGCACGACTGCGTCAATATCACCATCAAGCAGCACACGGTCACCACCACC
ACCAAGGGGGAGAACTTCACCGAGACCGATGTGAAGATGATGGAGCGCGT
GGTGGAGCAGATGTGCGTCACCCAGTACCAGAAGGAGTCCCAGGCCTATTA
CGACGGGAGAAGATCC

Site 1,4 only rPrP Protein Sequence

K K R P K P G G W N T G G S R Y P G Q G S P G G N R Y P P Q G G T W G Q P H
G G G W G Q P A G G S W G Q P A G G S W G Q P H G G G W G Q G G G T A N
Q W N K P S K P K T N L K A V A G A A A A G A V V G G L G G Y **M** L G S A **M**
S R P **M** I H F G N D W E D R Y Y R E N **M** Y R Y P N Q V Y Y R P V D Q Y S N
Q N N F V H D C V N I T I K Q H T V T T T T K G E N F T E T D V K **M** **M** E R V
V E Q **M** C V T Q Y Q K E S Q A Y Y D G R R S

Site 1,2 Only PrP Sequence

AAAAAGCGGCCAAAGCCTGGAGGGTGGAACACCGGTGGAAGCCGGTATCC
CGGGCAGGGAAGCCCTGGAGGCAACCGTTACCCACCTCAGGGTGGCACCTG
GGGGCAGCCCCACGGTGGTGGCTGGGGACAACCCCATGGGGGCAGCTGGG
GACAACCTGCTGGTGGTAGTTGGGGTCAGCCCGCTGGCGGTGGATGGGGCC
AAGGAGGGGGTACCGCTAATCAGTGGAACAAGCCCAGCAAACCAAAAACC
AACCTCAAGGCTGTGGCAGGGGCTGCGGCAGCTGGGGCAGTAGTGGGGGG
CCTTGGTGGCTACATGCTGGGGAGCGCCATGAGCAGGCCCATGATCCATTTT
GGCAACGACTGGGAGGACCGCTACTACCGTGAAAACATGTACCGCTACCCT
AACCAAGTGTACTACAGGCCAGTGGATCAGTACAGCAACCAGAACAACTTC
GTGCACGACTGCGTCAATATCACCATCAAGCAGCACACGGTCACCACCACC
ACCAAGGGGGAGAACTTCACCGAGACCGATGTGAAGATGATGGAGCGCGT
GGTGGAGCAGATGTGCGTCACCCAGTACCAGAAGGAGTCCCAGGCCTATTA
CGACGGGAGAAGATCC

Site 1,2 only rPrP Protein Sequence

K K R P K P G G W N T G G S R Y P G Q G S P G G N R Y P P Q G G T W G Q P H
G G G W G Q P H G G S W G Q P A G G S W G Q P A G G G W G Q G G G T A N
Q W N K P S K P K T N L K A V A G A A A A G A V V G G L G G Y **M** L G S A **M**
S R P **M** I H F G N D W E D R Y Y R E N **M** Y R Y P N Q V Y Y R P V D Q Y S N
Q N N F V H D C V N I T I K Q H T V T T T T K G E N F T E T D V K **M** **M** E R V
V E Q **M** C V T Q Y Q K E S Q A Y Y D G R R S

Site 1,2,3,5,6 Only PrP Sequence

AAAAAGCGGCCAAAGCCTGGAGGGTGGAACACCGGTGGAAGCCGGTATCC
CGGGCAGGGAAGCCCTGGAGGCAACCGTTACCCACCTCAGGGTGGCACCTG
GGGGCAGCCCCACGGTGGTGGCTGGGGACAACCCCATGGGGGCAGCTGGG
GACAACCTCATGGTGGTAGTTGGGGTCAGCCCGCTGGCGGTGGATGGGGCC
AAGGAGGGGGTACCCATAATCAGTGGAACAAGCCCAGCAAACCAAAAACC
AACCTCAAGCATGTGGCAGGGGCTGCGGCAGCTGGGGCAGTAGTGGGGGG
CCTTGGTGGCTACATGCTGGGGAGCGCCATGAGCAGGCCCATGATCCATTTT
GGCAACGACTGGGAGGACCGCTACTACCGTGAAAACATGTACCGCTACCCT
AACCAAGTGTACTACAGGCCAGTGGATCAGTACAGCAACCAGAACAACTTC
GTGCACGACTGCGTCAATATCACCATCAAGCAGCACACGGTCACCACCACC
ACCAAGGGGGAGAACTTCACCGAGACCGATGTGAAGATGATGGAGCGCGT
GGTGGAGCAGATGTGCGTCACCCAGTACCAGAAGGAGTCCCAGGCCTATTA
CGACGGGAGAAGATCC

Site 1,2,3,5,6 only rPrP Protein Sequence

K K R P K P G G W N T G G S R Y P G Q G S P G G N R Y P P Q G G T W G Q P H
G G G W G Q P H G G S W G Q P H G G S W G Q P A G G G W G Q G G G T H N
Q W N K P S K P K T N L K H V A G A A A A G A V V G G L G G Y **M** L G S A **M**
S R P **M** I H F G N D W E D R Y Y R E N **M** Y R Y P N Q V Y Y R P V D Q Y S N
Q N N F V H D C V N I T I K Q H T V T T T T K G E N F T E T D V K **M** **M** E R V
V E Q **M** C V T Q Y Q K E S Q A Y Y D G R R S

Site 2,3,4,5,6 Only PrP Sequence

AAAAAGCGGCCAAAGCCTGGAGGGTGGAACACCGGTGGAAGCCGGTATCC
CGGGCAGGGAAGCCCTGGAGGCAACCGTTACCCACCTCAGGGTGGCACCTG
GGGGCAGCCCGCCGGTGGTGGCTGGGGACAACCCCATGGGGGCAGCTGGG
GACAACCTCATGGTGGTAGTTGGGGTCAGCCCCATGGCGGTGGATGGGGCC
AAGGAGGGGGTACCCATAATCAGTGGAACAAGCCCAGCAAACCAAAAACC
AACCTCAAGCATGTGGCAGGGGCTGCGGCAGCTGGGGCAGTAGTGGGGGG
CCTTGGTGGCTACATGCTGGGGAGCGCCATGAGCAGGCCCATGATCCATTTT
GGCAACGACTGGGAGGACCGCTACTACCGTGAAAACATGTACCGCTACCCT
AACCAAGTGTACTACAGGCCAGTGGATCAGTACAGCAACCAGAACAACTTC
GTGCACGACTGCGTCAATATCACCATCAAGCAGCACACGGTCACCACCACC
ACCAAGGGGGAGAACTTCACCGAGACCGATGTGAAGATGATGGAGCGCGT
GGTGGAGCAGATGTGCGTCACCCAGTACCAGAAGGAGTCCCAGGCCTATTA
CGACGGGAGAAGATCC

Site 2,3,4,5,6 only rPrP Protein Sequence

K K R P K P G G W N T G G S R Y P G Q G S P G G N R Y P P Q G G T W G Q P A
G G G W G Q P H G G S W G Q P H G G S W G Q P H G G G W G Q G G G T H N
Q W N K P S K P K T N L K H V A G A A A A G A V V G G L G G Y **M** L G S A **M**
S R P **M** I H F G N D W E D R Y Y R E N **M** Y R Y P N Q V Y Y R P V D Q Y S N
Q N N F V H D C V N I T I K Q H T V T T T T K G E N F T E T D V K **M** **M** E R V
V E Q **M** C V T Q Y Q K E S Q A Y Y D G R R S